The development of a reverse genetics system for the study of chikungunya pathogenesis in the mouse model

John F. Chamberlain

Thesis submitted in accordance with the requirements for the degree of

Doctor of Philosophy
University of London

January 2015

Department of Immunology and Infection

Faculty of Infectious and Tropical Diseases

LONDON SCHOOL OF HYGIENE & TROPICAL MEDICINE

Funded by the Health Protection Agency, the National Institute of Health Research and the Centre for Health Protection Research

Research group affiliation(s): Virology and Pathogenesis group Porton Down

DECLARATION

I John Frederick Chamberlain, confirm that the work presented in this thesis is my own except where contributions by others have been acknowleged. Where information has been derived from other sources, I confirm that this has been indicated in the thesis.

ABSTRACT

The genus *Alphavirus* is one of two within the family *Togaviridae* and comprises approximately 30 species, including several pathogens of humans and other animals that are of medical, veterinary and economic importance. Most alphaviruses are maintained in nature by a biological transmission cycle between susceptible vertebrate hosts and blood-feeding arthropods such as mosquitoes. In common with many Old World alphavirus pathogens Chikungunya virus (CHIKV) is the aetiological agent of a syndrome characterized by fever, skin rash and acute or chronic poly-arthralgia or arthritis. Whereas previously CHIKV outbreaks were sporadic and self-limiting, in 2004 it re-emerged in coastal Kenya and there followed a series of outbreaks that have continued until the present day, resulting in many millions of cases.

Inroads into understanding the pathogenesis of CHIKV disease were until recently hampered through the lack of a convenient small animal model capable of exhibiting symptoms similar to those observed in humans in response to viral challenge. By contrast, studies with other alphaviruses, most notably Sindbis and Semliki Forest viruses (SINV and SFV), have provided insights into many aspects of the infectious process including several key determinants of virulence.

In the present study a reverse genetics system was developed to investigate the pathogenesis of CHIKV disease, the virus replication cycle and its interactions with susceptible hosts. This tool was used to investigate the hypothesis that a CHIKV encoded virulence factor is located within the cleavage domain of the non-structural polyprotein precursor of the viral replicase. Results from this study indicate that a unique amino acid within this conserved site is instrumental in contributing the inhibition of the type 1 IFN response in infected hosts. It was also shown that the type 1 IFN response was induced at an earlier stage in mice challenged with virus containing an engineered mutation at this site and that joint-swelling was less severe than with wild-type virus.

TABLE OF CONTENTS

LIST OF FIGURES

LIST OF TABLES

ABBREVIATIONS AND SYMBOLS

^{0}C	degrees centigrade
h	Hours
m	milli-
µ	micro-
n	nano-
M	molar
l	litre(s)
g	gram
cm	centimetres
hr	hour(s)
min	minute(s)
n	Sample size
<	Less than
sec	seconds
rpm	revolutions per minute
x g	multiples of relative centrifugal force
kb	kilobases
bp	base-pairs
Ae.	*Aedes* mosquito species
C	Capsid
CHIK	chikungunya
CHIKV	chikungunya virus
ONNV	O'Nyong nyong virus
SFV	Semliki Forest virus
SINV	Sindbis virus
EEEV	Eastern equine encephalitis viruses
RRV	Ross River virus

VEEV	Venezuelan equine encephalitis viruses
WEEV	Western equine encephalitis viruses
DNA	deoxyribonucleic acid
cDNA	complementary DNA
dNTP	2’-deoxynucleotide 5’-triphosphate
DMEM	Dulbecco’s modified Eagle medium
DPBS	Dubecco’s phosphate buffered saline
ESCA	East-South-Central African (chikungunya virus genotype)
ELISA	enzyme-linked immunosorbent assay
H&E	Haematoxylin and eosin stain
IFN	interferon
LB	Lauria-Bertani (broth / agar)
MHC	Major histocompatibility complex (types I or II)
H&E	Haematoxylin and eosin stain
PBS	phosphate-buffered saline
PCR	polymerase chain reaction
pfu	plaque-forming units
qRT-PCR	quantitative (real-time) reverse transcription polymerase chain reaction
RNA	ribonucleic acid
RT	reverse transcriptase
MOI	multiplicity of infection
Tm	Melting temperature
ORF	open reading frame
UTR	un-translated region
CSE	conserved sequence elements
PCR	polymerase chain reaction
RT-PCR	reverse transcription-PCR

qRT-PCR	quantitative RT-PCR
RACE	rapid amplification of cDNA ends
TF-PCR	template-fusion PCR
LAMP	Loop-mediated isothermal amplification
w/t	wild type (virus)

ACKNOWLEDGEMENTS

I should like to thank the following:

My supervisors, Roger Hewson and John Raynes for their help, advice and patience throughout the course of this study; the Biological Investigations group at PHE for conducting the mouse-related work, the Histology group also at PHE, Porton for their help in analysing the tissue samples and Howard Tolley (Microbial Imaging Laboratory, PHE, Porton) for preparing the electron micrographs. Finally thanks are due to my wife, Norma for her endless support and encouragement.

CHAPTER 1

General Introduction

1.1 Alphaviruses

1.1.1 Overview

The genus *Alphavirus* is one of two within the family *Togaviridae* and currently includes approximately 30 members (table 1.1). The other genus, Rubivirus contains a single species, Rubella virus (RUBV). Alphaviruses can infect a wide range of host organisms ranging from arthropods to vertebrates and are geographically widespread, being found in each of the world's continents. Most known Alphavirus species circulate in relatively restricted geographic locations and can be considered in terms of sub-groups based on whether they are endemic in the New World (North and South America) or the Old World (Europe, Africa, Australasia and Asia). Recently alphaviruses have been isolated in fish in the North Atlantic Ocean and in marine mammals in the southwest Pacific Ocean, although the distribution of these are currently unknown. The Old World alphaviruses include Chikungunya virus (CHIKV), O'Nyong nyong virus (ONNV), Ross River virus (RRV), Semliki Forest virus (SFV) and Sindbis virus (SINV). New World alphaviruses include Eastern, Western and Venezuelan equine encephalitis viruses (EEEV, WEEV and VEEV). Although some infected hosts show no clinical signs of disease, the genus includes several pathogens of humans and other animals that are of medical, veterinary and economic importance (Griffin 2013, Queyriaux 2008).

Alphavirus Species	Abbreviation	Antigenic Complex	Distribution
Barmah Forest virus	BFV	Barmah Forest virus	Australia
Eastern equine encephalitis	EEE	EEE (4 subtypes)	North, Central, South America
Middelberg virus	MIDV	Middelburg	South Africa, Zimbabwe
Ndumu virus	NDUV	Ndumu virus	South Africa
Semliki Forest virus	SFV	SFV	Central, Eastern, South Africa
Bebaru virus	BEBV	SFV	Malaysia
Chikungunya virus	CHIKV	SFV	Africa, Asia
Mayaro virus	MAYV	SFV	South America, Trinidad
Una virus	UNAV	SFV	South America, Panama
O'nyong Nyong virus	ONNV	SFV	Africa
Getah virus	GETV	SFV	Asia, Oceania
Ross River virus	RRV	SFV	Australia
Venezuelan equine encephalitis virus	VEEV	VEE (6 subtypes)	South, Central, North America
Cabassou virus	CABV	VEE	French Guiana
Everglades virus	EVEV	VEE	Florida, North America
Mosso das Pedras virus	MDPV	VEE	South America
Mucambo virus	MUCV	VEE	South America
Pixuna virus	PIXV	VEE	South America
Rio Negro virus	RNV	VEE	South America
Tonate virus	TONV	VEE	French Guiana
Western equine encephalitis virus*	WEE	WEE	North, South America
Aura virus	AURAV	WEE	Brazil, Argentina
Sindbis virus (Ockelbo, Pogosta and Karelian fever)	SINV	WEE	Africa, Australia, Central Asia, Northern Europe
Whataro virus	WHAV	WEE	New Zealand
Fort Morgan virus*	FMV	WEE	Western North America
Highlands J virus*	HJV	WEE	Eastern North America
Trocara virus	TROV	TROV	Brazil
Salmon pancreas disease virus	SPDV	-	Northern Europe, North America
Southern elephant seal virus	SESV	-	Macquarie Island, Australia

Table 1.1: Alphavirus antigenic complexes**:** table showing the Alphavirus species listed in the ninth report of the International Committee on Taxonomy of Viruses (ICTV) (King *et al* 2011) the antigenic complex to which they have been assigned (where this has been determined) and their Old/New World origins. Eilat virus (EILV) is not included as it had not been described at the time of this publication (Nasar *et al* 2012). An asterix denotes a species believed to be descended from an ancestral alphavirus resulting from a recombination event between a SINV-like virus and an EEEV-like virus Hahn *et al* 1988).

1.1.2 Classification of Alphaviruses

Togaviruses belong to group IV of the Baltimore classification system (Baltimore 1971) by virtue of their genomic makeup (single-stranded positive-sense RNA genome). Historically, members of the genus had been classified on the basis of serological cross-reactions, as group A arboviruses within the family *Togaviridae*. A second group of viruses including dengue, yellow fever, West Nile and tick-borne encephalitis viruses were also included in the family on the basis of shared physical properties, morphology and mode of transmission, and termed group B arboviruses. The term *arbovirus* was used to refer to the predominant mode of transmission between vertebrates. Most are maintained in nature in arthropod reservoirs and passed to a secondary host when the arthropod obtains a blood meal, hence: *ar*thropod-*bo*rne *vi*ruses.

However advances in molecular techniques in the late 20th century showed that the two groups are also distinct in terms of phylogenetic grouping, genomic organization and replication strategies (table 1.2). Alphaviruses are now placed in one of two genera within the family *Togaviridae* (Calisher *et al* 1980, Weaver *et al* 2005, King *et al* 2011). RUBV, the single member of the other genus (Rubivirus) has similarities in terms of morphology and genome organisation to alphaviruses (Weaver *et al* 2005), but shows little genome sequence homology and no detectable antigenic homology, thus any evolutionary relationship that exists between the two genera appears to be distant (Forrester *et al* 2012, King *et al* 2011). The former group B arboviruses have been re-classified to form the *Flavivirus* genus, one of three belonging to the family *Flaviviridae*.

***Alphavirus* Genus**	***Flavivirus* Genus**
Family *Togaviridae*	Family *Flaviviridae*
Genome length 11.6-11.9 kb	Genome length 10-11kb
Two open reading frames	One open reading frame
Separate structural and non-structural polyproteins	Single polyprotein
5 structural and 4 non-structural proteins	3 structural and 7 non-structural proteins
Non-structural genes at 5'end, structural genes at 3'end of genome	Structural genes at 5'end, non-structural genes at 3' end of genome
3' poly-A tail on genomic and sub-genomic RNA	3' stem-loop structure on genomic RNA
No significant genome homology between genera	
No detectable serological cross-reactivity between genera	

Table 1.2 A summary of the major differences between virus species formerly known as group A and B arboviruses (King *et al* 2011). They were later consigned to the genera *Alphavirus* within the family *Togaviridae* and *Flavivirus* in the family *Flaviviridae* respectively (Calisher *et al* 1989).

Early studies led to the classification of alphaviruses into seven antigenic complexes based on the serological relationship between the envelope glycoproteins E1 and E2, determined by haemagglutination inhibition and complement fixation assays (Calisher *et al* 1980). More recent studies in which partial or complete genomic RNA and amino acid sequences have been determined have led to phylogenetic trees being compiled, which shed light on their probable evolutionary history. These have resulted in broadly similar grouping patterns to those based on serology.

Within each antigenic complex distinct virus species typically show a minimum of 21% nucleotide and 8% amino acid divergence, whereas those in different complexes diverge by 38% and 40% respectively (King *et al* 2011). A further (eighth) complex

based on both antigenic and genetic characteristics was proposed following the discovery of Trocara virus (TROV) in *Aedes serratus* (*Ae. serratus*) mosquitoes in Brazil (Travassos da Rosa *et al* 2001) (table 1.1).

However some anomalies have surfaced with the availability of genomic data, such as the placement of Middelburg virus (MIDV) as the only member of the Middelburg virus complex, on serological grounds, whilst it groups with members of the SFV complex on the basis of whole genome nucleic acid sequence criteria (Luers *et al* 2005). It has been suggested that phylogenetic analyses of the structural protein amino acid sequences indicate that this discrepancy is due to recombination events within the E1 gene that occurred between two ancestral members of the SFV complex (Attoui *et al* 2007). In addition, there are conflicting views on the most appropriate classification of several of the more recently discovered alphaviruses such as Southern elephant seal virus (SESV), Salmon pancreas disease virus (SPDV) and Sleeping disease virus (SDV) and Eilat virus (EILV) (Weston *et al* Luers *et al* 2005, Nasar *et al* 2012, Forrester *et al* 2012) .

The division of alphaviruses on the basis of Old or New World distribution is largely supported by genomic nucleotide and amino acid sequence alignments, although there are exceptions to this general pattern among SFV complex members, with Myaro and Una viruses being present in the New World (Lavergne *et al* 2006, Powers *et al* 2006). These viruses cluster in the Old World SFV group according to phylogenetic and serological criteria but are mainly distributed in Brazil, Venezuela and

neighbouring countries of South America (Weaver et al 1992, Powers *et al* 2001), possibly as a result of introduction through human activity or bird migration.

Until recently phylogenetic trees that included all alphaviruses were only possible if based on alignments of incomplete genomic fragments as the complete sequences of several species were not known. However Forrester *et al* (2012) determined the sequences of the remaining genomes enabling alignments of the full length sequences of all known alphaviruses. Phylogenetic trees were developed with this new data which led to placement of the marine alphaviruses SDV, SPDV and SESV in basal positions in relation to terrestrial species (figure 1.1). The authors suggest that this finding indicates that terrestrial alphaviruses may have evolved from a common aquatic ancestor which subsequently diverged into the Old and New World species.

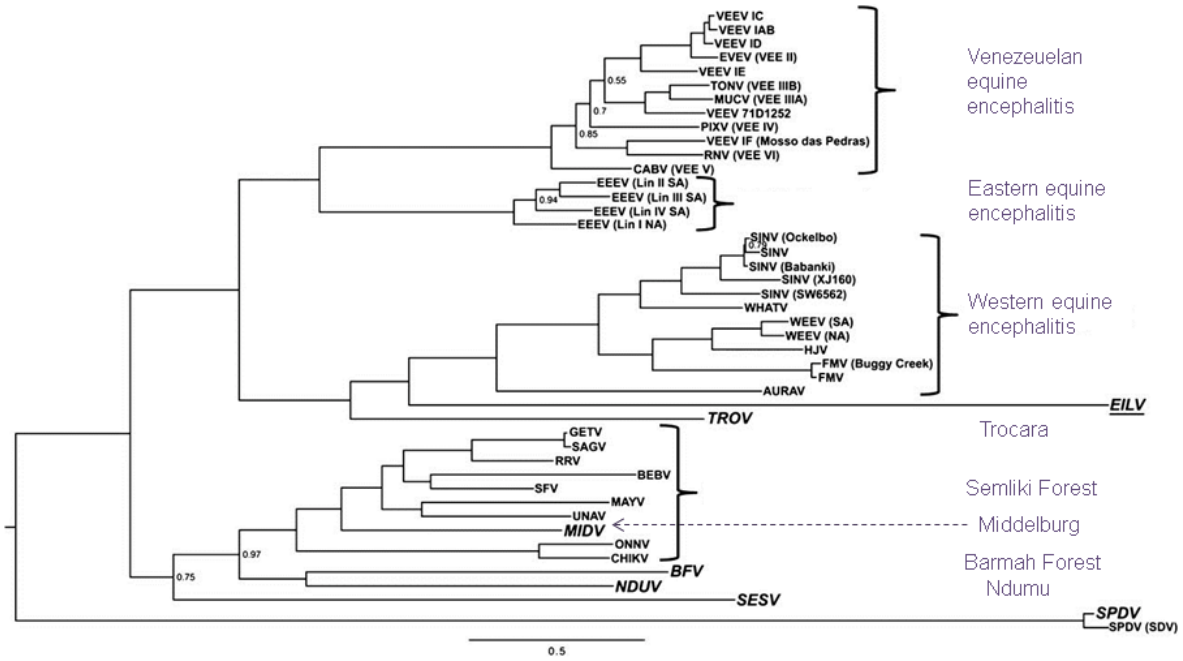

Figure 1.1 A Bayesian phylogenetic tree of alphavirus genomes based on alignment of the structural ORF adapted from Nasar *et al* (2012). Alphavirus antigenic complexes are denoted using a purple font. MIDV is classified as the only member of the Middelburg virus complex but groups with members of the SFV complex on the basis of genomic nucleic acid sequence criteria.

1.1.3 Recombinant species

Amongst the New World viruses, several species including WEE, Highlands J and Whataroa viruses, are believed to have evolved from a common ancestor that resulted from recombination between ancient Old and New world-type viruses (Hahn *et al* 1988, Weaver *et al* 1992, Weaver *et al* 1993, Weaver *et al* 1997). The ancestral virus is thought to have obtained the non-structural and capsid genes from an EEEV- like virus and envelope glycoproteins from a SIN-like virus. Hence SINV, a species geographically restricted to the Old World is placed in a group consisting otherwise of New World viruses (Hahn *et al* 1988, Weaver *et al* 1997).

1.1.4 Arthropod vectors of alphaviruses

In the majority of cases alphaviruses are maintained in nature through an enzootic cycle between a haematophagous arthropod vector and any of a wide range of vertebrate hosts from which they feed. It is the distribution of these species that determines the geographic range in which such alphaviruses can be isolated. In contrast to the lifelong chronic infection that occurs in the arthropod host, infection of vertebrates is usually of short duration and any symptoms are acute. Most alphaviruses have evolved to utilize specific vectors through which efficient transmission occurs, the most common of these being various mosquito species, although in the case of SESV, the louse *Lepidophthirus macrorhini* is believed to fulfil this function (La Linn *et a*l 2001). No arthropod vector has yet been identified for the fish viruses SPDV and SDV (Weston *et al* 1999, Villoing *et al* 2000). Conversely, the recently described alphavirus, Eilat virus (EILV) was isolated from mosquitoes (*Anopheles coustani*) and appears to be unable to replicate in vertebrate cell lines, only infecting insect cell lines (Nasar *et al* 2012).

1.1.5 Physical, biochemical and genomic properties of Alphaviruses

Alphaviruses are spherical particles (figure 1.2) with a diameter of approximately 60-70nm and a mass of 52 MDa. The genome is composed of a single 49S molecule of single-stranded, positive sense RNA with a 7-methylguanosine cap at its 5' terminal and a polyadenylate (poly-A) tail at its 3' terminal. The genomic RNA is linear and has a length of approximately 11.8kb (figure 1.3). Within it are two open reading frames (ORFs), each preceded and followed by untranslated regions (UTRs).The largest ORF comprises approximately two thirds of the 5'end of the genome and encodes a polyprotein precursor of the viral replicase. The second occupies most of the final third of the genome and encodes a polyprotein that is subsequently processed to produce the structural proteins (Strauss and Strauss, 1994, Griffin, 2013). Untranslated regions (UTRs) are present immediately preceding the 5'ORF, between the two ORFs and between the 3'ORF and the poly-A tail. (figure 1.3).

1.1.6 Conserved sequence elements

Four regions in the RNA sequence of alphavirus genomes that appear to have been conserved throughout their evolution, are of particular interest. These conserved sequence elements (CSEs) are predicted to form stem loop structures and are believed to have important roles in the regulation of transcription either of the genomic RNA or of the negative-sense replication intermediate that serves as a template for progeny genomic RNA and sub-genomic RNA.

In the 5’ UTR region there is a CSE consisting of approximately the first 44 nucleotides. Experiments in which deletion mutants were generated from an infectious SINV clone, indicated that the analogous region, present in the negative-strand RNA intermediate product, acts as a promoter for the production of genomic RNA (Niesters and Strauss 1990). A second CSE located approximately 150 nucleotides from the 5’ terminus of the genome has been described in both Old and New World alphaviruses (Ou *et al* 1983). This conserved 51 nucleotide sequence is located within the nsP1coding region and is believed to carry out roles in initiation of both genomic and negative-strand RNA (Strauss and Strauss 1994, Frolov *et al* 2001).

The CSEs in the 3’UTR in different alphaviruses vary considerably in length, ranging from 77 nucleotides in Pixuna virus to 609 nucleotides in Bebaru virus (Pfeffer *et al* 1998). Within each are repeated sequence elements composed of units varying in nucleotide sequence and length, the function of which is yet to be defined. However the final 19 nucleotides immediately preceding the poly-A tail are highly conserved in all members of the genus. It has been shown in SINV that this region plays a key role as a co-promoter of negative-strand RNA synthesis and that the introduction of substitutions or deletions significantly inhibits virus replication (Hill *et al* 1997, Kuhn *et al* 1990, Hardy and Rice 2005). Thus the early stages of replication appear to require interaction between the two termini (Strauss and Strauss 1994, Hardy 2006, Kuhn 2007).

The junction region is located between the two open reading frames and consists of a minimum stretch of 24 nucleotides of which 19 are upstream of the 3’ORF and 5 are

downstream (Strauss and Strauss 2002). The complement of this region in the negative-strand intermediate, acts as a promoter for transcription of the 26S sub-genomic RNA (Strauss and Strauss 1994).

Finally, conserved regions in alphavirus genomes function as packaging signals, enabling the rapid assembly of nucleocapsids soon after the detachment of the capsid protein from the structural polyprotein. Weiss *et al* (1994) identified a 132 nucleotide fragment within the nsP1-coding region of the SINV genome as a packaging signal that interacts with amino acids 81-112 in the capsid protein. It is thought that a variety of such signals are located at several sites within alphavirus genomes, although since only genomic RNA is encapsidated they are likely to be contained within the 5'two-thirds (Strauss and Strauss 1994, Frolova *et al* 1997). However an exception to this trend may occur with Aura virus in which a significant proportion of capsids have been reported to contain sub-genomic RNA when grown in cell cultures (Rümenapf *et al* 1994). The authors suggested that this species contains a packaging signal in the 26S RNA, although an altenative interpretation is that amongst the packaging signals present in the genome, those in the 5'two-thirds are weak and therefore the recognition element in the capsid protein is unable to distinguish between the two RNA species (Frolova *et al* 1997). Newly synthesized genomic 49S RNA and nucleocapsid protein self-assemble in the cytoplasm into icosahedral nucleocapsids which subsequently migrate to the plasma membrane where they form clusters.

The alphavirus nucleocapsid is approximately 40nm in diameter and consists of the genome enclosed by 240 copies of the capsid protein (C) to form an icosahedral

structure with T=4 symmetry (Kuhn 2013) (figure 1.2). The viral envelope is composed of a lipid bilayer derived from the host plasma membrane and is traversed by 240 heterodimers made up of E1 and E2 glycoproteins arranged as trimers to form 80 spike structures. These protrude from the outer surface where they form an icosahedral shell and are stabilised on the inner surface by interactions between the E2 endodomains and hydrophobic clefts on the capsid proteins. Small amounts of a hydrophobic 6kDa protein (6K) and the recently discovered 8kDa trans-frame (TF) protein are reported to be incorporated into the envelope, although their exact location and orientation has yet to be established (Liljeström and Garoff 1991, Jose *et al* 2009, Firth *et al* 2008, Snyder *et al* 2013). A further small cysteine-rich glycoprotein, E3 is a component of some alphavirus envelopes such as SFV (Parades 1998, Garoff and Simons 1974) but absent in others including SINV, CHIKV and WEEV (Simzu *et al* 1984).

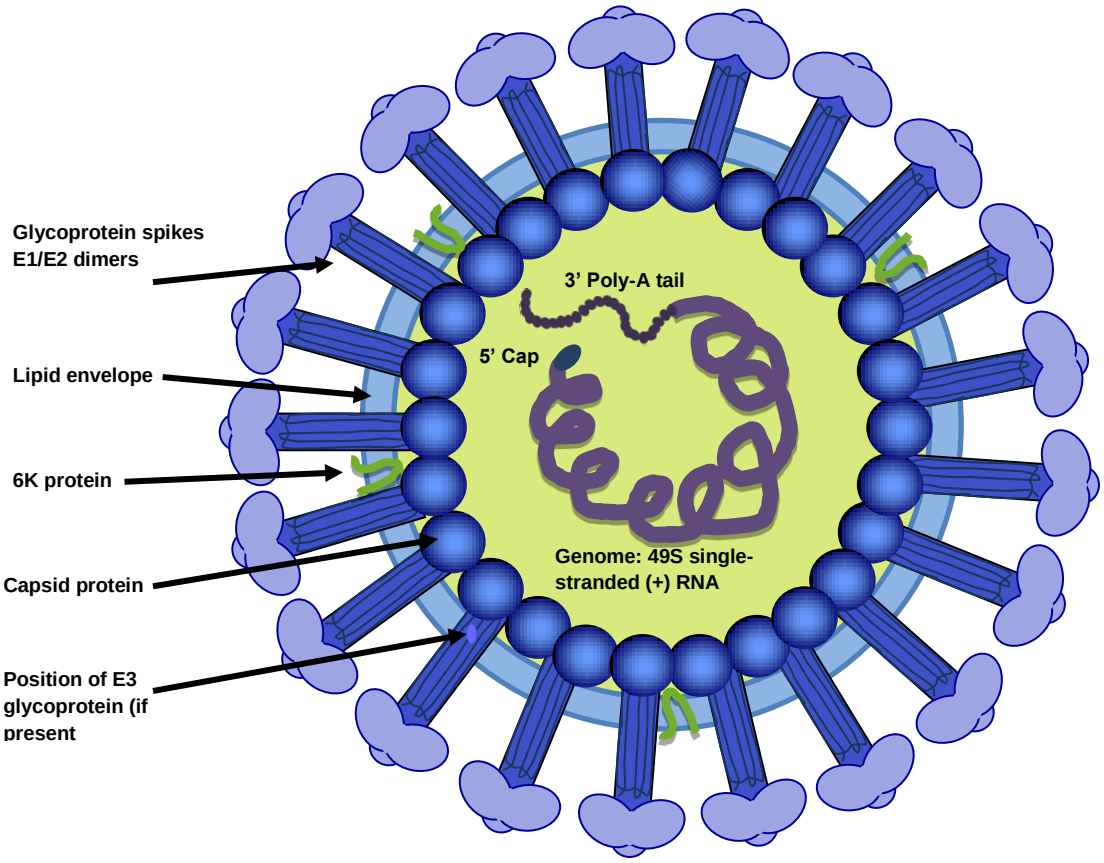

Figure 1.2 Alphavirus structural components: the alphavirus virion consists of a spherical/icosahedral particle with a diameter of 70nm. A single positive-sense RNA molecule with a 5' 7-methylguanosine cap and a 3'poly-A tail is encased by a shell of 240 copies of capsid protein and an envelope derived from the host cell plasma membrane. Protruding from the envelope are 80 glycoprotein spikes each composed of heterodimers of the glycoproteins E1 and E2 arranged as trimers. In addition, small amounts of the 6K protein and in some cases E3 are incorporated into the envelope.

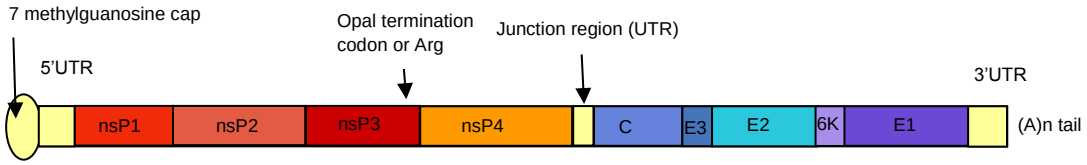

Figure 1.3 Schematic illustration of the alphavirus genome. The single-stranded positive-sense RNA contains two open reading frames (ORF) bordered by un-translated regions. The 5' ORF occupies approximately two thirds of the genome and codes for a single polyprotein which is processed to generate the non-structural proteins, forming the viral replicase. A structural polyprotein is encoded by the 3' one third of the genome. At the 5' terminal is a 7 methylguanosine cap and at the 3' terminal a poly-A tail. The opal termination codon is found in some isolates, but is replaced in others by an arginine codon.

1.2 Alphavirus replication cycle

Many of the details of the alphavirus replication cycle have been determined through studies on SINV, the prototype specific species and SFV, largely because they have been most extensively studied. This is due to the ease with which they can be grown in the laboratory and to their low pathogenicity in humans. Both are currently classified as human hazard group 2 agents on the approved list of biological agents published by the Health and Safety Executive (HSE). However the various stages are thought to be similar in all members of the genus (Kuhn 2007).

1.2.1 Attachment

Infection of a susceptible host cell begins with the attachment of the viral E2 envelope glycoprotein to the host cell receptor which is followed by endocytosis. Alphaviruses infect a range of host cells in both vertebrates and arthropods, however it is not known whether the glycoprotein is able to target multiple cell surface receptor molecules in different types of host cell or a single ubiquitous receptor that has been conserved between animal species (Wang *et al* 1991, Strauss *et al* 1994). To date, the identities of putative receptors for several alphaviruses have been identified using anti-idiotype antibodies as probes (Wang *et al* 1991), however none of these appears to be used exclusively and thus attachment may occur through interactions between E2 and more than one receptor / coreceptor (Griffin 2013).

Studies with SINV have shown that attachment can be initiated with several different cell surface proteins. Laminin, a relatively conserved component of the basement membrane of most animal cells, acts as a receptor in BHK 21 (baby hamster kidney) cell cultures and in C6/36 (*Aedes albopictus*) cell cultures for both SINV and VEEV (Wang *et al* 1992, Ludwig *et al* 1996). However it does not appear to carry out this function in chicken embryo fibroblasts, where a 63kDa protein is reported to act as a receptor (Wang *et al* 1991). Two proteins of unknown identity of 110kDa and 74kDa have been identified in mouse neuroblastoma cells as possible SINV receptors (Ubol and Griffin (1991).

SINV that has been propagated in BHK 21 cell cultures for a number of passages has been reported to employ heparin sulphate molecules as attachment receptors, following the accumulation of adaptive mutations (Klimstra *et al* 1998). These linear polysaccharides are components of proteoglycans located near the plasma membrane of most animal cells where they bind to protein ligands and mediate signal transduction. It is not clear whether the viruses use this or an alternative receptor for the initial attachment when the cells are infected. However, acquisition of these mutations was reported to correlate with reduced pathogenicity in neonatal mice. A similar phenomenon has been shown in VEEV and RRV, in the case of the latter this has been shown to result from a single amino acid substitution (N218R) in the E2 glycoprotein (Bernard *et al* 2000, Heil *et al* 2001). The diversity of cell surface receptors described for SINV and those identified for other alphaviruses indicates that alphaviruses can both utilize ubiquitous conserved molecules and readily adapt to alternative ones (Helenius *et al* 1978, Ludwig *et al* 1996, La Linn *et al* 2005, Wintachhai *et al* 2012).

1.2.2 Internalisation of virus

Following attachment, alphaviruses are internalised by endocytosis which is thought in most cases to be mediated by the formation of clathrin-coated pits; this has been shown to occur with SFV and SINV (Helenius *et al* 1980, DeTulleo and Kirchhausen 1998, Kielian *et al* 2010). However a study with SFV showed that at high concentrations this process becomes saturated, indicating that the virus does not itself induce the formation of clathrin-coated vesicles (Marsh and Helenius 1980). Instead it

is thought that virus enters the host cell through a pre-existing mechanism similar to that used for the uptake of physiological macromolecules.

Studies with cell cultures pre-treated with agents designed to eliminate clathrin and other endocytosis-associated proteins, have provided evidence of the use of clathrin-independent pathways by some alphaviruses. The use of anti-clathrin antibodies was reported to only partially reduce SFV infection, indicating that this virus may be able to utilise an alternative pathway (Doxey *et al* 1987). Furthermore an investigation employing a variety of inhibitors concluded that CHIKV is able to enter cells using a clathrin-indepenent, Eps 15-dependent endocytosis (Bernard *et al* 2010).

1.2.3 Fusion of viral envelope with endosomal membrane

Viruses are subjected to a progressively lower pH as their environment develops from that of an early to late endosome (Schmid *et al* 1989). Fusion of the alphavirus envelope with that of the endosome depends on the vacuolar pH reaching a threshold value that varies with different species. Once this has occurred conformational changes are triggered in the glycoprotein heterodimers resulting in their dissociation. A consequence of this is the exposure of the fusion peptide in the distal tip of E1, which penetrates the endosomal membrane through a hydrophobic interaction with the lipid bilayer (Lescar *et al* 2001, Kiellian *et al* 2010). In a process requiring the presence of cholesterol and sphingolipids, fusion between the viral envelope and the endosomal membrane occurs creating a pore through which the nucleocapsid core is released into the host cell cytoplasm.

1.2.4 Capsid uncoating

Viral genomic RNA is released into the cytoplasm following uncoating of the nucleocapsid at the ribosomes. Two theories have been put forward to explain how this occurs. In the first it is proposed that capsid proteins are detached from the incoming virion by a mechanism triggered by their binding to the host 60S ribosomal sub-unit in the host cell. Later in the replication cycle, newly synthesised capsid protein is produced in quantities that saturate the ribosome binding sites, thus progeny virions are able to assemble (Wengler *et al* 1992, Singh and Helenius 1992). The alternative theory suggests that capsid proteins are exposed to acidic conditions in the endosomes by means of ion channels formed by the E1 and 6K membrane proteins and that this primes the capsid for uncoating (Wengler *et al* 2003). Once it has gained entry to the host cytoplasm, whether through natural infection or through *in vitro* techniques in the laboratory, the 49S RNA is capable of initiating the process of producing progeny virus.

1.2.5 Translation of 5'ORF

The first open reading frame (ORF) following the 5'UTR comprises approximately two thirds of the genome and serves as messenger RNA (mRNA) for the non-structural polyprotein, P1234 (figure 1.4). In some alphaviruses species, or strains within a species, an opal termination codon (UGA) occurs near the 3' end of the nsP3 gene. This is invariably followed by a codon beginning with the nucleotide cytidine, the effect of which is to render the stop codon "leaky", enabling read-through to occur with low frequency (10-20%). In consequence, the quantity of the P123 polyprotein greatly exceeds that of P1234 (Strauss *et al* 1983). In viruses lacking the opal

termination codon it is replaced by an arginine codon (CGA) with the result that only P1234 is produced. It is not clear whether any essential function is facilitated by either of the two genotypes at any stage of viral relication. It has been reported that ONNV clones containing the nsP3 opal codon are more efficient at establishing persistent infections in mosquitoes than those containing arginine (Myles *et al* 2006). Furthermore an avirulent strain of SFV has been shown to become neurovirulent in BALB/c mice when the wild-type opal codon was replace by the CGA arginine codon (Tuittila and Hinkkanen 2003). To date no molecular basis has come to light for either of these observations and neither phenomenon has been shown to be applicable to other alphavirus species.

1.2.6 Cleavage

Following translation the non-structural polyprotein is cleaved by the virus-encoded papain-like protease located in carboxy-terminal half of the non-structural protein 2 (nsP2). Cleavage occurs at three conserved sites, thereby liberating each of the component proteins (figure 1.4). This occurs in a strictly regulated order in which the intermediate products as well as the individual proteins regulate cytoplasmic RNA synthesis within infected cells (Hardy and Strauss 1989, De Groot *et al* 1990, Strauss and Strauss 1994, Shirako and Strauss 1994, Merits *et a*l 2001, Kim *et al* 2004).

For cleavage at the nsP1/nsP2 and nsP2/nsP3 junctions, the nsP2-associated protease functions in *trans*, thus negative-strand (genome-complementary) RNA production predominates until levels of P123 reach a sufficiently high concentration. Next, nsP1

is released and a second transient complex consisting of nsP1, nsP23 and nsP4 is formed which mainly synthesises genome-length positive RNA, although low yields of negative-strand RNA may also be produced. Cleavage at the nsP2/nsP3 junction results in a more stable replication complex composed of mature forms of the four component proteins which no longer synthesises negative-strand RNA. Instead, negative-strand RNA is utilised as a template for the production of sub-genomic (26S) and genomic (49S) positive-strand RNA. In the case of SINV, it has been reported that the sub-genomic product is synthesised at threefold greater quantities than the genome length product (Strauss and Strauss 1994). In common with other positive-strand RNA viruses, the replicase complex of alphaviruses associates with the cytosolic surface of cytoplasmic membranes within host cells prior to the start of RNA synthesis (Salonen *et al* 2004).

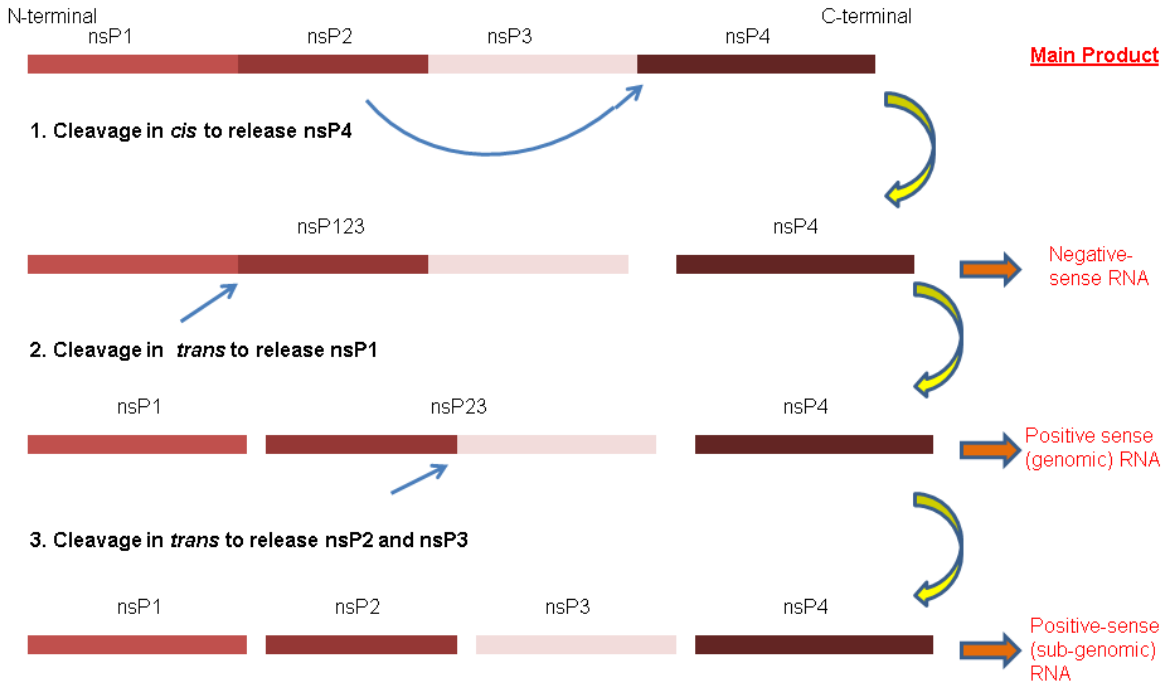

Figure 1.4 The cleavage products of the Alphavirus non-structural polyprotein (nsP) and the predominant RNA species synthesised at each stage. The non-structural polyprotein is translated from the 5' two thirds of the genomic RNA. The nsP4 is liberated by *cis*-proteolytic activity of nsP2. Through this catalytic region further cleavage is made in *trans* to separate the individual proteins from other polyproteins. The final replicase consists of an association of all four nsPs. At each stage of the processing of the polyprotein different RNA products are synthesised (as indicated).

1.2.7 Processing of structural proteins

The order in which the structural genes are arranged in the 26S mRNA is: C-E3-E2-6K-E1 (see figure 1.3). Like the non-structural proteins, the structural protein genes are translated into a single polyprotein which is subsequently processed to produce mature products destined for progeny virions (figure 1.5).

The capsid (C) protein is released into the cytosol through autoproteolysis activity soon after translation by the action of a chymotrypsin-like serine protease (Choi *et al* 1999). Cleavage occurs between two conserved residues: a C-terminal tryptophan in the C protein and a serine at the new N-terminal of the remaining polyprotein. The catalytic domain is present in the C-terminal half of the capsid protein and is composed of a β-barrel motif containing a triad of three crucial amino acids, histidine, aspartic acid and serine. Co-translational folding precedes cleavage so as to position these residues in the correct orientation (Nicola *et al* 1999). The tertiary structure of the protein places the C-terminal tryptophan residue (W267 in SFV) in the catalytic site, blocking and rendering it inactive after cleavage has taken place (Thomas *et al* 2010). Liberated capsid protein next associates with newly synthesised positive-sense RNA in response to the packaging signals mentioned above.

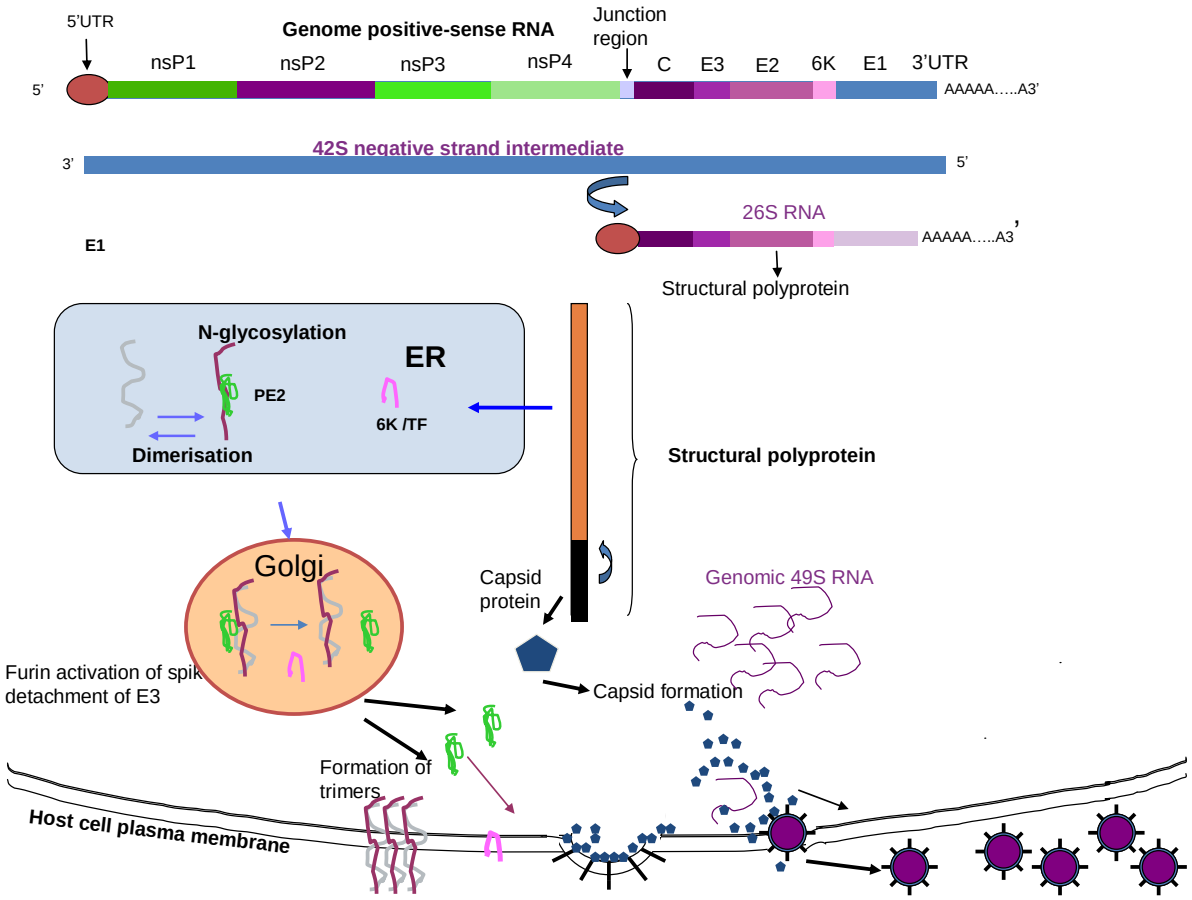

Figure 1.5 Processing of Alphavirus structural proteins: the viral replicase, consisting of the proteins nsP1, nsP2, nsP3 and nsP4 associates with the sub-genomic promoter on the negative-strand RNA and synthesises the 5'- capped, 3' polyA-tailed 26S RNA. This is translated at the cellular ribosomes into a single polyprotein. The N-terminal capsid protein separates through autoproteolysis, whilst the remaining polyprotein is processed in the endoplasmic reticulum and the Golgi complex.

At the N-terminal of the capsid protein is a region of about 100 amino acids that are not highly conserved, however a high proportion are arginine or lysine residues, which results in a net positive charge. It is thought that this results in an electrostatic attraction with negatively charged genomic RNA and contributes to the process of nucleocapsid packaging (Strauss and Strauss 1994). Although this is generally an

efficient process, in at least one species (Aura virus), virions containing sub-genomic 26S RNA may also be assembled (Rümenapf *et al* 1994).

A region near the C-terminal of the capsid protein protrudes from the outer surface and enables association of similar domains on adjacent proteins to produce capsomeres and ultimately new nucleocapsids (Cheng *et al* 1995). Studies of the crystal structure of Aura virus capsid have identified a hydrophobic pocket present in the C-terminal region that interacts with a cytosolic region of the E2 glycoprotein and is thought to have a role in initiation of budding (Metsikkö and Garoff 1990, Aggarwal *et al* 2012). A short conserved region that follows immediately to the C-terminal side of the protein is reported to enable capsids to bind to ribosomes prior to disassembly (Singh and Helenius 1992).

In the capsid protein of New World alphaviruses a conserved domain has been identified near the N-terminal region that plays a critical role in inducing host cell transcriptional shutoff (Garmashova *et al* 2007a, Garmashova *et al* 2007b). This function represents one of the means by which alphaviruses are able to supress the synthesis of effectors of the innate immune response. In Old World alphaviruses transcriptional shutoff is mediated by a domain present in nsP2 (Frolova *et al* 2002, Garmashova *et al* 2006, Akhrymuk *et al* 2012).

1.2.8 Envelope glycoproteins

Each spike consists of three heterodimers which in turn are composed of one copy each of the glycoproteins, E1 and E2 (439 and 417 amino acids long respectively in the CHIKV S27 strain). Following the detachment of the capsid protein a signal sequence at the N-terminal of the remaining polyprotein is exposed and this translocates the remaining structural polyprotein (E3-E2-6K-E1) across the endoplasmic reticulum (ER) membrane. Within the lumen of the ER this product is processed by the host cell enzyme signalase to yield pE2 (a precursor of E3 and E2), 6K and E1 (Garoff *et al* 1994, Strauss and Strauss 1994). Further signal sequences at the C-terminals of pE2 and 6K promote translocation of the 6K and E1 proteins into the ER. Subsequently pE2 and E1 form into heterodimers in a process that has been shown in SFV to involve almost exclusively, components originating from the same polyprotein (Barth *et al* 1995). The E3 portion of pE2 provides a disulphide isomerase function which facilitates the formation of several disulphide bonds essential for the correct folding of E2 during spike formation (Parrott *et al* 2009).

The spikes are translocated to the plasma membrane within the Golgi complex which provides a similar acidic environment to that which triggers viral-host membrane fusion following receptor-mediated endocytosis in the initial stages of the infectious process. However, as a component of pE2, E3 prevents activation of E2 by stabilising an acid sensitive region which would otherwise interact with the fusion loop domain (Lobigs and Garoff 1990, Sjöberg *et al* 2011). Furthermore, when in the trans Golgi complex, pE2 is cleaved by the action of the host enzyme furin to form E2 and E3, the two proteins remain closely associated whilst the environment remains acidic, thus

maintaining this shielding effect. The E1 and pE2 proteins are glycosylated in stages as they move from the endoplasmic reticulum through the Golgi complex to regions of the plasma membrane where E1 and E2 form stable heterodimers. Here, interactions between the nucleocapsid core and the carboxy-terminal cytoplasmic domain of E2 promote virion assembly and budding (Jose *et al* 2012).

1.2.9 6K / TF protein

The 6K protein is so named because it has long been thought to be a single 6KDa polypeptide, however, as mentioned below this may not be the case. This protein has been reported to have a role in various stages of the replication cycle, including uncoating, membrane fusion, budding and virus release (Wengler *et al* 2003, McInerney *et al* 2004, Loewy *et al* 1995, Liljestrom *et al* 1991, Gaedigk-Nitschko *et al* 1990). Although translated in equimolar amounts relative to the other structural proteins, significantly smaller amounts of the 6K protein are incorporated into the viral envelope (Lusa *et al* 1991).

Recent studies have revealed a novel ribosomal -1frame-shifting mechanism that occurs at a conserved motif within the 6K coding region of the structural polyprotein ORF. This results in translation into two predicted protein products: the 6K protein and an additional product termed TF (Trans Frame protein) of approximately 8kDa (Firth *et al* 2008, Chung *et al* 2010). These authors report that it is predominately the latter which is incorporated into the viral envelope.

1.3 Non-Structural Proteins

Non-structural polyproteins (nsPs) in different alphaviruses range in size from approximately 2470 to 2500 amino acid residues (Strauss and Strauss 1994). Many functions of the replicase complex have been mapped to specific domains within the polyprotein and mature nsPs, as summarized below.

1.3.1 nsP1

The nsP1 in alphaviruses comprises approximately 532 to 540 amino acid residues (in the S27 strain of CHIKV it is 535 amino acids). The N-terminal region contains catalytic regions which enable it to cap the 5' end of newly synthesised genomic and sub-genomic RNA by a process distinct from that by which host cells cap mRNA (Cross 1983, Mi and Stollar 1991, Laakkonen *et al* 1994). GTP is methylated at its N7 position by guanyl-7-methytransferase to produce ^{me7}GTP which is next covalently attached to nsP1 as ^{me7}GMP-nsP1 (Ahola and Kaariainen 1995). The critical amino acids in the catalytic site of nsP1 for methylation have been identified and shown by sequence alignment to be conserved amongst several virus families (Rosanov *et al* 1992). However details of the process by which the cap is transferred to the target RNA and the domain catalyzing this step have yet to be established.

The attachment of the viral replicase to cytoplasmic vacuoles has been shown in both SFV and SINV to be due to the action of an amphipathic alpha helix sited in the central region of the nsP1(Salonen *et al* 2003, Spuul *et al* 2007). Hydrophobic amino acids present in this structure are thought to interact with acyl groups within the membrane to anchor it in place. An additional feature that contributes to this affinity

for host cell membranes is the presence of one or more palmitoylated cysteine residues located towards the 3' end of nsP1 (three amino acids from the N-terminal in CHIKV S27 [residues 416 to 419]). A further role attributed to nsP1 is its proposed interaction with nsP4 leading to the initiation of negative-strand RNA synthesis (Wang *et al* 1991, Shirako *et al* 2000, Fata *et al* 2002).

1.3.2 nsP2

The nsP2 is the largest of the replicase sub-units varying amongst different alphavirus species and ranges from 794-807 amino acids in length (Kääriäinen and Ahola 2002). Near the N-terminal is a helicase domain which is involved in unwinding dsRNA, an intermediate transcription product in the synthesis of negative-sense and genomic RNA (Gomez de Cedron *et al* 1999). Also present is a domain with nucleotide triphosphatase activity which is thought to be essential for the function of RNA helicase (Karpe *et al* 2011).

Although RNA replication and polyprotein processing take place in the host cell cytoplasm, a proportion of the nsP2 in alphavirus infected cell cultures has been reported to be present in the host cell nucleus. Nuclear localization signals (NLS) responsible for this phenomenon have been mapped to the central region of nsP2 (Rikkonen *et al* 1992, Rikkonen *et al* 1994, Montgomery and Johnston 2007).

Also towards the N-terminal is a domain exhibiting RNA triphosphatase activity. This contributes to the process of RNA capping by cleaving the phosphoanhydride bond at the 5' end of positive-sense RNA, releasing the gamma phosphate and thus enabling

the capping function of nsP1 to proceed (Vasiljeva *et al* 2000). Near the C-terminal of nsP2 is a papain-like cysteine protease essential for cleaving the non-structural polyprotein at specific sites to yield both intermediate and mature replicase components (Strauss and Strauss 1994, De Groot *et al* 1990). The catalytic site is able to cleave the nsP3/nsP4 junction in *cis* whilst the nsP1/2 and nsP2/3 are processed in *trans*.

In addition to the active methyl transferase catalytic site in nsP1, a highly conserved but non-functional methyl transferase-like domain has been identified in the C-terminal half of nsP2.This has been reported to have roles in the regulation of negative-sense RNA synthesis and in the induction of cellular cytopathic effects (Mayuri *et al* 2008).

In addition to its roles in viral replication, nsP2 has been shown to function through two mechanisms that result in inhibition of the innate immune response. In the Old World alphaviruses SINV, SFV and CHIKV, a determinant located close to the helicase domain, promotes the rapid degradation of the host cell RNA polymerase II component, Rpb1 (Frolova *et al* 2002, Akhrymuk *et al* 2012). In a process thought to involve ubiquitination of the target protein and its subsequent degradation through host cell pathways, cellular gene activation is inhibited (Wilkinson 2005). One of the consequences of the resulting down-regulation of host protein synthesis is the reduction in synthesis of host IFN signalling components and IFN stimulated gene products. In addition, the nsP2 in CHIKV has been shown to contain a C-terminal

motif that blocks the phosphorylation of the Signal Transducer and Activator of Transcription (STAT) thus inactivating the IFN signalling pathway (Fros *et al* 2010).

1.3.3 nsP3

The nsP3 ranges in size amongst alphaviruses from approximately 514 to 570 amino acid residues (Strauss and Strauss 1994). Although three distinct domains are recognised in nsP3, the precise contribution each makes to the infectious process is less clear than those made by nsPs 1, 2 or 4. A 160 amino acid region at the N-terminal is conserved in alphaviruses and categorised as a member of the *macro* domain family. Domains with a high degree of homology are also found in a diverse range of life forms including distantly related viruses, certain bacterial species, archae and many eukaryotes, including mammals (Pehrson and Fuji 1998). Macro domains are reported to carry out ADP ribosylation, an important modification of proteins associated with functions such as cell signalling, DNA repair and apoptosis (Karras *et al* 2005). A study of the crystal structures of both CHIKV and VEEV showed evidence of ADP ribose 1-phosphate phosphatase activity and of RNA binding (Malet *et al* 2009). Lulla *et al* (2012) have provided evidence that elements contained within the *macro* domain in SFV bring about the precise positioning of the nsP2/3 precursor to allow the nsP2 encoded protease access to the previously unexposed cleavage site.

Towards the central region in nsP3 is a zinc-binding domain, which has been suggested to have a role (along with the C-terminal part of nsP2 and the *macro* domain) in binding to RNA, resulting in the preferential production of the negative-

sense form (Shin *et al* 2012). After the cleavage of nsP2/3 the changes in substrate affinity of the mature replicase lead to production of genome and subgenomic RNA only.

The C-terminal region of nsP3 shows great variation in terms of sequence and length, accounting for much of the difference in overall sizes between alphavirus species. However one common characteristic is that of extensive phosphorylation, particularly on serine and threonine residues. The significance of this feature has not been fully explained and studies with SFV have shown no kinase activity. SFV mutants, totally defective in nsP3 phosphorylation remain viable, but are reported to exhibit a decreased rate of RNA synthesis and reduced pathogenicty in mice (Vihinen *et al* 2001). A study in which genetically engineered clones of virulent and avirulent strains of SFV were characterized have shown that the major determinant for neurovirulence in BALB/c mice is carried in nsP3 (Tuittila and Hinkkanan 2003). The authors also demonstrated that in this model the replacement of an opal termination codon for an arginine codon conferred virulence on an otherwise non-virulent strain.

Finally, recent studies with CHIKV and ONNV have shown that elements present in nsP3 determine the vector specificity (Saxton-Shaw *et al* 2013). The majority of mosquito-transmitted alphaviruses rely on haemophagous *Aedes* species for transmission to vertebrate hosts, however ONNV is exclusively transmitted by anopeline species (*A. gambiae* and *A. funestus*). The authors constructed a series of chimeric clones of the two viruses and evaluated their ability to infect *A. gambiae.*

CHIKV clones were only able to establish an infection at a level comparable to wild-type ONNV when their nsP3 was replaced by the equivalent gene from ONNV.

1.3.4 nsP4

The overall size of nsP4 in alphaviruses is approximately 607 to 614 amino acid residues (Strauss and Strauss 1994). It includes a large C-terminal domain comprising the catalytic region of the RNA-dependent RNA polymerase (RdRp) containing the GDD motif common to polymerases in other RNA viruses (Rubak *et al* 2009). This is activated to use genomic RNA as a template to produce negative-sense RNA, by the action of the nsP2-encoded protease. In addition nsP4 functions as a terminal adenyl transferase, thus facilitating the generation and maintenance of the poly-A tail in genomic and sub-genomic RNA (Tomar *et al* 2006).

1.4 Clinical features of alphaviruses

Overt disease symptoms in hosts involved in the natural transmission cycles of alphaviruses are often absent. However, when transmission to alternative, often "dead-end" host species occurs such as domestic animals or humans, severe disease may result. When symptoms do occur in humans these are generally manifested in one of two distinctive syndromes which are generally (although not exclusively) associated with the geographic location in which the virus is endemic. Most of the Old World viruses cause a fever and skin rash that lasts for 1-2 weeks followed by polyarthralgia polyarthritis of varying duration (Tesh 1982, Griffin 2013, Queyriaux 2008, Lakshmi *et al* 2008) as seen typically in members of the Semliki Forest virus

antigenic group such as SFV, RRV or CHIKV (see table 1.3). The clinical features seen in CHIK patients are dealt with in more detail in section 1.6.2. The predominant clinical features of most New World alphavirus infections consist of fever, followed by severe and frequently fatal encephalitis and neurological symptoms (see examples in table 1.4).

1.4.1 Alphavirus infection of domestic and wild animals

Most alphaviruses are maintained in nature through natural cycles in which arthropod vectors infect and acquire virus from vertebrate hosts (Strauss and Strauss 1994). In many cases the vertebrate host suffers only mild symptoms or is asymptomatic, however in others morbidity of varying severity does occur. SFV is able to cause lethal encephalitis in rodents, but is rarely pathogenic in humans. The New World viruses, WEE, VEE and EEE cause severe encephalitis in horses, EEE is also associated with encephalitis in pheasants and emus. Highlands J virus (HJV) is a pathogen of domestic birds such as chickens, turkeys, pheasants, partridges and ducks and causes decreased yields in egg production or mortality (Eleazer and Hill 1994, Griffin 2013). Getah virus (GETV) causes febrile illnesses in horses, pigs and calves (Powers *et al* 2001). Diseases of Atlantic salmon and rainbow trout caused by salmonid alphavirus or salmon pancreas disease virus (SPDV) have had a significant impact on the commercial production of these species in the North Atlantic region since the mid-1980s. Infected fish develop lesions at various sites, particularly in the pancreas and in skeletal and heart muscle. Widely varying mortality rates have been reported in outbreaks, ranging from 0.7-26.9% (Jansen *et al* 2010).

Virus	Geographic range
Chikungunya	Eastern, central and western Africa, India Sri Southeast Asia, Indian Ocean islands, Italy*, France**
O'nyong-nyong	East Africa
Igbo Ora	Nigeria, Central African Republic
Ross River	Australia
Barmah Forest	Australia
Ndumu	Southern Africa
Mayaro	Central and South America
Sindbis	Many regions in Africa, NW Europe (Ockelbo, Pogosta and Karelian fevers), India, Malaysia Southern and Eastern Africa
Semliki Forest	Central, Eastern and Southern Africa, former USSR, India,

* Single outbreak of 217 cases in the Emilia-Romagna region of northern Italy in 2007 (Rezza *et al* 2007)
** Two indigenous cases in south-eastern France (Grandadam *et al*, 2010)

Table 1.3 Alphaviruses associated with rash and polyarthritis

Virus	Geographic range
Eastern Equine Encephalitis	North and South America
Venezuelan Equine Encephalitis	South and Central America
Western Equine Encephalitis	North and South America
Highlands J	Eastern USA

Table 1.4 Alphaviruses causing encephalitis in humans and other mammals

1.5 Diagnosis of alphaviruses

Virus isolation by intra-cerebral inoculation of suckling mice was for many years the method of choice for diagnosis of alphaviruses (Precious *et al* 1974), however in recent years this has been replaced by cell culture-based methods. This may involve the use of vertebrate cell lines such as Vero or BHK-21 cells or mosquito cell lines. Virus identification is subsequently carried out by immunofluorescence (IF), haemagglutination inhibition (HI), complement fixation (Litzba *et al* 2008, Clarke and Casals 1958, Calisher *et al* 1980) or by enzyme immunoassays on infected cell supernatant (Yap *et al* 2010).

Routine diagnosis during alphavirus epidemics is commonly carried out by IgM capture enzyme immunosorbent assay (ELISA). The IgM response to alphaviruses in an individual is relatively specific for members of each antigenic complex and can be detected from 4-7 days after the onset of symptoms and persist for a further 2-3 weeks (Pialoux *et al* 2007). Molecular techniques such as reverse transcription-polymerase chain reaction (RT-PCR) and Loop-mediated isothermal amplification (LAMP) assays are rapid and specific alternatives but must be used on specimens taken early in the course of infection (Hasbe *et al* 2002, Edwards *et al* 2007, Lakshmi *et al* 2008).

1.6 Chikungunya virus

CHIKV is an Old World alphavirus that is transmitted by *Aedes* mosquitoes and is the aetiological agent of chikungunya fever, a condition first described following an outbreak between 1952 and 1953 in the Makonde plateau, located near the south-

eastern border between Tanganyika (now Tanzania) and Mozambique (Robinson 1955, Ross 1956). The name of the virus is derived from a word used by the Makonde tribe who were one of the main groups of people to be affected and describes the characteristic stooped posture seen in many of those suffering from the condition as a result of the severe arthritic condition it causes: it translates as, "that which bends up". From these earliest recognized cases in 1952 until 2003, localised periodic re-emergences were documented in several countries between West Africa and Southeast Asia.

However in 2004, CHIKV re-emerged in coastal Kenya (Njenga *et al* 2008, Schuffenecker *et al* 2006, Sergon *et al* 2008) and spread rapidly to islands in the Indian Ocean. At an early stage in the epidemic that followed, CHIKV isolates obtained from patients had acquired a mutation that facilitated their efficient replication in the Asian tiger mosquito, *Ae. albopictus*. There followed a major epidemic resulting in several million human cases with autochthonous outbreaks reported in a wider geographic range than had previously been recorded.

Several of the early clinical signs seen in CHIK patients such as high fever, skin rash, myalgia and arthralgia are also indicative of other Old World alphaviruses and dengue fever. Both types of virus co-circulate in many tropical and sub-tropical parts of Africa and Asia with a range of arthropod-borne pathogens causing diseases such as malaria, leptospirosis, West Nile disease and Japanese encephalitis. Since these conditions also include an acute non-specific febrile phase, the potential for mis-diagnosis is significant in settings where reliable diagnostic procedures are not

available. CHIKV was first isolated during an outbreak initially thought to be dengue fever in 1953 and only identified as an alphavirus after subsequent serological characterisation (Robinson 1955). Retrospective case reviews have provided evidence that several earlier outbreaks attributed to dengue fever may have actually been CHIK fever and not recognised as distinct conditions (Carey 1971).

1.6.1 Clinical features of Chikungunya

The main clinical manifestations caused by CHIKV infection are summarized in figure 1.6. The incubation period for CHIKV infections of humans is typically 2-5 days. A small proportion of those known to have been infected on the basis of serological evidence (3-25%) show no symptoms (Queyriaux *et al* 2008). In common with most of the other Old World alphaviruses, human cases of chikungunya are characterised by an illness consisting of an acute phase with a high fever (often with a temperature in excess of 39°C), a petechial or maculopapular skin rash and joint pains. The febrile phase is usually accompanied by the skin rash, both of which develop abruptly and coincide with a viraemia. The viraemic phase typically lasts for 5-12 days beyond the onset of symptoms and is often extreme with virus titres reaching 10^{10} to 10^{12} genome copies per ml of blood (Rezza *et al* 2007, Pialoux *et al* 2007, Hoarau *et al* 2010). The range of symptoms experienced by an individual varies, but frequently also includes myalgia, headache, fatigue, conjunctivitis and gastrointestinal symptoms (Queyriaux *et al* 2008, Borgherini *et al* 2008, Cavrini *et al* 2009).

The most significant symptoms seen in a high proportion of patients consist of arthralgia or arthritis. The pain suffered by patients varies, but is often extreme and incapacitating presenting in a fluctuating manner. Although most infections resolve in 2-3 weeks, in chronic cases joint pain persists for many months or even years (Queyriaux *et al* 2008, Borgherini *et al* 2008, Cavrini *et al* 2009). Most commonly, fingers, wrists, elbows, knees, ankles and toes are affected and joints that have previously been injured are particularly susceptible (Tesh 1982). It has been observed that the majority of patients presenting with chronic arthralgia are over 60 years of age and have significantly higher viral loads during the preceding acute viraemic phase than those with less severe symptoms (Hoarau *et al* 2009). This age-related pattern has also been reported in a Rhesus macaque model (Messaoudi *et al* 2013). In this study, increased CHIKV titres were detected in older animals when compared to young adults and this correlated with both weaker innate and adaptive immune responses.

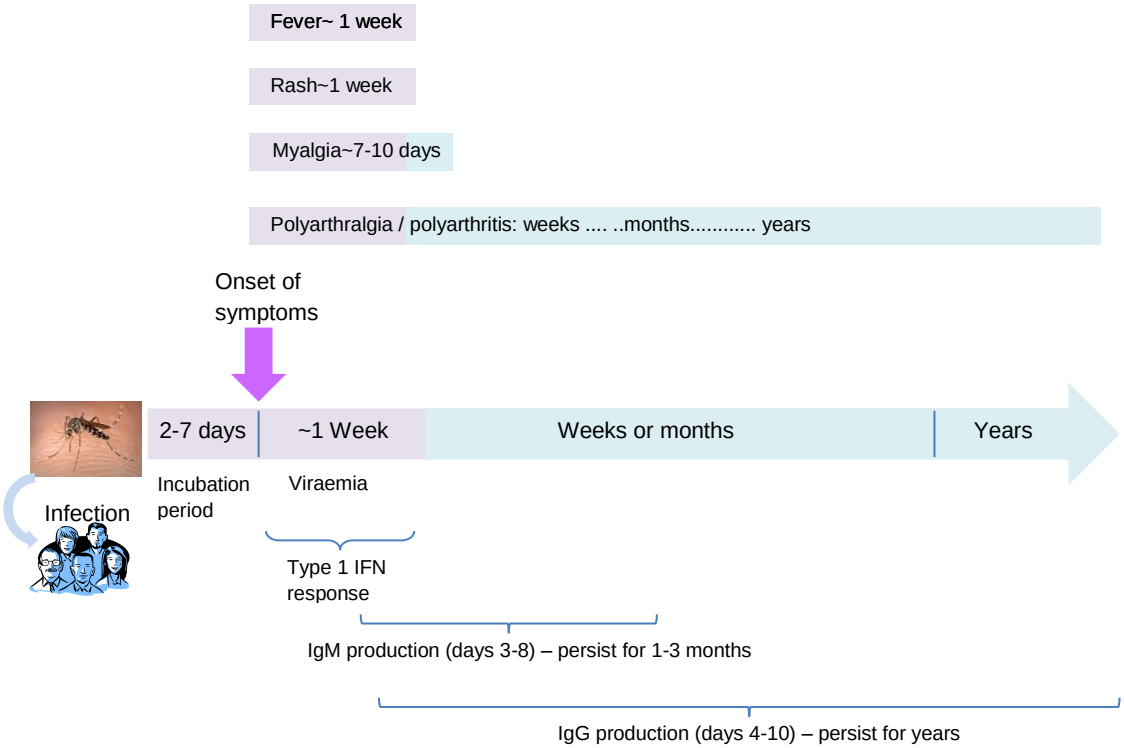

Figure 1.6 Schematic representation of the typical course of CHIKV disease in humans, showing symptoms, biomarkers and approximate times. Asymptomatic infections are also seen in 3-25% of cases and additional symptoms may occur in others (see section 1.6.2).

Other less common but serious complications associated with CHIKV include myocarditis, meningoencephalitis and Guillan-Barré Syndrome. In addition, recent cases involving strains with the E1 A226V mutation have been linked with previously unreported symptoms including flaccid paralysis, brain stem encephalitis, seizures, retinitis and haemorrhagic manifestations (Sarkar *et al* 1965, Lewthwaite *et al* 2008, Singh *et al* 2008, Staples *et al* 2009, Gauri *et al* 2012). A study of the 2005-2006 CHIKV outbreak on La Réunion Island in the Indian Ocean provided evidence linking CHIKV to patient deaths. However although it was shown that a significant excess in mortality coincided with the epidemic incidence peak, it was not determined to what extent other underlying medical conditions contributed to death (Renault *et al* 2008).

1.6.2 Diagnosis of Chikungunya

Laboratory confirmation of CHIKV infection may be requested when a patient has a recent history of having visited or lived in an area where the virus is known to be endemic and presents with symptoms such as fever and severe arthralgia or arthritis. The likely effectiveness of diagnostic techniques depends upon the stage in the disease at which patient samples (usually blood serum) have been obtained. The viraemic phase typically persists for approximately one week after onset of symptoms, thus limiting the period during which methods relying on virus culture or detection of viral RNA can be reliable (figure 1.6).

A variety of RT-PCR assays using both SYBR® green and probe-based technologies and LAMP assays have been described as means for rapid confirmation of a CHIKV diagnosis. To use these methods however, it is essential that specimens are obtained early in the course of infection (Hasbe *et a*l 2002, Edwards *et al* 2007, Lakshmi *et al* 2008).

The production of IgM antibodies typically begins between 3 and 8 days after onset of symptoms and is closely followed by that of IgG antibodies. These can, in most cases be detected for several months or years after disease onset respectively, so CHIKV antibody detection methods are of particular use when the acute phase sample tests negative. Routine diagnosis during alphavirus epidemics is commonly carried out by immunofluorescence (IF) and enzyme immunosorbent assays (ELISAs) which can be used to detect both IgM and IgG anti-CHIKV antibodies from acute or convalescent-phase sera using whole antigen or recombinant capsid or envelope antigens, (Litzba *et al* 2008, Yap *et al* 2010, Pialoux *et al* 2007, Panning et al 2008, Burt *et al* 2012).

1.6.3 CHIKV transmission cycles

Two distinct patterns of CHIKV transmission are recognised which vary with environmental conditions. In rural West and Central Africa, a reservoir of infection is maintained through a sylvatic cycle in which forest-dwelling non-human primates are infected through contact with *Aedes* (*Ae*) mosquitoes (Powers and Logue 2007). The species involved varies with the geographical location, but is believed to include *Ae.*

taylori, *Ae. luteocephalus*, *Ae. furcifer*, *Ae. africanus* and *Ae. neoafricanus*. Spread to human populations through these vectors tends to involve small communities and therefore occurs on a small scale.

In urban settings, *Ae. aegyptii* and since 2005, *Ae. albopictus* are the principal vectors in a mosquito-human-mosquito transmission cycle. Zoonotic cycles involving animal reservoirs have not been shown to exist in endemic regions of Asia, where transmission from person to person through mosquito bites appears to be the prominent route. Serological evidence of CHIKV infection in long tailed macaques has been reported in Malaysia (Apandi *et al* 2009) but it is not clear whether this represents a major source of human outbreaks. Evidence of an alternative route of infection was obtained by a study conducted during the La Réunion Island outbreak in 2005 where it was found that mother to child transmission occurred in 19 out of 39 cases where the mother had been infected between 7 and 3 days prior to delivery (Gérardin 2008, Fritel *et al* 2010).

Of particular concern from a public health perspective is the rapid increase in geographic distribution of *Ae. albopictus* in recent decades (Benedict *et al* 2006, Delatte *et al* 2008). This species is is more widespread than *Ae. aegyptii* and from being largely confined to Southeast Asia until the mid-1970s it has become established in many other countries in Africa, North and South America and Europe (Urbanelli *et al* 1999, Gratz 2004) (table 1.5). It is thought that international trade in goods that may harbour stagnant water such as tyres and timber, has facilitated the introduction of mosquito larvae to new territories and this has been compounded by

the increase in insecticide resistance. To date there are at least 45 countries or territories in which CHIKV is known to have been transmitted to humans (table 1.6), however as mosquitoes capable of transmitting the pathogen are present in many more, further populations are also at risk.

Year first recorded	**Country**	**References**
1979	Albania	Adhami and Reiter 1998
1983	Trinidad	Le Maitre and Chade 1983
1985	USA	Sprenger and Wuithiranyagool 1986
1986	Brazil	Forattini 1986
1990	Italy	Sabatini *et al* 1990
1991	Nigeria	Savage *et al* 1992
	South Africa	Cornel and Hunt 1991
1993	Barbados	Reiter 1998
	Dominican Republic	Peña 1993
1995	Cuba	Broche and Borja 1999
	Guatemala	Ogata and Samayoa 1996
	Honduras	
1997	Cayman Islands	Lounibos *et al* 2003
1998	Argentina	Rossi *et al* 1999
	Colombia	Velez *et al* 1998
1999	France	Schaffner and Karch 2000
2000	Cameroon	Fontenille and Toto 2001
2001	Equatorial Guinea	Toto *et al* 2003
2002	Panama	
2003	Nicaragua	Lugo *et al* 2005
	Switzerland	Flacio *et al* 2004
	Israel	Pener *et al* 2003
2004	Belgium	Schaffner *et al* 2004
	Spain	Nart 2004
2005	Netherlands	Sholte *et al 2007*
	Greece	Samanidou-Voyadjoglou *et al* 2005
	Australia	Scott *et al* 2009
2006	Croatia	Klobučar *et al* 2006
	Gabon	Krueger and Hagen 2007
2007	Germany	Pluskota *et al* 2008
	Lebanon	Haddad *et al* 2007
	Syria	
2011	Tonga	Guillaumot *et al* 2012

Table 1.5 Countries in which *Aedes albopictus* became established between 1979 and 2012 (adapted from Benedict *et al* 2007)

1.6.4 Emergence of CHIKV strains transmitted by *Ae. albopictus*

Until the 2004 re-emergence of CHIKV its principal vector was found to be *Ae aegyptii,* however in the 2005-2006 outbreak on La Réunion Island several factors indicated that this was not the case in this instance. In view of the explosive nature of the outbreak, vectors would be expected to be present in significant numbers, however *Ae. aegyptii* were relatively scarce in this region but *Ae. albopictus*, a species known to be susceptible to CHIKV infection were abundant.

CHIKV isolated from patients during the early months contained alanine at position 226 in the E1 glycoprotein whereas those isolated later contained valine. Experiments in which the sensitivity of *Ae.albopictus* mosquitoes to infection with the two CHIKV phenotypes were compared, showed that those containing the A226V mutation replicated and disseminated to the host salivary glands most efficiently (Vazeille *et al* 2007). Studies using CHIKV clones containing either of the two variants to infect mosquitoes in the laboratory, confirmed that this mutation provides a selective advantage to the virus in utilizing this species (Tsetsarkin *et al* 2007). Further evidence that *Ae. albopictus* was the primary vector was provided by the detection of CHIKV genomic RNA by qRT-PCR from mosquitoes collected in the area.

In the majority of the subsequent CHIKV outbreaks (until December 2013), *Ae. albopictus* is believed to have acted as the principal vector (Tsetsarkin *et al* 2011). The results of phylogenetic studies indicate that the E1 A226V mutation has occurred on at least two other separate occasions in strains from the ESCA lineage, thus

representing an example of evolutionary convergence (De Lamballerie *et al* 2008, Arankalle *et al* 2007, Gould and Higgs 2009).

Evidence suggested that in earlier outbreaks in Asia documented over a period of approximately 60 years, despite the presence of *Ae. albopictus*, CHIKV strains belonging to the Asian lineage have predominately been transmitted by *Ae. aegyptii* (Power and Logue 2008). It has recently been demonstrated that these strains are restricted in their ability to adapt to *Ae. albopictus* through acquisition of the E1 glycoprotein A226V mutation because of the presence of a threonine residue at position 98 (Tsetsarkin *et al* 2011). In experiments using infectious clones derived from representatives of these two lineages, it has been shown that the adaption depends on a crucial epistatic interaction between an alanine residue at position 98 and the valine residue at position 226. In further experiments using chimeric clones, amino acid residues in the E2 glycoprotein at positions 60 and 211 also play important roles in adaption (Tsetsarkin *et al* 2009).

1.6.5 Epidemiology of Chikungunya

Three distinct clades of CHIKV are currently recognized on the basis of phylogenetic criteria (Powers *et al* 2000), these being termed according to the geographic region from which members were originally isolated: West African, East / South / Central/ African (ESCA) and Asian. Outbreaks that occurred between 1952 and 2003 followed a general pattern of relatively localized self-limiting outbreaks followed by intervals, ranging from years to decades before re-emergence was seen. The most recent of

these in Africa occurred in the Democratic Republic of Congo in 1999-2000 (Pastorino *et al* 2004) and in Asia, in an outbreak in Java from 2001-2003 (Laras *et al* 2005).

However in 2004 a new pattern emerged in the form of a major epidemic infecting several million people with viruses belonging to the ESCA clade. The epidemic is believed to have emerged on the Kenyan island of Lamu (Sergon *et al* 2008, Njenga 2008) and in the following months and years spread both to other African countries and in an easterly direction to countries and territories from the Indian Ocean islands to India and Southeast Asia, resulting in the largest recorded epidemic (table 1.6 and figure 1.7). On the island of La Rèunion in the Indian Ocean 266,000 cases were reported in 2005, representing 38% of the population and an estimated 1.4 million cases occured in India in 2006-2007 (Powers 2008, Schwartz and Albert 2010).

The epidemic spread with respect to evolution, vector specificity and clinical characteristics has been monitored in detail throughout up to the present day. From Kenya it spread into other African countries and in an easterly direction to Madagascar, the Indian Ocean islands, India, Sri Lanka and Southeast Asia, reaching the Philippines in 2011. In addition to the many countries in which outbreaks have occurred, imported cases involving travellers returning from endemic regions have been recorded in at least 18 countries (Powers 2008). In 2007 the first recorded outbreak in Europe was reported in the North-eastern region of Emilia Romagna in Italy. Genomic evidence identified a patient who had recently returned from a trip to India, as the index case in an outbreak that led to a further 207 cases (Rezza *et al*

2007, Cavrini *et al* 2009). Two further European cases were reported in 2010 in the town of Fréjus, South-eastern France (Grandadam *et al* 2010).

Although CHIKV outbreaks in the period between 2011 and 2014 have been of a lower magnitude, the pre-2004 pattern has not resumed and regular notifications of further cases continue to be reported to the present day (http://www.promedmail.org). In parts of Oceania, two other Old World alphaviruses that cause similar diseases, namely Ross River and Barmah Forest viruses, are endemic. However in 2011 and 2012, CHIKV outbreaks were reported for the first time on the islands of Papua New Guinea and New Caledonia (Horwood *et al* 2013, Dupont-Rouzeyrol *et al* 2012). Furthermore, in late 2013 and early 2014 the first documented cases of CHIKV were reported on several Carribean islands and on the mainland of South America (Cassadou *et al* 2014, Van Bortel *et al* 2014).

Countries and territories where chikungunya outbreaks have been recorded:		
Africa	**Asia**	**Elswhere**
Tanzania	**Thailand**	
Uganda	**Cambodia**	
Democratic Republic of Congo	**India**	
Zimbabwe	**Vietnam**	
Senigal	**Malaysia**	
Nigeria	**Myanmar (Burma)**	
South Africa	**Indonesia**	
Kenya	**Pakistan**	
Burundi	**Philippines**	
Gabon	Timor	
Malawi		
Guinea		
Central African Republic		
Countries in which the first recorded chikungunya outbreak occurred after its re-emergence in 2004:		
Africa	**Asia**	**Elswhere**
Benin	Bangladesh	**1. Americas**
Cameroon	Bhutan	Anguilla
Comoros	China	Aruba
Equatorial Guinea	Laos	British Virgin Islands
Madagascar	Maldives	Dominica
Mauritius	Singapore	French Guiana
Mayotte	Sri Lanka	Guadeloupe
Republic of Congo	Taiwan	Martinique
Rèunion	Yemen	St Barthelemy
Seychelles		St Kitts and Nevis
Sierra Leone		St Martin
Sudan		St Maarten
		2. Europe
		Italy
		France
		3. Oceania/Pacific islands
		Federal states of Micronesia
		New Caledonia
		Papau New Guinea

Table 1.6 Countries and territories in which autochthonous cases of chikungunya disease have been recorded as of March 31st 2014. Countries in which cases were recorded after the 2004 re-emergence, but had a history of earlier outbreaks are indicated with bold lettering.

Figure 1.7 Map showing the approximate geographic locations (indicated by red stars) in which chikungunya outbreaks have been reported as of March 31st 2014. Areas with a history of CHIKV outbreaks prior to the 2004 re-emergence are enclosed by blue dotted lines.

1.7 CHIKV Pathogenesis

1.7.1 Overview

Until recently, research into the pathogenic processes caused by CHIKV infection was limited due to the lack of a suitable animal model replicating human disease. However following the first report of the use of young and inbred mice in 2008, others have followed in which adult wild-type (w/t) mice and non-human primates have been used (Couderc *et al* 2008, Gardner *et al* 2010, Ziegler *et al* 2008, Morrison *et al* 2011, Labadie *et al* 2010).

A recent report suggests that the differences in susceptibility seen between humans and w/t mice to CHIKV infection may be related to differences in the process of autophagy (Judith *et al* 2013). When human cell lines were infected with CHIKV, capsid protein was degraded following ubiquitination and binding of the autophagy receptor p62, whereas interaction of the autophagy receptor NPD52 with nsP2 was found to promote viral replication. By contrast, both orthologues carried out antiviral roles in infected mouse cells *in vitro* and *in vivo*.

CHIKV can be grown in a wide range of cell lines derived from both human and non-human sources (Sourisseau *et al* 2007, Hahon and Zimmerman 1970, Thon-Hon *et al* 2012, Puiprom *et al* 2013). Infection of susceptible mammalian cell cultures with alphaviruses usually results in a cytopathic effect (CPE) which in many cases is due to apoptosis (Jan and Griffin 1999, Glasgow *et al* 1997, Sourisseau *et al* 2007, Dhanwani *et al* 2012). This appears to be induced through more than one mechanism;

in SINV apoptosis is dependent on virus entry and does not require replication, whereas in SFV it occurs following RNA synthesis.

1.7.2 Cellular tropism of CHIKV

In a study to determine the celluar tropism of CHIKV in human cell cultures Sourisseau *et al* (2007) found that primary fibroblasts, epithelial and endothelial cells were particularly susceptible to infection and monocyte-derived macrophages were susceptible to a lesser extent. In contrast, virus replication was not seen in primary lymphocytes, monocytes, or monocyte-derived dendritic cells. CHIKV has also been shown to grow in muscle satellite cells although not in muscle fibres (Ozden *et al* 2007).

1.7.3 Disease progression

The sequence of events following intradermal inoculation of a mouse model lacking the IFN type 1 receptor ($IFNAR^{-/-}$) with CHIKV, was investigated by Couderc *et al* (2008). This study revealed that virus replication initially occurs in skin fibroblasts near the site of injection and then disseminates in the blood to the liver, muscle, joints, lymphoid tissue and brain. In studies using a non-human primate model the detection of CHIKV RNA was reported from similar sites during the acute phase of the disease and in addition, a transient acute lymphopenia and neutropenia were reported (Labadie *et al* 2010). In contrast to *in vitro* studies by this group and that of Sourisseau *et al* (2007), evidence of dendritic cell infection was obtained. A proposed explanation for this phenomenon is that CHIKV is able to utilize the process of apoptosis as a means of assisting virus dissemination within the infected host.

Macrophages and dendritic cells may become infected by taking up progeny virus contained in apoptotic blebs from susceptible cells such as fibroblasts and transport it to other sites (Schwartz and Albert 2010, Krejbich-Trotot *et al* 2011).

1.7.4 Innate immune responses to CHIKV infection

The early host response to CHIKV infections is largely mediated by the innate immune system through the induction of type 1 interferons (IFN-α and IFN-β) which are detected at high levels during the acute phase and return to normal at the end of the viraemic phase (Schwartz and Albert 2010, Schilte *et al* 2010). The crucial role played by type 1 IFN in the acute phase of CHIKV infections has been illustrated in several studies. In one of these, mice were intradermally infected with CHIKV and disease severity compared between adult wild type (w/t) C57BL/6, neonatal w/t and two groups of transgenic mice, one partially (IFN-α/βR$^{-/+}$) and the other totally deficient (IFN-α/βR$^{-/-}$) in type 1 IFN receptor genes (Couderc *et al* 2008). It was demonstrated that adult w/t mice and those aged over 12 days remained healthy whereas neonates developed disease of decreasing severity with advanced age. Whilst mild disease symptoms were observed in the IFN-α/βR$^{-/+}$ mice the CHIKV infection was lethal in the IFN-α/βR$^{-/-}$ group. Furthermore, Gardner *et al* (2012) reported a greatly increased severity of w/t CHIKV induced joint inflammation in mice deficient in STAT-dependent IFN responses when compared to w/t mice, an observation not seen with the vaccine candidate strain 181/25 (Levitt *et al* 1986).

1.7.5 Interferons

IFNs are a group of cytokines that are produced and secreted by most cells in vertebrate organisms and are grouped into three classes on the basis of their amino acid sequences: types I, II and III (Randall and Goodbourn 2008, Janeway *et al* 2005). After binding to specific cell surface receptors, IFNs act both as autocrine and paracrine stimulators of a range of antiviral genes and have been shown to be crucial effectors of the innate immune response to alphaviruses (figure1.8). Following their release from infected cells, IFN-α and IFN-β (type I IFNs) interact with the IFNAR receptor on the plasma membrane leading to the activation of tyrosine and Janus kinases (TYK2 and JAK1). These phosphorylate the signal transducers and activators of transcription (STAT1 and STAT2) which then form complexes consisting of STAT1/2 heterodimers and IFN regulatory factor 9 (IRF-9). This product, known as IFN-stimulated gene factor 3 (ISGF-3), migrates from the cytosol to the nucleus where it binds to a *cis*-acting DNA element, termed ISRE (IFN-stimulated response element) and activates the transcription of IFN-α/β-stimulated genes (ISGs).

Signalling in response to IFN-γ (type II IFN) follows its interaction with a receptor composed of two major sub-units, IFNGR1 and IFNGR2 (figure 1.8). The cytoplasmic regions of these two components are associated with the tyrosine kinases JAK1 and JAK2 respectively. The binding of IFN-γ to its receptor subunits stimulates their dimerization and is followed by the activation of JAK1 and JAK2. These, in turn phosphorylate a tyrosine residue in two STAT1 molecules resulting in the formation of a STAT1-STAT1 homodimer. Finally the homodimer translocates to the nucleus where it binds to the gamma-activation sequence (GAS) where it stimulates the transcription of ISGs.

IFN-γ is a pleiotrophic cytokine secreted by Th0-cells, activated Th1-cells (CD4+), cytotoxic T cells (CD8+) and by natural killer (NK) cells in response to viral infections (Janeway *et al* 2005). Its roles include the activation and differentiation of macrophages, NK cells, T cells, B cells and the induction of class II major histocompatibility complex (MHC) molecules.

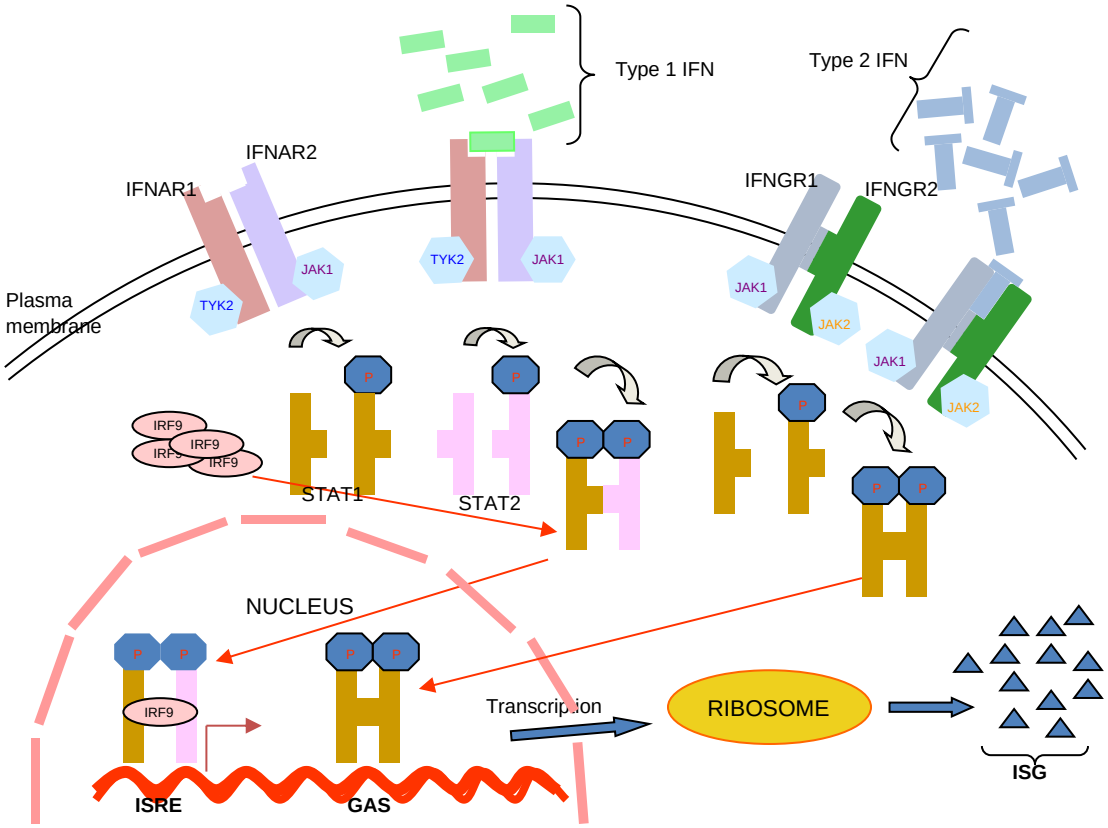

Figure 1.8 Types 1 and 2 IFN receptor signalling: α and β IFNs engage the receptors consisting of IFNAR 1 and IFNAR 2 sub-units which leads to the activation of the kinases TYK2 and JAK1. These phosphorylate the STAT proteins resulting in the formation of heterodimers. These products (consisting of STAT1 and STAT2) migrate to the nucleus where they recruit IRF9 to form the complex ISGF3 which binds to the ISRE region present in the promoters of ISGs leading to their synthesis. The binding of IFN-γ to its receptor results in the activation of JAK2 and JAK1 which in turn phosphorylate a tyrosine residue in two STAT1 molecules resulting in the formation of a STAT1-STAT1 homodimer. This translocates to the nucleus where it binds to the gamma-activation sequence (GAS) and stimulates the transcription of ISGs.

Products encoded by ISGs inhibit invading viruses in a variety of ways. Amongst those that have been identified are the following: protein kinase-R (PKR), 2'-5'-oligoadenylate synthetase, RNase-L and the Mx GTPases, MxA and MxB (Haller *et al* 2005). The overall effect of many of these proteins is to degrade RNA, inhibit protein synthesis and to promote apoptosis.

In addition to their key roles in the innate immune response, type I IFNs have immunomodulatory properties on the adaptive immune response. Most nucleated cells are capable of processing antigenic peptides derived from the degradation of pathogen proteins and forming compexes with major histocompatibility complex (MHC) class I molecules. These are presented at the cell surface in a form that is recognised by antigen-specific $CD8^+$ cytotoxic T lymphocytes which are able to destroy the infected cell. Type I IFN signalling upregulates the expression of MHC class I expression and the activities of $CD8^+$ T cells, thus increasing the likelihood of this occurring (Randall and Goodbourn 2008).

The innate immune response is initiated by the detection of products resulting from the viral infection process, such as single and double-stranded RNA (ssRNA and dsRNA). It is triggered by pattern recognition receptors (PRRs) present in both the cytoplasm and in membranous structures of the host cell that are stimulated by molecular motifs known as pathogen-associated molecular patterns (PAMPS). The toll-like receptors (TLRs) are PRRs present in the endosomal and plasma membranes, each of which is activated by a particular PAMP (Blasius and Beutler 2010). As discussed in section 1.2, CHIKV has a single-stranded RNA genome which is

replicated in two transcriptional stages; first a complementary (negative-sense) version is made and later this product is used as a template to generate progeny RNA. It is thought that a transient dsRNA form exists during this process. TLR7 and TLR8 are activated by ssRNA and signal via the myeloid differentiation primary response gene 88 (MYD88), whereas TLR3 is activated by dsRNA and utilizes the TIR domain-containing adaptor-inducing interferon-β (TRIF). Thus these PRRs are of particular importance in the innate immune response to CHIKV. Further PRRs present in the cytoplasm include retinoic acid inducible gene-1 (RIG-1) and melanoma differentiation-associated gene 5 (MDA-5), which detect RNA with 5'triphosphorylated ends and dsRNA (Meylan *et al* 2005, Hornung *et al* 2006). These receptors interact with the adaptor protein mitochondrial antiviral signalling protein (MAVS, also known as VISA, IPS-1 and CARDIF) triggering a signalling cascade that leads to the activation of interferon regulatory factors 3 and 7 (IRF3 and IRF7) resulting in their migration into the nucleus (Sun *et al* 2006). Here they bind to the IFN-stimulated response elements (ISREs) and trigger the production of early type 1 interferons.

Although CHIKV does not directly activate PRRs in peripheral blood monocytes or dendritic cells, MAVS-regulated induction of interferon-β occurs in infected fibroblasts (Schilte *et al* 2010). In addition it has been proposed that endosomal TLRs may be activated as a result of the phagocytosis of infected cells containing CHIKV-specific PAMPS and apoptotic bodies by haemopoietic cells.

The activation of inflammasomes may also lead to the induction of a type 1 interferon response following CHIKV infection. Inflammasomes are cytoplasmic multi-protein complexes that perform an essential role in apoptosis, inflammation and necrosis and include a member of the Nod-like receptor (NLR) family of PRRs and one of a family of cysteine-aspartic acid proteases, known as caspases. The caspase component catalyses the proteolytic processing of immature forms of the pro-inflammatory cytokines IL-18 and IL-1β rendering them bioactive. Amongst the functions of IL-1β is its interaction with MYD88 on the surface of non-infected cells, which sets in motion a cascade that leads to activation of NFκB and the induction of type 1 interferons.

The importance of type I IFNs as mediators of the early immune response may be reflected by the apparent evolutionary trend for alphaviruses to evolve with the means to suppress their action. Key factors that promote successful infection of CHIKV in humans and the associated pathological effects are its ability to inhibit type 1 IFN induction or the function of IFN-stimulated genes. Mechanisms that achieve this both by interfering with host protein synthesis (but allowing that of virus) and inhibiting specific type I IFN activity have been identified. In one study it was demonstrated that the avirulent V42 SFV strain showed no cytopathic effect compared to the virulent L10 strain when grown in type 1 IFN-treated Vero cells and that the yield was 100-fold greater in the former (Deuber and Pavlovic 2007). It was concluded that the ability of the L10 strain to overcome the IFN-induced antiviral state in host cells was a significant contributing factor in its increased virulence. The nsP2 from VEE and EEE viruses, have been shown to cause shutdown of cellular protein synthesis (Akhrymuk *et al* 2012), whilst a similar action is mediated by a region near the N-

terminal of the capsid protein of VEE and EEE viruses (Garmashora *et al* 2007). A separate contribution made by nsP2 in both CHIKV and SFV involves the inhibition of type I IFN-induced JAK-STAT signalling pathways (Fros *et al* 2010, Breakwell *et al* 2007).

1.7.6 Adaptive immune response to CHIKV

Although evidence of an adaptive immune response to CHIKV infection is not seen until 5-7 days after infection, it appears to have an important role in the chronic phase. Couderc *et al* (2009) demonstrated that adult mice deficient in IFN-α/β receptors and w/t neonates were protected from otherwise lethal doses of CHIKV when inoculated with polyclonal immunoglobulins prepared from human convalescent sera. Fric *et al* (2013) showed that the survival times for CHIKV-infected mice, deficient in receptors for IFN types 1 and 2 (AGR129) were significantly extended by passive immunisation using virus-specific human monoclonal antibodies. The importance of antibodies in controlling infection was indicated in a study that showed the persistence of viraemia for over a year in B-lymphocyte deficient mice challenged with CHIKV (Lum *et al* 2013). In contrast, both w/t and CD4 deficient mice produced sufficient antibody levels to control infection.

In another study, CHIKV-specific RNA could be detected in w/t mice for at least 16 weeks after infection, in joint tissues near the site of infection (the rear left footpad). However higher virus titres in a variety of tissues were consistently seen in *Rag*$^{-/-}$ mice (lacking mature B and T lymphocytes) than in w/t mice, together with

histological findings indicative of synovitis, arthritis and tendonitis (Hawman *et al* 2013). Furthermore prophylactic administration of CHIKV-specific monoclonal antibodies prevented the establishment of this persistent infection. These findings provide evidence that persistent CHIKV infection is a cause of chronic musculoskeletal tissue pathology and that it can be controlled by adaptive immune responses.

1.8 Prevention and Treatment

Treatment of CHIKV infection is currently aimed at alleviating the symptoms and generally consists of supportive care and pain management through the use of non-steroidal anti-inflammatory drugs and non-salicylate analgesics (Pialoux *et al* 2007). Preventative measures are focused on protecting those at risk from mosquito bites and on controlling local mosquito populations (Lloyd, 1994). These precautions include the wearing of garments that completely cover the limbs and the use of mosquito nets for those who require rest during the day such as babies, the elderly and the sick. A study aimed at controlling *Ae. albopictus* populations in Spain recommended a multiple intervention study to achieve this aim. These were: the education of householders in affected areas about measures to prevent mosquito-borne disease, the treatment of public sources of vegetation with larvicides and the removal of potential mosquito breeding sites such as uncontrolled rubbish dumps (Abramides *et al* 2011).

1.8.1 Antivirals

Although several potential antiviral agents have been tested for anti-CHIKV activity *in vitro*, none are currently licensed for the treatment of CHIKV infections in humans.

However several substances such as ribavirin and harringtonine that have been approved for the treatment of other medical conditions have been reported to inhibit CHIKV *in vitro* (Kaur and Jang Hann Chu 2013). As such compounds have undergone the necessary testing for use in patients, they show particular promise as therapeutic agents.

Ribavirin, a synthetic purine analog, shows antiviral activity against several RNA viruses including SFV and CHIKV in vitro and has been licensed by the USA Federal Drug Agency (FDA) for the treatment of hepatitis C virus infections (Briolant *et al* 2004, Smee *et al* 1988, Pedicone 2009). The results of a small scale trial in India where CHIK patients were treated with ribavirin provided further evidence that it may represent an effective treatment (Ravichandran and Manian 2008). In six out of ten subjects who had experienced arthritis and lower limb pain for over two weeks following the end of the febrile phase, a rapid reduction in soft tissue swelling was reported after ribavirin treatment accompanied by a significant reduction in pain.

Harringtonine and its derivative homoharringtonine, are alkaloids derived from the Japanese plum yew, *Cephalotaxus harringtonia*, that have been shown to exert inhibitory effects on CHIKV replication *in vitro* (Kaur *et al* 2013). Although *in vivo* studies have not been reported, this agent has been approved by the FDA for the treatment of chronic myeloid leukemia.

An investigation to determine the inflammatory gene expression profiles in a mouse model exhibiting CHIKV-induced arthritis found a high level of similarity with those derived from rheumatoid arthritis (RA) patients (Nakaya 2012). The authors of this study proposed that despite the apparent differences in pathogenesis in the two conditions, a variety of drugs currently used to treat RA may be effective in treating patients suffering from chronic CHIKV arthritis.

1.8.2 CHIKV candidate vaccines

Passive transfer of human immunoglobulin purified from convalescent patients has been shown to be effective in protecting a IFN-$\alpha\beta^{-/-}$ mouse model (Couderc *et al* 2008) from a lethal dose of CHIKV. It is thought that his approach may be applicable to humans known to have been exposed to CHIKV and in whom the disease is likely to be particularly severe, such as immunocompromised patients and neonates borne to viraemic mothers (Couderc *et al* 2009).

Both live-attenuated (Levitt *et al* 1986) and inactivated (Harrison *et al* 1967), virus vaccines have been developed in the past, although neither was made commercially available. The former (known as 181/25) resulted from 18 serial passages of a w/t strain in cell cultures and was shown to be highly immunogenic, however adverse side-effects (transient arthralgia) were seen in 8% of human volunteers in phase II trials (Edleman *et al* 2000). Inactivated vaccines prepared by treatment with formalin, (Harrison *et al* 1967) and Tween-80/ether (Eckels *et al* 1970) were only moderately immunogenic. However since the 2004 CHIKV emergence it has become clear that

CHIKV has the potential to be distributed over an even wider geographical area, particularly in view of the adaption of recently emerged strains to use *Ae. albopictus* as a vector. This has stimulated a resurgence of interest in CHIKV vaccines and resulted in several innovative approaches to what is perceived as both a public health threat and a potential bioterrorism agent.

Recently the application of reverse genetic techniques to produce a live attenuated vaccine candidate has been reported (Plante *et al* 2011). This consists of live virus produced by transfecting Vero cell cultures with RNA generated from an infectious clone derived from a patient in La Réunion Island in 2005. In the vaccine strain, the sub-genomic promoter was replaced with the internal ribosome entry site (IRES) from encephalomyocarditis virus conferring on it the advantage of being incapable of replication in mosquitoes. The authors of this study have shown the vaccine to be highly immunogenic in an adult C57BL/6 mouse model. It has been shown that antibodies isolated from immunized animals were effective in conferring passive immunity to further mice challenged with the same virus strain, however, adoptive transfer of $CD4^+$ or $CD8^+$ T cells did not confer protection.

Two research groups have demonstrated protective immune responses in laboratory animals vaccinated with engineered virus-like particles coated with CHIKV glycoproteins E1 and E2 (Akahata *et al* 2010, Metz *et al* 2013). Other candidate vaccines recently developed include: a recombinant adenovirus that expresses CHIKV structural proteins (Wang *et al* 2011) and a DNA vaccine (Mallilankaraman *et al* 2011).

1.9 Project Aims

Arthrogenic alphaviruses cause significant morbidity and are a public health concern in a wide range of geographic locations. Prominent amongst these is CHIKV, which has emerged in the form of a series of devastating outbreaks during the past decade. However, in contrast to the relatively localised distribution of alphaviruses such as RRV, ONNV, and MAYV, that of CHIKV has markedly expanded during recent years. Many aspects of the pathogenesis of CHIKV-induced disease, the resulting host immune response and the means by which the virus subverts these, remain to be elucidated. A clearer understanding of these is desirable in order to develop vaccines and therapeutic agents in order to minimise the impact of CHIKV.

The actions of IFN represent a powerful means by which animals are able to control many viral infections even in the absence of an adaptive immune response. However viruses have evolved several strategies that enable them to evade or suppress the host IFN response. Several alphaviruses have been shown to achieve this is by inhibiting host cellular transcription by mechanisms mediated by the capsid protein in New World viruses and nsP2 in Old World viruses (Garmashova *et al* 2007a, Garmashova *et al* 2007b, Akhrymuk *et al* 2012, Frolova *et al* 2002). Reduced type 1 IFN susceptibility was shown to be a key determinant in the virulence of the L10 SFV strain in mice (Deuber and Pavolic 2007). In contrast to this non-specific effect, the nsP2 in CHIKV has been shown to target key components involved in the IFN-induced JAK-STAT signaling process (Fros *et al* 2010).

The absence until recently of an animal model for CHIKV in which clinical symptoms comparable to those seen in human patients could be recreated, represented a barrier to investigations into disease induced by this virus. However, progress into the understanding of pathogenesis of other alphaviruses has been made through studies using members of the genus for whom such models are well established. A large proportion of these have utilised SINV and SFV, agents capable of causing disease in laboratory animals, but which are classified as ACDP Hazard Group 2 pathogens and therefore can be studied using relatively inexpensive laboratory facilities. Although such investigations have provided valuable insights into virulence determinants and their role in pathogenesis, the relevance of many to CHIKV induced disease and interactions with the host immune system, remain to be established.

Studies on the SINV strain S.A.AR86 have identified a crucial determinant of virulence in mice within the nsP1/nsP2 cleavage domain, namely a threonine (T) at position P3.This contrasts with non-virulent strains in which the amino acid at this position is isoleucine (I). Substitution of this single amino acid (by isoleucine) was sufficient to greatly reduce virulence in mice (Heise *et al* 2000). Subsequent investigations demonstrated that virulent strains containing T at this site resulted in slower non-structural protein processing and delayed 26S RNA synthesis (Heise *et al* 2003). The authors speculated that this modulating effect might be crucial in the induction of neurovirulence in adult mice and its absence, to attenuation.

Since the cleavage domains in non-structural polyproteins are highly conserved within each alphavirus species (Strauss and Strauss 1994), the possibility exists that similar

virulence determinants exist in the nsP1/nsP2 junction in other members of the genus. The work described in this thesis was conducted to test the hypothesis that disruption of the analogous polyprotein region in other alphaviruses may also reduce virulence. More specifically the study was directed at investigating whether the proposed determinant is present in CHIKV and if its function is related to type 1 IFN induction.

The specific aims were as follows:

- To characterise a CHIKV isolate from a human case of CHIK.
- To construct an infectious clone of the virus to serve as a tool for investigating CHIKV pathogenesis.
- To construct a mutant clone containing an amino acid substitution in the P3 region of the nsP1-coding region of the CHIKV genome (position 533) in order to disrupt the proposed virulence factor in this conserved region.
- To investigate the phenotypical differences of the two cloned viruses in terms of growth dynamics *in vitro*.
- To evaluate the relative ability of each clone to induce arthritic disease in a mouse model and to investigate whether any differences observed are related to induction of type 1 IFN in host cells.

CHAPTER 2

Construction of CHIKV clones for use in reverse genetics studies

Several members of the Alphavirus genus have been shown to be sensitive to type I IFN and to exhibit increased pathogenicity in mammalian hosts unable to mount an effective type I IFN response (Jordan 1973, Couderc *et al* 2010, Gardner *et al* 2012, Xu *et al* 2010, Deuber, and Pavlovic, 2007). Successful infection of immunocompetent hosts relies to a large extent upon virus properties that have evolved to mediate a general shutdown of host protein synthesis or to inhibit specific components of the IFN pathways, thus enabling them to evade the expression or effects of IFNs.

Many studies have employed reverse genetics techniques to investigate the genomic location of determinants of these activities (Garmashova *et al* 2007a, Garmashova *et al* 2007b, Akhrymuk *et al* 2012, Frolova *et al* 2002, Breakwell *et al* 2007, Simmons *et al* 2010). Reverse genetics techniques are designed to investigate the phenotypical traits that are determined by a defined genomic sequence and the outcomes that result from the experimental introduction of variations in it. This approach contrasts with that of classical genetics which involves the identification of a genetic basis for observed phenotypes. The application of reverse genetics has proved invaluable in the study of alphaviruses, enabling the design of experiments in which an exact copy of the genome can be manipulated to investigate key questions related to the virus life cycle and pathogenesis (Cruz *et al* 2010, Davis *et al* 1989, Liljeström *et al* 1991,

Kuhn *et al* 1992, Tsetsarkin *et al* 2006, Saxton-Shaw *et al* 2013). In addition, alphavirus cDNA clones have been engineered to produce potential vaccines by the introduction of attenuating mutations and as vehicles for the delivery of heterologous proteins (Rayner *et al* 2002, Schultz-Cherry *et al* 2000, Moriette *et al* 2006, Plante *et al* 2011, Quetglas *et al* 2010).

In order to study an RNA virus by reverse genetics, its complete genome must be transcribed into a complementary DNA (cDNA) version from which an infectious transcript can be synthesized *in vitro*. In its simplest form, this can be achieved by using a DNA primer that hybridizes specifically to the 3' end of the genome and which is extended to produce a RNA-DNA heterodimer by the action of reverse transcriptase. Following the elimination of the RNA template, a second primer corresponding to nucleotides at the 5' end of the genomic RNA is used to initiate the production of double-stranded DNA and its amplification, using the polymerase chain reaction (PCR). However there is often a limit to the length of cDNA that can be synthesized from an RNA template because of the presence of secondary structures that interfere with the progress of reverse transcriptase as it moves between the 3' and 5' ends. Thus it is often necessary to construct a full-length cDNA by combining a series of fragments derived from different regions of the genome. Many commercially available plasmid vectors provide the means for achieving this. These often contain a multiple cloning site which has been engineered downstream from an RNA polymerase promoter, so facilitating features that facilitate the insertion and *in vitro* transcription of DNA sequences under investigation. In addition, such vectors contain an origin of replication and an antibiotic resistance gene that acts as selectable marker to inhibit growth of bacteria lacking the plasmid in the presence of the antibiotic.

As the genome in positive-sense viruses such as alphaviruses is directly utilized as messenger RNA (mRNA) in permissive host cells, its delivery into the host cytoplasm facilitates the production and replication of infectious virus. A range of techniques have been developed to induce the uptake of nucleic acids in a process known as transfection. Amongst these are methods using chemical reagents such as DEAE-dextran or calcium phosphate and physical methods such as electroporation or the formation of complexes with cationic lipids (Kim and Eberwine 2010). A reverse genetics system allows not only the rescue of a cloned version of the original wild-type (w/t) virus, but that of further sub-clones with altered genomes derived through the introduction of defined mutations. Thus questions regarding functions of virus-specific proteins can be addressed by comparing w/t with mutated virus clones.

Several important determinants of virulence within the Alphavirus genome have been mapped using reverse genetics. In some cases their disruption through the introduction of mutations results in attenuated viruses (White *et al* 2001, Suthar *et al* 2005, Fros *et al* 2010 Simmons *et al* 2010). Examples of domains in viral proteins that are instrumental in inhibiting the host immune response have been identified in both the structural and non-structural proteins (nsP) of various alphaviruses and are discussed in chapter 1 (sections, 1.2.5, 1.2.7 and 1.3.2).

Suthar *et al* (2005) identified four major determinants of adult mouse neuroviulence that were present in the S.A.AR86 SINV strain by challenging adult mice with virus from a series of chimeric cDNA clones derived from AR86 and the avirulent

Girdwood S.A. strain. These determinants were threonine at position 538 in nsP1, cysteine at position 386 in nsP3, serine at position 243 in E2 and 18 amino acid fragment deletion in nsP3 and and an a8 amino acid deletionin nsP3.

The nsP1 determinant is located in the conserved domain at which nsP1is cleaved from the nsP2 component of the polyprotein precursor, at position P3 (table 2.1). Further investigations in which infectious virus from cDNA clones of wild type strain S.A.AR86 and a second clone containing isoleucine at this site (the amino acid present in avirulent strains), were used to challenge adult mice and showed that threonine is absolutely critical for neurovirulence (Heise *et al* 2000). More recently, Cruz *et al* (2010) reported that although SINV containing the T538I mutation virus showed similar growth characteristics in cell cultures and was able to infect similar regions of the brains of laboratory mice to the wild type (w/t) virus, clinical signs were greatly reduced. In addition it was found that higher levels of type 1 IFN were induced in animals receiving the I538 genotype than w/t virus, indicating that the presence of threonine at this position is important in the process by which SINV is able to reduce the effects of the host innate immune response. The T538 genotype was subsequently reported to inhibit the tyrosine phosphorylation of STAT1 and STAT2 thus down-regulating the response to IFN types I and II (Simmons *et al* 2010).

Virus	GENBANK Accession number	Antigenic complex	nsP1/2 cleavage domain							
			P4 532	P3 533	P2 534	P1 535	P1[1] 536	P2[1] 537	P3[1] 538	P4[1] 539
CHIK	**NC004162**	**SF**	**R**	**A**	**G**	**A**	**G**	**I**	**I**	**E**
ONN	NC001512	SF	R	A	G	A	G	I	V	E
RR	GQ433359	SF	R	A	G	A	G	V	V	E
MID	EF536323	SF	R	A	G	A	G	V	V	N
MAY	KJ013266	SF	R	A	G	A	G	V	V	T
SF	AY112987	SF	H	A	G	A	G	V	V	E
UNA	HM147992	SF	R	A	G	A	G	V	V	E
BF	NC001786	BF	R	A	G	E	G	V	V	E
NDU	JX644171	NDU	R	A	G	A	G	V	E	E
WHA	NC016961	WEE	D	I	G	A	A	L	V	E
AUR	NC003900	WEE	D	A	G	A	A	L	V	E
WEE	KJ554991	WEE	E	A	G	A	G	S	V	E
SIN	NC001547	WEE	D	I*	G	A	A	L	V	E
TROC	HM147991	TROC	D	I	G	A	A	L	V	D
VEE	L01442	VEE	E	A	G	A	G	S	V	E
EEE	AY722102	EEE	E	A	G	A	G	S	V	E

*In the neuro-adapted strain S.A.AR86 (GENBANK accession number U38305), isoleucine is replaced by threonine.

Table 2.1 Alphavirus nsP1/nsP2 polypeptide cleavage domains. The four mature non-structural proteins (nsPs) encoded by Alphavirus genomes are derived from a single polyprotein by cleavage at sites within conserved domains. The domains present between nsP1 and nsP2 in the polyproteins of CHIKV (highlighted in red) is aligned with those of a further 15 alphaviruses as shown, cleavage is mediated by a virus-encoded protease between the amino acids at P1 and P1[1]. Amino acid positions are numbered from the polyprotein N-teminal based on the genome of the CHIKV S27 African prototype strain (Khan *et al* 2002).

This phenomenon does not appear to be restricted to SINV as it has also been demonstrated that the amino acid at the P3 position in the nsP1/nsP2 cleavage domain of RRV plays a similar role (Cruz *et al* 2010). In this case the w/t virus contains alanine at the P3 site (nsP1 532), which when replaced by isoleucine resulted in a

virus that grew poorly in cell cultures, however virus obtained from a clone containing an alanine to valine substitution (A232V) had similar growth characteristics to the w/t clone but induced a relatively strong IFN response.

The presence of virulence factors in similar positions in two alphaviruses from different antigenic complexes and phylogenetic branches indicates that it may be active in other members of the genus. In the present study it was decided to develop a cDNA clone as a tool to investigate whether a substitution at this site would bring about a similar effect in CHIKV. A comparison of the nsP1/nsP2 cleavage domains of alphaviruses belonging to particular antigenic complexes shows a high degree of similarity (table 2.1). Most notably, the first four amino acids at the N-terminal end of the cleavage site of those belonging to the SFV antigenic complex, are identical (RAGA). In view of this degree of conservation, it seems likely that the phenotype reported for RRV (Cruz *et al* 2010) resulting from an alanine to valine substitution may be replicated in other members of the complex. For this reason it was decided to test the effect of introducing a mutation (A533V) at this site in a recently circulating CHIKV strain and to establish whether this would lead to the induction of increased amounts of type1 IFN and the development of an attenuated strain.

MATERIALS AND METHODS

2.1 Safety considerations

CHIKV has been classified by the Advisory Committee on Dangerous Pathogens (ACDP) as a class 3 pathogen (www.hse.gov.uk), therefore all procedures in which viable virus was handled (those prior to the addition of AVL buffer) were carried out in a class 2 cabinet in a CL3 laboratory. All subsequent steps took place in CL2 laboratories.

2.2 Cell culture

The cell lines used in this study, BHK-21 (baby hamster kidney fibroblasts), Vero (adult African Green monkey epithelial cells) and L929 mouse fibroblasts, were obtained from the European Collection of Cell cultures (ECCAC), Porton Down, Salisbury, UK (ECACC catalogue numbers 85011433, 84113001 and 85011425 respectively).

BHK-21 cells were grown and maintained in Glasgow Minimum Essential Medium (GMEM) and Vero and L929 cells were grown and maintained in Dulbecco's Minimal Essential Media (DMEM) (Sigma-Aldrich products G6148 and D6046 respectively). All media were supplemented with fetal bovine serum (FBS) at concentrations of 2% for propagation of virus stocks and 10% for cell line maintenance. In addition, Anti-Anti antibiotic-antimycotic solution (Gibco®) was used resulting in final concentrations of 100 units/mL of penicillin, 100 µg/mL of streptomycin, and 0.25 µg/mL of amphotericin B. Washing steps were carried out using Dulbecco's phosphate-buffered saline (DPBS). The incubation conditions in all

cases were 37°C in an atmosphere of 5% CO_2 at 6% humidity. Cell concentration was determined by staining trypsinized cells in an equal volume of 0.4% trypan blue dye and counting in a haemocytometer.

2.3 Cell passage

When cultured cells had reached 80-100% confluence the supernatant was removed, rinsed twice and replaced with a minimal volume of trypsin-EDTA (0.25 % w/v trypsin, 1mM EDTA in PBS). Following incubation at 37°C for 2min the detached cells were resuspended in an appropriate volume of culture medium and transferred to a fresh flask.

2.4 Virus isolate history

The virus isolate used in this study (SL-R233) was isolated from one of a panel of blood serum specimens taken from febrile patients between 2006 and 2007 and was supplied in a cell supernatant by Dr Mark Bailey (HPA, Porton, Salisbury, Wiltshire SP4 0JG). The collaborative study was carried out in Sri Lanka and at HPA Porton. Its aims were to identify the causes of febrile illnesses over the course of a year, in patients at the Columbo North Teaching Hospital in Western Sri Lanka. The patient from whom the specimen was obtained was a 58 year old male living in the Thimbirigasayaya region of Colombo and it was isolated by the Special Pathogen Reference Unit (SPRU) at CEPR. The sample was shown to be positive for CHIKV by qRT-PCR with a high titre. It also was tested and found to be negative for dengue virus, leptospirosis and Coxiella burnettii; furthermore no growth was seen on blood agar cultures, thus a co-infection appeared to be unlikely.

2.5 Virus propagation *in vitro*

Virus was grown from infected supernatant as follows. Cell monolayers (approximately 75-90% confluent) were washed once and drained. Virus diluted in serum-free medium to the minimum volume judged to cover the monolayer was added (for T25 and T75 flasks this was 1ml and 5ml respectively).

The flasks were incubated for 1hr to allow adsorption of virus after which the excess liquid was removed and replaced with growth medium (10ml for T25 flasks and 20ml for T75 flasks). Flasks were returned to the incubator and inspected periodically for the appearance of cytopathic effects (CPE) in order to gauge the most appropriate time to harvest virus.

2.6 Virus harvesting

CHIKV was harvested as follows. The infected cell-supernantant suspensions from T25 flasks (approximately 10ml) and T75 flasks (approximately 20ml) were transferred to 15ml or 50ml polypropylene centrifuge tubes (Falcon) respectively. These were centrifuged at 3,000rpm for 10min at 4°C, and 1ml aliquots of supernatant were distributed into 2ml cryogenic vials (Nunc™Thermo Scientific™) prior to being stored at -80°C.

2.7 Transfection by electroporation

BHK-21 monolayers from three T75 flasks grown to 80-90% confluence were washed twice, then treated with trypsin-EDTA. The wash steps were carried out using DPBS

without calcium and magnesium. After loss of adherence, the cells from each flask were pooled in 10ml DMEM medium containing 2% FBS and aspirated to break up cell clumps. The suspension was centrifuged at 1500 rpm for 15min and after decanting the supernatant, the pellet was resuspended in 20ml chilled wash buffer. The centrifugation step was repeated and the pellet resuspended in 1ml chilled wash buffer. The cell suspension was distributed in 200µl aliquots in 2mm electrocuvettes and placed on ice. Electroporation was carried out with two alternative volumes of transcribed RNA, 10 and 20µl. In each case cells were subjected to a single pulse of 140kV using a BioRad Genepulser Xcell™ at 25F capacitance. Cells were allowed to recover for 10min at room temperature, then mixed with 20ml pre-warmed medium supplemented with 10% FBS in T75 culture flasks. The flasks were immediately transferred to an incubator in a CL3 laboratory and incubated under standard conditions (section 2.3). The cells were inspected twice daily for signs of cytopathic effects (CPE) and when these were observed, the virus was harvested.

2.8 Nucleic acid purification

Water used in all protocols involving the manipulation of nucleic acids was certified to be nuclease-free (Promega UK). This was used for elution of nucleic acids in all cases except for medium scale plasmid DNA purification, so as to minimize the presence of substances capable of inhibiting enzyme activity in downstream manipulations. Medium-scale plasmid preparations were carried out in order to provide stock reagents for long term storage and here 10mM Tris, 1mM EDTA pH8.0 (TE buffer), was used for elution in order to minimize the activity of any contaminating nucleases.

At various stages of this study it was necessary to purify nucleic acids (viral RNA, amplified dsDNA from PCR, cDNA and plasmid DNA) from serum, mammalian tissue samples and enzyme catalyzed reaction mixtures. This was carried out using techniques based on the principle that nucleic acids bind to silica particles in a buffer of high ionic strength and at a defined pH range. Samples containing mixtures of biomolecules are applied to silica-containing microcolumns by centrifugation under conditions that favour the capture of nucleic acids. Subsequent washes with buffers containing a chaotrophic agent such as guanidinium thiocyanate, followed by one with a high salt concentration and ethanol remove undesired components such as proteins and phospholipids. Finally the pure nucleic acid is eluted with a low-salt buffer or with water. A range of commercially produced kits for the purification of RNA or DNA from various samples are available. A list of those used in this study is shown in table 2.2 and relevant protocols are provided in Appendix A.

Product	Manufacturer	Catalogue number	Purpose
QIAquick® PCR purification kit	Qiagen	28106	Amplicon DNA purification
QIAquick® Gel Extraction kit	Qiagen	28706	Purification of linear DNA fragments from agarose gels
QeneElute® Plasmid miniprep kit	Sigma-Aldrich	PLN350	Small-scale plasmid DNA purification
Megaclear™ kit	Ambion (Life Technologies)	AM1908	RNA from *in vitro* procedures
QIAfilter Plasmid Midi kit	Qiagen	12245	Preparation of stock plasmids
QIAamp® Viral RNA Mini Kit	Qiagen	52906	Purification of viral RNA from serum or cell culture supernatant
Minielute gel extraction kit	Qiagen	28606	Purification of linear DNA from agarose gels for elution at maximum concentration
RNeasy Mini Kit	Qiagen	74106	Extraction of RNA from mouse tissues

Table 2.2 Silica-based products used for nucleic acid purification

2.9 Design of PCR and sequencing primers

The complete nucleic acid sequences of a number of CHIKV genomes associated with several outbreaks are available on the National Center for Biotechnology Information (NCBI) website (http://www.ncbi.nlm.nih.gov/). This facility was used to obtain a selection of genome sequences of isolates from the Indian Ocean outbreak (post-2005). Alignments were conducted using the MegAlign component of the DNASTAR software package, to identify conserved regions. Primers previously used to determine the genome sequence of a CHIKV isolate (D570) isolated from a traveller returning to the UK from Mauritius in 2006 (GenBank accession number EF012359) were available in this laboratory. In the initial steps, primers from this source that were predicted to anneal to conserved genomic regions were used in amplification by RT-PCR and sequencing of the SL-R233 genome (table 2.3). Once sequencing data had

been generated by this means, further CHIK SL-R233-specific primers were designed and purchased (Sigma, UK).

Where possible primers were designed to be 19-25 nucleotides in length, with a guanine/cytidine content of 40-50% and with a Tm value of 60-65°C and otherwise in accordance with the generally accepted rules summarized by Dieffenbach *et al* (1993). Each was checked for predicted secondary structure and primer dimer formation using the online Sigma primer design tool (sigmaaldrich.com). Additional primers were designed for use in Rapid Amplification of cDNA Ends (RACE) and for site-directed mutagenesis; these will be discussed further below. A full list of RT-PCR primers can be seen in table 2.3.

Amplicon	Primer name	Primer sequence 5' to 3'	Primer position from 5' end	Length (bp)
158.1	*CH11F* *CH1329R*	GACACACACGTAGCATACCAGT CAGCAGGTCAGTGTTCTTTCT	11-32 1309-1329	1318
158.2	*CH7870F* *CH9155R*	CAGAGAGAGGGATGTGCATG CCACCGCAATTACACTTGTAC	7870-7887 9135-9155	1285
159.1	*CH741F* *CH2912R*	GAGGCAAGTTGTCTATTATGAGAG TGACGTGCTCTGACGTTGATG	741-764 2892-2912	2171
159.2	*CH2246F* *CH5332R*	GGATCTGGCAAGTCAGCTAT CCTTCTCTCTCGTCACATGTC	2246-2265 5311-5331	3085
159.3	*CH5580F* *CH7654R*	CAGGAGAAGTGGATGACTTG GCCTGATGATTTGGATAGTAG	5580-5599 7634-7654	2074
165.1	CH4658F CH6977R	GGCGCACTGTACTCATATCTAGA GAACAGAGTTAGGAACATACC	4659-4680 6956-6976	2317
165.2	CH6035F CH8229R	GCATGCAATGAGTTCTTAGCTA CTTGTTGTCGAAGATCGGTCT	6035-6056 8209-8229	2194
165.3	CH7920F CH9218R	GCACGAAGGTAAGGTAACAGG TGACATTGATCAACCTTGCAG	7920-7940 9198-9218	1298
165.4	*CH8984F* CH11770R	GTAAAGAGCTACCTTGCAGCA GTTCGGAGAATCGTGGAAGAG	8984-9004 11750-11770	2786*
167.1	CH8984F CH10239R	GTAAAGAGCTACCTTGCAGCA GGTGAAGACCTTACAGCTGTAG	8984-9004 10218-10239	1255
167.2	*CH999F* CH1789R	ACGCAGACGGATTCCTGATGTG CTGGCTACGTAGTACGGTCTG	999-1020 1769-1789	770*
167.3	CH741F CH2523R	GAGGCAAGTTGTCTATTATGAGAG GGGTCACCACAAAGTACAACT	741-764 2503-2523	1782
167.4	CH2534F CH4224R	GGCTTCTTCAATATGATGCAGA GTTGCACTGTTCTTAAAGGACTC	2534-2555 4202-4224	1690
167.5	CH3909F CH4992R	CGCAAGTTTAGATCATCTAGAG GAGCATTTGACTTTTTGCACTC	3909-3930 4971-4992	1083
167.6	CH4915F CH5771R	CGTCACAAGCATAATTGTGTG AACACTTCTCCTCGTGGACTTC	4915-4935 5750-5771	856
169.1	CH10033F CH11501R	CGTATAAGACTCTAGTCAATAGAC CACCTACATACAATGTGTCTC	10033-10057 11481-11501	1468
169.2	CH10033F CH11770R	CGTATAAGACTCTAGTCAATAGAC GTTCGGAGAATCGTGGAAGAG	10033-10057 11750-11770	1737
169.3	CH10033F CH11700R	CGTATAAGACTCTAGTCAATAGAC AGCTTAAGTACCTACATCTC	10033-10057 11700-11681	1648
171.1	CH1411F CH2241R	CGAGTTTGACAGCTTTGTGGT ACTCCGAAGACTCCTATGACTG	1411-1431 2220-2241	830
171.2	CH8809F CH10210R	CCGTGTACGATTACTGGAACA GGTTTTTGTCCTTGCACTCTG	8809-8829 10190-10210	1401
199.1	CH11266F Poly-dT primer	GCACTGATTCTAATCGTGGTG GGATCCTTTTTTTTTTTTTTT	11267-11286 Poly-A tail	n/a
229.1	CH548R poly-dG primer	CGTGTACAGCATAGACGTCTTG AAGCTTACGGGIIGGGIIGGGIIG	527-548 Non-genomic	n/a
229.2	CH498R poly-dG primer	CATGAGACGTCTGTGTGTAAGC AAGCTTACGGGIIGGGIIGGGIIG	477-498 Non-genomic	n/a

Table 2.3 Primers used to amplify the entire genome of CHIKV strain SL-R233 in a series of sub-genomic RT-PCRs. The use of italics in the table indicates primers designed to anneal to conserved regions of recently circulating CHIKV strains, whereas the remainder were based on data obtained from the isolate under study. The resulting cDNA was subsequently used as a template in sequencing reactions. In the column showing amplicon length, the figure given indicates the anticipated product size in base-pairs based on the forward and reverse primer positions in the CHIKV prototype strain S27. An asterix indicates that no band or one below the expected size was seen in samples analysed by agarose gel electrophoresis.

2.10 Standard RT-PCR conditions

The RT-PCR conditions described below represent the general protocol used. Adjustments in the cycling conditions were introduced where necessary to accommodate variations in the Tm values of primers and the anticipated length of the amplicon.

Template RNA was amplified with Superscript III One-step RT-PCR Platinum® Taq HiFi kit (Life Technologies™, UK). All reactions were in a total volume of 50µl and consisted of 25µl 2 x reaction buffer, 20µl water, 0.2µM forward and reverse primers, 1µl enzyme mixture and 2µl template RNA.

The thermocycling conditions were as follows: 50° C for 30min, 94°C for 2min, 40 cycles of (94°C for 15sec, 58-62°C for 30sec, 68° C for 1min per kb (based on the expected length of the amplicon). Finally a single step of 68°C for 5min was included. All genomic fragments were amplified using one-step RT-PCR on a GeneAmp 2700 thermal cycler (Life Technologies™, UK).

2.11 Amplification of the 5' and 3' ends

In order to determine the genome sequence of the UTR at the 5' end of the genome a short amplicon was produced using the RACE technique (Rapid Amplification of cDNA Ends), the main steps of which were as follows. A cDNA copy of the 5' genomic RNA was generated by reverse transcription using Superscript III reverse transcriptase (Life Technologies, UK). 2µl template RNA was combined with a reaction mixture consisting of 2µM primer CH548R, 200u (1µl) reverse transcriptase, 5mM DTT, 50mM Tris-HCl pH8.3, 75mM KCl and 3mMNaCl, in a total volume of

20µl. The template and primer components were pre-heated to 70°C for 5min, and placed on ice for 2min prior to mixing with the remaining components by gently tapping the tube. The reaction was incubated at 50°C for 20min and the enzyme inactivated by heating to 70°C for 15min. Template RNA was removed by the addition of 2u of *E. coli* RNase-H followed by incubation at 37°C for 20min.

The cDNA was purified using a PCR purification kit and eluted in 50µl of water (see table 2.2 for details and Appendix 1 for protocol). A 5' poly-dCTP tail was generated to this product using the Terminal Deoxynucleotidyl Transferase (TdT) kit (Life Technologies, UK) in a 40µl volume reaction containing 27µl cDNA, 8µl of 5 X TdT buffer, (15u) enzyme and 0.2mM dCTP. The reaction was incubated at 37°C for 30min. The reaction was treated with the PCR purification kit and the product eluted with 50µl of water.

Amplification of the 5'end was carried out in a 50µl volume reaction using 20mM Tris-HCl (pH 8.4), 50mM KCl, 1.5mM $MgCl_2$, 1mM each dATP, dCTP, dGTP and dTTP, 0.4µl each of poly-dG and reverse primers and 0.25u Taq polymerase (Life Technologies, UK). The primer sequences used for RACE reactions are shown in table 2.3. Reactions were carried out with the poly-dG primer in combination with each of the reverse primers: CH548R and CH498R (table 2.3). The thermocycling conditions were: 40 cycles of 94°C for 15sec, 55°C for 30sec and 72°C for 35 sec, followed by a single step of 72°C for 5min. The 3'-terminal end of the genome was

amplified using a reverse transcriptase primer designed to anneal to the poly-A tail (Poly-dT primer) and an internal forward primer, CH11266F (table 2.3).

2.12 Analysis of DNA samples by agarose gel electrophoresis

DNA was separated by agarose gel electrophoresis using the mini-SUB®CELL GT apparatus (BioRad, UK). Gels were prepared by mixing 0.8-1.5% w/v agarose powder (Sigma, UK) in Tris-borate buffer (TBE, 89mM Tris, 89mM boric acid, 20mM EDTA, pH 8.0), containing 0.5µg/ml ethidium bromide. This was dissolved by boiling, cooling to approximately 60°C and mixing. Gels were poured at approximately 45-55°C and left to set at room temperature for 20min. Gels were placed in the electrophoresis tank containing TBE buffer and after loading the samples, subjected to a constant voltage of 100V for 20-40min. Samples were mixed with 1µl of 10X Bluejuice gel loading buffer (Life Technologies™, UK) prior to loading. DNA bands were visualized with ultraviolet light (302nm) and sizes were assessed by comparison with those of a 1kb plus molecular weight ladder (Life Technologies™, UK).

2.13 Gel extraction of DNA

When the banding pattern of DNA samples seen on analytical gels appeared satisfactory in terms of size and yield, the remainder of the reaction mixtures was gel extracted. This process entailed agarose gel electrophoresis, followed by visualization using high wavelength UV light (365nm) so as to minimize damage to the sample. Bands corresponding to the desired products were visualized from behind a Perspex® screen, excised using a scalpel and purified using one of the extraction kits detailed in table 2.2 (for protocols see appendix 1).

2.14 Template-fusion PCR (TF-PCR)

Template-fusion PCR was used to in order to generate large amplicons (greater than 3.1kb) from DNA fragments previously cloned into a plasmid vector. The 5’ and 3’template fragments were designed to have overlaps of a minimum of 100 base nucleotides. The plasmids were linearized by digestion using a restriction enzyme present only in the vector, samples were then denatured to separate the complementary DNA strands, by heating to 95°C. Next a combined annealing and extension step was carried out in which the samples were cooled to 68°C. At this temperature hydrogen bonding between complementary strands leads to the formation of two products, (1) dsDNA similar to that in the original sample and (2) positive-sense strands from one product paired with negative-sense strands from the other, annealed at the overlap region. The strands are extended in a 5’ to 3’ direction by the action of a suitable thermostable DNA polymerase in a process in which the double-stranded region acts in the same way as a PCR primer (figure 2.1).

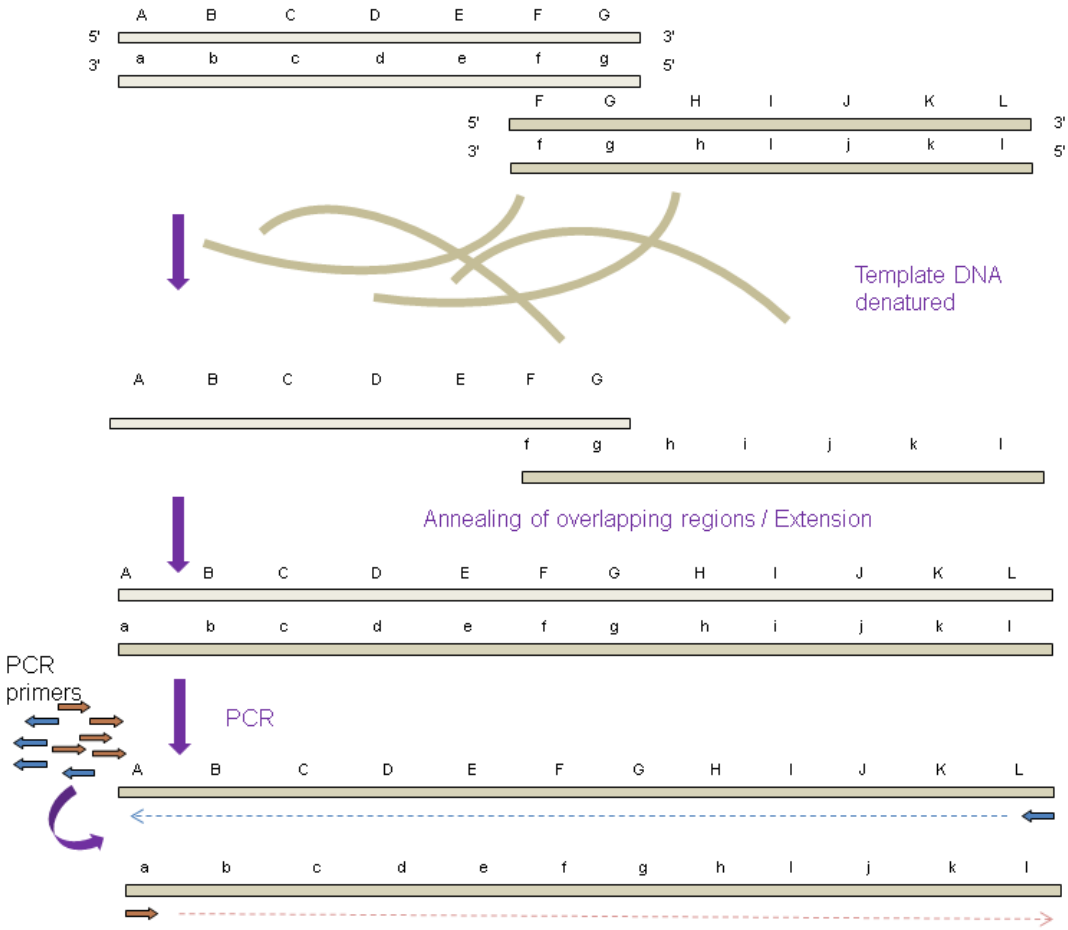

Figure 2.1 The use of template-fusion PCR to combine overlapping DNA fragments in order to synthesise a single product comprising a dsDNA version of the original template. The fragments A to G and F to L represent overlapping regions of the genome of interest present in two recombinant plasmids (upper and lower case letters indicate complementary DNA strands). The template DNA is first denatured by heating to 94°C, then cooled to 68°C to enable hydrogen bonds to form between the complementary strands of the two DNA species and for their Taq DNA polymerase-catalysed 3' to 5' extension. After 10 cycles of these two temperatures, primers complementary to the ends of each of the two products are added and thermocycling is continued to amplify the full-sized product.

Reaction mixtures were prepared as follows. Two plasmids, containing DNA inserts of adjacent CHIKV fragments, were linearized by digestion with a suitable restriction enzyme (ApaI) and template was prepared by adding 0.5µl of each to 14µl water. This mixture was heated to 94°C for 2min, then cooled on ice for 2min. Amplification was carried out using the Elongase® enzyme kit (Life Technologies, UK) and included two thermal-cycling stages. For the first amplification step the template was amplified in a 50µl reaction mixture consisting of 60mM Tris-SO_4 (pH 9.1), 18mM $(NH_4)_2SO_4$, 2mM $MgSO_4$, 0.2mM each of dATP, dCTP, dGTP and dTTP, 19µl water and 1µl Elongase polymerase. The first thermocycling step comprised 10 cycles of: 94°C for 15sec and 68°C for 3min.

The second amplification step followed the addition of forward and reverse primers to a final concentration of 0.4µM and consisted of 35 cycles of a two-step thermo-cycling process. Samples were denatured at 94°C for 15sec followed by a combined annealing-extension step at 68°C for a period determined by the anticipated amplicon size (1min per kb of amplicon). Finally, a single step at 68°C/ 8min was included.

2.15 DNA Sequencing

Purified DNA (PCR fragments or plasmid) was sequenced by dideoxy chain termination using an Applied Biosystems BigDye™ Terminator v3.1 cycle sequencing kit (catalogue No. 4336917). In brief, 1-11µl DNA was mixed with 2µl BigDye™ Terminator, 4µl 5x buffer and 1µl 10mM primer. The volume was made up to 20µl with nuclease-free water. The reaction mixture was subjected to 25 cycles of 96°C for 10sec, 50°C for 5sec, 60°C for 4min. Unincorporated dye terminator was

removed by gel filtration using a Qiagen® DyeEx™ 2.0 spin kit (Qiagen®, UK) and 2µl of eluted DNA was diluted in 13µl Hi Di Formamide (Life Technologies, UK). Sequencing data was obtained by running samples on an ABI PRISM™ 3130 Genetic analyzer. Overlapping sequence reads (contigs) were assembled into continuous consensus data using the SeqMan component of the DNASTAR sequence analysis software (Lasergene®, UK). The entire CHIKV genome was sequenced in both directions using primers that covered the entire genome (tables 2.3, 2.4 and 2.5). The genome was analyzed using MegAlign and SeqEdit software (DNASTAR, Lasergene®, UK).

Sequencing Primer	Primer Sequence 5' to 3'	Primer position (from 5'end)
CH1F	*ATGGCTGCGTGAGACACAC*	*1-19*
CH269F	GGCAGTGCGCCAGCAAGGAGG	269-289
CH525F	ACCAAGACGTCTATGCTGTACAC	525-547
CH742F	AGGCAAGTTGTCTATTATGAGAGG	742-765
CH1008F	GATTCCTGATGTGCAAGACTAC	10081020
CH1387F	CCAGTCAATTCAGAAGGTTCAG	1387-1408
CH1561F	AGAAGCAGAGGAAGAACGAGAAG	1561-1583
CH1620F	CAGCACAGGAAGATGTTCAGG	1620-1640
CH2079F	TCTACGACGTGGATCAGAGAAG	2079-2100
CH2487F	TGAGACCAAGGCAGAAAGTTG	2487-2507
CH2886F	TCTATGCATCAACGTCAGAGC	2886-2909
CH2971F	*GTGGATAAAGACGCTGCAGAAC*	*2971-2992*
CH3416F	TGGAACATCAACAAGCAGATCTG	3416-3438
CH3559F	GCTGGTTAACAAGATAAACGG	3559-3579
CH3726F	TGGTCATAAACATCCACACACC	3726-3747
CH4037F	AATGCAGCCTTTGTAGGACAG	40347-4057
CH4211F	AAGAACAGTGCAACACCAGTG	4211-4231
CH4338F	CCTATCGAGAAGTCGCAAAG	4338-4349
CH4402F	CTCTCCACAGGTGTATACTCAGG	4400-4422
CH4556F	CAAGTAGAGCTGCTGGATGAG	4556-4577
CH4730F	ATGTGGCCAAAGCAAACAGAG	4730-4750
CH5306F	*ACTGTGACATGTGACGAGAGAG*	*5306-5327*
CH5295F	GGAGAAACCTGACTGTGACAT	5295-5215
CH5412F	ACACAGCAATGTCTCTTCAGG	5412-5432
CH5997F	TCAACGTTCGATTGTCCAATC	5997-6017
CH5751F	AAGTCCACGAGGAGAAGTGTTAC	5751-5773
CH6099F	ATGATGCATATCTAGACATGGTGG	6099-6122
CH6319F	GGACTCAGCAGTATTCAACGTG	6319-6340
CH6642F	TTCACAGAGAGCTGGTTAGGAG	6642-6663
CH7109F	AGATGTGCCACTTGGATGAACATGGAAG	7109-7136
CH7278F	CAGGTGACGAACAAGATGAAG	7278-7298
CH7533F	CCGACAGCAAGTATCTAAACAC	7533-7554
CH7633F	CTACTATCCAAATCATCAGGC	7633-7654
CH7924F	*GAAGGTAAGGTAACAGGTTACG*	*7924-7945*
CH8486F	GGTACTATCAGCTGCTACAAGC	8486-8507
CH8804F	CAGCACCGTGTACGATTACTG	8804-8824
CH8812F	CCGTGTACGATTACTGGAACA	8812-8829
CH9201F	CAAGGTTGATCAATGTCATGC	9201-9221
CH9385F	CAAGTCATCATGCTACTGTATCC	9385-9409
CH9441F	*GGAGAAGAACCAAACTATCAAGAAG*	*9441-9466*
CH9723F	CAGATGCATCACACCGTATG	9723-9742
CH9842F	GAACGAGCAGCAACCTTTGT	9842-9861
CH9995F	ACGAACACGTAACAGTGATCC	9995-10015
CH10340F	CAGAATTTGCATCAGCATACAGG	10340-10362
CH10609F	CGCACACCTGAGAGTAAAGAC	10609-10629
CH11042F	CTCAGCTGCAAATCTCTTTCTC	11042-11063
CH11344F	GCGACTGATACCTGCTTCTGTT	11344-11355
CH11481F	GAGACACATTGTATGTAGGTGATAAG	11481-11506

Table 2.4 Forward primers used for sequencing CHIKV isolate SL-R233. In addition the primers shown in italics were used as RT-PCR primers for the production of the cDNA clone as discussed in section 2.21.

Reverse Primers	Sequence 5' to 3'	Primer position (from 5'end)
CH425R	CGATCTTTCCAGAGATGTTTCTG	403-425
CH699R	TTAGCCTTCAGTACCTGCTCATC	677-699
CH923R	CACACGAAACCACTGTATCAC	903-923
CH1097R	GGTCATTTGATCACAAATGGTC	1084-1105
CH1836R	GTGCACGTCTTCACTTGCTC	1817-1836
CH1814R	CCAAAGCGTGAATCAGACTG	1696-1814
CH2289R	TGCCTGGTAACTAGGTTCTTG	2269-2289
CH2413R	TCTGTTGCATCCATTCAAGAG	2393-2413
CH2657R	ATGCAACGATGACACAATGG	2637-2657
CH3055R	CATTATTGATGCATGCTCCAC	3035-3055
CH3090R	*GTATCGAAGGTCATTTGGTGA*	*3071-3090*
CH3623R	TAGGCAGTGCAAGGTTATAGC	3603-3623
CH4003R	CTTCTGCCATTGTCAAAGTTG	3982-4003
CH4056R	TGTCCTACGAAGGCTGCATTC	4036-4056
CH4101R	CGATGTCCATGCGTTTTACC	4090-4109
CH4129R	GCACTCTTCATCGTTCTTCG	4110-4129
CH4493R	CAGTAGATGACCACGTGTGC	4473-4493
CH4649R	TGCTGTATCCTTTTCTGCCTG	4629-4649
CH4984R	GAGCATTTGACTTTTTGCACTC	4971-4992
CH5330R	CTTCTCTCTCGTCACATGTCAC	5309-5330
CH5432R	CCTGAAGAGACATTGCTGTGT	5410-5432
CH5533R	CTTTCGATTTCTCCTTCGTTG	5521-5533
CH5771R	AACACTTCTCCTCGTGGACTTC	5750-5771
CH5864R	*GCGACTGATACCTGCTTCTGTT*	*5843-5864*
CH6122R	CCACCATGTCTAGATATGCATC	6101-6122
CH6434R	CATAGGTTGCTAAATTCTCAGTTG	6411-6434
CH6769R	TCCGTTTCCAAAACAGTGTCTC	6756-6777
CH7214R	AGCTGTTCCTGTCACAGTATCG	7201-7222
CH7311R	GCTCGTCTTCTATCTTCATCTTG	7289-7311
CH7449R	TTCTCGAAATTGGATCTGGAG	7438-7459
CH7944R	GTAACCTGTTACCTTACCTTCGTG	7921-7944
CH8225R	TTGTCGAAGATCGGTCTGC	8208-8225
CH8273R	*GCTCCTTCATTAGCTCCTCCTAA*	*8251-8273*
CH8654R	CTGATGCGTTCTAGTGCTACG	8634-8654
CH9123R	GCCATTGACTGTGATCTTTACG	9102-9123
CH9485R	CGACTTCCTTCTTATGCATCAC	9472-9493
CH9585R	*GGCTGTACCGTTTGTAGATAACT*	*9563-9585*
CH9942R	TTACAGCAGCATGGTAAGAGTC	9920-9942
CH10230R	CGGTGAAGACCTTACAGCTGTAG	10218-10240
CH10533R	GTACACCACAATTTTGTTGTCG	10512-10533
CH10595R	CCAAATTGTCCTGGTCTTCCTG	10574-10595
CH10708R	CAGATGGTGCCTGAGAGTATG	10687-10708
CH11164R	GGTAGTTGACTATGTGGTCCTTC	11142-11164
CH11360R	GCTATGTACAGTGTGTCTCTTTGG	11346-11369
CH11811R(3'Term)	*GAAATATTAAAAACAAAATAACATCTCCTA*	*11783-11811*

Table 2.5 Reverse primers used for sequencing CHIKV isolate SL-R233. In addition the primers shown in italics were used as RT-PCR primers for the production of the cDNA clone as discussed in section 2.21.

2.16 Plasmid digestion

DNA (15-25µg) was digested with 5-10u of restriction enzyme in the appropriate buffer in a final volume of 20µl. Details of the enzymes and buffers used are provided in table 2.6. Reaction mixtures were incubated at 37°C for 1hr and digestion confirmed by agarose gel electrophoresis (section 2.12).

Restriction enzyme	**Supplier (10x Buffer)**	**Buffer components and concentrations under reaction conditions (1X)**
AgeI	Promega K	10mM Tris-HCl, 10mM $MgCl_2$, 150mM KCl, pH7.4
ApaI	Promega A	6mM Tris-HCl, 6mM $MgCl_2$, 6mM NaCl, 1mM DTT, pH 7.5
HindIII	Promega E	6mM Tris-HCl, 6mM $MgCl_2$, 100mM NaCl, 1mM DTT, pH7.5
PfIMI	NE buffer 3	100mM NaCl, 50mM Tris-HCL, 10mM $MgCl_2$, 1mM DTT, pH7.9
ScaI	Promega K	10mM Tris-HCl, 10mM $MgCl_2$, 150mM KCl, pH7.4
SgrAI	NE buffer 4	50mM K-acetate, 20mM Tris-acetate, 10mM Mg acetate, 1mM DTT, pH7.9
SpeI	Promega B	6mM Tris-HCl, 6mM $MgCl_2$, 50mM NaCl, 1mM DTT, pH7.5
SacI	Promega J	10mM Tris-HCl, 7mM $MgCl_2$, 50mM KCl, 1mM DTT, pH7.5
XhoI	Promega D	6mM Tris-HCl, 6mM $MgCl_2$, 150mM NaCl, 1mM DTT pH7.9
NotI	Promega D	6mM Tris-HCl, 6mM $MgCl_2$, 150mM NaCl, 1mM DTT pH7.9

Table 2.6 Details of restriction enzymes and buffers used. Reaction mixtures with a final volume of 10-20µl consisted of 15-25 µg DNA and 5-10u of the appropriate enzymes in buffer as recommended by the manufacturer.

2.17 Transformation of chemically competent *E.coli*.

In order to produce stocks of recombinant plasmid DNA, chemically competent One Shot® TOP10 or One Shot® Mach 1 *E.coli* were transformed by heat shock according to the manufacturer's instructions. Briefly, 1-2µl DNA was mixed with a 50µl aliquot of *E.coli* in a 1.5ml microcentrifuge tube and incubated for 30min on ice. The cells were heated to 42°C for 30sec before being returned to the ice for a further 2min. Finally 250µl SOC medium (Life Technologies product No 15544-03) was added and the tube was incubated at 37°C with agitation at 300rpm, for 1hr in an orbital incubator.

2.18 Purification of plasmid stocks

Subsequent growth of plasmid-transformed *E. coli* K12 strains was carried out in Lennox LB broth or on LB agar plates (Sigma-Aldrich UK). LB broth consists of 5g /L NaCl, 10 g/L tryptone and 5 g/L yeast extract, pH7.2. In addition to these ingredients LB agar contains 10g/L agar. Plasmid-transformed *E. coli* were spread onto the surface of LB agar supplemented with the appropriate antibiotic (100µg/ml ampicillin or 50µg/ml kanamycin) and incubated overnight at 37°C.

Individual colonies resulting from the agar cultures were used to inoculate 3ml Lennox LB broth containing antibiotic. These cultures were grown overnight with agitation at 37°C on an orbital incubator at 250rpm. Recombinant plasmid DNA was purified using the QeneElute® Plasmid miniprep kit (table 2.2) and analysed first by gel electrophoresis of restriction digest fragments and finally by DNA sequencing.

Medium-scale plasmid purifications were carried out using the QIAfilter Plasmid Midi kit (table 2.2).

2.19 Nucleic acid quantification

The quantity and purity of stocks of both DNA and RNA were determined by analysis of 1-2µl samples using the NanoDrop® ND-1000 spectrophotometer according to the manufacturer's instructions.

2.20 Ligation of PCR-generated fragments into plasmids

DNA fragments were digested with restriction enzymes (section 2.16) at the sites present in the overlapping regions and ligated into the MCS or to unique sites in the insert. This was accomplished using T4 DNA ligase (Life Technologies™) in accordance with the manufacturer's protocol. The approximate DNA concentrations were assessed by their relative band intensities under UV light on ethidium bromide-stained agarose gels (section 2.12). Typically, the concentration ratio of insert to vector in a ligation reaction mixture was 3:1. For DNA fragments with 5' or 3' recessed ends, the remainder of the reaction mixture consisted of 1u T4 DNA ligase, 1 x reaction buffer (supplied with the kit) and water, to make a final volume of 20µl. Incubation was at 22°C for 10min. Blunt-ended ligation reactions differed in the enzyme concentration used (5u T4 DNA ligase) and the incubation conditions (14°C for 1hr).

2.21 Cloning strategy

The cloning strategy for the cDNA clone derived from CHIKV SL-R233 is illustrated in figure 2.2. A series of restriction sites that were rare or absent in the cDNA sequence of isolate SL-R233 were determined using the DNASTAR SeqBuilder software (Lasergene®). Using this information, oligonucleotide primers were selected to enable the entire genome to be amplified by RT-PCR in the form of five contiguous amplicons. These were arranged in such a way that the 3'and 5' ends of adjacent amplicons contained overlapping regions in which selected restriction sites were present.

The amplicons detailed in table 2.7 were initially cloned using TOPO 2.1, DNA pCR® and Zero Blunt® TOPO® PCR Cloning kits (Life Technologies, UK) in accordance with the manufacturer's instructions. These plasmid vectors facilitate the rapid cloning of amplicons with 3'dA overhangs or blunt ends produced by Taq polymerase or proof-reading polymerases respectively. The key features provided by vectors in these kits are the presence of multi-cloning sites (MCSs) and antibiotic resistance markers that enable the subsequent selection of host bacterial cells containing the desired clones. Recombinant products cloned from the amplicons 172.1, 172.2, 172.3, 172.4 and 172.5 were named p172.1, p172.2, p172.3, p172.4 and p172.5 respectively.

Amplicon	Primers	Amplicon size (base-pairs)	Gene
172.1	CHIK1F / CH3090R	3090	5'UTR/nsP1/nsP2
172.2	CH2971F / CH5864R	2893	nsP2/nsP3/nsP4
172.3	CH5306F / CH8273R	2966	nsP3/nsP4/C
172.4	CH7924F / CH9585R	1665	C/E3/E2
172.5	CH9441F / 11811R	2327	E2/6k/E1/3'UTR

Table 2.7 Primers used to amplify CHIKV genome fragments used to construct the cDNA clone.

The cloned sub-genomic CHIKV fragments were recombined in stages through a further series of plasmid vectors each propagated using One-Shot® Mach 1™ *E. coli* (Life Technologies). Fragments 1-3090 and 2971-5864, contained in p172.1 and p172.2 were combined by TF-PCR and cloned into the Zero Blunt® TOPO® PCR vector to produce p236.7 (containing the 5' 5864 nucleotide fragment). In a similar manner, fragments 7924-9585 and 9441-11811 were combined by TF-PCR and cloned into the Zero Blunt® II TOPO® PCR vector to produce p197.1 containing the 3' 3887 nucleotide fragment).

The 5307-8273 CHIKV fragment was excised from p172.3 by restriction enzyme digestion at the vector BamHI and XhoI sites, and ligated into plasmid pGEM 7Z(+) (Promega, UK) also digested with BamHI and XhoI. The ScaI site present in the β-lactamase coding region present in this vector was eliminated by creating a silent mutation by site-directed mutagenesis [clone p238.1(S-)]. The G1872A substitution in the vector converted a GAA codon to a GAG codon, both coding for glutamic acid. The purpose of this step was to enable the use of the single remaining ScaI site present between nucleotides 8150 and 8155 in the CHIKV genome to attach the next fragment to the 3' end whilst the ampicillin resistance marker remained active.

Plasmid p238.1(S-) was linearized by digesting with ScaI and Bam HI p197.1 was also digested with ScaI and Bam HI and the CHIKV fragment extending from 8153, through the 3' end (11811) to the vector MCS was ligated to these sites, resulting in plasmid p25.6. The CHIKV fragment 5308-11811 flanked by parts of the vector MCS was cut from p25.6 by digestion with NotI and SpeI and ligated into pGEM 5Z(+) (Promega, UK) to produce plasmid p31.2. Finally the 5' 5864 nucleotide fragment was cut from p236.7 by digestion with AgeI (CHIK-specific) and SacI (vector specific). The resulting plasmid (p31.10) contained a cDNA copy of the CHIKV genome from nucleotides 1-11811.

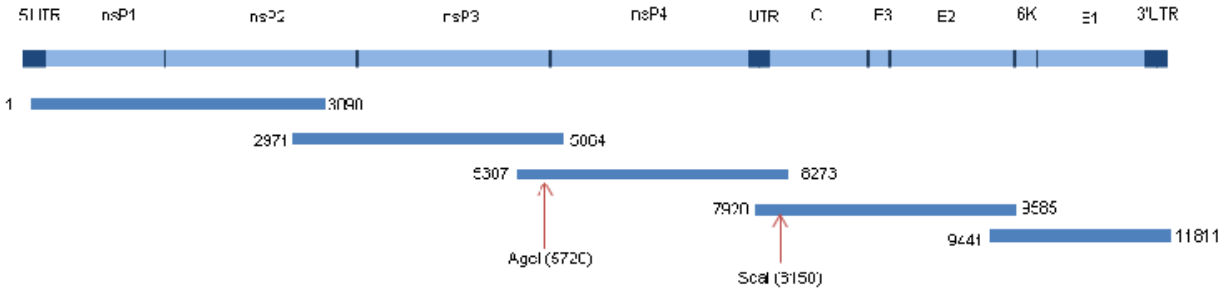
5'UTR
nsP1
nsP2
nsP3
nsP4
UTR
C
E3
E2
6K
E1
3'LTR
1
3080
2971
5004
5307
8273
7920
9585
9441
11811
AgeI (5720)
ScaI (3150)

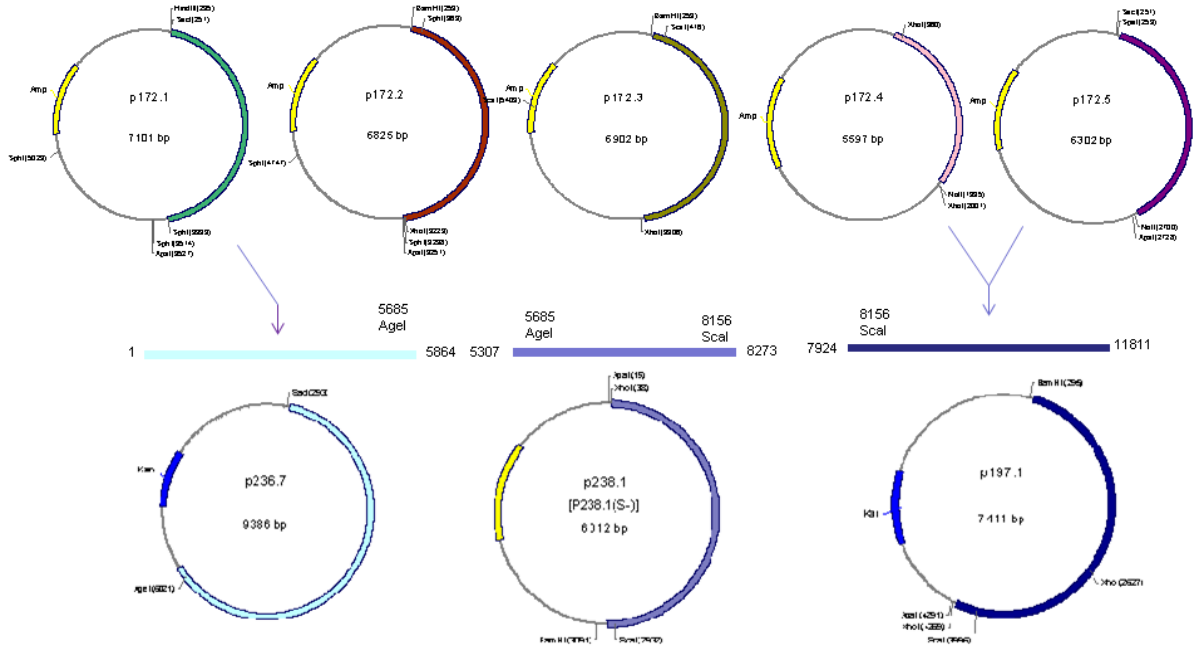
p172.1
7101 bp
p172.2
6826 bp
p172.3
6902 bp
p172.4
5597 bp
p172.5
6302 bp
Amp
1
5685
AgeI
5864
5307
5685
AgeI
8156
ScaI
8273
7924
8156
ScaI
11811
p236.7
9386 bp
p238.1
[P238.1(S-)]
6312 bp
p197.1
7411 bp


SacI
1
AgeI
5685
5864


NotI
5307
Age
5685
11811
SpeI

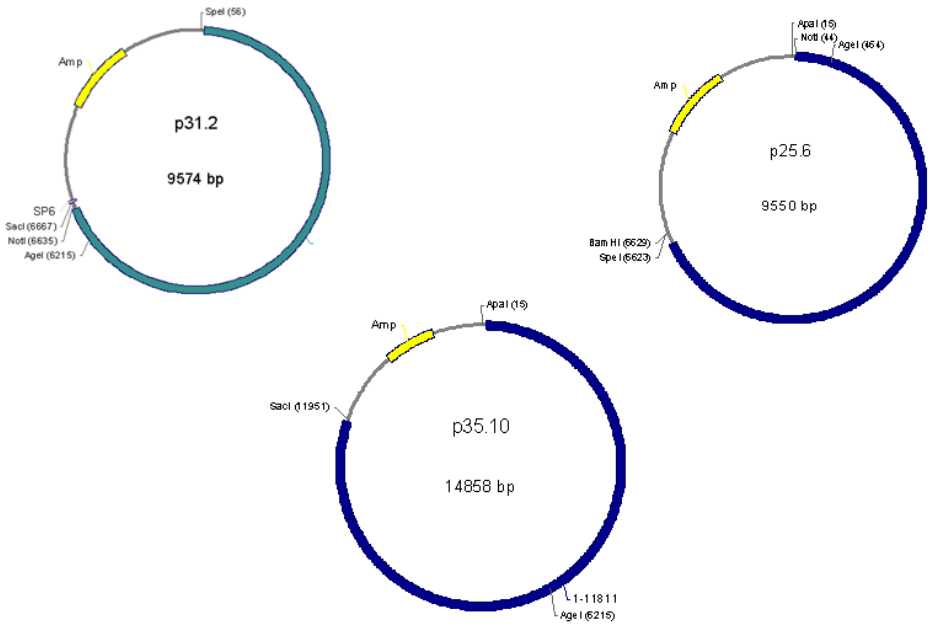
p31.2
9574 bp
Amp
SP6
SacI (6667)
NotI (6635)
AgeI (6215)
p25.6
9550 bp
Amp
BamHI (6629)
SpeI (6623)
p35.10
14858 bp
Amp
SacI (1951)
1-11811
AgeI (6215)

Figure 2.2 Strategy for cloning a cDNA clone from RT-PCR products of CHIKV isolate SL-R233. A series of five overlapping amplicons was cloned into the TOPO 2.1 DNApCR® vector. The CHIKV-specific inserts of 172.1, 172.2 and 172.4, 172.5 were combined by TF-PCR.and cloned into Zero Blunt® TOPO® PCR. Clones containing cDNA coding for nucleotides 1-5864, 5307-8273 and 7924-11811 were, next used to assemble the entire CHIKV genome in pGEM5Z(+) by cleaving the inserts and vectors at the restriction sites indicated and combining by the action of T4-DNA ligase.

2.22 Site-directed mutagenesis

Genetic modification was carried out on cDNA clones by site-directed mutagenesis using a Stratagene QuikChange®II Site-Directed Mutagenesis kit according to the manufacturer's instructions (Appendix A9), using the primers listed in table 2.8. Following the introduction of five point mutations to the CHIKV-derived 11,811kb insert in plasmid p35.10, a corrected version [**pCHIK-SL (-)**] was produced. This clone contained an identical genome to the original isolate up to the end of the 3'UTR apart from the presence of 3 silent mutations.

Primer	**Mutation**	**Sequence**
CH11238F	A11263G	TGTGCACCGCCTGGAGATACTTTTGTGGTACACTTG
CH11272R		GATTAGAATCAGTGCGGCAACAGCAACAACCAGTC
CH4609F	-4636A	ACAGCAGCTTGGCAGGCAGAAAAGGATACAGCAGCAC
CH4654R		TGGTGCTGTATCCTTTTCTGCCTCCCAAGCTGCTG
CH3500F	T3527C	ACACTCATTAGTGGCCGAACACCGCCCAGTAAAAGG
CH3535R		CCTTTTACTGGGCGGTGTTCGGCCACTAATGAGTG
CH2584F	C2609T	TGTACCACAAAAGTATCTCCAGGCGGTGCACACTG
CH2617R		TGTGCACCGCCTGGAGATACTTTTGTGGTACACTTG
CH9016F	G9042A	CGCAACTACCGAGGAGATAGAGGTACACATGCCCC
CH9050R		GGGGCATGTGTACCTCTATCTCCTCGGTAGTTGCG
CH1655F	C1674T	GAACAGCTTGAGGACAGAGTGGGCGCAGGAATAATAGAGAC
CH1696R		AGTCTCTATTATTCCTGCGCCCACTCTGTCCTCAAGCTGTTC
Amp Sca(-) For	β-lactamase ScaI site (-)	TGCTTTTCTGTGGACTGGTGAGTATTCAACCAAGTCATTCTGAG
Amp Sca(-) Rev		TCTCAGAATGACTTGGTTGAATACTCACCAGTCACAGAAAAGC

Table 2.8 Oligonucleotide primers used to carry out site-directed mutagenesis

Clone pCHIK-SL(A-) was subsequently modified by the addition of a 3' poly-A tail as detailed below (section 2.23) to produce clone **pCHIK-SL(wt)**. A further variant clone was produced from this product resulting in a phenotype with an A533V substitution in the P3 position in the nsP1-nsP2 cleavage domain of the ns-polyprotein

clone **pCHIK-SL(A533V)**. The nucleotide substitution (C1674T) was carried out in the subgenomic clone p172.1 (section 2.21). A chimera was constructed in which a fragment bordered by the SpeI site (present in the pGEM5Z(+) MCS) and PflMI (1735-1745 from the 5'end of the CHIKV genome) was excised from p172.1 and used to replace the analogous region in pCHIK-SL(wt).

2.23 Addition of a poly-dA tail to the cDNA clone

A 3' tail consisting of 40 adenosine monophosphate residues was added to the CHIKV genome cDNA in clone pCHIK-SL(wt) in two stages (figure 2.3). This involved incremental extensions of the 3' UTR by PCR. 2µl of a 1:20 dilution in water of the sub-clone, p197.1 was used as template to amplify a region corresponding to nucleotides 9384-11811 (the end of the 3'UTR). In a standard 50µl PCR, primers CH9385F (table 2.4) and a reverse primer, CHIK(A)15-term, were used the latter contained 15 thymidine molecules at its 5' end followed by a sequence complementary to the final 28 nucleotides of the 3'UTR (table 2.9). The amplicon produced by this reaction was cloned into the pCR Blunt II TOPO® vector. In a second PCR 2µl of a 1:20 dilution (in water) of the cloned product of the first PCR was used as template. This reaction differed from the first by the replacement of the reverse primer CHIK(A)15-term by CHIK$(A)_{40}$ ApaI. (table 2.9). This primer consisted of three sections: a stretch of 40 copies of the nucleotide, thymidine the ApaI recognition sequence (GGGCCC), and finally the nucleotides, guanosine and adenosine, these being complementary to the final two nucleotides of the 3'UTR. The latter two were intended to have the effect of ensuring that annealing to the 15 adenosine template occurred in the correct orientation. The pCR Blunt II TOPO® cloning procedure was repeated with the resulting amplicon.

After confirming the correct sequence of this construct, the modified 3' end was added to the CHIKV clone lacking a 3'poly-A tail (pCHIK-SL(A-) by constructing a chimera. A unique restriction site (SgrAI), identified 10236–10243 nucleotides from the 5' end of the CHIV genome was used in tandem with ApaI to cleave the 3' regions form the two constructs. Finally the 3'-tailed SgrAI-ApaI fragment was ligated into pCHIK-SL(A-) to produce the clone (pCHIK-SL(wt).

Primer	Sequence
CHIK(A15)term	TTTTTTTTTTTTTTTGAAATATTAAAAACAAAATAACATCTCC
CHIK(a)A40 ApaI	GGGCCCTTTTTTTTTTTTTTTTTTTTTTTTTTTTTTTTTTTTTTGA
CH9384F	CCAAGTCATCATGCTACTGTATCC

Table 2.9 PCR primers used to construct a 3' $(A)_{40}$ tail on the cDNA CHIKV clone. These were used as described in section 2.23.

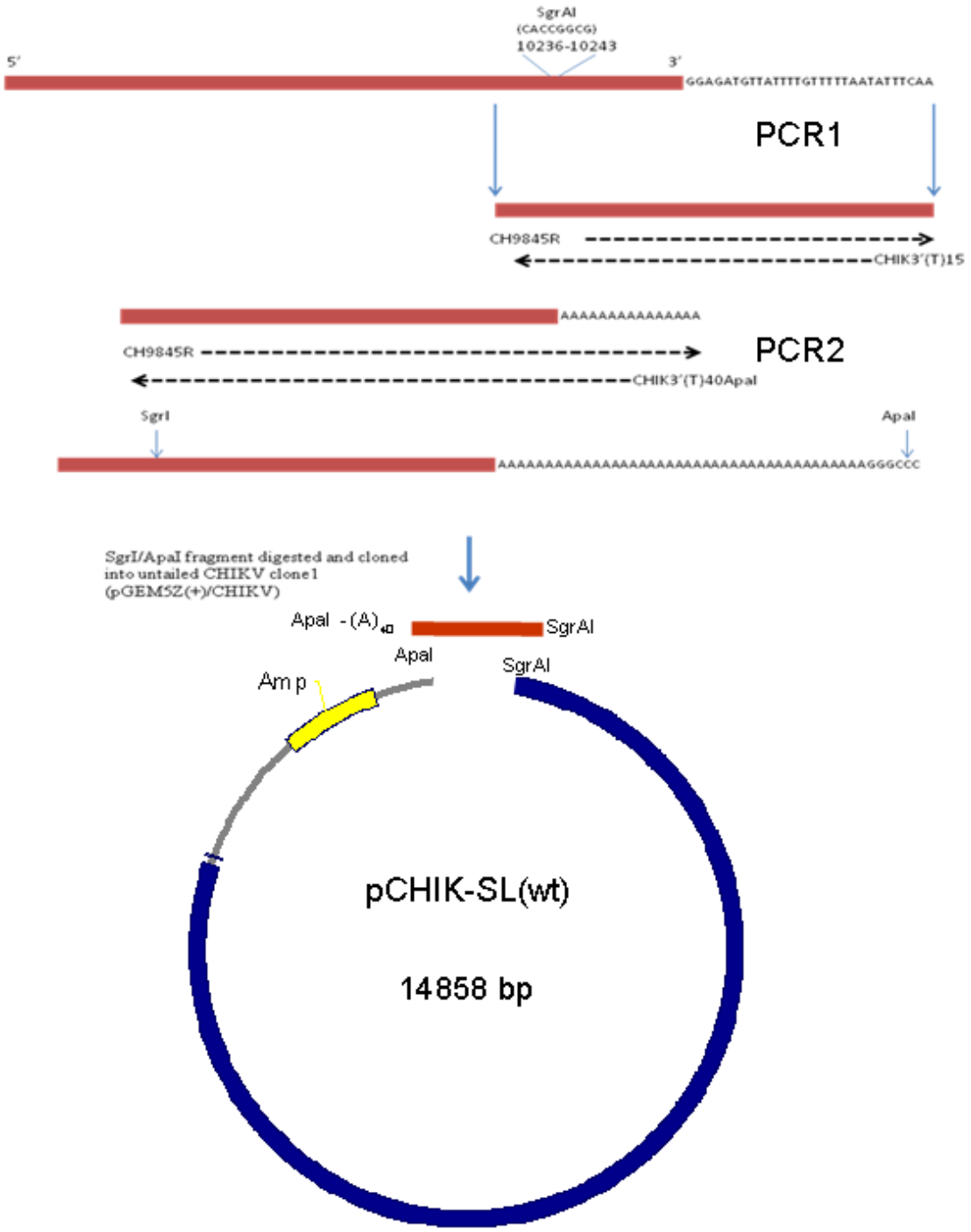

Figure 2.3 The amplification steps used to generate a 3' poly-dA tail by PCR. The 3' region contained in the plasmid construct p197.1 (section 2.26) was amplified in two stages: in the first of these the reverse primer, CHIK(A15)term was used with the forward internal primer CH9384F and the resulting amplicon cloned into the pCR Blunt II TOPO® vector. The CHIKV-specific region of this product was amplified using the same forward primer with a second reverse primer, CHIK$(A)_{40}$ ApaI and the amplicon cloned in the same way. A chimeric clone was constructed using a CHIKV-specific fragment present between the restriction sites, SgrAI and the added ApaI site in this clone and the pGEM5Z(+) based CHIKV clone, pCHIK-SL(A-).

2.24 Measurement of CHIKV 3'poly-A tail

The 3' poly-A tail of SL-R233 RNA and that of the S27 African CHIKV prototype (supplied by Dr CH Logue, PHE, Porton, UK), were determined using the USB® Poly(A) Tail-Length Assay Kit (Affymetrix, Inc. USA) to tail and amplify the 3' ends (Appendix protocol A11). Amplicons were subsequently sequenced, and reads from multiple PCRs compared.

2.25 *In vitro* transcription

Genome RNA was generated from clones, pCHIK-SL(wt) and pCHIK-SL(A533V), by *in vitro* transcription. The cDNA clones were linearized by digesting 25µl of each stock plasmid (4.05 and 6.7µg respectively) at the unique ApaI site immediately downstream from the 3' poly-A tail in the inserts, in a final volume of 30µl. Linear DNA was ethanol precipitated by adding one tenth of the volume of 3M sodium acetate and two volumes of 100% ethanol, mixing after each addition. The mixture was incubated at -20°C for 1hr, centrifuged at 16,060 x g for 15min at 20°C and the pellet dried. Finally the pellet was resuspended in 20µl water.

Capped viral RNA was generated from linearized cDNA by utilizing the SP6 polymerase promoter situated upstream from the CHIKV insert on the pGEM5Z(+) vector, using a mMESSAGE mMACHINE® kit (Ambion Life Technologies™, UK). The protocol provided by the manufacturer was followed exactly and is reproduced in appendix A10. Remaining DNA was removed by the addition of 2µl TURBO DNase (supplied with the kit) and incubation at 37°C for 15min.Transcribed RNA was

purified using a MEGAclear™ kit (Ambion, Life Technologies product No AM1908). After a final ethanol precipitation step the RNA was resuspended in 20µl water.

RESULTS

2.26 Amplification of CHIKV genome fragments by RT-PCR

In order to develop a reverse genetics system for the CHIKV isolate SL-R233 it was first necessary to determine its genome sequence so that an effective cloning strategy could be devised. To this end a series of 20 RT-PCRs were conducted (including those later used to construct clones) resulting in the coverage of the entire genome, and at least two amplicons for each region throughout its length (tables 2.3 and 2.7). In this way it was likely that errors in transcription would be detected when contigs were built from the sequencing reads (figure 2.4). Although it was recognized that the length of an RNA template that can be amplified in a single RT-PCR is often limited to 3-3.5kb, it was originally planned to construct the cDNA clone from the minimum number of sub-clones. It was intended to combine the virus-specific inserts from these, by utilizing restriction sites present in overlapping regions and then using the action of T4 DNA ligase to attach adjacent regions of the genome when assembling the final clone. However in cases where unique restriction sites were not present in the required region it was necessary to combine of cDNA fragments by an alternative means; in these cases TF-PCR was used.

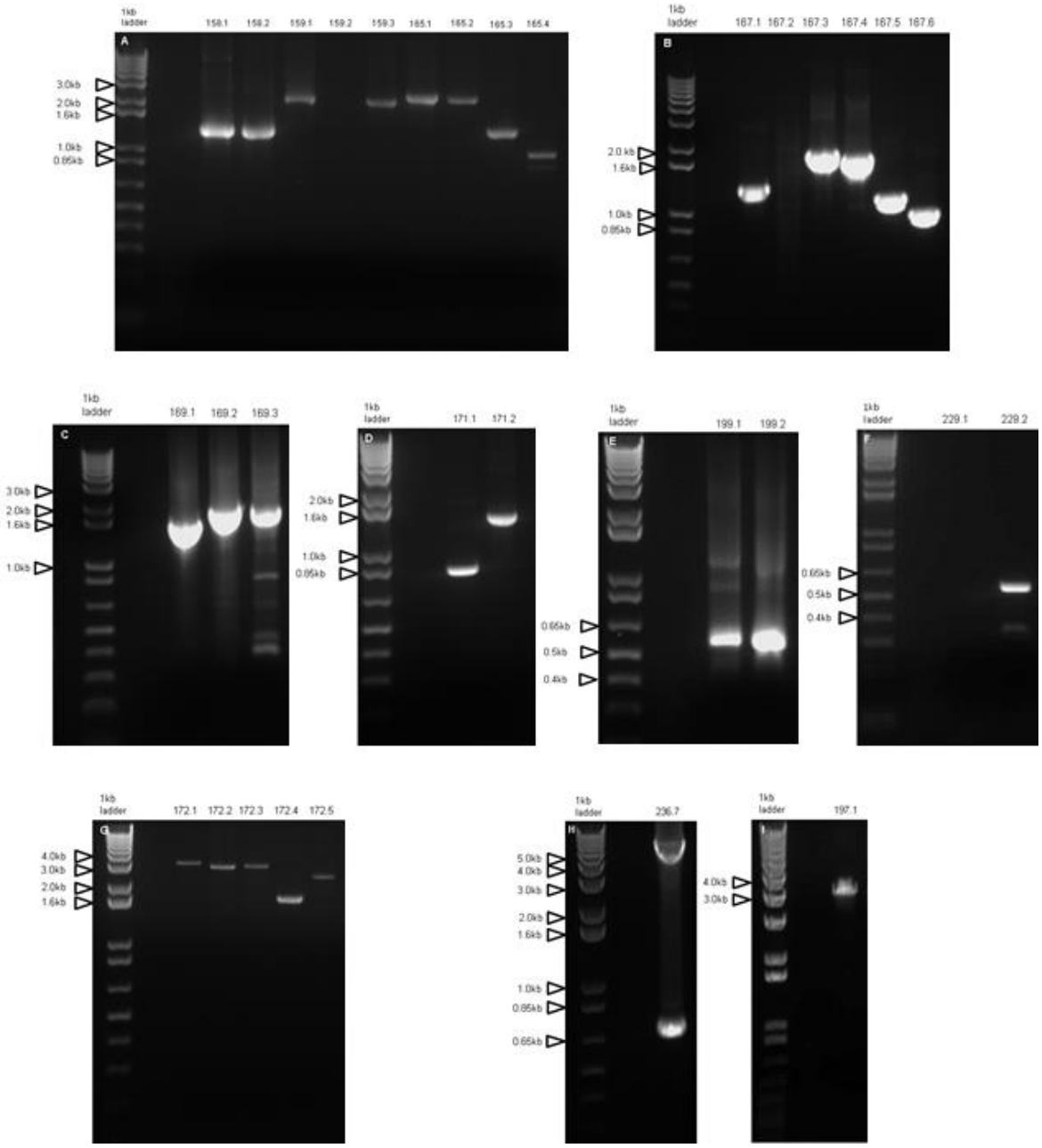

Figure 2.4 Ethidium bromide-stained agarose gels containing separated CHIKV SL-R233 amplicons. A series of fragments covering the entire genome was amplified by RT-PCR from which the sequence was determined (A to F). A second series of amplicons comprising the entire genome containing overlapping regions was used to construct sub-clones and to confirm the genomic sequence (G). The cloned fragment 1-3090 was combined with that of 2971-5864 by TF-PCR as were fragments 7920-9585 and 9441-11811 to produce fragments of 5864 and 3887 nucleotides respectively (H and I).

2.27 Sequence analysis of CHIKV isolate SL-R233

The complete genomic nucleotide sequence of the Sri Lankan CHIKV strain, SL-R233 was determined from cDNA obtained by RT-PCR and is shown in appendix C1. The linear genome was found to be 11811 nucleotides in length (excluding the 3'-terminal poly-A tail).

The genome organization was found to be typical of members of the alphavirus genus, consisting of two open reading frames (ORFs) flanked on either side by an untranslated region (UTR). Following a 5' UTR of 76 nucleotides was the non-structural ORF beginning with a methionine codon (ATG) between positions 69-71 and terminating with the codon TAG at positions 7491-7493. The second UTR (known as the junction region) separating the two ORFs, was found to extend for a further 65 nucleotides. The ORF coding for the structural polyprotein started with codon ATG (nucleotides 7559-7561) and ended with the codon TAA (nucleotides 11311-11313). The 3'UTR was 501 nucleotides long.

The base composition was analysed using the EditSeq component of the DNASTAR software package and shown to be: A = 29.62%, C = 24.94%, G = 25.16% and T = 20.27%. This software was used to determine the location of the two ORFs and to translate them to obtain the amino acid sequences of the two polyproteins. By comparing this data with the sequences and cleavage domains from other known Old World alphaviruses, the polyprotein cleavage sites (in the amino acid sequences) were located and the sizes of the resulting translation products determined (figure 2.5).

In the course of determining the genome sequence of SL-R233, a total of seven amplicons containing the region coding for the nsP3/nsP4 cleavage domain were produced and sequenced. In each case the CGA codon (arginine) was seen at position 5634-7 (figure 2.6), however inspection of the chromatogram traces revealed that in each case, beneath the dominant cytidine peak was a smaller one indicating the presence of thymidine (uridine in the original RNA). The E1 – A226V mutation seen in the latter half of the outbreak in the Indian Ocean outbreak (Schuffenecker *et al* 2006, Tsetsarkin *et al* 2007, Powers and Logue 2007), was absent.

An alignment (Clustal W) showing the relationship of isolate SL-R233 to strains of other members of the ESCA clade and to those of the Indian and West African clades, was used to construct a phylogenetic tree (figure 2.7). This demonstrated a close relationship between SL-R233 and other Southern Asian isolates (Sri Lanka, Singapore, Thailand and India) obtained at about the same time (2005-2008).

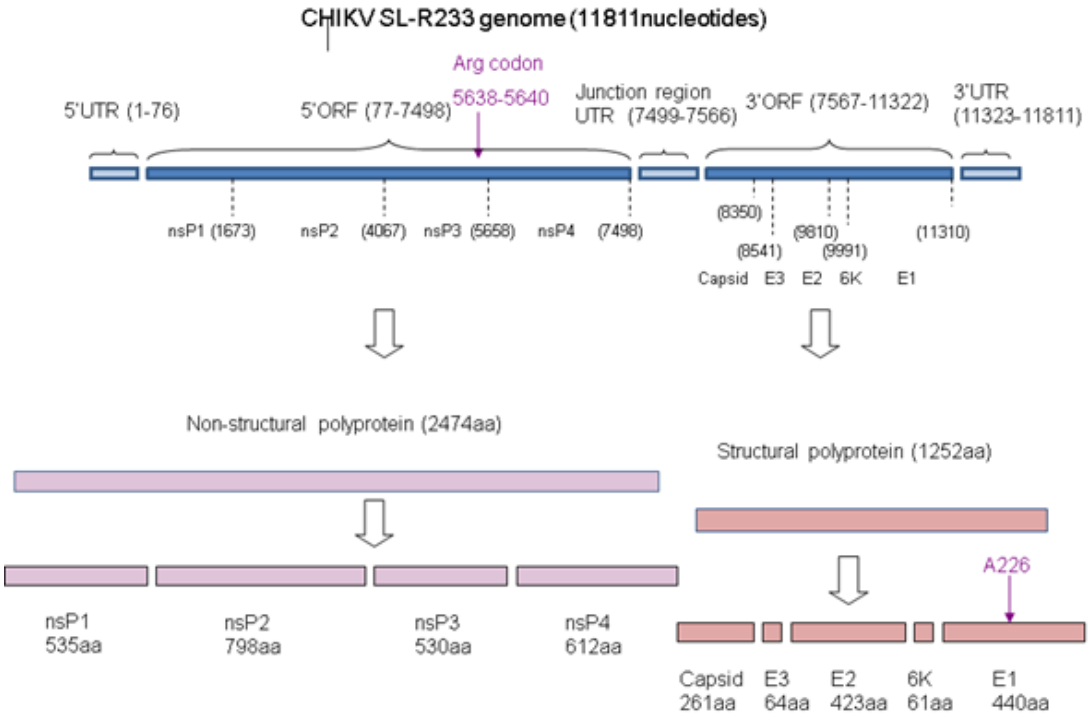

Figure 2.5 Schematic representation of the SL-R233 genomic features and translational protein products. The sizes of individual proteins are shown, following proteolytic processing of the non-structural and structural polyproteins. In common with isolates from the Indian sub-continent prior to mid-2007, when strains of the ESCA clade with the A226V mutation were first reported, alanine was present at this site.

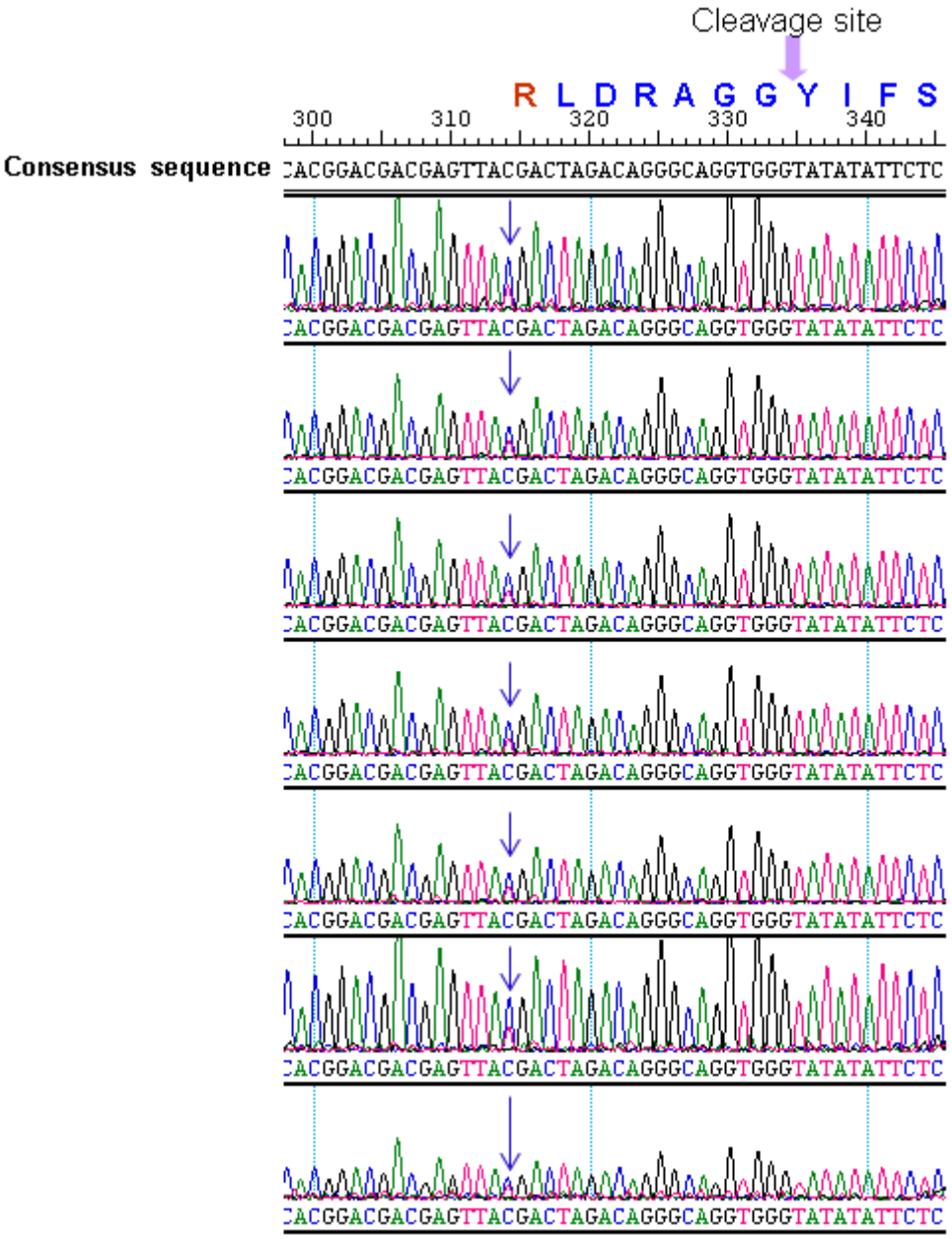

Figure 2.6 Alignment of the cDNA sequence traces from seven RT-PCR products covering the junction between the nsP3 and nsP4 genes on the 5' ORF. The amino acid sequence of the cleavage domain is marked in blue and the site of the arginine codon (CGA) is marked in red. Close examination of the sequence traces for each amplicon indicates that the first nucleotide in the codon is cytidine, however in each case a smaller peak (corresponding to thymidine) immediately below provides evidence that a second product with an opal (TGA) termination codon is also present.

Percent Identity

	1	2	3	4	5	6	7	8	9	10	11	12	13	14	15	
1		93.4	99.6	96.8	99.5	99.9	99.6	99.6	84.4	99.6	99.7	99.5	94.0	96.9	99.5	1
2	6.1		93.5	94.0	93.5	93.4	93.6	93.5	83.5	93.6	93.4	93.6	98.0	94.0	93.7	2
3	0.3	6.1		96.9	99.8	99.7	99.7	99.6	84.6	99.6	99.8	99.6	94.1	97.0	99.6	3
4	3.0	5.4	3.0		97.0	96.8	97.1	97.1	84.9	97.1	96.8	97.2	94.9	99.8	97.2	4
5	0.3	6.1	0.1	3.0		99.5	99.8	99.8	84.8	99.8	99.7	99.7	94.2	97.1	99.7	5
6	0.1	6.0	0.2	3.0	0.2		99.7	99.7	84.5	99.6	99.8	99.5	94.1	96.9	99.5	6
7	0.2	6.0	0.2	2.9	0.2	0.1		99.9	84.8	99.9	99.6	99.7	94.2	97.2	99.7	7
8	0.2	6.0	0.2	2.9	0.2	0.1	0.1		84.8	99.8	99.6	99.7	94.2	97.2	99.7	8
9	17.1	17.9	17.1	16.7	17.0	17.1	17.0	17.0		84.9	84.5	84.9	83.8	85.0	84.9	9
10	0.2	5.9	0.2	2.8	0.2	0.2	0.1	0.1	16.9		99.6	99.8	94.3	97.3	99.8	10
11	0.3	6.1	0.1	3.0	0.1	0.2	0.2	0.2	17.0	0.2		99.5	94.1	96.9	99.5	11
12	0.3	5.9	0.3	2.8	0.3	0.2	0.2	0.2	16.8	0.1	0.3		94.2	97.3	99.9	12
13	5.8	1.2	5.8	5.1	5.8	5.8	5.7	5.7	17.9	5.7	5.8	5.6		94.8	94.4	13
14	3.0	5.5	3.0	0.1	3.0	2.9	2.9	2.9	16.7	2.8	3.0	2.7	5.1		97.3	14
15	0.3	5.9	0.3	2.8	0.3	0.3	0.3	0.3	16.9	0.2	0.3	0.0	5.6	2.8		15
	1	2	3	4	5	6	7	8	9	10	11	12	13	14	15	

1 CHIKV_LK6008_SriLanka_(2008).seq
2 CHIKV_PHH_strain_(Phillipines).seq
3 CHIKV_MY-08-065_(Malaysia2009).seq
4 Chikungunya_S27_African_prototype_str
5 CHIKVThailand_CU_Chik683(2009).seq
6 CHIKV_3408_SriLanka_(2008).seq
7 CHIKV_SL-R233_(2006).seq
8 CHIKV_SL15649_(Sri_Lanka_2006).seq
9 CHIKV_strain37997_Senegal.seq
10 Chik31_EU564335_(Rajastan_2006).seq
11 CHIKV_122508_(Singapore_2008).seq
12 CHIKV_Reunion_LR2006-OPY1.seq
13 CHIKV181-25_vaccine_strain.seq
14 CHIKV_Ross_strain_(Feb_2011).seq
15 CHIKV_SPRU_D560-06_(2006).seq

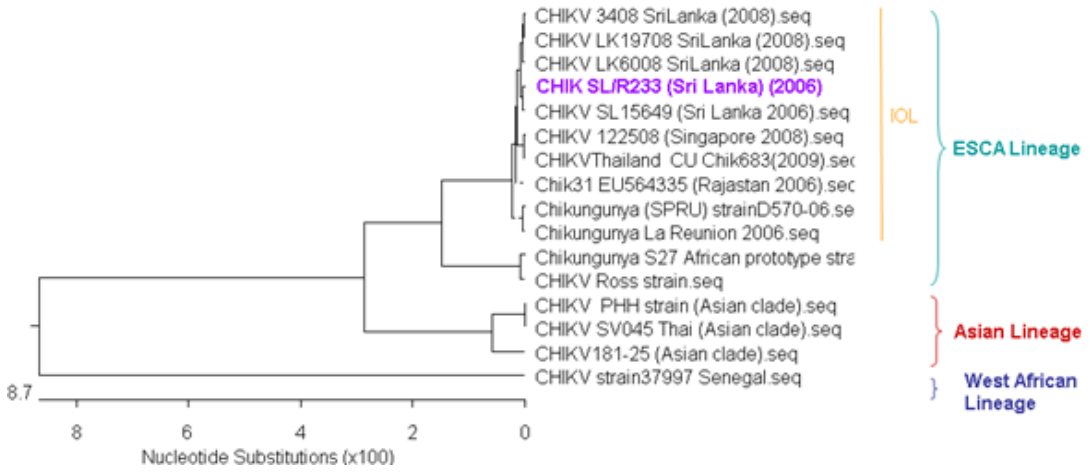

Figure 2.7 Phylogenetic tree (Clustal W) showing the genome of isolate SL-R233 to be closely related to those of other recent isolates of the Indian Ocean sub-lineage (IOL). Although forming a distinct group, these isolates from Sri Lanka, Singapore, India and Mauritius (D570-06) group significantly closer to the prototype Eastern/Southern/Central (ESCA) African strain, S27 than to strains in either the West African or Asian genotypes.

2.28 Construction of CHIKV sub-clones

Although the TOPO 2.1 pCR® and Zero Blunt® II TOPO pCR® vectors are convenient for cloning PCR products they are not recommended for inserts greater than 3-4kb. As CHIKV genomes are approximately 11.8kb, it was necessary to base the construct containing the complete viral genome on an additional more suitable vector. The plasmid, pGEM5Z(+) (Promega, UK) was initially selected to form the backbone of the final construct. This product contains a suitable MCS which is flanked by T7 and SP6 RNA polymerase promoters which facilitate *in vitro* transcription of inserts in either direction. The TOPO 2.1 pCR® vector contains a 3'-thymidine overhang at the cloning site to facilitate the cloning of amplicons generated by Taq-polymerase which have a terminal 3'-adenosine (dA) overhang. As amplifications were carried out using a high fidelity DNA polymerase, the resulting amplicons were blunt ended and thus required an additional step to add the dA overhang. It became apparent at this stage that a better approach would be to use the pCR®BluntII TOPO vector as this has similar range of restriction sites in the MCS, and is designed for blunt ended amplicons.

In order to utilize the ScaI restriction site at position 8150-8155 in the CHIKV genome a silent mutation was introduced into the sub-clone containing this region (p238.1) to remove the ScaI site present in the β-lactamase gene in the pGEM7Z(+) vector (position G1872A). Thus the gene remained functional and conferred ampicillin resistance to host *E.coli* whilst the CHIKV ScaI site became unique in the resulting product (p238.1(S-).

2.29 Sequence analysis of CHIKV cDNA clone 35.10

A genomic alignment of SL-R233 and the virus-derived insert in p35.10, revealed seven point mutations comprising six nucleotide substitutions and one deletion (figure 2.8). Three of the former (T3946C, A6811G and T7024C) were silent, but the remainder were missense mutations and would have translated into altered polyproteins (figure 2.8). Searches in the NCBI GENBANK website revealed that each of the silent mutations occurred in several other naturally occurring isolates. This being the case, it was decided that additional steps to correct them in order to produce a clone with an identical nucleotide sequence to the wild type (w/t) isolate was not necessary. To construct a clone containing the (w/t) coding sequences, a series of five intermediate clones derived from p35.10 were produced, in which the missense errors were sequentially corrected through site-directed mutagenesis.

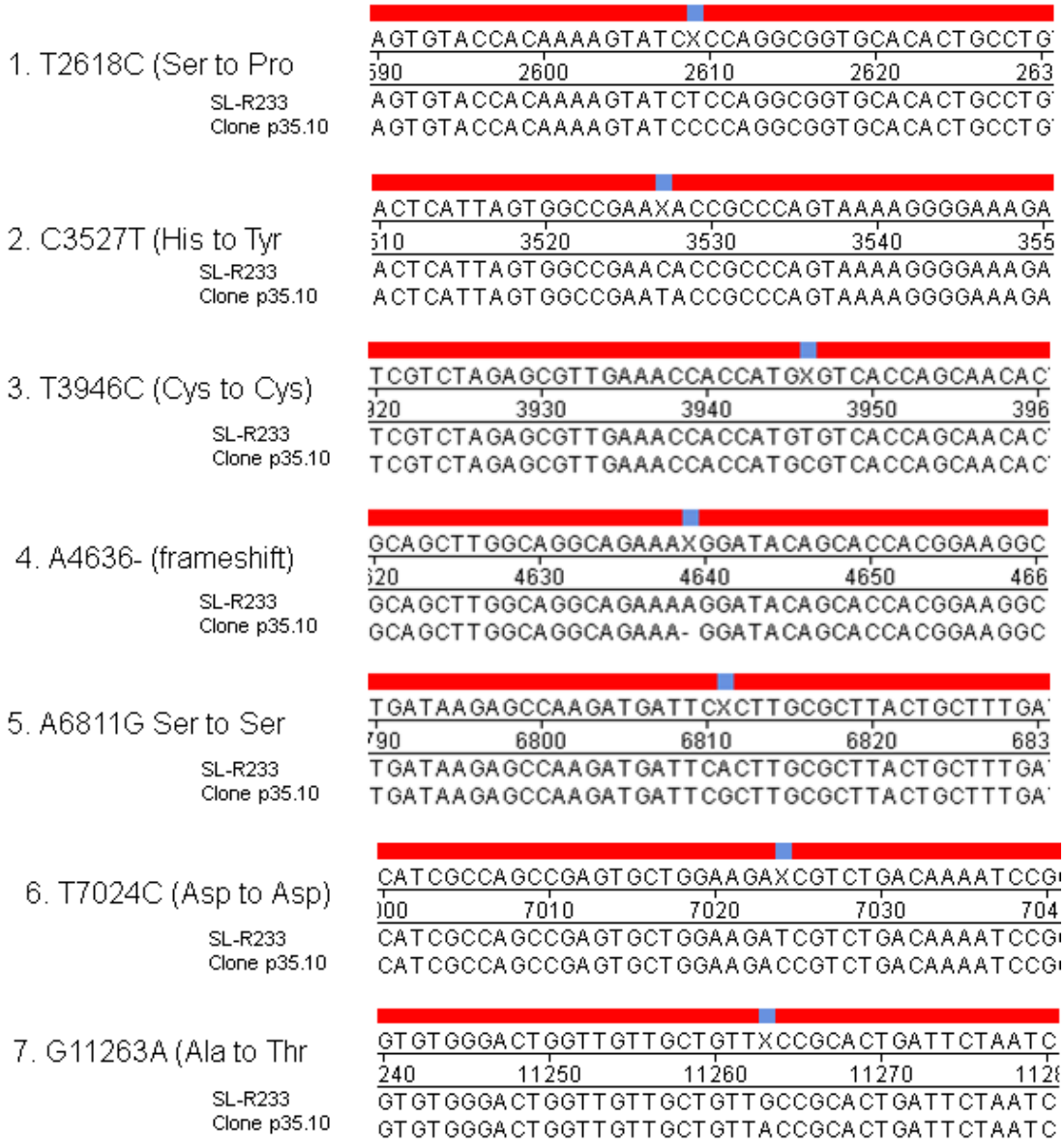

Figure 2.8 Alignment of CHIKV isolate SL-R233 with cDNA clone p35.10 using MegAlign software (Lasergene®, DNASTAR). The cDNA clone was a pGEM5Z(+) based construct containing the full-length genome assembled from PCR products (Clustal W). Point mutations are highlighted in blue on a red background.

2.30 Modification of CHIKV cDNA clone pCHIK-SL(A-)

The inclusion of a 3' poly-A tail had not been included in the strategy to produce the initial CHIK clone [pCHIK-SL(A-)] as it was reasoned that successful transfection of RNA transcribed from this construct would require the 5' two thirds of the genome to be translated to produce a functioning replicase. This being the case, all the functions necessary to synthesise progeny RNA and proteins, including a tailing function would be carried out by a domain in nsP4. Early attempts at transfection of mammalian cells (BHK21 cells), indicated that this was a correct assumption, in that viable w/t SL-R233 CHIKV was rescued from resulting cell culture supernatants. However, when this process was repeated under identical electroporation conditions virus rescue was not efficient.

In order to determine the poly-A tail length required, all CHIKV strains available in the GENBANK database were analysed. However this resource provided only limited guidance, as only eight entries reported this feature (table 2.10). It was therefore decided to measure the poly-(A) tails in CHIKV RNA available in this laboratory to provide information which to base a strategy.

CHIKV Strain	Accession Number	Poly-(A) tail length (nucleotides)
SL15649	GU189061	28
IND-06-Guj	JF274082	31
LR2006 OPY1	DQ443544	29
Lamu33	HQ456255	25
KPA15	HQ456254	25
SL10571	AB455494	19
MY/08/068	FN295487	7
BNI-CHIIKV899	FJ959103	20

Table 2.10 CHIKV genomes accessed from GENBANK with reported 3' poly-(A) tail lengths (only those greater than two nucleotides included).

Agarose gel analysis of amplification products obtained using the Affymetrix© Poly(A) Tail-Length Assay Kit failed to provide a clear answer as to the length of tail in virus rescued from cell cultures transfected with RNA transcribed from pCHIK-SL(A-) or CHIK S27. Furthermore, sequencing of the 3' region of PCR products showed no clear boundary between the end of the poly-(A) tail and the beginning of the poly-(G) section added during the assay (Appendix 1.11). This finding was interpreted as indicating the presence of a mixed population of genomes with varying tail lengths.

In order to obtain a more precise result, PCR products obtained from the assay of CHIKV clone pCHIK-SL(A-) and from S27 were cloned into the pCR2.1 TOPO vector and a selection of ten transformed *E.coli* colonies were used to prepare purified plasmid; in each case nine provided suitable DNA for sequencing. The sequencing results indicated that virus both from an un-tailed clone and w/t strain S27 generated viruses containing a mixed population with regard to genomic poly-(A) tails with length ranging from 23 to 78 nucleotides (figure 2.9).

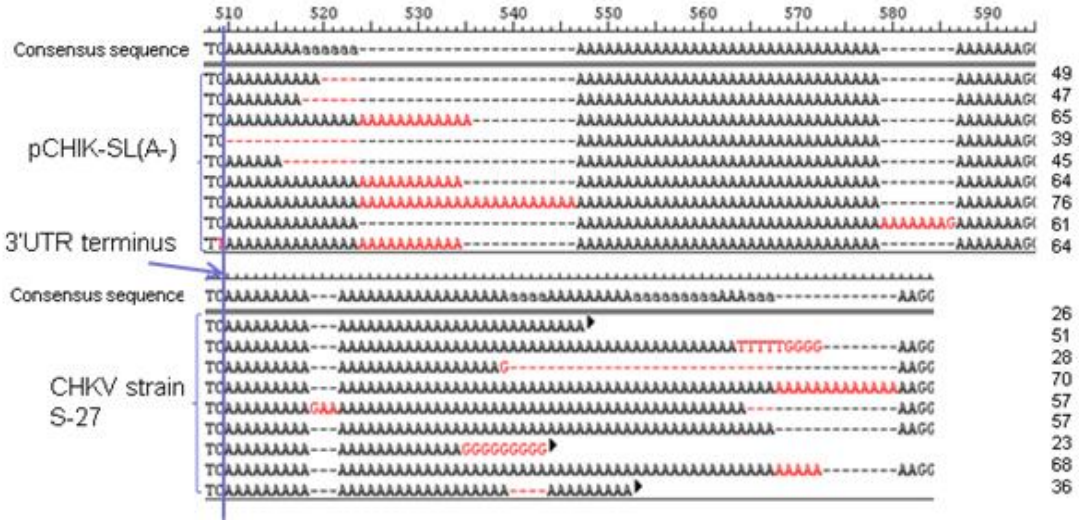

Figure 2.9 Alignment of CHIKV-specific PCR products covering the 3'UTR and poly-(A) tail region. The Affymetrix© Poly(A) Tail-Length Assay Kit was used to amplify the 3'terminal region of CHIKV genomic RNA from strain S27 and from rescued SL-R233 obtained from cDNA clone pCHIK-SL(A-).Nine aliquots of each amplicon were cloned into the Zero Blunt® II TOPO® PCR vector, sequenced and the adenine residues in the tail region counted.

In light of these results, clone pCHIK-SL(A-) was further modified to include a 3' (dA) tail consisting of 40 adenosine monophosphate molecules (approximately midlength in the range observed above). In addition to the CHIKV genome components present in pCHIK-SL(A-) a section of DNA derived from the MCS of earlier sub-clones, was removed and the poly-(A) tail was followed immediately by an ApaI recognition sequence (GGGCCC), used to linearize the plasmid prior to *in vitro* transcription, thus reducing the distance between the end of the cloned virus genome and this site. The new clone was called pCHIK-SL(wt).

2.31 Rescue of progeny virus

The earliest signs of cytopathic effect (CPE) was observed 5 days following the transfection of BHK-21 cells with *in vitro* transcribed RNA generated from plasmids pCHIK-SL(wt) and pCHIK-SL(A533V). This was characterized by cells first adopting a rounded appearance, then becoming detached from the culture vessel surface. Supernatant was harvested and stored in 1ml aliquots at -80°C. In order to confirm that the CPE was due to an infectious agent 0.5ml of each supernatant was used to infect confluent BHK-21 monolayers in T75 flasks. The appearance of CPE after incubating these for a further 72hr indicated that this was the case. The presence of CHIKV was confirmed by extracting RNA from 140µl of each supernatant and amplifying a 1.3kb fragment covering the genome region in which the mutation discussed in section 2.22 had been introduced (nucleotides 1008-2405), by RT-PCR. The amplicons were sequenced using the PCR primers and analysed using the MegAlign software to ensure their correct identities.

This confirmed that two genotypically distinct viruses had been recovered from BHK-21 cells transfected with plasmids pCHIK-SL(wt) and pCHIK-SL(A533V). It is these viruses, hereafter termed CHIK-SL(r-wt) and CHIK-SL(r-mut) respectively, that were the subjects of the remainder of this study.

DISCUSSION

Since the onset of a series of epidemics first seen in Eastern Africa and the Indian Ocean islands in 2004, several changes have been reported both in the epidemiology and phylogeny of CHIKV. Whereas formerly CHIK outbreaks tended to be relatively limited in size, sporadic and self-contained, waves of the disease have now spread across India to the Far East, into Southern Europe and to numerous African countries. Moreover, during the time that has elapsed since this was recognized, a range of atypical clinical conditions have been attributed to the strains that have emerged. Genomic analysis of recent strains has demonstrated significant evolution from the strains isolated from the early outbreaks when compared to those currently circulating. Prior to the period 2004-2005, the predominant invertebrate vector implicated in transmitting CHIKV to urban populations was the mosquito species, *Ae. aegyptii* and thus the geographic distribution of this species reflected that of the virus. However, more recently several key mutations are believed to have enabled CHIKV to more efficiently colonize and be disseminated by an alternative vector, *Ae. albopictus*. Although once thought to limited in its distribution to sub-tropical regions in the Far East, *Ae. albopictus* has been introduced to many new territories in the past 20-30 years (table 1.5, chapter 1). Thus, the potential exists for the exposure of large immunologically naïve populations to CHIKV.

Several pathological aspects of CHIK disease have yet to be explained. One reason for this until recently, was the lack of a suitable animal model, susceptible to CHIKV and in which symptoms similar to those seen in humans could be reproduced. However, since 2010 both mouse and primate models have been reported, (as discussed in section 1.7, chapter 1). These advances have paved the way for the use of

reverse genetics techniques to investigate viral genes, their products, functions and potential as virulence factors.

Three full length cDNA clones of the virus genome have been produced and used to transcribe infectious RNA. In the first version of the w/t clone the genome was inserted into the pGEM5Z(+) vector between the SacI and SpeI restriction sites in the orientation that would allow transcription by SP6 RNA polymerase. The viral insert terminated at the end of the 3'UTR and did not include a poly-A tail. In order to carry out efficient *in vitro* transcription it was necessary to linearize the recombinant plasmid downstream from the insert, ideally close to the 3'end. A single ApaI site present at the 3' end of the vector MCS (with respect to the orientation of the CHIKV insert) remained after completion of the construct. This site which is absent in the genome of SL-R233, resulted in the addition of 78 nucleotides between the end of the 3' UTR and the cleavage site.

Early attempts at transfecting mammalian cells by electroporation were successful, resulting in w/t virus with a genome that differed from the original isolate only by the presence of 3 silent mutations. The translation products would thus be predicted to be identical in amino acid sequence. However, several attempts were made to repeat this procedure using identical conditions, without success. It was clear that for this reverse genetics system to be of use it would be necessary to routinely recover infectious virus from cells. It also became clear that clone pCHIK-SL(A-) differed from other published alphavirus clones in that it lacked a 3' poly-A tail.

Interestingly, it was possible to detect large stretches of virus-specific RNA (>1kb) in the supernatant taken from BHK21 cell cultures that had been electroporated with virus RNA but failed to produce progeny virus after 8 days. This was interpreted as indicating that the function of the poly-(A) tail was not to impart stability to virus RNA in the host cell environment.

Although several descriptions of infectious clones of CHIKV and other alphaviruses have been published in the scientific literature (Vanlandingham *et al* 2005, Mareilke Kümmerer *et al* 2012, Akhrymuk *et al* 2012, Frolova *et al* 2002, Breakwell *et al* 2007, Simmons *et al* 2010), details of poly(A) tail length are sparse. A search was conducted in the GENBANK database for CHIKV genome submissions and revealed that this feature is rarely included. Assays were performed with cloned RNA extracted from virus recovered from cloned CHIKV SL-R233 and from the African prototype strain S27. A comparison of nine clones made from single amplified reaction mixtures showed the presence in both samples of a range of tail lengths, between 21 and 78 adenosine repeats. It was concluded from these results that infectious CHIKV may have tails of a range of lengths and from the small sample analyzed here, a minimum of 23.

A second version of the w/t CHIKV clone was produced with a 3' tail consisting of 40 adenine residues, immediately followed by the unique ApaI restriction site. In addition a small DNA region of 78 nucleotides carried over from the MCS of earlier sub-clones, (between the virus 3'UTR and the ApaI site) were eliminated. RNA transcribed from this second version of the w/t CHIKV (CHIK-SL(r-wt)) showed

increased efficiency for transfecting BHK21 cell cultures, indicating that although not essential, the inclusion of a 3' poly-A tail has a positive effect on this process.

The w/t CHIKV clone constructed in this study is a single genome representative of the ESCA lineage of viruses present in Southeastern Asia in 2006. It has been demonstrated that w/t virus, genotypically identical to the parent isolate can be rescued when transcribed RNA is used to transfect cell cultures. This product will facilitate reverse genetics studies to elucidate the contribution of specific genomic structures and amino acids in the viral life cycle and in interactions with host factors.

It was next decided to develop a third clone with which to investigate whether the virulence determinant reported by Heise *et al* (2000) in the nsP1/nsP2 cleavage domain of SINV is also present in CHIKV. This construct, pCHIK-SL(A533V) contained a CHIKV-specific insert that differed from the w/t clone by the presence of a A533V mutation at the P3 position in the nsP1/nsP2 cleavage domain in the polypeptide precursor. Although this region is highly conserved, the mutation had no effect on virus viability. Progeny virus derived from each clone was sequenced to verify its genotype. In the remainder of this investigation it is planned to compare the phenotypes of w/t and A533V mutated virus, CHIK-SL(r-wt) and CHIK-SL(r-mut) both *in vivo* and *in vitro* with particular regard to the induction of type I interferon.

CHAPTER 3

Study of the phenotypes of wild type and A533V mutant CHIK viruses by *in vitro* studies

As discussed in the earlier chapters, the overall aim of this study was to develop a reverse genetics system with which to investigate potential factors involved in CHIKV pathogenesis. In chapter two the construction of cDNA clones pCHIK-SL(wt) and pCHIK-SL(A533V) and their use as templates for transcribing infectious RNA virus was described. Whereas pCHIK-SL(wt) encodes the consensus sequence of the virus isolate, SL-R233, pCHIK-SL(A533V) contains a mutation in the 5' ORF resulting in its translation into a non-structural polyprotein that contains an alanine to valine substitution at the p3 position in the nsP1/nsP2 cleavage domain. Having constructed the infectious clones, it was necessary to generate virus stocks and characterize each in terms of their plaque morphology, growth kinetics and their effect on host cell gene expression.

Two cell lines were used in this study, L929 and Vero cells. The L929 cell line is a murine fibroblast cell line that is susceptible to alphavirus infection and capable of mounting an IFN response (Sourisseau *et al* 2007, Cruz *et al* 2010). This cell line was chosen as a host cell line with which to assess the ability of the two viruses CHIK-SL(r-wt) and CHIK-SL(r-mut) to induce type 1 IFN. The Vero cell line is derived from kidney epithelial cells from a vervet (African green monkey) and one in which CHIKV can be grown to high titres (Sam *et al* 2012 Sourisseau *et al* 2007). For this reason it was chosen for plaque purification and propagation of stock virus for further

studies. In contrast to the majority of mammalian cell types Vero cells are incapable of producing type 1 IFN, although they possess the appropriate receptors and respond to IFN when it is provided exogenously (Emeny and Morgan 1978, Desmyter *et al* 1968, Rhim *et al* 1969).

METHODS

3.1 Virus titration by plaque assay

Assays were conducted in triplicate using Vero cell monolayers at 90-100% confluence in the wells of 6-well (35mm) cell culture dishes. For growth curve experiments, these were infected in duplicate with 10-fold dilutions of virus in DPBS essentially as described in section 2.5 except that the total volume added to each well was 0.25ml. For titration of stock virus, the cells in four wells were infected with each dilution. During the 1hr incubation period for virus attachment, the added virus suspension was gently rocked every 15min to allow an even distribution. Next the cells were aspirated and covered with 3ml of molten overlay consisting of 50% DMEM supplemented with 5% FBS and 1% agarose.

This was allowed to solidify at room temperature, after which the culture dishes were transferred to an incubator where they remained under standard incubation conditions for 65-72 hr. A delay between addition of the virus and commencement of incubation was inevitable as a result of the surface decontamination procedure required when removing potentially contaminated items from a class 3 safety cabinet. For the incubation time stated above, timing commenced only when the culture trays were placed in the incubator.

The cells were fixed by adding 3ml of 10% formalin v/v in water to each well and incubating at room temperature for a minimum of 1hr. The agar was removed using a spatula under a running tap and the adherent cells stained by the addition of 2ml 0.2%

crystal violet (Sigma, UK) in 50% v/v methanol. Staining was allowed to proceed for a minimum of 15min, after which time the cells were rinsed under a running tap. The dishes were dried by inverting over tissue paper at room temperature and plaques counted against a light background. Plaques were counted in those wells containing a minimum of 10 and a maximum of 80 plaques, in order to minimize errors selected for estimation of the virus titre (expressed in terms of plaque-forming units (pfu) per ml).

3.2 Plaque size estimation

In order to determine differences in plaque size, assays were conducted under identical conditions and images produced by digital photography. These were magnified by a factor of 3 and were used to measure the diameter of fifty plaques of w/t and fifty plaques of A533V mutant viruses using proportional dividers. The average plaque diameter for each type was determined after adjusting for the magnification factor.

3.3 Virus plaque purification

Plaque assays were conducted as described in section 3.1. Prior to fixing the cell monolayer, plaques were picked from beneath the overlay in the assay well, using the tip of a sterile 10ml pipette. After mixing each agarose plug obtained in this way by briefly vortexing in 1ml serum-free DMEM, they were transferred to a -80°C freezer and stored overnight. Vero cell monolayers grown to 90-100% confluence in T25 culture flasks were infected with 0.5ml of each plaque harvest and incubated until

CPE was visible. The cell-supernatant suspension was harvested and stored at -80°C until required.

3.4 Virus stock preparation

Two Vero cell monolayers grown in T75 flasks to 90-100% confluence were infected with 0.5ml supernatant from a plaque purification harvest diluted in serum-free medium. Virus was harvested from the supernatant after the appearance of CPE and stored in 1ml aliquots in cryogenic vials at -80°C. RNA was extracted from both CHIK-SL(r-wt) and CHIK-SL(r-mut) stocks and fully sequenced.

3.5 Virus growth kinetics

Vero and L929 cells were grown in T25 culture flasks to 90-100% confluence then infected with virus with a multiplicity of infection (MOI) of 0.01 pfu per cell. At various times post-infection flasks were transferred from the incubator to a -80°C freezer where they were stored for a minimum of 2hr. The process of freezing and subsequent thawing to room temperature was conducted to ensure lysis of host cells. Virus was harvested from the thawed supernatants prior to plaque assay titration.

3.6 Preparation of virus for electron microscopy of virus samples

Two Vero cell monolayers grown to 90-100% confluence in T75 flasks were infected with 1 $x10^6$ pfu of stock virus; in a third flask DPBS was used in place of virus (negative control). The two virus infected flasks were incubated for periods intended

to provide the maximum yield of cell-associated virus; one was incubated for 20hr and the other (and the negative control), for 24hr. These times were judged to be sufficient to enable maximum virus growth prior to the appearance of CPE.

Following incubation, the supernatant was decanted and primary fixation conducted. Sufficient 2.5% glutaraldehyde was added to submerge the cells (approximately 10ml) which were next incubated at room temperature for 2hr. The monolayer was scraped off and the cell-glutaraldehyde suspensions transferred to 15ml Falcon polypropylene centrifuge tubes. The samples were centrifuged at 3,000 rpm for 10min and the pellets resuspended in 1ml Sorrensen's phosphate buffer (0.133 M Na_2HPO_4, 0.133 M KH_2PO_4 pH 7.4). Further processing and production of transmission electron microscope (TEM) images were carried out by Mr H Tolley, Microbial Imaging Laboratory, PHE, Porton Down. The main steps of this were as follows: the cells were centrifuged and the resulting pellet resuspended in osmium tetroxide solution at 2-8°C and incubated for 2-4hr. Following a further centrifugation step the pellet was mixed with molten agar. After cooling, the agar cubes were dehydrated through a graded ethanol series (from 30% to 100%) at room temperature and then embedded in Araldite® resin. Finally after a 72hr polymerisation step, ultrathin sections were cut, stained and visualised by TEM.

3.7 RNA extraction

RNA was extracted from w/t and A533V mutant virus-infected cell cultures. T25 flasks containing a monolayer of 1 x 10^6 L929 cells were infected at an MOI of 0.01 and harvested at various times after inoculation by transferring to a freezer at -80°C and thawing to room temperature. After removing from the freezer the pellet was

resuspended in 600µl of RLT buffer containing 10µl per ml β-mercaptoethanol taken from an RNeasy mini kit (Qiagen®, UK). Samples were then homogenized by centrifuging at 16000 x g for 2min in a QIAshredder RNA immediately prior to purification which was performed by following the protocol supplied by the manufacturer (Appendix A7). This process included the optional on-column DNase digestion step.

3.8 QRT-PCR assays

For analysis of Mx1, IFNa2 and IFNb1 expression TaqMan gene expression assays on demand™ (Life Technologies) were used. These proprietary reagents consist of premixed primer-probe sets, designed to amplify an amplicon across at least one exon junction of the gene of interest in a two-step reaction. Each probe incorporates a sequence-specific probe with a 5-FAM (5-carboxyfluorescein) label at its 3' end and a minor groove binding (MGB) protein.

Prior to PCR-amplification, cDNA was prepared from 50µl of eluted RNA after adding an equal volume of RT master-mix, consisting of 10 x random primer solution, 10 x RT buffer, 25 x dNTP solution and Multiscribe™ Reverse Transcriptase taken from a High-Capacity cDNA Reverse Transcriptase kit (Applied Biosystems, UK). This reaction mixture was incubated in an ABI® 2720 Thermal Cycler (Applied Biosystems, UK) at 25°C for 10 min, 37°C for 2hr, 85°C for 10min and was finally cooled to 4°C.

For each gene of interest 16µl per sample of pre-mix was prepared and distributed into the appropriate wells of a MicroAmp® Fast Optical 96-well reaction plate

(Applied Biosystems, UK). The pre-mix consisted of 10µl 2x TaqMan® Universal Master Mix II (Applied Biosystems, UK), 1µl 20x TaqMan® Gene Expression Assay and 5µl water. To each well 4µl cDNA (test samples) or nuclease-free water (negative controls) was added. Thermocycling was carried out using an Applied Biosystems 7500 Fast Real-Time PCR System, conditions were as follows: 50°C for 2min, 95°C for 10min and 40 cycles of 95°C for 15sec and 60°C for 1min. Samples were run in triplicate and the mean average cycle threshold (Ct) values calculated.

3.9 HPRT assays

A NanoDrop 1000 spectrophotometer was used to determine the total RNA concentration present in un-infected and CHIKV-infected cell supernatants harvested at various times post-infection. Each assay was conducted in triplicate using a wavelength of 260nm. Samples containing approximately 30ng RNA were used as template in an Rn_Hprt1_QF_1 QuantiFast® Probe qRT-PCR one step assay according to the manufacturer's protocol (Appendix A12).

3.10 Normalisation of gene expression assays

To calculate the relative quantity of samples assayed by qRT-PCR the Ct value of the gene of interest was normalized against that of the endogenous reference gene (HPRT). The ΔCt value for each sample was determined by calculating the difference between the two ($Ct_{sample} - Ct_{HPRT\ gene}$). Similarly, an appropriate sample was selected as a calibrator for which all other samples were to be compared ($Ct_{calibrator} - Ct_{HPRT\ gene}$). The ΔΔCt value for all other samples was calculated from the formula

($\Delta\Delta Ct = \Delta Ct_{sample} - \Delta Ct_{calibrator}$). To calculate the quantity relative to the calibrator sample, RQ (relative quantity) values were calculated as being equal to $2^{-\Delta\Delta Ct}$.

RESULTS

3.11 Preparation of cloned virus stocks

The supernatants resulting from the transfection of BHK-21 cell cultures with plasmids pCHIK-SL(wt) and pCHIK-SL(A533V), were used to plaque-purify virus. Virus-containing supernatant from each plaque infected monolayer was used to seed secondary flasks for the production of stocks for future work. The storage of harvested virus in small (1ml) aliquots made it possible to recover convenient volumes when needed for multiple experiments without the risk of reducing the titre through repeated thawing and re-freezing. RNA from both cloned viruses [CHIK-SL(r-wt) and CHIK-SL(r-mut)] were fully sequenced and found to be identical to the parent plasmids except that they both contained an additional silent point mutation, an A133G substitution (figure 3.1).

Figure 3.1 Alignment of the genome sequence of plaque-purified CHIK-SL(r-w/t) with that of the parent virus strain SL-R233 revealed that it differed by the presence of a single point mutation (A133G) near to the 5' end of the nsP1 gene. This silent mutation was also present in CHIK-SL(r-mut),

3.12 Virus titration

In order to ensure that subsequent experiments with the w/t and A533V mutant viruses could be conducted at a known MOI it was necessary to obtain accurate virus titres. To achieve this three plaque assays were carried out on virus taken from separate aliquots of each virus. The mean average titres obtained for the two cloned CHIKV working stocks are shown in tables 3.1 and 3.2. These are $2.49x10^7$pfu/ml CHIK-SL(r-w/t) and $3.7x10^6$pfu/ml CHIK-SL(r-mut).

Assay	Total plaques (10^{-5} dilution)	Virus titre x pfu/ml	Mean average titre
w/t 1	252	2.52×10^7	$2.49x10^7$
w/t 2	259	2.59×10^7	
w/t 3	236	2.36×10^7	
A533V	41	4.1×10^6	$3.7x\ 10^6$
A533V	38	3.8×10^6	
A533V	32	3.2×10^6	

Table 3.1 Plaque assay results. Assays were conducted in triplicate, the plaque numbers refer to the total in each well of 6-well assay plates from 250µl of diluted virus and are (a) CHIK-SL(r-w/t) and (b) CHIK-SL(r-mut).

Assay	Dilution	Plaque count (pfu)				Mann-Whitney statistical p-value		
		Well 1	Well 2	Well 3	Well4	Assays 1v2	Assays 1 v 3	Assays 2 v 3
w/t 1	10^{-5}	73	54	61	64	0.7728	0.5637	1.0000
w/t 2	10^{-5}	59	81	58	61			
w/t 3	10^{-5}	53	62	48	73			
Mut 1	10^{-5}	12	14	8	7	1.000	0.3865	0.5637
Mut 2	10^{-5}	11	6	13	8			
Mut 3	10^{-5}	6	9	7	10			

Table 3.2 Mann-Whitney statistical analysis indicates that the titres obtained for each virus type are not significantly different at the level of $P<0.05$.

3.13 Plaque morphology

The appearance of plaques derived from w/t and mutant viruses differed in all assays (figure 3.2). Those produced by w/t virus were larger and had a less regular border than those observed from the mutated virus. When plaque assays with the two virus types were conducted under identical conditions, the average plaque diameter produced by CHIK-SL(r-wt) was 3.34 mm (n=50, SD= 0.348993, whereas that produced by CHIK-SL(r-mut) was 1.64mm, (n=50 SD= 0.161271).

3.14 Morphology of w/t virus by electron microscopy

To observe the physical presence of virus from SL-R233(r-wt)-infected cell cultures, supernatants were analysed by electron microscopy (figure 3.3). The resulting images revealed the presence of large numbers of particles with a similar appearance to wild-type Alphavirus virions in terms of size and morphology, with diameters of approximately 65-75nm (Kuhn 2013, Strauss and Strauss 1994).

3.15 Growth kinetics of CHIKV

In order to determine whether the A533V mutation would result in a defect in replication compared to the w/t virus, the growth kinetics of plasmid-derived viruses CHIK-SL(r-wt) and CHIK-SL(r-mut) were investigated in Vero cells and L929 cells. Both cell lines were infected at a MOI of 0.01 pfu. In Vero cells the growth curves for both w/t and mutated virus (figure 3.4, table 3.3) were similar, reaching a peak titre of 2.6-2.8 x 10^8pfu/ml after 20-24hr. When each virus was used to infect L929 cells at the same MOI, the peak titres observed were three orders of magnitude lower than those obtained with Vero cells (figure 3.5). Virus containing the A533V mutation

reached a peak titre at an earlier stage than CHIK-SL(r-wt) and were shown to significantly differ in growth kinetics (Mann-Whitney statistical test <0.05) (table 3.4).

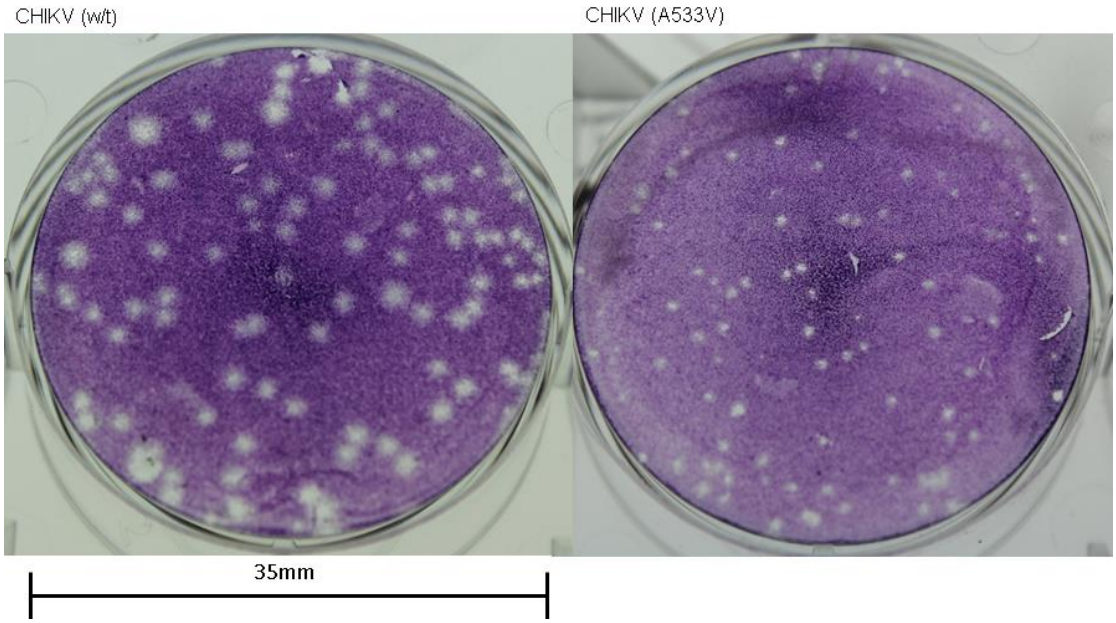

Figure 3.2 Plaque morphology (A) CHIK-SL(r-wt) and (B) CHIK-SL(r-mut). Supernatant from Vero cells infected with each virus was used to infect a confluent Vero cell monolayer in 35mm diameter dishes. Two days after infection, cells were fixed and crystal violet staining was performed.

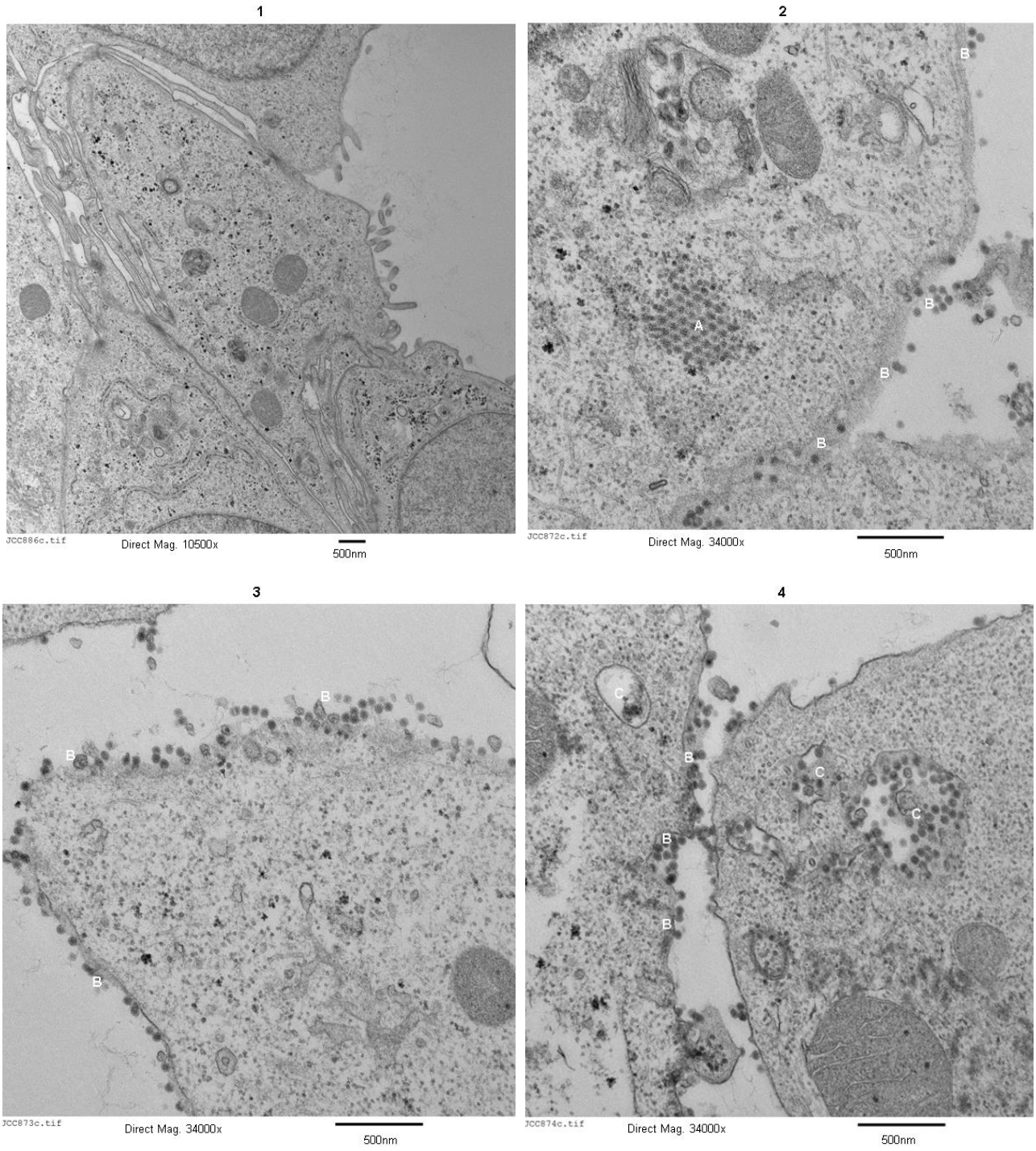

Figure 3.3 Electron micrographs showing Vero cell sections: un-infected (panel 1) and infected with chikungunya virus (panels 2, 3 and 4). Infection was carried out with CHIK-SL(r-wt), rescued from the cDNA clone pCHIK-SL(wt) and cells harvested 24hr post-infection. Nucleocapsids are seen as dark circular structures within the cell cytoplasm (A), in various stages of development at the plasma membrane (B) and in association with intracellular vesicles (C).

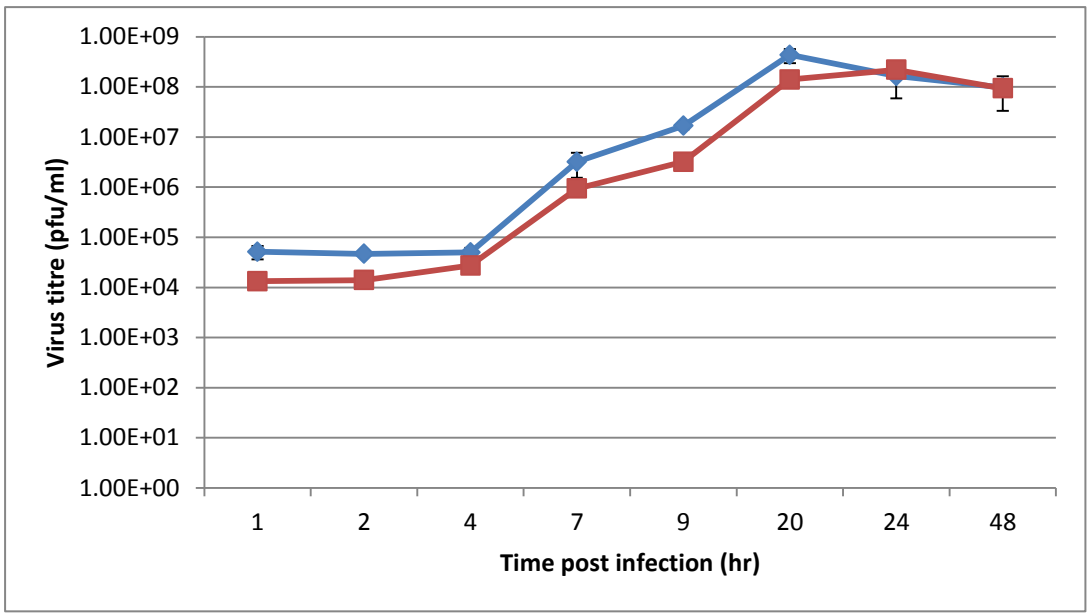

Figure 3.4 Growth curves of wild type (wt) and A533V mutant (mut) viruses (blue and red respectively). Vero cells were infected at a multiplicity of infection (MOI) of 0.01pfu with CHIK-SL(r-wt) and CHIK-SL(r-mut). Cell culture supernatants were harvested at the indicated times and viral progeny titres determined by plaque assays in triplicate. Each data point represents the mean average of the virus titre and the error bars denote standard deviation.

Time post-infection (hr)	Mann-Whitney statistical p-value
	Vero cells
1	0.0129
2	0.0510
4	0.1093
7	0.0108
9	0.0400
20	0.0150
24	0.9362
48	0.4433

Table 3.3 Mann-Whitney statistical analysis comparing CHIKV titres determined by plaque assay, of CHIK-SL(r-wt) and CHIK-SL(r-mut) over the study period. Yellow shading indicates significant values where $P<0.05$.

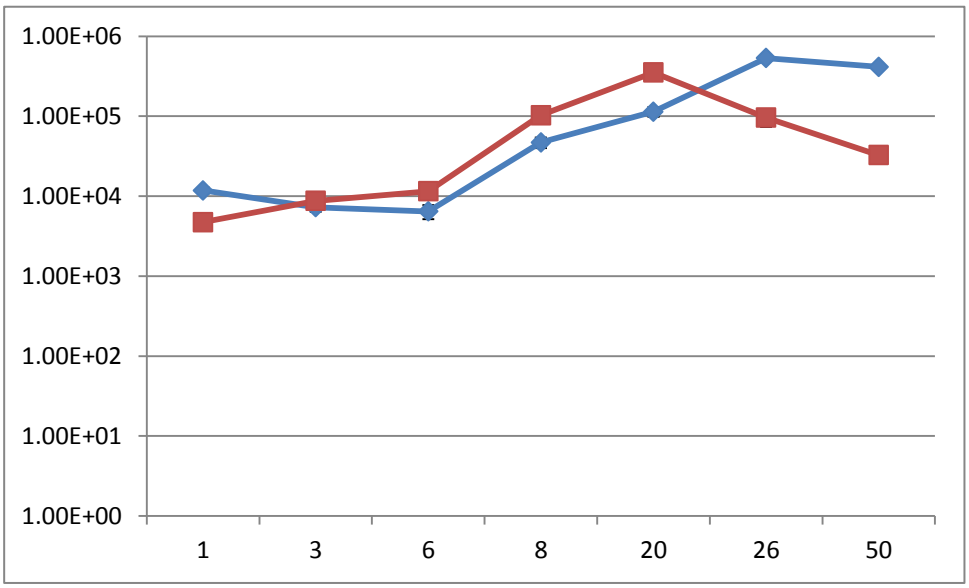

Figure 3.5 Growth curves of wild type (wt) and A533V mutant (mut) viruses (blue and red lines respectively). L929 cells were infected at a multiplicity of infection (MOI) of 0.01pfu with CHIK-SL(r-wt) and CHIK-SL(r-mut). Cell culture supernatants were harvested at the indicated times and viral progeny titres determined by plaque assays in triplicate. Each data point represents the mean average of the titre error bars denote standard deviation.

Time post-infection (hr)	Mann-Whitney statistical p-value
	L929 cells
1	0.0122
3	0.2482
6	0.3123
8	0.0304
20	0.0150
26	0.0021
50	0.0051

Table 3.4 Mann-Whitney statistical analysis comparing CHIKV titres determined by plaque assay, of the two virus populations over the study period. Yellow shading indicates significant values where P <0.05.

3.16 Host cell expression of type 1 IFN and Mx1

Expression of the IFNa2, IFNb1 and Mx1 genes were detected from 26, 20 and 20hr post inoculation respectively in cells infected with w/t virus (figure 3.6). Cells infected with A533V mutated virus showed expression of Mx1 and IFNa2 at an earlier time post-infection than w/t virus. Although IFNb1 expression was detected in cells infected with both virus types at 20hr post infection, the lower threshold cycle observed with mutated virus indicates a higher level of expression.

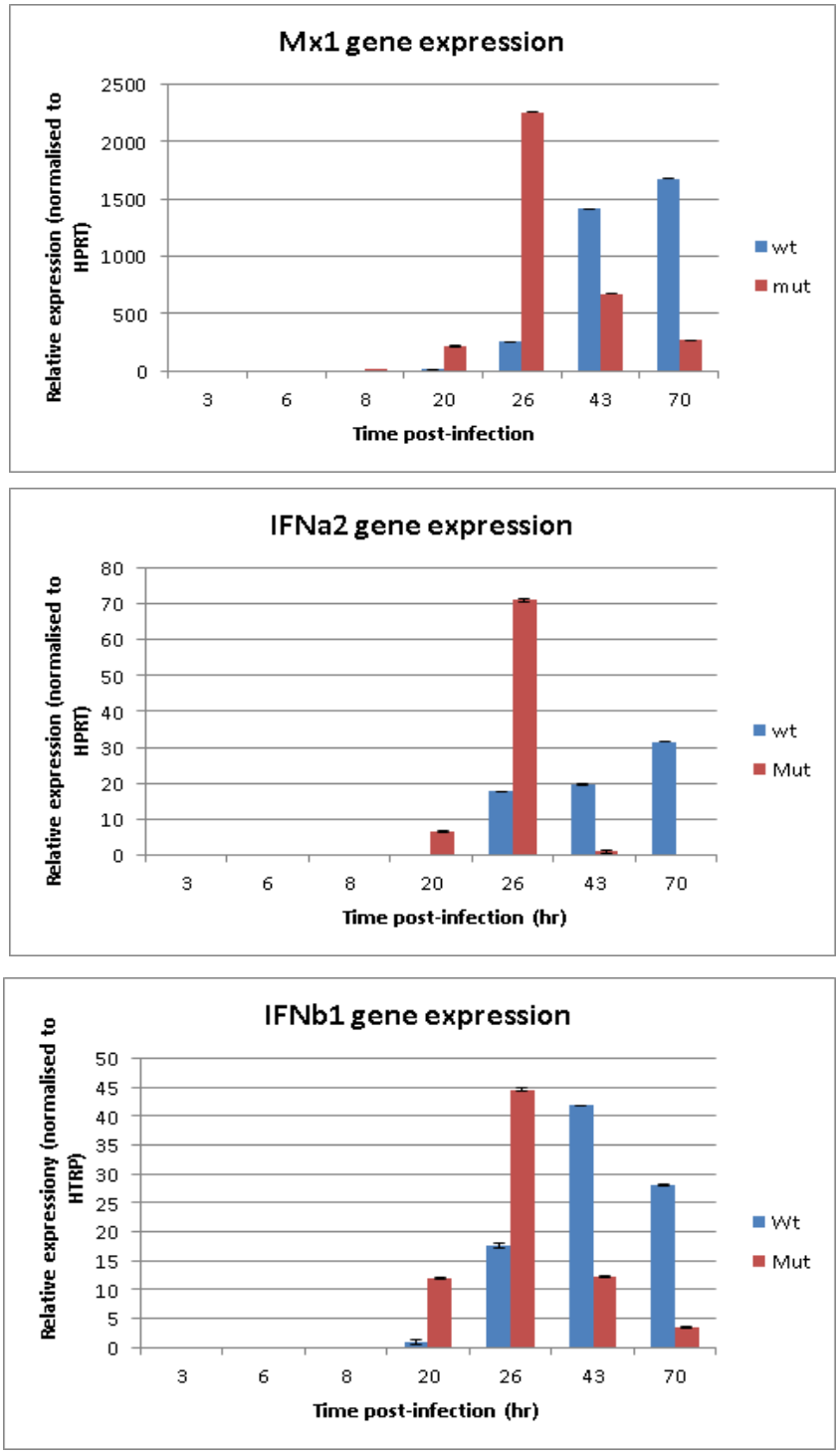

Figure 3.6 Total RNA extracted from L929 cell cultures harvested at various periods post-infection with either CHIK-SL(r-wt) or CHIK-SL(r-mut), was assayed in triplicate by two-step TaqMan qRT-PCR to determine expression of Mx1(a), IFNa2 (b) and IFNb1 (c) genes. The mean C(t) values were normalised with HTRP. The error bars denote the standard deviation of samples.

DISCUSSION

It has been confirmed that infectious CHIKV can be generated from RNA transcribed from the plasmids pCHIK-SL(wt) and pCHIK-SL(A533V) as described in chapter 2. In addition to the three silent mutations known to be present in the precursor of these constructs (figure 2.8), a further mutation, A133G was detected when the genomes from rescued viruses were sequenced. This additional mutation, resulted in a CAA codon being substituted for a CAG codon; both of these encode glutamine. The ORF encoded by the R233-SL(r-wt) genome was predicted to encode identical amino acid sequences to the parental isolate, SL-R233 and R233-SL(r-mut) to differ only by the presence of the engineered A533V mutation,

Particles with features typical of alphaviruses in various stages of their life cycle, were observed in Vero cell cultures infected with w/t virus with an electron microscope. The growth curves produced when both w/t and mutant viruses were grown in Vero cells reached a peak titre of 2-4.3 x 10^8pfu/ml at approximately 20-24hr post-infection, however at the earlier time-points the w/t virus exhibited higher yields, indicating that the introduction of the nsP1 A533V mutation may confer a slight replication defect. This contrasts with the titres estimated for each of the stock virus preparations which were CHIK-SL(r-wt) = 2.49 x 10^7 and CHIK-SL(r-mut) = 2.97 x 10^6. A possible reason for the reduced titres found in the stock viruses is that they were propagated by seeding cell cultures at unknown MOIs. Supernatants that resulted from infecting Vero cell cultures with single plaques were used directly to prepare virus stocks as described in section 3.2 and these were not titrated. The growth kinetics studies were conducted using a low MOI (0.01pfu) which is

conducive to producing a high virus titre, whereas a high MOI may have unknowingly been used for the stock virus cultures.

The A533V mutant virus displayed a smaller plaque phenotype in Vero cells, a finding also reported by Cruz *et al* (2010) who introduced a similar mutation into the RRV genome. In the growth kinetics experiment using L929 cells, the peak titres of both viruses was significantly lower than those observed with Vero cells.

The graph shown in figure 3.5 showing virus titres in samples obtained at various time points after infection of L929 cell cultures indicates that the A533V mutant reached a peak titre earlier that of the w/t clone. The titres obtained from w/t virus declined at a slower rate than those of the A533V mutant virus thereafter; the significance of these observations are supported at <P 0.05 using the Mann-Whitney statistical test.

The relative quantity of transcripts of the IFNa2 and IFNb1 genes and that of the gene encoding the IFN-induced GTP-binding protein, Mx1 were found to be higher at an earlier interval post-infection with the A533V mutated virus. This is consistent with the subsequent studies of other alphaviruses indicating that the introduction of this mutation induces the type 1 IFN response in host cells more efficiently (Cruz *et al* 2010).

Taken together, these results show that the introduction of the A533V mutation to an otherwise w/t clone results in progeny with altered growth characteristics from the parental virus, produces smaller plaques and induces type 1 IFN at an earlier stage in the infectious process. This is consistent with the hypothesis outlined in chapter 1 proposing the presence of a virulence determinant at the site of interest and is supported by subsequent studies showing that analogous mutations modulated the ability of SINV and RRV to inhibit host cell type 1 IFN responses (Cruz *et al* 2010, Simmons *et al* 2010). To investigate in more detail the different CHIKV phenotypes and their influences on disease pathogenesis, it was decided to conduct *in vivo* studies in a mouse model.

CHAPTER 4

Study of the phenotypes of wild type and A533V mutant CHIK viruses in a mouse model

The aim of this part of the study was to evaluate the relative ability of each clone to induce arthritic disease in a mouse model and to investigate whether any differences observed are related to induction of type 1 IFN in host cells. Thus it was necessary to examine the phenotypes of the two cloned viruses described in chapters 2 and 3, in an informative animal model.

Although a macaque model has been developed and shown to reproduce the pathological features seen in humans including viral persistence (Labadie *et al* 2010), the high maintenance costs of multiple experiments for statistically sound results and ethical issues associated with experiments using non-human primates precluded it from consideration. A small animal model that would be suitable for conducting multiple experiments and conform to the available laboratory facilities and financial constraints, was required.

In recent years several mouse models have been developed that mimic clinical symptoms observed in humans and shed light on the pathogenesis of CHIKV disease (table 4.1). Two of these utilised neonatal or adult interferon-deficient mice (Couderc *et al* 2008, Zeigler *et al* 2008). These exhibited overt CHIK disease symptoms, provided information on tissue tropism and highlighted the importance of innate immunological pathways in recovery. However the reliance of this model on an immature or defective immune system limited its relevance to disease in humans. It

was later reported by two separate groups that a localized arthritic condition similar to the disease observed in human cases, could be induced in adult wild type C57BL/6 mice following CHIKV injection in the ventral side of the footpad.

In the first of these studies, mice that were a minimum of 6 weeks of age were used (Gardner *et al* 2010) whereas in the second, 14 day old mice were used, (Morrison *et al* 2010). In both cases a viraemic phase of 4-5 days was observed followed by inflammation of musculoskeletal tissues. As the present study is focussed on immunological responses to infection with CHIKV containing the A533V mutation, the mouse models possessing defective immune systems would not be suitable. Thus the mouse model described by Gardener *et al* (2010) was adopted for the present study as it has been reported to exhibit pathological features consistent with CHIKV disease in humans and does not entail prohibitively high purchasing, housing and maintenance costs.

Animal	Reference	Details
Mouse (129s/v) IFN-α/βR$^{-/-}$ and IFN-α/βR$^{-/-}$	Couderc *et al* (2008)	Intradermal administration. Identified fibroblasts as prominent target cell, disease severity dependent on age and type 1 IFN response.
Mouse ICR and CD-1 strains outbred Newborn and 14 days old	Ziegler *et al* (2008)	Showed age-dependent pathology, however not reported to develop arthritis, so limited relevance to human cases. Young mice more costly.
C57BL/6J and NIH Swiss mice 5 and 10 week old mice	Wang *et a*l (2008)	Intranasal and intra-peritoneal administration. Symptoms seen in younger group only.
Mouse C57BL/6 strain adult ♀ (≥6 weeks old)	Gardner *et al* (2010)	Administration in footpads, established a local persistent infection with disease symptoms similar to human infection.
Mouse C57BL/6J strain wild –type 14 days old	Morrison *et al* (2010)	Established a local persistent infection when virus injected in footpads with disease symptoms similar to human infection. Younger mice than Gardner *et al* therefore more expensive.
Cynomolgus macaques captive-bred 3-5 years old immunocompetent	Labadie *et al* (2010)	Intradermal administration. Similar disease symptoms to those seen in humans. High costs for purchase and maintenance of primates compared to mouse models.

Table 4.1 A summary of the CHIKV disease animal models available at the time of this study.

It was first decided to evaluate the suitability of the C57BL/6 model for the study by confirming its potential to produce measurable foot-swelling when infected with the w/t CHIKV clone and to determine the optimum infectious dose required.

With this information available, a follow-up experiment was planned to compare a range of clinical parameters in tissues obtained in mock-infected mice with those infected from w/t and A533V mutant viruses. The results obtained from *in vitro* studies of the two CHIKV genotypes (in chapter 3) indicated that the A533V mutant virus grew to a lower titre than the w/t virus in cells capable of producing type 1 IFN and that IFN induction occurred earlier in the course of infection. It was next decided

to investigate whether this effect would be reproduced *in vivo* and if so, whether the presence of the mutation would result in an attenuated phenotype, thus testing the hypothesis. Mice infected with the two virus clones would be evaluated from two perspectives. Levels of IFN-α and IFN-β present in samples would be monitored throughout the challenge to determine whether their induction was significantly affected by the presence of the A533V mutation. For evidence of this it was planned to monitor fluctuations in the expression of IFN-α and IFN-β and of the IFN-induced Mx1 gene by qRT-PCR and also to measure the translated products through serological assays.

In order to obtain a more comprehensive picture of the disease profile, the levels of other markers indicative of an innate immune response were also to be measured, namely IFN-γ, haptoglobin (Hp), serum amyloid A (SAA**)** and serum amyloid P (SAP). The anticipated inflammatory response to the CHIKV challenge is a well characterized phenomenon observed following infections or other trauma in mammals. It consists of a coordinated release of a diverse range of inflammatory mediators which induce fever, changes in vascular permeability, vasodilation and changes in the metabolism and catabolism of many organs, both locally and at more distant sites. As the protein mediators of this process have specific roles in controlling inflammation they serve as useful markers of disease pathology.

Hp is a haemoglobin-binding protein, mainly produced in the liver and is known as an acute phase reactant (Dobryszycka 1997). It is present in serum in increasing amounts during acute conditions such as infection, injury, tissue destruction and some cancers.

Its purpose is to remove damaged cells and debris and to prevent loss of iron through the kidneys. Acute phase SAA proteins are also synthesised principally in the liver in response to pro-inflammatory cytokines released by activated monocytes and macrophages (Uhlar and Whitehead 1999). Also synthesised in liver cells, SAP is a member of the pentraxin family of molecules, thought to play a role in innate immunity and reported to be an acute phase reactant in mice (Pepys *et al* 1979).

METHODS

4.1 Animals

Experimental procedures involving live animals, measurements, dissections and husbandry were carried out by the Biological Investigation Group (BIG), an expert team of animal procedure license holders who have mandatory control over all experimental work with animals at PHE, Porton, Salisbury, UK. C57BL/6 mice aged at least 6 weeks old were purchased from Harlan Laboratories, UK. Animals were housed in flexible film isolators under climate controlled CL3 conditions and were allowed free access to food and sterile water throughout the study. All animals were treated in strict accordance with the UK Animals (Scientific Procedures) Act 1986.

Prior to the study period, a microchip implant **(idENTICHIP** with Bio-Thermo™, Animalcore Ltd, UK) facilitating identification and body temperature monitoring, was inserted into the subcutaneous tissue of the neck region of each mouse according to the manufacturer's instructions.

4.2 Animal assessments

The distance between the tarsometatarsal joint and the phalanges and width of the perimetatarsal area of the hind feet (figure 4.1), were measured daily using digital calipers. The temperatures and weights were also measured daily. Visual clinical assessments were conducted twice daily in order to identify symptoms such as postural changes, lethargy or ruffled fur that might indicate the onset of disease. Statistical analysis was conducted using the Minitab 16 statistics software package (Minitab Ltd, UK)

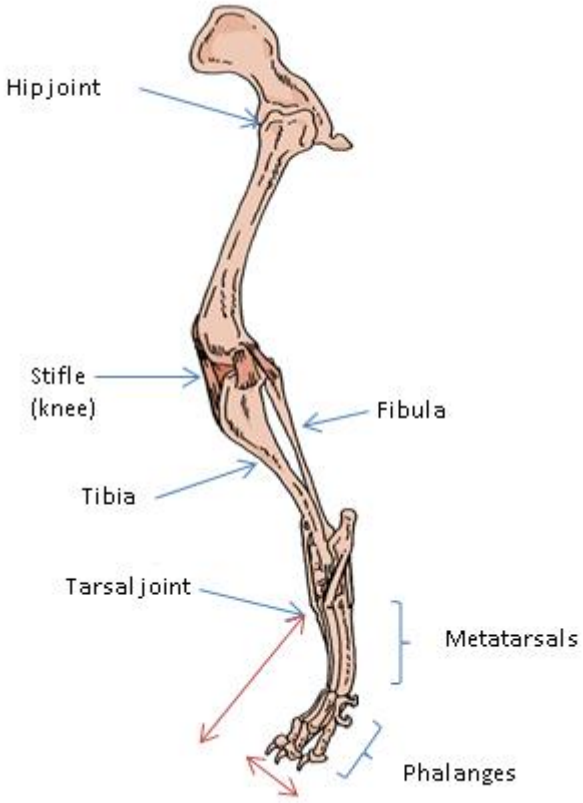

Figure 4.1 Distal view of the spatial relationship of the bones of the mouse hind leg. Red arrows show the approximate areas measured for width and height in order to assess the degree of swelling observed in the C57BL/6mouse model following inoculation with CHIKV.

An initial pilot experiment was conducted to confirm replication of CHIK disease in C57BL/6 mice in our hands and in accordance with Gardner *et al* (2010). Additionally this enabled the optimum infectious dose to be determined. Animals were assigned to seven groups each of which was injected subcutaneously with either w/t or A533V mutant virus at a range of titres as detailed in table 4.2, or with DPBS that constituted a negative control group. As the R233-SL(r-mut) stock was prepared at a lower titre than R233-SL(r-wt), it was possible to challenge mice over a wider titre range with the latter than the former. Mice were inoculated subcutaneously into the ventral side of the left hind foot as detailed in table 4.2 and euthanized 14 days after inoculation. Blood samples were collected from each mouse from which sera were separated and stored at -80°C until required.

Group	**Virus / DPBS**	**Virus inoculum (pfu/40µl**
1	CHIK-SL(r-wt)	1.00E+06
2	CHIK-SL(r-wt)	1.00E+05
3	CHIK-SL(r-wt)	1.00E+04
4	CHIK-SL(r-mut)	2.00E+04
5	CHIK-SL(r-mut)	1.00E+04
6	CHIK-SL(r-mut)	8.00E+03
7	DPBS	Negative control

Table 4.2 Details of the inoculum administered subcutaneously to the left hind foot in seven groups of five C57BL/6 mice, to determine the optimum dose required to induce measurable foot swelling (first challenge experiment).

Following the pilot study, the main series of challenge experiments in this work were set out. Animals were assigned to four groups, each defined by their subsequent treatment. Members of group 1 received 1 x 10^4 pfu of cloned w/t virus suspension, group 2, received 1 x 10^4 pfu A533V mutant virus and group 3 received diluent only (serum-free DMEM). As with the first challenge experiment, inoculum volumes were 40µl. Groups 1 to 3 comprised 18 mice each. A further 3 animals, group 4, did not receive an inoculation.

4.3 Tissue sampling

Three mice from groups 1-3 were culled at pre-defined time periods following challenge (1, 3, 6, 9, 12 and 15 days), by the administration of anaesthetic overdose. The group 4 mice were culled on day 9. The following samples were collected for molecular studies: the right hind leg, the right axillary lymph node, the right inguinal lymph node, a spleen sample and a liver sample. These were placed in reinforced 2ml homogenization tubes compatible with the Precellys® tissue homogenizer (Precellys, UK) and immediately transferred to a -80°C freezer until required. Blood was collected in BD Microtainer® serum separator tube**s** (Fisher Scientific UK Ltd), allowed to clot at room temperature for 30-40min and stored on ice prior to further processing. After separation from the clotted material by centrifuging at 9500 x g for 3min, serum samples were recovered. A 140µl aliquot of each was added to 560µl AVL buffer taken from a Qiagen QIAamp® Viral RNA Mini Kit (Appendix A5) and this was subsequently used to purify RNA. The remaining serum was transferred to cryogenic screw-capped tubes and stored at -80°C until required for immunoassays. The remaining (left) hind leg from each animal was placed in neutral buffered 10% formalin (approximately 4% formaldehyde w/v) and sent for histological examination.

4.4 Histopathology investigation

Tissue specimens were processed for histological analysis by the Histology Department at PHE, Porton, Salisbury, UK. Leg samples from the stifle and tarsal regions were processed to paraffin wax and 5-6µm sections cut and stained with hematoxylin and eosin (H&E). Slides were examined "blind" by light microscopy and advice on interpretation was provided by pathologists Prof Em.GR. Pearson and Dr EL. Rayner.

4.5 Tissue processing

The weight of each mouse tissue sample was estimated by subtracting the mean average weight of 50 prefilled bead homogenization tubes from that of each sample-containing tube. Samples were suspended in 1ml chilled DPBS and subjected to 3 cycles x 6200rpm for 5 seconds separated by 30 second pauses, using a Precellys® 24 tissue homogenizer (Bertin Technologies UK). A 140µl aliquot of each tissue suspension was mixed with 560µl RLT buffer containing 10µl per ml β-mercaptoethanol taken from an RNeasy mini extraction kit (Appendix A7). The remainder was stored at -80°C until required.

4.6 Serological assays

Serological assays were conducted using a range of commercially available ELISA kits. For mouse haptoglobin, SAA and SAP assays, kits purchased from Life Diagnostics Ltd, UK were used (catalogue numbers 2410-1, 3400-1 and 3410-1 respectively). IFN-αand IFN-β were assayed with Verikine™ mouse interferon ELISA kits (catalogue numbers BPL-42410 PBL-42120), IFN-γ was assayed with a Nova® mouse IFN-γ kit (Life Technologies, UK catalogue number KMC4022). Each

assay was performed in accordance with the relevant protocol provided by the manufacturers (Appendices A15-19).

4.7 Assessment of viraemic phase by block RT-PCR

RT-PCR assays were used to detect the presence of virus in 5µl of RNA samples purified from mouse serum infected with w/t virus, in a total volume of 50µl (chapter 2, section 2.10). RNA purification was carried out on 35µl of serum mixed with 140µl AVL buffer taken from a Qiagen QIAamp® Viral RNA Mini Kit (Appendix A5). This four-fold reduction in the volumes from those recommended by the manufacturer was undertaken to conserve the limited volumes of serum available; for the remainder of the process the manufacturer's protocol was adhered to. The primers CHIK1F and CH425F (tables 2.4 and 2.5) were used to amplify and analyse the 5'-terminal 425 nucleotides of the CHIKV genome using the methods detailed in chapter 2 (sections 2.10 to 2.12) and thermocycling at 50°C for 15min, 94° for 2min, 40 cycles of 94°C for 15sec, 55°C for 30sec, 68°C for 30sec and finally 68°C for 5min. Agarose gel electrophoresis and imaging was conducted on 10 µl samples as described in chapter 2, section 2.12.

4.8 Analysis by qRT-PCR assay

All qRT-PCRs were conducted using the MiniOpticon™ system (BioRad, UK) or the Applied Biosystems® 7500 Fast Real-time PCR system (Life Technologies). Assays to detect relative expression of IFNA2 and IFNB1 and Mx1 genes were performed as described in section 3.8 of Chapter 3.

Assays to detect and quantify CHIKV-specific amplicons were conducted using a one-step RT-PCR method developed in this laboratory (Edwards *et al* 2007).The sensitivity of this method was determined using *in vitro* transcribed RNA, generated from a cloned cDNA copy of the amplicon (pCH127) as template. The 127bp cDNA amplicon was cloned downstream from a T7 promoter sequence in the pMK plasmid vector by GeneArt (Life Technologies, UK). An XbaI site was engineered immediately downstream from the 3' end of the insert to enable linearization prior to *in vitro* transcription. Lyophilized plasmid DNA supplied by the manufacturer was resuspended in 50µl water prior to use as a template for *in vitro* transcription.

Linearization was carried out by adding 10µl pCH127 DNA to a reaction mixture consisting of 10u XbaI and 300mg bovine serum albumin in 1 x Promega restriction buffer D (table 2.6, chapter 2) in a total volume of 30µl. The reaction was incubated for 3hr at 37°C. *In vitr*o transcription was initiated at the T7 polymerase promoter and ended at the XbaI digestion site immediately following the CHIKV insert. Three transcription reactions were conducted using 8µl of linearized plasmid as template with the reagents from a MEGAshortscript™ kit, according to the manufacturer's instructions (Appendix A13). The resulting RNA was pooled and purified using a Qiagen RNeasy Mini-Elute kit, eluting with 30µl water. The sample absorbance was measured at the ultraviolet wavelength of 260nm using a NanoDrop 2000® spectrophotometer. It was then possible to calculate the RNA concentration on the basis that an absorbance of 1.0 unit at 260nm corresponds to 40µg per ml (Sambrook *et al* 1989) and thus to produce a standard curve to determine and compare genome copy numbers. The molecular weight the of ribonucleotide monophosphates AMP, CMP, GMP and UMP are 347.2, 323.2, 363.2 and 324.2 Daltons (Da) respectively.

The 5’ end of the RNA transcript from the linearized clone begins immediately after the final uridine molecule in the T7 promoter and ends after the first thymidine molecule in the XbaI site. The molecular weight was estimated to be 62220, by multiplying the total number of nucleotides in this region (183 nucleotides), by 340 (the approximate mean average of the individual nucleotides shown above). The transcribed RNA copy number was calculated using the Avogadro constant in the equation:

$$n = \frac{6.0221 \times 10^{23} \text{ molcules/mole}}{62220 \times 1 \times 10^{9} \text{ ng}}$$

The standard value series was made by making a series of ten-fold dilutions of the *in vitro* transcribed RNA prepared in water containing 1×10^{7} to 1×10^{1} copies and used as template in qRT-PCRs. The average C(t) from three assays was used to prepare a standard curve through which the relationship between C(t) and template copy number could be extrapolated. The standard curve was subsequently used to estimate amplicon copy numbers in tissue samples assayed by qRT-PCR and this was taken as an approximate measure of genome copy number as has been done in other studies (Gentilomi *et al* 2008, Huang *et al* 2009, Dhanwani *et al* 2014).

RESULTS

4.9 Clinical assessment of mice

The purpose of the first (pilot) mouse challenge was to determine the optimum dose required to induce measurable foot swelling. As this exercise was limited to determining whether the chosen mouse model was suitable for evaluating the CHIKV clones under study and in order to minimize discomfort in the mice, injection of virus was restricted to a single (left) hind limb. No indication of inhibited mobility or other overt signs of ill health were observed in any animal, consequently, the local ethics committee considered it acceptable to infect both hind legs in the main challenge, thereby providing additional material for analysis.

For the pilot experiment, an analysis of the measurements made on the hind legs demonstrated significant swelling from days 9-13 post-challenge in the feet injected with virus (left feet), when compared with the DPBS control group. The corresponding right feet of the virus-challenged animals also showed swelling, although this was less extensive than those observed in the injected feet (figures 4.1-4.6). The Mann-Whitney Statistical test was used for the analysis of all treatment groups compared with negative controls. Swelling did not significantly vary in severity between animals challenged with w/t virus and the A533V mutant even when the viral dose was identical (groups 4 and 5). No increase in swelling was observed between animals receiving the lowest w/t viral dose (10^4 pfu) and those receiving higher titres (10^5 and 10^6 pfu). Consequently it was decided to conduct the subsequent challenge with this lower dose (10^4 pfu).

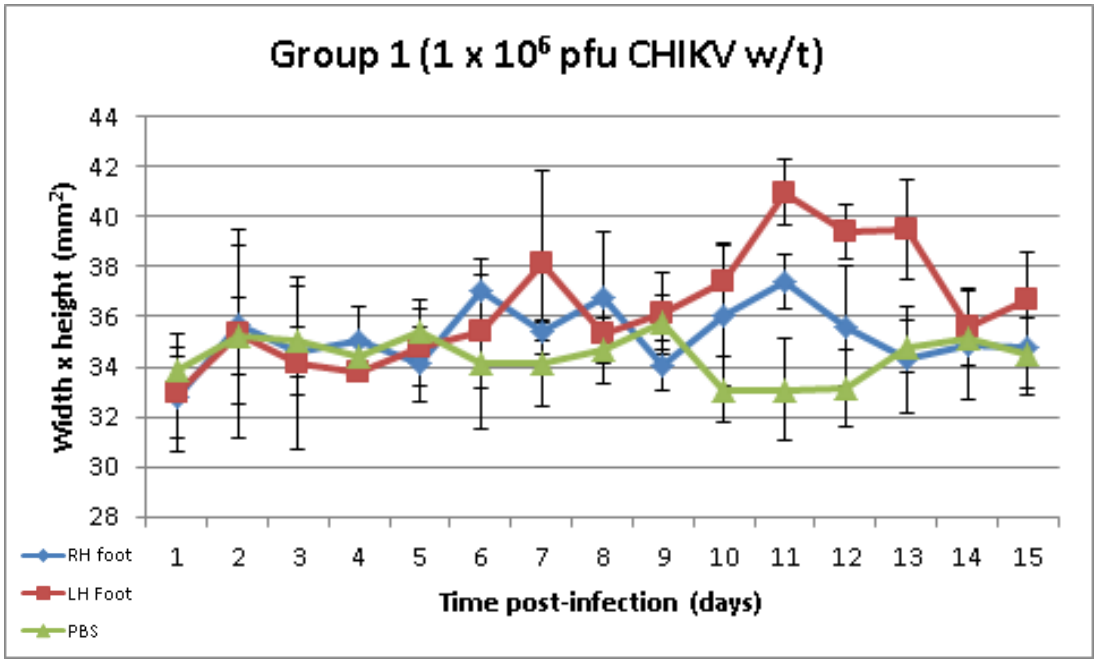

Figure 4.2 Changes in foot size as an indication of inflammation, observed over a 15 day period following the injection of w/t CHIKV (10^6 pfu in 40µl) to the left hind feet of C57BL/6 mice. The width and height (from the heel joint to the end of the foot) were multiplied together to estimate the approximate area (mm^2). Results show mean values from five mice with error bars denoting the standard deviation.

Time post-challenge (days)	Group 1 Mann-Whitney statistical p-value	
	Left foot v diluents	Right foot v diluents
1	0.2703	0.2721
2	0.7133	0.9025
3	0.5403	0.7133
4	0.2703	0.3913
5	0.5403	0.1113
6	0.7133	0.1779
7	0.1779	0.1779
8	0.3913	0.1779
9	0.7133	0.1113
10	0.0200	0.0662
11	0.0200	0.0200
12	0.0200	0.2703
13	0.0200	0.6242
14	0.4624	0.5303
15	0.1113	0.9025

Table 4.3 The Mann-Whitney statistical test was used to determine differences between the injected foot (left hind) and both the right hind foot of the same animal and the DPBS control group: $P < 0.05$. Yellow shading indicates that Mann-Whitney statistical test is significant.

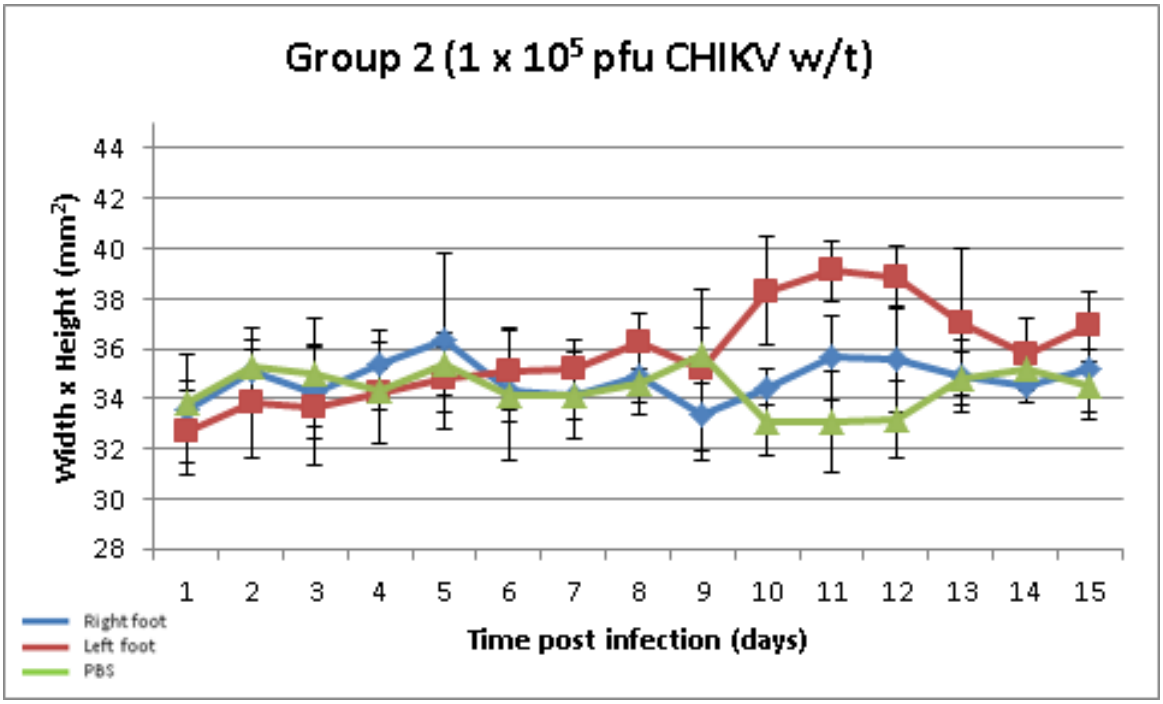

Figure 4.3 Changes in foot size as an indication of inflammation, observed over a 15 day period following the injection of w/t CHIKV (10^5 pfu in 40µl) to the left hind feet of C57BL/6 mice. The width and height (from the heel joint to the end of the foot) were multiplied together to estimate the approximate area (mm^2). Results show mean values from five mice with error bars denoting the standard deviation.

Time post-challenge (days)	Group 2 Mann-Whitney statistical p-value	
	Left foot v diluents	Right foot V diluents
1	0.2101	0.2101
2	0.2963	0.2963
3	0.5309	0.5309
4	0.6761	0.6761
5	0.4034	0.4034
6	0.2101	0.2101
7	0.1437	0.1437
8	0.0947	0.0947
9	0.6761	0.6761
10	0.0122	0.0122
11	0.0122	0.0122
12	0.0122	0.0122
13	0.0601	0.2101
14	0.6761	0.6761
15	0.0601	0.0601

Table 4.4 The Mann-Whitney statistical test was used to determine differences between the injected foot (left hind) and both the right hind foot of the same animal and the DPBS control group: $P < 0.05$. Yellow shading indicates that Mann-Whitney statistical test is significant.

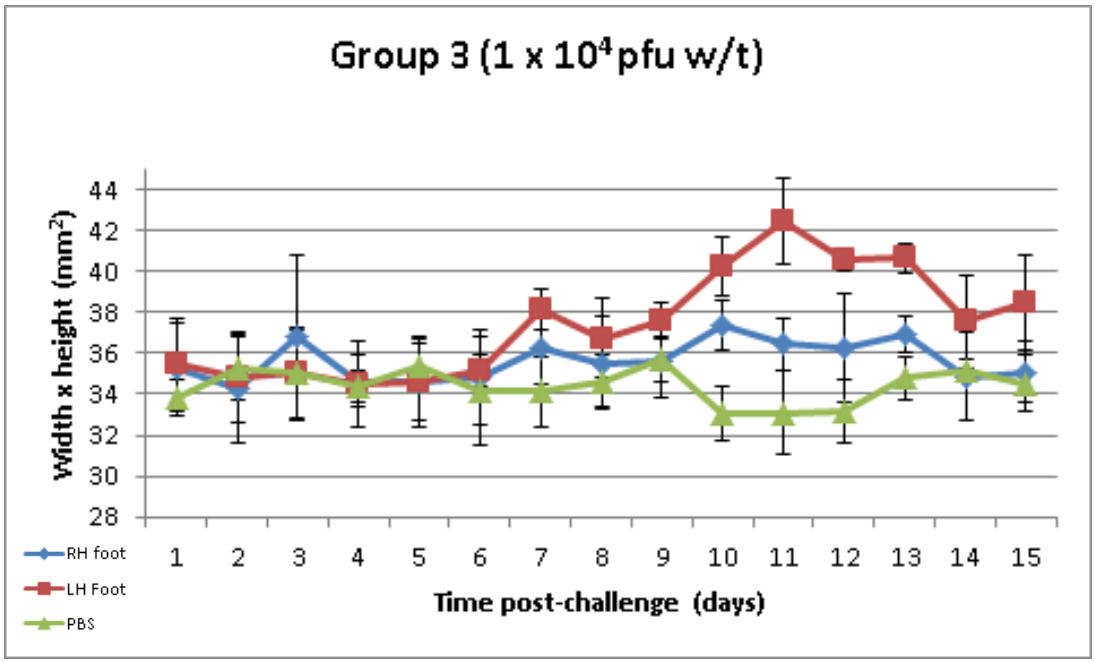

Figure 4.4 Changes in foot size as an indication of inflammation, observed over a 15 day period following the injection of w/t CHIKV (1 x 10^4 pfu in 40µl) to the left hind feet of C57BL/6 mice. The width and height (from the heel joint to the end of the foot) were multiplied together to estimate the approximate area (mm^2). Results show mean values from five mice with error bars denoting the standard deviation.

Time post-challenge (days)	Group 3 Mann-Whitney statistical p-value	
	Left foot v diluents	Right foot V diluents
1	0.2963	0.2963
2	0.6761	0.6761
3	1.0000	0.4034
4	0.8345	1.0000
5	0.2963	0.4034
6	0.2101	0.4034
7	0.0122	0.2101
8	0.2963	1.0000
9	0.0367	0.8345
10	0.0051	0.0122
11	0.0344	0.0367
12	0.0122	0.0601
13	0.0122	0.0122
14	0.1437	0.8345
15	0.0601	0.5309

Table 4.5 The Mann-Whitney statistical test was used to determine differences between the injected foot (left hind) and both the right hind foot of the same animal and the DPBS control group: $P < 0.05$. Yellow shading indicates that Mann-Whitney statistical test is significant.

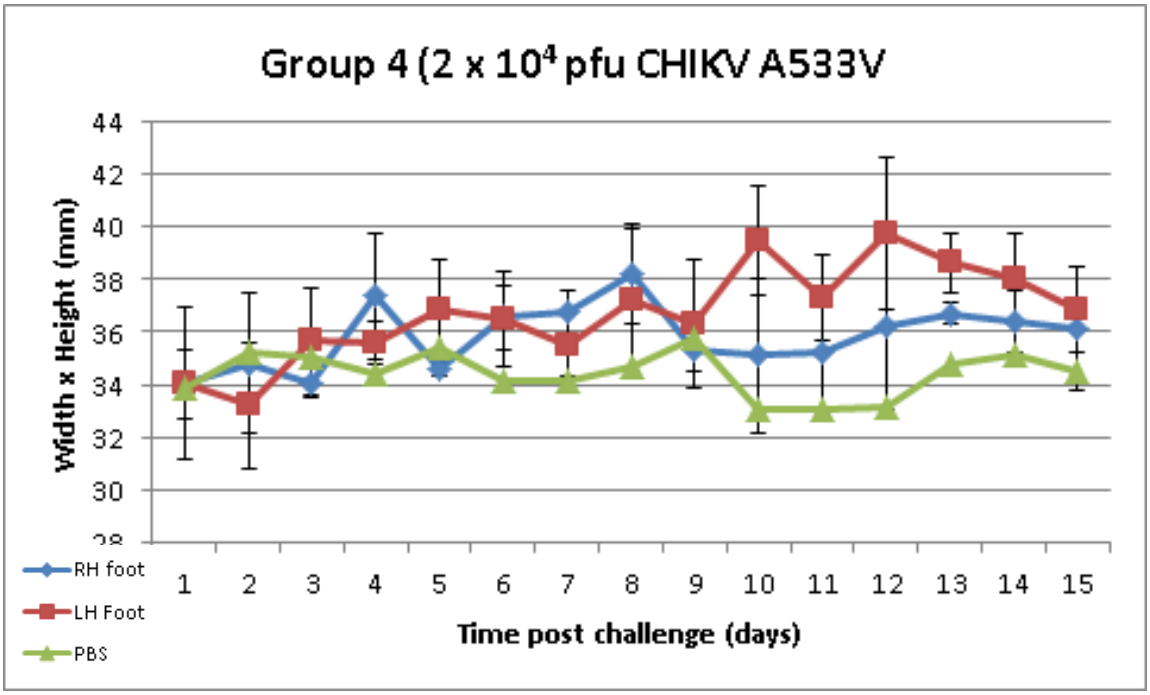

Figure 4.5 Changes in foot size as an indication of inflammation, observed over a 15 day period following the injection of A533V mutated CHIKV (2 x 10^4 pfu in 40µl) to the left hind feet of C57BL/6 mice. The width and height (from the heel joint to the end of the foot) were multiplied together to estimate the approximate area (mm^2). Results show mean values from five mice with error bars denoting the standard deviation.

Time post-challenge (days)	Group 4 Mann-Whitney statistical p-value	
	Left foot v diluents	Right foot v diluents
1	0.7133	0.7133
2	0.1779	1.0000
3	0.5403	0.5403
4	0.0662	0.1113
5	0.1779	0.1779
6	0.2703	0.1779
7	0.1779	0.1113
8	0.1113	0.2207
9	0.9025	0.5403
10	0.0367	0.1779
11	0.0200	0.1779
12	0.0200	0.2207
13	0.0200	0.0200
14	0.0122	0.1779
15	0.1113	0.4624

Table 4.6 The Mann-Whitney statistical test was used to determine differences between the injected foot (left hind) and both the right hind foot of the same animal and the DPBS control group: P< 0.05. Yellow shading indicates that Mann-Whitney statistical test is significant.

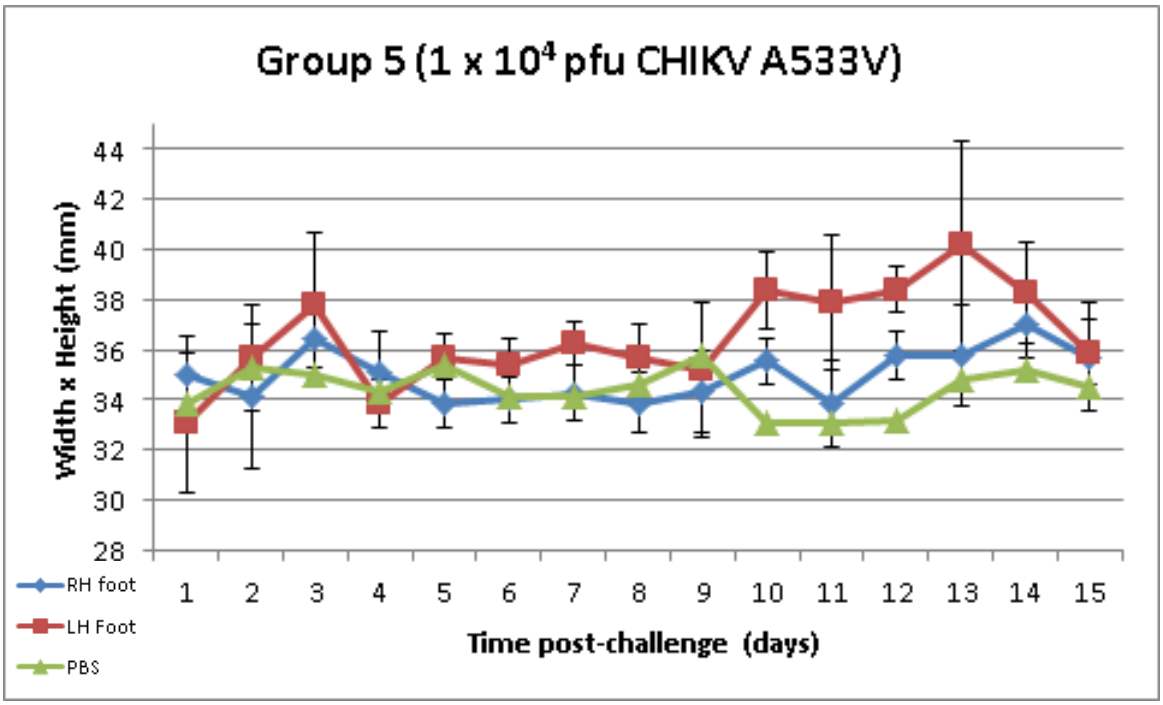

Figure 4.6 Changes in foot size as an indication of inflammation, observed over a 15 day period following the injection of A533V mutated CHIKV (1 x 10^4 pfu in 40µl) to the left hind feet of C57BL/6 mice. The width and height (from the heel joint to the end of the foot) were multiplied together to estimate the approximate area (mm^2). Results show mean values from five mice with error bars denoting the standard deviation.

Time post-challenge (days)	Group 5 Mann-Whitney statistical p-value	
	Left foot v diluents	Right foot v diluents
1	0.4034	0.4034
2	0.8345	0.5309
3	0.2963	0.2963
4	0.4647	0.5309
5	1.0000	0.1437
6	0.2101	0.4034
7	0.0601	1.0000
8	0.0947	0.1437
9	0.8345	0.1437
10	0.0122	0.0367
11	0.0122	0.8345
12	0.0122	0.0367
13	0.0601	0.6761
14	0.0367	0.0947
15	0.2963	0.5309

Table 4.7 The Mann-Whitney statistical test was used to determine differences between the injected foot (left hind) and both the right hind foot of the same animal and the DPBS control group: $P < 0.05$. Yellow shading indicates that Mann-Whitney statistical test is significant.

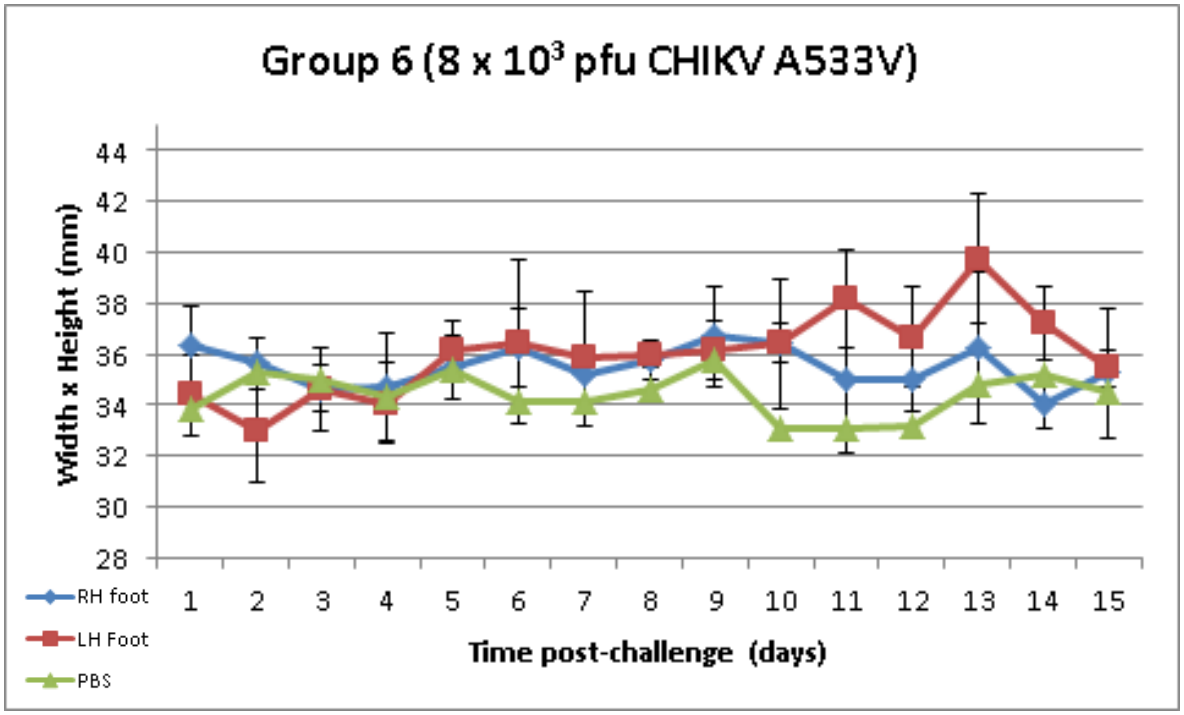

Figure 4.7 Changes in foot size as an indication of inflammation, observed over a 1 day period following the injection of A533V mutated CHIKV (8 x 10^3 pfu in 40µl) to the left hind feet of C57BL/6 mice. The width and height (from the heel joint to the end of the foot) were multiplied together to estimate the approximate area (mm^2). Results show mean values from five mice with error bars denoting the standard deviation.

Time post-challenge (days)	Group 6 Mann-Whitney statistical p-value	
	Left foot v diluents	Right foot v diluents
1	0.5309	0.0521
2	0.0601	1.0000
3	0.6761	0.8345
4	0.6761	0.8345
5	0.4034	0.8345
6	0.4034	0.2101
7	0.2101	0.4034
8	0.0367	0.0947
9	0.6015	0.5309
10	0.0947	0.0122
11	0.0122	0.2963
12	0.0367	0.0601
13	0.0122	0.5309
14	0.0367	0.0601
15	0.5309	0.8345

Table 4.8 The Mann-Whitney statistical test was used to determine differences between the injected foot (left hind) and both the right hind foot of the same animal and the DPBS control group: $P < 0.05$. Yellow shading indicates that Mann-Whitney statistical test is significant.

Several modifications to the main experimental procedure were made in light of the results from the pilot study. In contrast to the first mouse challenge, a group injected with DPBS was not included as a negative control since this was not considered necessary. This was replaced by a diluent control group consisting of mice challenged with the cell culture medium in which the virus stocks had been prepared (DMEM supplemented with 5% FBS). This was to prevent changes caused by components of the growth medium being mistaken for those caused by virus. Finally a negative control group was included, consisting of three mice that received no treatment and were euthanized on the ninth day post-challenge. Figure 4.1 confirms the area measured on the mice to determine swelling; Figure 4.8 and table 4.9 show results from the inflammation assessment.

Throughout the study no significant differences in body temperature or fluctuations in weight gain were observed between the four groups (figure 4.9). Data from the different groups was compared using the Mann-Whitney statistical analysis test $P<0.05$) (tables 4.10 and 4.11).

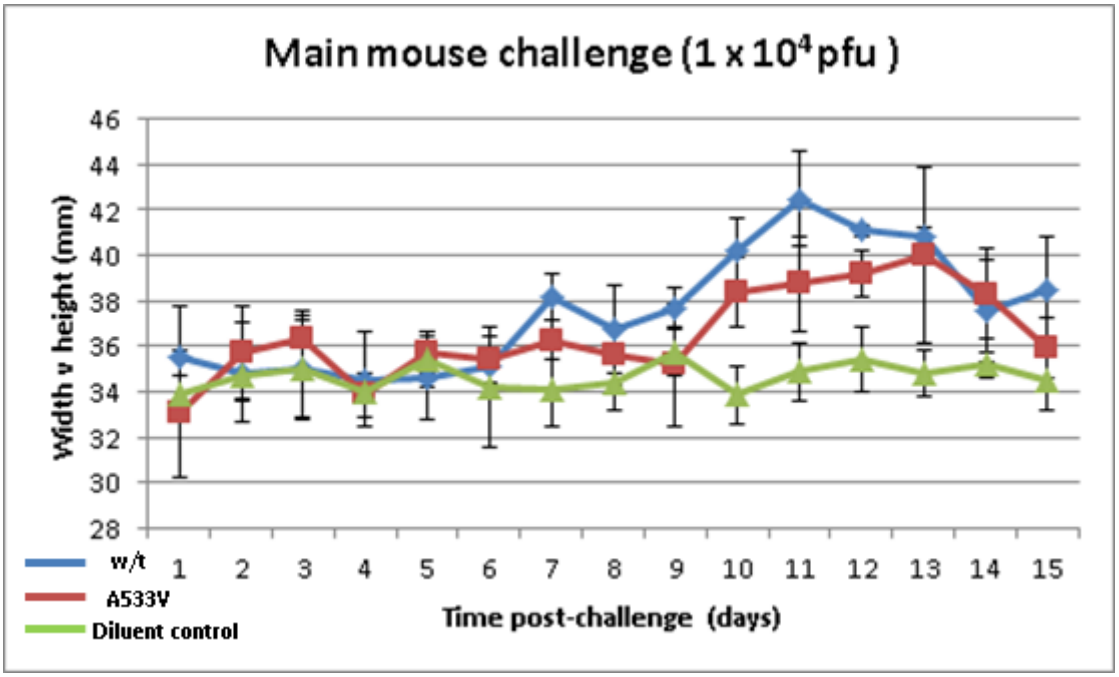

Figure 4.8 Changes in foot size as an indication of inflammation observed over a 12 day period in three groups of C57BL/6 mice. Groups 1 and 2 were challenged with 1 x 10^4 pfu w/t or A533V mutated CHIK-SL viruses respectively diluted in DMEM medium supplemented with 5% FBS in a total volume of 40µl. Group 3 received a similar volume of diluent in the absence of virus. In each case the site of injection was the ventral sides of the hind feet. The width and height were multiplied together to estimate the approximate area. Results show mean values from five mice with error bars denoting the standard deviation.

Time post-challenge (days)	Mann-Whitney Test	
	w/t v diluent control	A533V mutant v diluent control
1	0.3785	0.4034
2	1.0000	0.6761
3	1.0000	0.5309
4	0.8345	0.9168
5	0.2963	1.0000
6	0.2101	0.2101
7	0.0122	0.0601
8	0.1437	0.0947
9	0.0367	0.8345
10	0.0122	0.0122
11	0.0122	0.0122
12	0.0122	0.0122
13	0.0122	0.0601
14	0.1437	0.0367
15	0.0601	0.2963

Table 4.9 The Mann-Whitney statistical test was used to determine differences in foot swelling in mice infected with w/t (group 1) and A533V mutant (group 2) CHIK-SL viruses with the diluent control (group 3): $P < 0.05$. Yellow shading indicates that Mann-Whitney statistical test is significant.

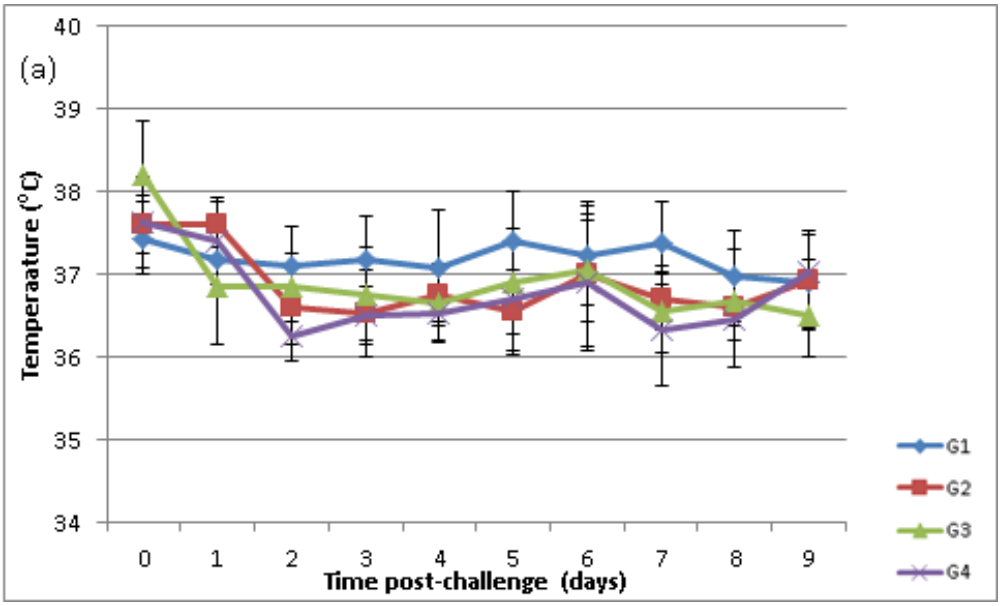

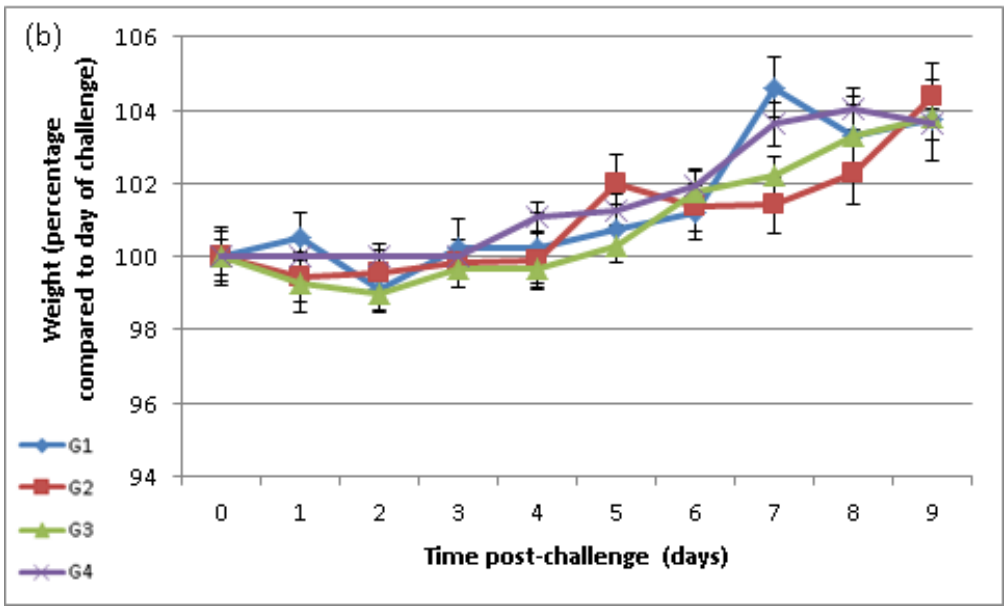

Figure 4.9 Clinical data from four groups of adult C57BL/6 mice. Groups 1 and 2 (G1 blue and G2 red) were challenged with 1 x 10^4 pfu of w/t and A533V mutant CHIK-SL viruses respectively diluted in a total of 40µl DMEM medium containing 5% FBS, group 3 (G3 green)were challenged with a similar volume of diluent and group 4 (G4 purple) received no treatment. The data represents the mean of six mice each from groups 1-3 and three from group 4 with error bars denoting standard deviation: (a) temperature differences between groups: (b) changes in body weight.

Temperatures	Mann-Whitney statistical p-value		
Time post-challenge (days)	w/t v diluent control	A533V mutant v diluent control	Diluent control v Un-infected control
0	0.0453	0.0656	0.1213
1	0.4233	0.0927	0.2453
2	0.3785	0.4223	0.0933
3	0.3367	0.4712	0.6985
4	0.3367	0.7488	0.7963
5	0.3367	0.2623	0.1556
6	0.7488	0.9362	0.7963
7	0.0250	0.5218	0.5186
8	0.3785	0.9362	0.4386
9	0.3785	0.2623	0.1213
10	0.1282	0.2980	-
11	0.8102	0.9362	-
12	0.6625	0.2980	-

Table 4.10 The Mann-Whitney statistical test was used to determine significant differences between the body temperatures of adult C57BL/6 mice challenged with w/t and A533V mutant CHIK-SL viruses with the diluent control group (n=6). The same test was applied to compare the diluent control group with an untreated group which was euthanized on day 9 (n=3) $P< 0.05$.

Weights	Mann-Whitney statistical p-value		
Time post-challenge (days)	w/t v diluent control	A533V mutant v diluent control	Diluent control v Un-infected control
0	0.1093	0.5752	0.3662
1	0.0453	0.5752	0.7963
2	0.1735	0.2298	0.5186
3	0.1282	0.4712	0.6056
4	0.1282	0.2298	1.0000
5	0.0782	0.0782	0.8973
6	0.1735	0.5218	0.6056
7	0.0306	0.3785	0.7963
8	0.2002	0.3785	1.0000
9	0.1735	0.3785	0.5186
10	0.1495	0.1735	-
11	0.6889	0.4712	-
12	0.4712	0.5752	-

Table 4.11 The Mann-Whitney statistical test was used to determine significant differences between the weight changes in adult C57BL/6 mice challenged with w/t and A533V mutant CHIK-SL viruses with a diluent the control group (n=6). The same test was applied to compare the diluent control group with an untreated group which was euthanized on day 9 (n=3) $P< 0.05$.

4.10 Assessment of viraemic phase

CHIKV RNA was detected by block RT-PCR in the sera of animals receiving w/t CHIKV from between days 1 and 6 post-challenge but not on days 9 and 12 (figure 4.10). This corresponds to the period immediately prior to the development of foot swelling (see figure 4.8) and is of similar duration to that reported for other CHIKV isolates with the same mouse model (Gardner *et al* 2010).

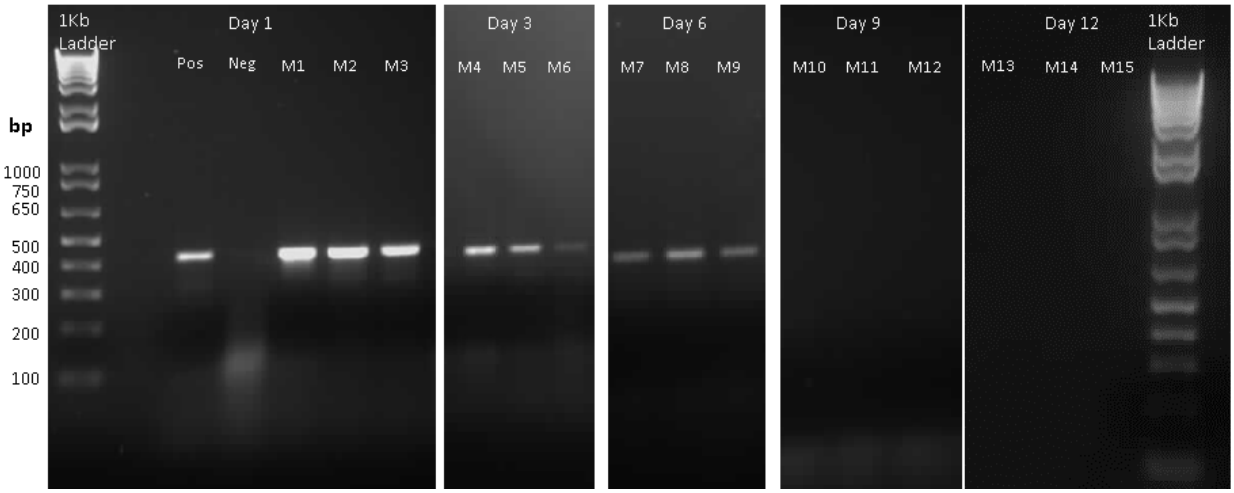

Figure 4.10 RT-PCR was used to amplify a 424bp CHIKV-specific amplicon. Products were visualised by separating 10µl out of 25µl total reaction mixtures by agarose gel electrophoresis and illuminating the ethidium bromide-stained gels with UV light (302nm).

4.11 Determination of virus titres by qRT-PCR

A standard curve was produced from the C(t) values obtained by performing the CHIKV qRT-PCR method of Edwards *et al* (2007) on RNA containing the predicted amplicon in a series of dilutions of known copy number (figure 4.11 and table 4.11). This enabled the approximate amplicon copy number to be estimated from C(t) values

obtained by assaying RNA from a variety of tissue samples. The assay was conducted on RNA extracted from pre-weighed tissue, derived from the right axial lymph node, the right inguinal lymph node, the right hind leg and sections from the spleen and liver in culled mice (figure 4.12, table 4.13). Although the use of block RT-PCR (figure 4.10) does not provide a quantitative measure of viraemia, the fluorescence intensity was greatest for the samples taken one day post-challenge, suggesting that it reached a peak at this time. In contrast the qRT-PCR profile shown in figure 4.12 indicates that the viral load remained high in the leg tissues for the first six days post-challenge for the w/t virus but only three days for the A533V mutant. For the remainder of the study period a rapid depletion of viral RNA in samples was observed. Interestingly this decline was more rapid in animals receiving the A533V mutant.

Viral loads in the spleen and inguinal lymph nodes were highest between 3 and 6 days post-challenge before progressively declining until day 15; levels in the axial lymph nodes remained high until day 9. Although there appeared to be no difference in the ability of virus to disseminate to these tissues, detectable mutant virus RNA declined more rapidly than w/t virus. In all cases viral loads were higher in tissues obtained from animals infected with w/t virus than those infected with the A533V mutant (table 4.13).

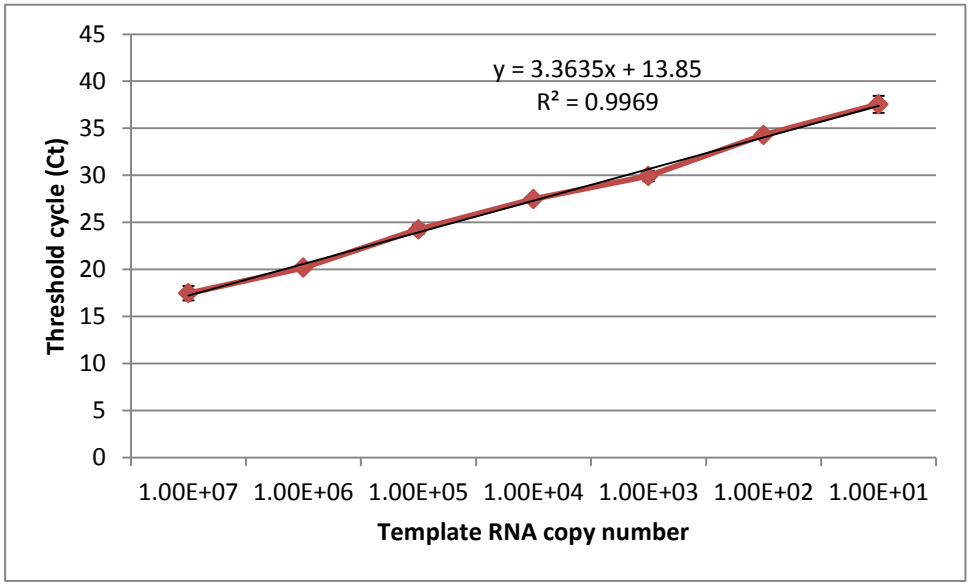

Figure 4.11 Graph showing the relationship between the calculated mean copy number of a 127bp cDNA CHIKV-specific amplicon and the threshold cycle (Ct value) obtained by qRT-PCR (Edwards *et al* 2007). Error bars show the standard deviation over three assays for each dilution..

Genome copy numbers	C(t)1	C(t)2	C(t)3	Mean Average	Standard deviation
1.00E+07	18.32	16.84	17.2	17.45333	0.771838
1.00E+06	20.11	19.92	20.51	20.18	0.301164
1.00E+05	23.65	24.56	24.52	24.24333	0.514231
1.00E+04	27.3	27.61	27.55	27.48667	0.164418
1.00E+03	29.31	30.38	30.1	29.93	0.554887
1.00E+02	34.46	34.19	34.19	34.28	0.155885
1.00E+01	37.54	38.46	36.65	37.55	0.905041

Table 4.12 The relationship between the average threshold cycle (Ct value) and genome copy numbers obtained by qRT-PCR (Edwards *et al* 2007).

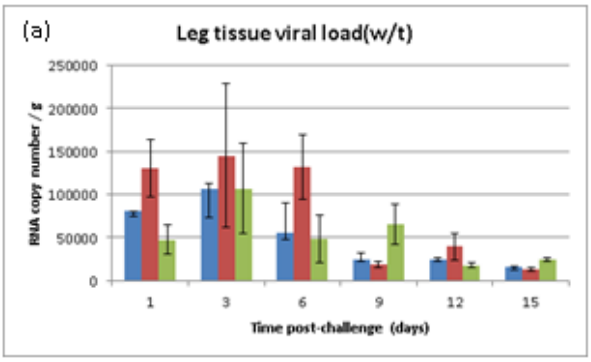
(a)
Leg tissue viral load(w/t)
RNA copy number / g
250000
200000
150000
100000
50000
0
1
3
6
9
12
15
Time post-challenge (days)

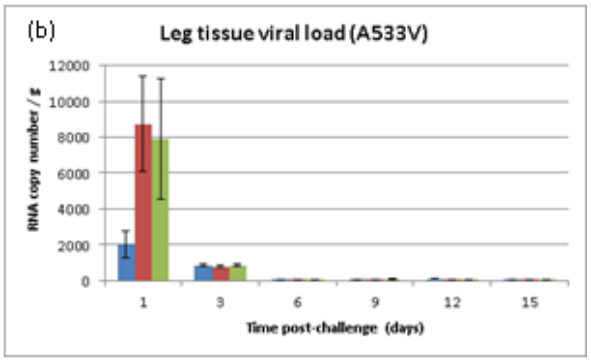
(b)
Leg tissue viral load (A533V)
RNA copy number / g
12000
10000
8000
6000
4000
2000
0
1
3
6
9
12
15
Time post-challenge (days)

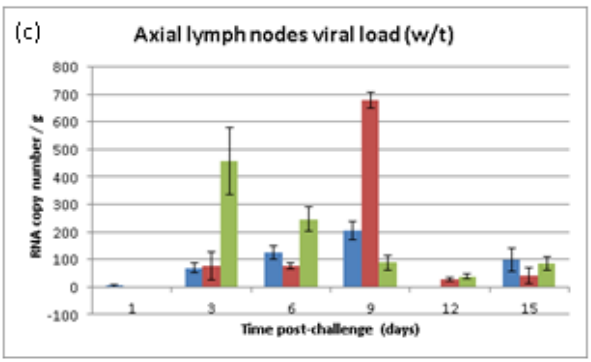
(c)
Axial lymph nodes viral load (w/t)
RNA copy number / g
800
700
600
500
400
300
200
100
0
-100
1
3
6
9
12
15
Time post-challenge (days)

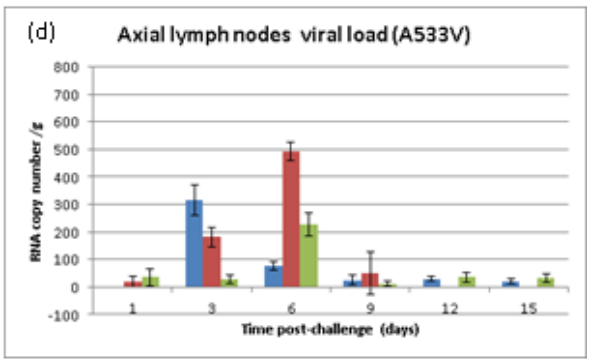
(d)
Axial lymph nodes viral load (A533V)
RNA copy number / g
800
700
600
500
400
300
200
100
0
-100
1
3
6
9
12
15
Time post-challenge (days)

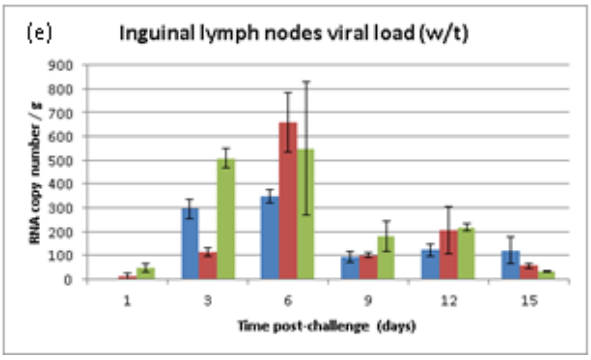
(e)
Inguinal lymph nodes viral load (w/t)
RNA copy number / g
900
800
700
600
500
400
300
200
100
0
1
3
6
9
12
15
Time post-challenge (days)

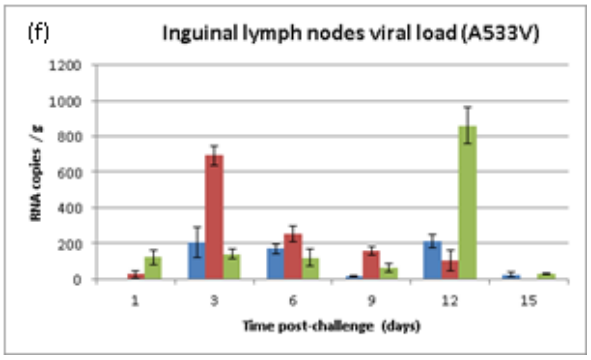
(f)
Inguinal lymph nodes viral load (A533V)
RNA copies / g
1200
1000
800
600
400
200
0
1
3
6
9
12
15
Time post-challenge (days)

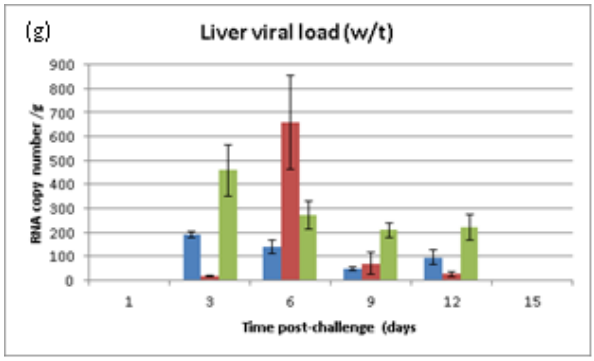
(g)
Liver viral load (w/t)
RNA copy number /g
900
800
700
600
500
400
300
200
100
0
1
3
6
9
12
15
Time post-challenge (days

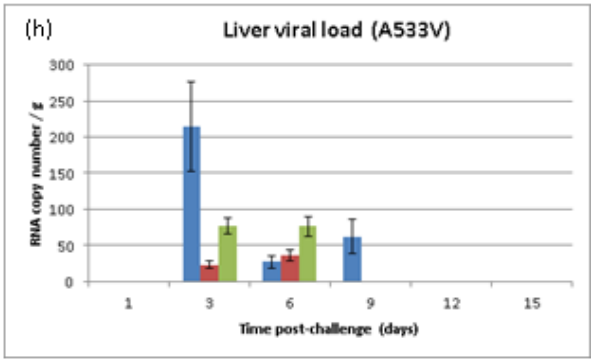
(h)
Liver viral load (A533V)
RNA copy number / g
300
250
200
150
100
50
0
1
3
6
9
12
15
Time post-challenge (days)

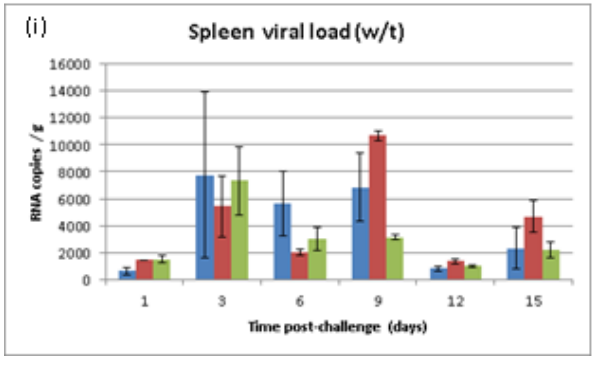
(i)
Spleen viral load (w/t)
RNA copies / g
16000
14000
12000
10000
8000
6000
4000
2000
0
1
3
6
9
12
15
Time post-challenge (days)

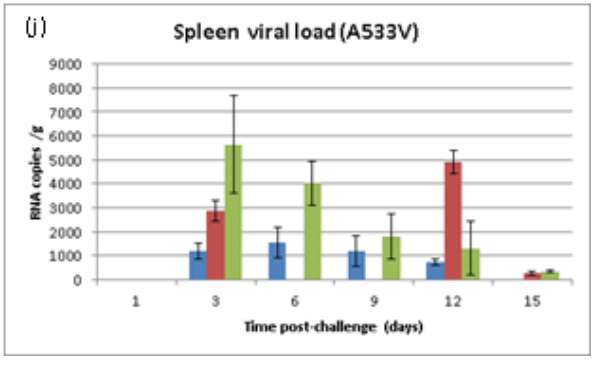
(j)
Spleen viral load (A533V)
RNA copies / g
9000
8000
7000
6000
5000
4000
3000
2000
1000
0
1
3
6
9
12
15
Time post-challenge (days)

Figure 4.12 Mouse tissues from animals infected subcutaneously with 1 x 10^4 pfu CHIK-SL(r-wt) or 1 x 10^4 pfu CHIK-SL(r-mut) were assayed for the presence of CHIKV RNA by qRT-PCR from the indicated tissues. Assays were performed in triplicate using the qRT-PCR method (Edwards *et al* 2007) C(t) values were converted into the approximate RNA copy number using the standard curve shown in figure 4.11 and the mean average values shown with error bars denoting standard deviation. The coloured bars (blue, red and green) represent individual mice euthanized on the days indicated from which tissues were obtained.

Mann-Whitney statistical p-value: w/t v A533 mutant					
Time post-challenge (days)	Leg tissue	Axial lymph nodes	Inguinal lymph nodes	Liver	Spleen
1	0.1451	*	0.4799	*	*
3	0.0004	0.9296	0.7239	0.3313	0.0027
6	0. 0122	0.2697	0.0004	0.0004	0.2164
9	0. 0240	0.0521	0.7911	*	0.0004
12	0. 0004	1.0000	0.2164	*	0.1120
15	0. 0004	0.0031	0.0020	*	0.0004

Table 4.13 The Mann-Whitney statistical test was used to determine significant differences in genome copy number determined by qRT-PCR in the indicated tissues from mice infected subcutaneously with 1 x 10^4 pfu CHIK-SL(r-wt) or 1 x 10^4 pfu CHIK-SL(r-mut). Significance (yellow shading) confirmed if $P<0.05$, asterix indicates insufficient data to perform the test.

4.12 Detection of innate immunity mediators by serology

To minimize deterioration of blood sample quality, samples were placed on ice immediately after collection and processed to obtain serum within approximately 1hr. However significant haemolysis was observed in the majority of samples. Storage prior to conducting serological assays was at -80°C.

No type I IFN, haptoglobin, SAA or SAP was detected in the mouse sera samples. However in each case satisfactory standard curves were produced, indicating that the quality of the assay reagents was unlikely to be a factor. Possible explanations are that the assays were adversely affected by poor sample quality or that the sera dilutions used were incorrect.

IFN-γ was detected between days 9 and 15 post-challenge in sera from w/t virus-infected animals and between 9 and 12 days post-challenge in those receiving A533V mutant virus (figure 4.13).

4.13 Detection of type 1 IFN gene expression in mouse tissues by qRT-PCR

In view of the limited data on innate immune responses from the serological assays, qRT-PCRs were used to measure the relative quantity of transcripts for type 1 IFNs and for the IFN-stimulated GTP-binding protein Mx1 (IFNa2, IFNb1 and MX1 genes). Template RNA was extracted from homogenized leg tissue and assays were conducted as described in section 3.7, chapter 3. The results show transient expression of IFNa2, IFNb1 and MX1genes in mice infected with the A533V mutant virus on

day 1 which declined 3 days post-challenge, (figure 4.14). Expression was detected at a later stage in mice challenged with w/t virus approximately 20-26hr post-challenge.

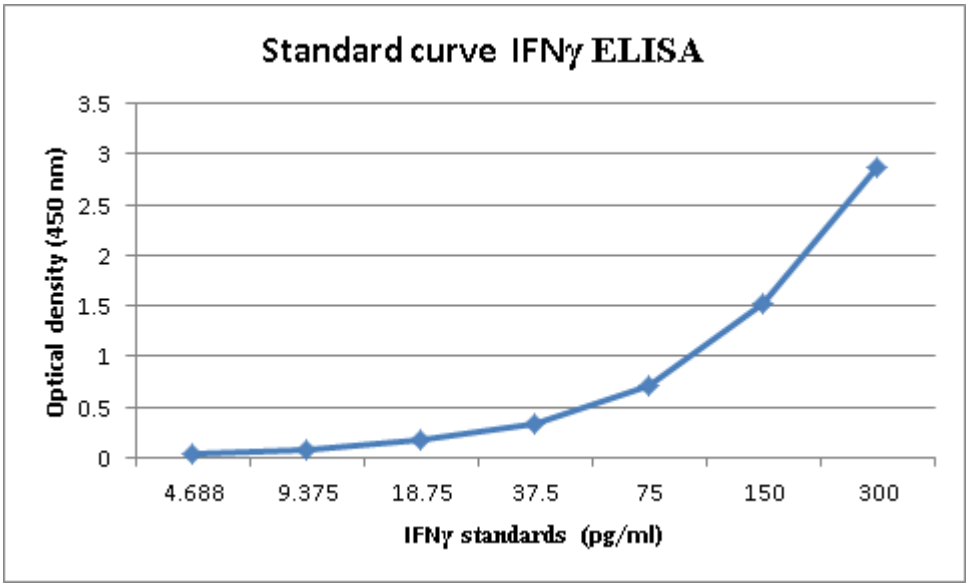

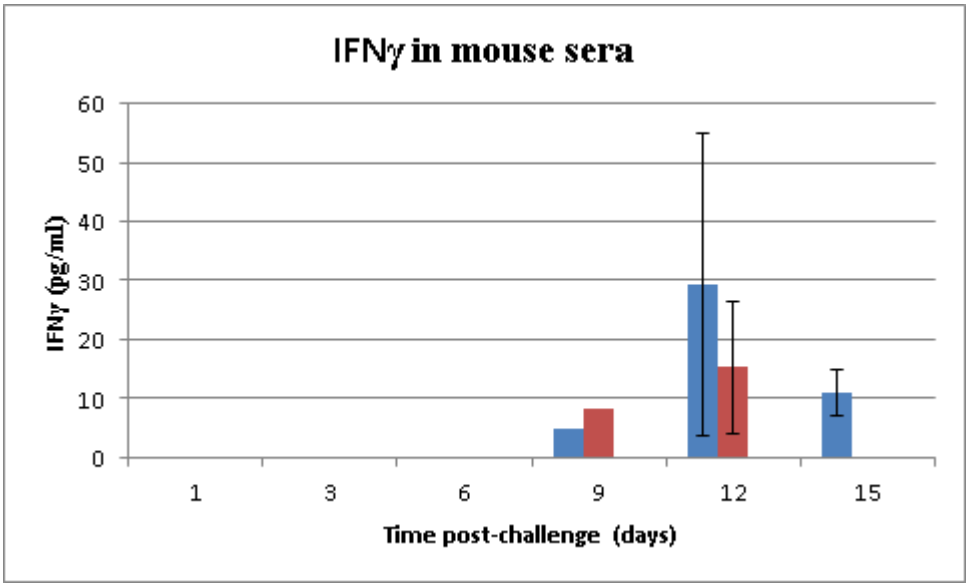

Figure 4.13 Graphs showing IFNγ standard curve and serum IFNγ detected in mice infected subcutaneously with 1 x 10^4 pfu CHIK-SL(r-wt) (blue) or 1 x 10^4 pfu CHIK-SL(r-mut) (red) as determined by ELISA. The values shown are the mean average from three assays (where this was possible) and the error bars denote standard deviation.

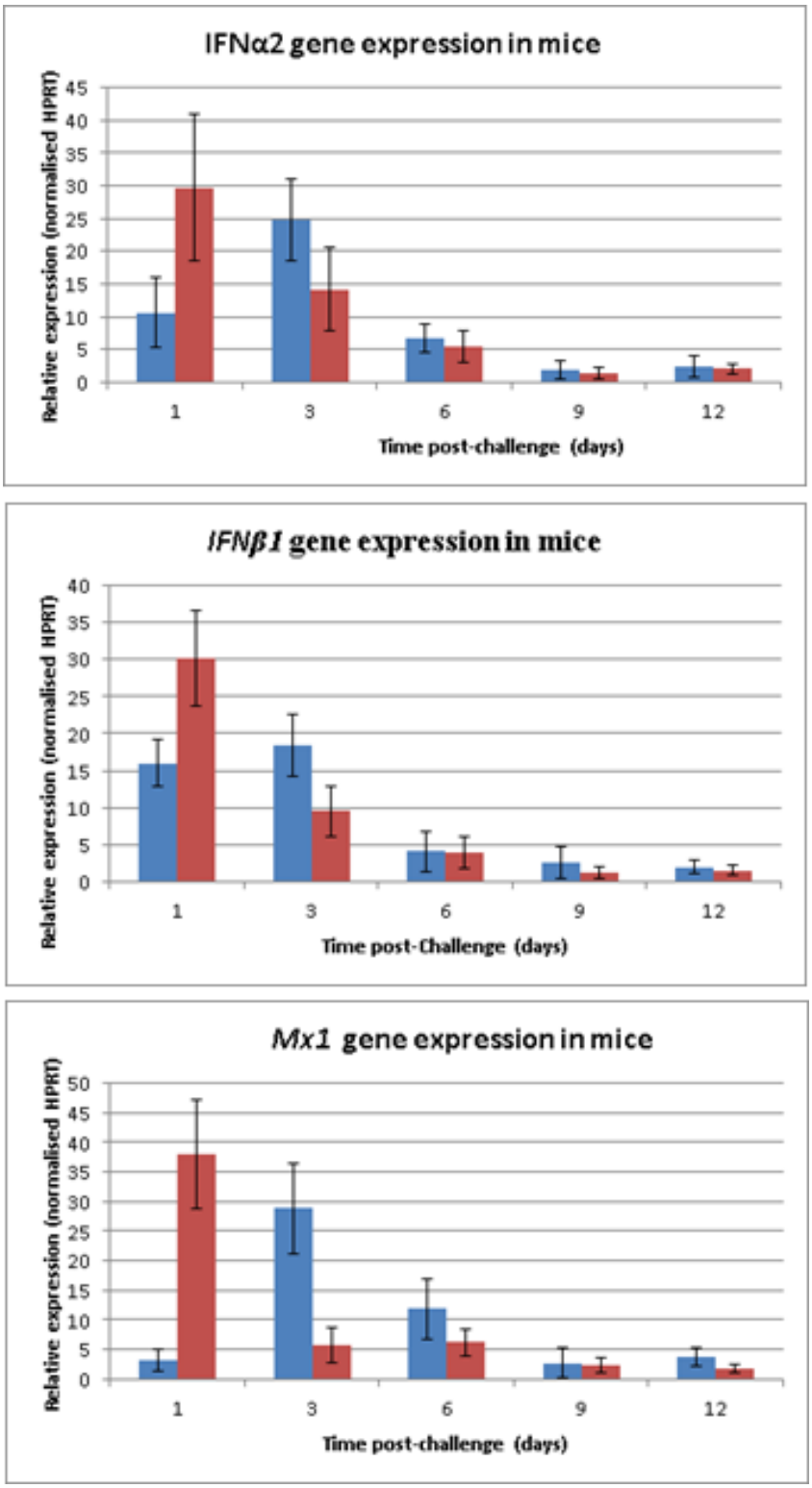

Figure 4.14 Graphs showing the levels of expression of IFNa2, IFNb1 and Mx1 genes in RNA extracted from homogenized tissue extracted from the hind leg of adult C57BL/6 mice. Mice were challenged with 1 x 10^4 pfu w/t (blue) or A533V mutant (red) CHIKV and groups of three were euthanized at the times indicated. Assays were performed in triplicate and the mean average result normalised to HPRT. Error bars denote standard deviations.

4.14 .1 Histolopathological changes in mouse leg tissue

Examination of H&E stained tissue specimens by light microscopy revealed histological changes indicative of inflammation in the tarsus region but not the stifle of the hind legs of animals challenged with virus. The three uninoculated mice culled on day 9 showed no morphological abnormalities, however minimal changes were noted in 2 of the 18 members of the diluent control group (1 mouse culled at day 1 and one at day 15). Similar tissues from the stifle region of all animals at each time point showed no signs of disease. Changes indicative of disease pathology were evaluated as normal, minimum, mild, moderate or marked and are summarised in tables 4.14-4.17.

4.14.2 Histolopathological changes in fibrovascular connective tissue

In tarsus tissue samples from each of the challenged groups, disease pathology was observed as indicated by the presence of varying levels of polymorphonuclear leukocyte (PMNL) cell infiltrate (table 4.14). This was minimal on day 1 post challenge in all animals (figure 4.15 panels a, c and e) and remained at a similar level or was normal throughout the 15 day study in individuals from the diluent control group (panel f). However in samples from animals culled on days 3, 6 and 9 a clear contrast between groups infected with w/t and A533V mutant virus was noted, with the most severe disease occurring in the former (figure 4.15 panels d and f). The extent of cellular infiltrate increased in group 1 mice from day 1 to day 6, remained at this high level on day 9, then decreased on days 12 and 15. A steady increase in the degree of tissue change was observed in group 2 mice from day 1 until day 9 and thereafter it declined.

4.14.3 Histopathological changes in skin

Minimal levels of inflammatory cell infiltrates were observed in skin from two animals from group 2 (1 from day 3 and 1 from 12) and none was observed in the diluent control group (table 4.15). However in group 1 histopathological changes were observed in individuals from each sampling day; these were minimal in 1 animal on days 1, 6 and 15 and in 2 animals on days 3, 9 and 12 (figure 4.16). Changes in the remaining mice were mild in 1 animal and moderate in one animal on day 6.

4.14.4 Histopathological changes in synovium

Synovium was not present in all samples analysed and no changes were observed in animals in groups 2 or 3 (table 4.14), however changes such as cellular infiltrates, necrosis and disruption of synovial membranes were observed in a total of four animals. These were assessed as mild to moderate, in one animal on day 6 and 1 animal on day 9 and they were minimal in 2 animals on day 15 (figure 4.17).

4.14.5 Histopathological changes in skeletal muscle

Differences in the appearance of skeletal muscle in mice from different treatment groups were particularly marked (figure 4.18). In animals receiving w/t virus, myocyte degeneration and necrosis was observed from days 1 to 15 in all animals at each time point apart from a single animal which remained normal (on day 3). On days 1 and 3 post-challenge all changes indicating inflammation were assessed as minimal or mild, but from days 6 to 15, samples from nine out of 12 mice had moderate or marked necrosis (figure 4.18 panels a and b respectively). Samples from

group 2 mice were assessed as normal or minimal on days 1 and 3 and minimal or mild on days 6, 12 and 15. The most severe changes amongst group 2 mice (2 moderate and 1 mild) were observed on day 9 (figure 4.18). Minimal myocyte degeneration was observed in 10 of 18 animals comprising group 3. A cellular infiltrate consisting mainly of mononuclear inflammatory cells was observed in 16 out of 18 mice from group 1, 5 from group 2 and a single animal from group 3 (table 4.17).

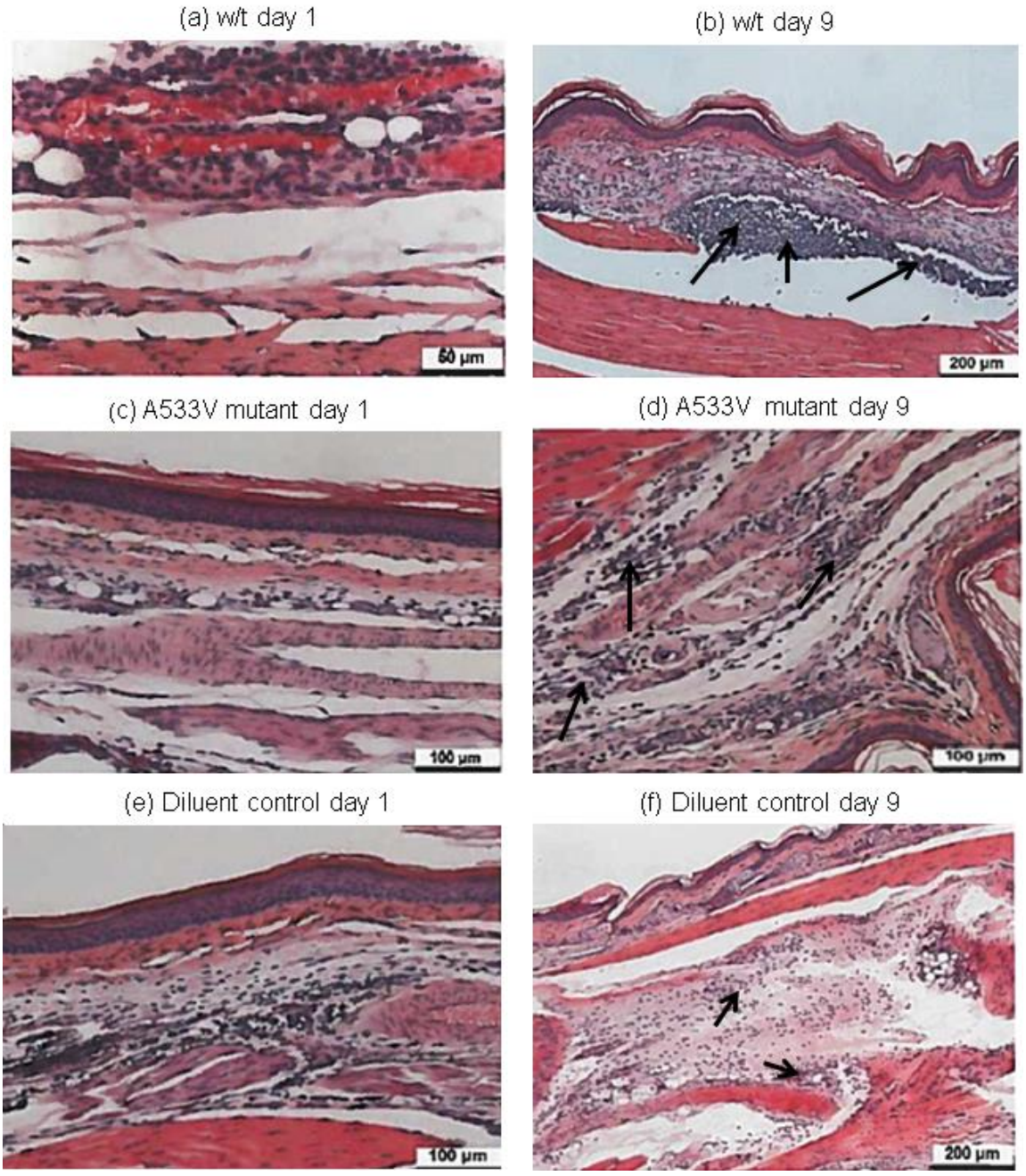

Figure 4.15 Haematoxylin and eosin stained sections of subcutaneous connective tissue obtained from the tarsus region of C57BL/6 mice challenged with 40µl of cell culture medium containing 1 x 10^4 pfu CHIK-SL(r-wt), 1 x 10^4 pfu CHIK-SL(r-mut), or diluent control. Sections were visualised by light microscopy and show samples obtained 1 (a, c, and e) and 9 (b, d and f) days post challenge. Day 9 images of virus-infected tissue show an accumulation of inflammatory cells, predominately neutrophils in the subcutaneous tissue (marked by arrows) which are minimal or absent in day 1 samples and diluent control samples.

Day	Group	Histological changes - severity				
		Normal	**Minimal**	**Mild**	**Moderate**	**Marked**
1	1	1	2	-	-	-
	2	2	1	-	-	-
	3	2	1	-	-	-
3	1	-	-	2	-	1
	2	3	-	-	-	-
	3	2	1	-	-	-
6	1	-	-	-	-	3
	2		1	2	-	-
	3	3	-	-	-	-
9	1	-	-	-	-	-
	2	-	1	1	1	-
	3	3	-	-	-	-
12	1	-	-	1	2	-
	2	1	1	1	-	-
	3	3	-	-	-	-
15	1	-	-	2	1	-
	2	2	1	-	-	-
	3	2	1	-	-	-

Table 4.14 Histopathological changes in fibrovascular connective tissues were assessed in haematoxylin and eosin stained tissue sections from the tarsus region of C57BL/6 mice challenged with 40µl of cell culture medium containing 1 x 10^4 pfu CHIK-SL(r-wt) (group 1), 1 x 10^4 pfu CHIK-SL(r-mut) (group 2), or diluent control (group 3). Three mice from each group were euthanized on the days indicated and samples visualised by light microscopy. Samples were assessed and allotted to one of the five categories shown to indicate the extent of histological change observed.

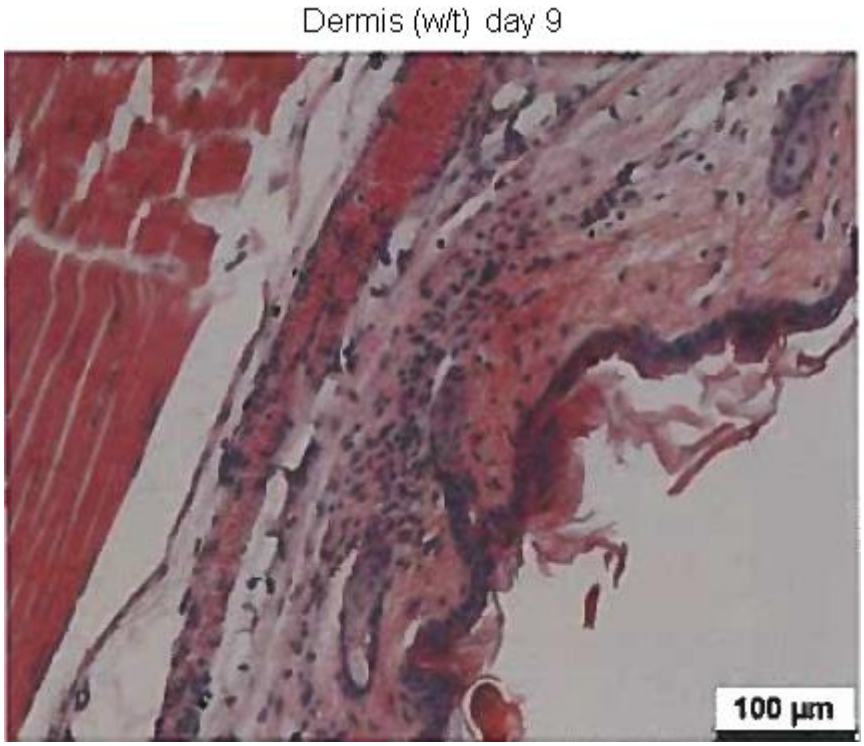

Figure 4.16 Haematoxylin and eosin stained section showing minimal inflammatory cell infiltrate, mainly consisting of neutrophils in the dermis in a C57BL/6 mouse challenged with 40µl of cell culture medium containing 1 x 10^4 pfu CHIK-SL(r-wt).

Day	Group	Histological changes - severity				
		Normal	**Minimal**	**Mild**	**Moderate**	**Marked**
1	1	2	1	-	-	-
	2	3	-	-	-	-
	3	3	-	-	-	-
3	1	1	2	-	-	-
	2	2	1	-	-	-
	3	3	-	-	-	-
6	1	-	1	1	1	-
	2	3	-	-	-	-
	3	3	-	-	-	-
9	1	-	2	-	1	-
	2	3	-	-	-	-
	3	3	-	-	-	-
12	1	1	2	-	-	-
	2	2	1	-	-	-
	3	3	-	-	-	-
15	1	2	1	-	-	-
	2	3	-	-	-	-
	3	3	-	-	-	-

Table 4.15 Histopathological changes in skin specimens were assessed in haematoxylin and eosin stained tissue sections from the tarsus region of C57BL/6 mice challenged with 40µl of cell culture medium containing 1 x 10^4 pfu CHIK-SL(r-wt) (group 1), 1 x 10^4 pfu CHIK-SL(r-mut) (group 2) or diluent control (group 3). Three mice from each group were euthanized on the days indicated and samples visualised by light microscopy. Samples were assessed and allotted to one of the five categories shown to indicate the extent of observed histological change in terms of inflammatory infiltrate.

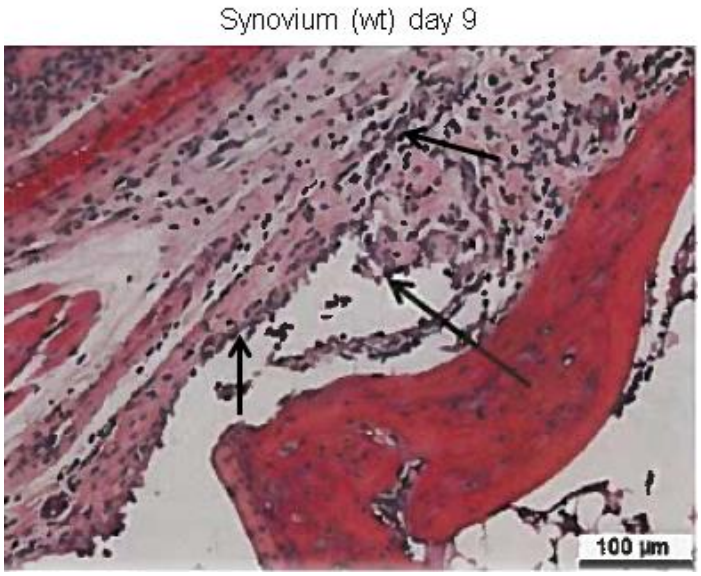

Figure 4.17 Haematoxylin and eosin stained section of tissue obtained from the tarsus region of C57BL/6 mouse challenged with 40µl of cell culture medium containing 1 x 10^4 pfu CHIK-SL(r-wt). Regions of moderate inflammation of the synovium are indicated by arrows.

Day	Group	Histological changes - severity				
		Normal	Minimal	Mild	Moderate	Marked
1	1	3	-	-	-	-
	2	3	-	-	-	-
	3	3	-	-	-	-
3	1	3	-	-	-	-
	2	3	-	-	-	-
	3	3	-	-	-	-
6	1	2	-	-	1	-
	2	3	-	-	-	-
	3	3	-	-	-	-
9	1	2	-	1	-	-
	2	3	-	-	-	-
	3	3	-	-	-	-
12	1	3	-	-	-	-
	2	3	-	-	-	-
	3	3	-	-	-	-
15	1	1	2	-	-	-
	2	3	-	-	-	-
	3	3	-	-	-	-

Table 4.16 Histopathological changes in synovium specimens were assessed in haematoxylin and eosin stained tissue sections from the tarsus region of C57BL/6 mice challenged with 40µl of cell culture medium containing 1 x 10^4 pfu CHIK-SL(r-wt) (group 1), 1 x 10^4 pfu CHIKSL(r-mut) (group 2), or diluent control (group 3) recieived no treatment. Three mice from each group were euthanized on the days indicated and samples visualised by light microscopy. Samples were assessed and allotted to one of the five categories shown to indicate the extent of histological change in terms of necrosis and inflammatory infiltrate, observed.

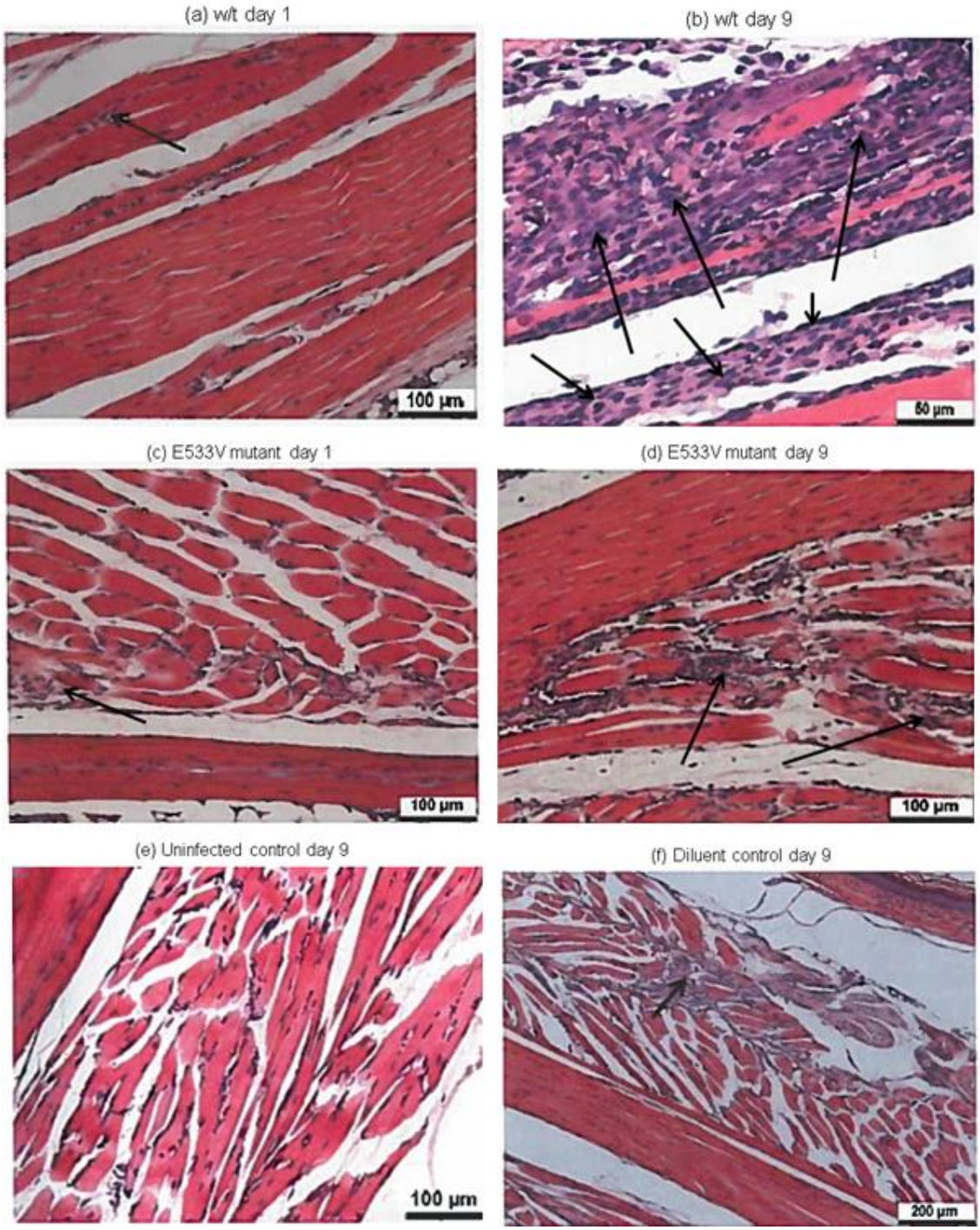

Figure 4.18 Haematoxylin and eosin stained sections of skeletal muscle tissue obtained from the tarsus region of C57BL/6 mice. Mice were challenged with either 1 x 10^4 pfu CHIK-SL(r-wt), 1 x 10^4 pfu CHIK-SL(r-mut), diluent control or received no treatment. Sections were visualised by light microscopy and show samples obtained 1 (a and c) and 9 (b, d, e and f) days post-challenge. Areas of myocyte degeneration and infiltration of mononuclear inflammatory cells (violet-staining regions) are indicated by arrows.

Day	Group	Histological changes - severity				
		Normal	Minimal	Mild	Moderate	Marked
1	1	-	3	-	-	-
	2	2	1	-	-	-
	3	**1**	2	-	-	-
3	1	1	1 (1)	1	-	-
	2	1	2	-	-	-
	3	1	2	-	-	-
6	1	-	1 (1)	-	2 (2)	-
	2	-	1	2	-	-
	3	1	1	1 (1)	-	-
9	1	-	-	-	1	2 (3)
	2	-	-	1	2 (1)	-
	3	1	2	-	-	-
12	1	-	- (1)	2 (1)	1 (1)	-
	2	-	2	1	- (1)	-
	3	1	2	-	-	-
15	1	-	-	- (3)	1	2
	2	-	2	1	-	-
	3	2	1	-	-	-

Table 4.17 Skeletal muscle pathology: monocyte degeneration (inflammatory infiltrate) Histopathological changes in skeletal muscle specimens were assessed in haematoxylin and eosin stained tissue sections from the tarsus region of C57BL/6 mice challenged with 40µl of cell culture medium containing 1 x 10^4 pfu CHIK-SL(r-wt) (group 1), 1 x 10^4 pfu CHIK-SL(r-mut) (group 2), or diluent control (group 3). Three mice from each group were euthanized on the days indicated and samples visualised by light microscopy. Samples were assessed and allotted to one of the five categories shown to indicate the extent of histological change in terms of myocyte degeneration and inflammatory cell infiltrate (shown in brackets), observed.

DISCUSSION

Experiments with the C57BL/6 adult mouse model showed that arthritic symptoms could be induced with both w/t and A533V mutant viruses derived from the CHIKV SL-R233 isolate. Swelling lasting for 4-5 days was observed in the injected legs of mice challenged with both virus types, reaching a peak at 10-11 days post exposure. In contrast to the report by Gardner *et al* (2010) swelling was also observed in the non-injected limb.

Viraemia in mice infected with w/t CHIKV was detected from 1-6 days post-challenge by block-based RT-PCR. High levels of virus RNA detected in homogenized leg tissue from animals challenged with w/t virus were also highest during this period. Viral RNA levels produced in leg tissue from animals receiving A533V mutant virus were lower at day 1 and had declined significantly after day 3 post-challenge. Viral RNA was detected in liver homogenates from day 3 post-challenge in mice challenged with both virus types, declining to undetectable levels by day 12 for w/t virus and day 9 for A533V mutant virus. In contrast, evidence of virus persistence in the axial and inguinal lymph nodes and in the spleen until the end of the study. These findings contrast with those of Gardner *et al* (2010), who reported the detection of virus in spleen, inguinal lymph nodes and liver for shorter periods post-challenge (until day 5 in lymph nodes and spleen and day 3 in liver tissue). This can be explained by the different methods used for virus detection; the qRT-PCR assay used in the present study detects genome RNA copy numbers whereas the endpoint dilution assay used by the authors of the former study, detects viable virus particles.

Inflammation of the virus-injected foot was observed in the tarsal region in mice treated intradermally with 10^4 pfu ofeither w/t or A533V virus types. The effective viral dose was determined by measuring changes in the area estimated by multiplying the width at the widest point of the phalanges by the distance from the end of the phalanges to the tarsometatarsal joint. The longest period of significant swelling for animals challenged with both virus types was observed with 10^4pfu and extended from days 9-13 post-challenge with w/t virus and days 10 -14 with the A533V mutant virus.

The timing of the foot swelling correlates with histological changes observed in leg tissue. These were most marked in the skeletal muscle and connective tissues and increased in severity from the first until the ninth day after infection, declining thereafter. Similar tissues to those studied in the tarsus were normal in samples from members of each treatment group at all time points. The contrasting histological findings from virus infected tissues with the diluent control and the absence of swelling in the legs of the latter indicate that these changes were brought about as a result of the viral challenge, however minimal changes in tissues from 4 (of a total of 18) animals in the diluent control group occurred. Ideally immunostaining would have been done to confirm virus involvement by demonstrating the presence of CHIKV-specific antigens at sites of pathogenic lesions.

The earliest time point at which IFN-γ was detected (day 9 post-challenge) coincided in both virus-infected groups with the period in which the virus RNA copy number peaked in leg tissues and the most severe histopathological changes were observed. In

samples obtained on days 12 and 15, a reduction in viral RNA and evidence of tissue regeneration were observed in subcutaneous connective tissue and skeletal muscle.

qRT-PCR analysis of RNA extracted from leg tissue indicated that earlier type I IFN induction occurred in animals challenged with the A533V mutant virus than those receiving w/t virus. This finding correlates with the *in vitro* studies discussed in chapter 3.

CHAPTER 5

General Discussion

Since the re-emergence of CHIKV in coastal Kenya in 2004, unprecedented epidemic activity over an expanding geographical range has been documented. Furthermore associations have been described with several clinical conditions hitherto rarely or never previously reported. Prior to this event CHIKV emerged sporadically in outbreaks that were usually self-limited and separated in time by years or decades. However, whilst the strains affecting Africa, the Indian Ocean islands, south-eastern Asia and southern Europe from 2004 until 2012 were predominately sub-lineages of the ESCA genotype (Hapuarachchi *et al* 2010, Powers 2008), a more recent emergence of chikungunya in the Phillipines, Indonesia, the Caribbean islands, Central and South America (Cassadou *et al* 2014, Van Bortel *et al* 2014) is due to the Asian genotype. This recent emergence may pose serious public health concerns, as *Ae. aegyptii* is prevalent throughout many tropical and sub-tropical regions in the Americas and, much of the population are likely to be at risk of infection. As a consequence of the devastating series of CHIKV outbreaks since 2004, there has been much interest in the biology and pathogenesis of this and other alphaviruses.

Until recently the lack of a suitable animal model for CHIKV and its classification as a hazard group 3 pathogen, have hampered progress in the study of CHIKV pathogenesis. In contrast other members of the Alphavirus genus have been more amenable to laboratory study. For example the hazard group 2 pathogens SFV and SINV have been extensively characterised, and details of their transmission cycles

and likely mode of pathogenesis established by numerous studies including reverse genetics. Such research has identified several virulence factors and molecular structures that enable these (now well studied) viruses to inhibit the host innate immune response or to evade its effects. Building on this body of knowledge, the work contained in this thesis has been conducted to investigate a hypothesis that CHIKV contains a sequence specific virulence determinant in the boundary between the non-structural proteins nsP1 and nsP2.

RNA replication in alphaviruses is a highly regulated process in which different phases predominate at different stages of the infection cycle. Following translation of the nsP ORF, either one of two versions of this nsP polyprotein (nsP123 or nsP1234) is synthesised, as an immature (polyprotein) form of the viral replicase. This polyprotein is cleaved by a protease action in nsP2 to produce the mature replicase complex, which consists of four closely associated nsPs. The co-translation cleavage events occur at three conserved sites: nsP1/2, nsP2/3 and nsP3/4. This proteolytic processing occurs in a strict order, so that different combinations of the polyprotein components predominate before the mature replicase complex is formed (i.e. nsP123 + nsP4, followed by nsP1+ nsP23 + nsP4 and finally nsP1+nsP2 +nsP3 +nsP4). The catalytic activity of each of these cleavage intermediates favours the synthesis of different RNA products. First, the predominant product is a negative-sense copy of the viral genomic RNA, next, this product is used as template to synthesise nascent genomic (positive-sense) RNA and finally, sub-genomic (26S) RNA which functions as mRNA to direct the synthesis of the structural polyprotein.

It seems likely that a mutation in the cleavage domain, such as the one engineered in this study, would disrupt this process and alter the ratio of RNA species present in CHIKV-infected cells. This has been shown to be the case with the nsP2/nsP3 cleavage site of SINV in a study where p23-cleavage defective clones continued synthesising negative-sense RNA in addition to positive genomic and sub-genomic forms throughout the infectious process instead of ceasing after the cleavage at the nsP1/nsP2 site (Mai *et al* 2009).

In this thesis an infectious cDNA clone of CHIKV has been created, so that genomic RNA can be precisely manipulated using recombinant technology. Since alphavirus RNA is infectious, this system enables phenotypic changes introduced through specific mutation to be investigated. Based on work which has focused on the low level alphavirus pathogen SINV, a specific mutation has been engineered into the nsP1/ nsP2 cleavage site of the CHIKV genome. The phenotypic consequences of this modification have been examined using classic virological techniques.

5.1 Characterization of circulating CHIKV and choice of infectious clone

The first step in this investigation was to select and characterise a recently circulating CHIKV isolate from a clinical case, rather than a laboratory strain. The virus selected (SL-R233) was isolated from the serum of a patient who presented with acute fever at a local hospital in Colombo, Sri Lanka in November 2006; through simple passage using Vero cells in culture. Essential parameters of this isolate such as effective growth in a variety of cell lines, the ability to develop plaques and consistent

behaviour following resuscitation from liquid nitrogen were established and the nucleotide sequence was then determined. As anticipated, phylogenetic analysis of SL-R233 genomic RNA showed that it grouped closely with other ESCA isolates from the Indian Ocean (IO) sub-lineage dating from 2006-2008.

5.2 ESCA and E1-A226V

The majority of CHIKV outbreaks that have been reported since 2004 have involved strains belonging to the ESCA lineage and the Indian sub-lineage. Many are characterized by a mutation in the E1 envelope glycoprotein (an A226V substitution). This mutation is has been shown to enhance the efficiency of dissemination and transmission of the virus by *Ae albopictus*, so fuelling the epidemic (Tsetsarkin *et al* 2007, Vazeille *et al* 2007). Phylogenetic evidence suggests that the substitution has arisen on at least four separate occasions in strains belonging to the ESCA genotype, in the Indian Ocean Islands, Cameroon or Gabon, India and Sri Lanka (De Lamballerie *et al* 2008, Kumar *et al*, 2008). During the outbreak from which isolate SL-R233 was obtained, the first evidence of this genotype appeared in early 2007 (Santosh *et al* 2008, Kumar *et al* 2008, Hapuarachchi *et al* 2010), thus the finding presented here of E1-226A was to be expected.

5.3 Sequence context of non-structural proteins

The presence of an in-frame opal termination codon (TGA) upstream from the nsP3/nsP4 cleavage domain has been reported in some alphavirus species including strains within species, whilst being replaced by an arginine codon (CGA) in others

(Strauss and Strauss 1994, Kim *et al* 2004). The role of this opal codon in the infectious cycle of alphaviruses has not been established, although several have been proposed. It has been reported to act as a virulence factor in SFV, as a component that enhances the efficiency of SINV growth in cell cultures and, in ONNV as a factor required for adaption to infectivity in arthropod cells, (as discussed in chapter 1 section 1.3.3) (Tuittila and Hinkkanen 2003, Li and Rice 1989, Myles *et al* 2006). Sequence analysis of the nsP3/nsP4 cleavage domain of SL-R233 virus indicated that a heterogeneous population was present with respect to this locus. Specifically the analysis of sequence traces from multiple RT-PCR products revealed that whilst there was a dominant signal for cytidine in the first nucleotide position of the codon, a weaker signal for thymidine was also present.

5.4 Construction of the infectious clone

The first version of the cDNA CHIKV clone constructed in this work, consisted of the entire 11.8kb sequence from the start of the 5'UTR to the junction of the 3'UTR with a short poly-A tail, determined directly from sequencing. It was named pCHIK-SL(A) to indicate that no poly-A tail had been added. It was reasoned that if infectious RNA obtained from *in vitro* transcription could be successfully introduced into susceptible host cells (by transfection), the 5' ORF encoding the replicase component proteins would be translated and initiate the virus replication cycle. Initially this approach was successful, as w/t virus was immediately rescued from BHK21 cells that were electroporated with this RNA product. However, subsequent attempts at rescuing infectious virus using the same conditions were inconsistent and generally less successful. Comparisons with other alphavirus cDNA clones indicated that the major

difference between these and pCHIK-SL(A-) was the shortness in length of a poly-A tail in the latter. Further investigations determined the presence of CHIKV-specific amplicons in excess of 1kb, in cell monolayers 8 days after electroporation, indicating that the poly-A tail in the virus genome was more likely to have a role in aiding efficient translation than in maintaining RNA stability. A poly-A tail with a minimum length of 11 residues has been reported to combine with the terminal 19 nucleotides of the UTR to function as the core promoter for negative-strand RNA synthesis in SINV (Hardy and Rice 2005). Attoui *et al* (2007) estimated that the poly-A tail length present in MIDV was between 200 and 250 adenine residues.

Thus an investigation was undertaken to determine the poly-A tail length present in w/t CHIKV RNA with a view to modifying pCHIK-SL(A-) accordingly. It was demonstrated in a series of amplicons derived from both pCHIK-SL(A-)-transcribed RNA and from the African prototype CHIKV strain S27 (Khan *et al* 2002), that tail lengths ranged from between 22 and 78 adenine residues. A strategy adding a tail in approximately the middle of this range (40 residues) were devised to modify clone pCHIK-SL(A-), creating the clone pCHIK-SL(wt). Repeated transfections using RNA transcribed from this new clone was shown to efficiently produce infectious virus, indicating that whilst not being essential, this component performs an important function. pCHIK-SL(wt) was subsequently used as the basis of the clone, pCHIK-SL(A533V) containing the A533V mutation.

5.5 *In vitro* studies

Experiments comparing *in vitro* growth kinetics of w/t and A533V mutant viruses discussed in chapter 3 showed that in the absence of a type I IFN response (in Vero cell cultures), they reached similar titres for the final two time-points (24 and 48hr post-infection). However, significantly lower viral yields for the A533V mutant were observed at the earlier time-points. Interestingly, the plaque sizes produced by the A533V mutant virus on the same host cells were significantly smaller than those of w/t virus, these observations indicating that the latter possesses a growth advantage. When the growth kinetics of the two virus types were compared in L929 cell cultures (a cell line capable of mounting a type 1 IFN response) a different profile was observed. In this case the A533V mutant grew to higher titres than w/t virus until a peak was reached at approximately 20hr post-infection, before markedly declining. This drop in titres was not observed with w/t virus between the peak reached at 26hr (post-infection) and the last time-point assayed (50hr post infection). A possible explanation for this observation is that the A533V mutant is more efficient than the w/t virus in inducing type 1 IFN in the host cells resulting in earlier viral clearance.

5.6 Virus induction of type 1 IFN

The data obtained from qRT-PCR assays to measure up-regulation of the genes encoding IFN-α, IFN-β and Mx1 in L929 cells indicates that the w/t virus is less efficient at inducing these genes than the A533V mutant. Induction of these genes first occurred in cells infected with the A533V mutant virus at 8-20hr post infection which coincides with the time that peak titres were obtained. The gene expression reached a maximum at 26hr post-infection, at which time virus titres had begun to

decline. In contrast, type 1 IFN induction in L929 cells infected with w/t virus was delayed and occurred at lower levels than the mutant-infected cells until 43hr post-infection. The hypothesis that the mutation engineered into the A533V clone is more effective at inducing a type 1 IFN response is thus supported by this work.

5.7 *In vivo* work

The course of infection and pathology induced in the mouse model was consistent and measurable, however it did differ slightly from that reported by Gardner *et al* (2010). These authors recorded maximum foot swelling on days 7 post-challenge whereas this was observed on days 11 (w/t) and 13 (A533V), in the present study. It is not known whether this was due to natural variation amongst C57BL/6J mice or a significant discrepancy. If significant, a possible explanation is that the CHIK-SL(r-wt) and CHIK-SL(r-mut) stocks used in mouse challenges were propagated in Vero cell cultures whereas the former authors passaged virus isolates in C6/36 (*Ae. albopictus*) cells. Although the Vero cell line is incapable of producing type 1 IFN, it is possible that other components of the innate immune system, perhaps initiated by host detection of pattern-associated molecular patterns (PAMPS), inhibited the ability of the virus to infect other mammal (mouse) cells. In contrast, the C57BL/6J model of Morrison *et al* (2011) produced foot swelling in younger (14 day old) mice which reached a peak at 7-10 days using virus prepared in Vero cells. Alternatively the selected mouse model is not equally susceptible to different CHIKV strains and may have produced rheumatic disease more efficiently if the SL-R233-based clones had been adapted to the mouse. Gardner *et al* (2010) reported that whereas a Réunion Island isolate, LR 2006-OPY1 produced consistent levels of viraemia, an Asian isolate required nine passages in order to adapt.

The animal-based studies show a similar pattern with regard to type 1 IFN induction as in L929 cell cultures. In each case transient expression of IFN-α and IFN-β and Mx1 in A533V mutant-infected mice was relatively higher 1 day post-challenge than for those infected with w/t virus though it was much reduced after day 3. *In vivo* w/t virus genome copy numbers (directly correlating to viral load) in tissue samples were higher at each time point than with the A533V mutant. In both cases high viral loads were detected in leg tissue at day 1 post-challenge, but whereas by day 6 the A533V mutant had declined to an undetectable level, a significant reduction in w/t virus was not seen until day 9, with low viral load still being detected until the end of the experiment. There was thus a period between the disappearance of virus in the leg tissue and the earliest indication of swelling in the legs (day 9). These observations are in contrast with virus assays conducted on the lymphoid tissues. Virus was detected in w/t mice in both the axial and inguinal lymph nodes in all mice infected with w/t virus from days 3 to 15 and in the spleen from days 1 to15. A533V mutated virus was detected in the inguinal lymph nodes and spleen in all mice from days 3 to 12 and in the axial lymph nodes and from days 3 to 9. In individual cases virus genomes were detected to the end of the experiment. These findings may be indicative of viable virus persisting at these sites as has been reported in a non-human primate model (Labadie *et al* 2010).

The continued presence of viral material may be linked to the activation of T cells in the lymphoid organs and to the appearance of IFN-γ on day 9. This coincides with the timing of the onset of leg swelling. CHIK-specific CD4+ T cells producing IFN-γ

were reported by Teo *et al* (2012) to be present in inflamed joints and to have a role in pathology in CHIKV-infected mice, however Messaoudi *et al* (2013) reported that an increased persistence of arthritic disease in older CHIKV-infected primates was associated with a reduced virus-specific T cell response, suggesting that they play a protective role. T cell production of IFN-γ has shown to play an important role in the clearance of other alphaviruses (Binder and Griffin 2001, Sun *et al* 2011).

5.8 Histopathological changes

The histology findings indicate that C57BL/6J mice challenged with w/t and A533V viruses at similar titres both developed significant changes indicative of an acute inflammatory condition, increasing in severity from day 1 to day 9 post-challenge followed by a progressive decrease in cell damage observed on days 12 and 15. However the overall severity for each time point (summarized in tables 4.14-4.17) was consistently greater in the w/t group, indicating that the introduction of the A533V mutation, at least partially attenuated the virus. Changes were most severe in the supporting connective tissue and the skeletal muscle of infected leg tissue, both being associated with a prolific infiltrate of mononuclear leukocytes. Changes indicative of inflammation in the synovium were only seen in a minority of animals and confined to those infected with w/t virus. In this respect the results differ from those reported in the C57BL/6 mouse model by Gardner *et al* (2010) and the primate model of Labadie *et al* (2010).

5.9 Conclusions

Taken together the results generated in this study indicate the presence of a virulence factor in the CHIKV nsP1/nsP2 cleavage site and thus support the hypothesis under investigation. Alphaviruses are distributed in all continents of the world and infect a diverse range of animal species. As discussed in chapter 1, many members of the genus encode proteins that function to antagonise the host IFN response, both by mediating shutoff of host protein synthesis and by interacting with specific effector molecules with roles in cell signalling pathways (Breakwell *et al* 2007, Garmashova *et al* 2006), Garmashova *et al* 2007b, Aguilar *et al* 2007, Fros *et al* 2010). Whilst the A533V mutation may partially attenuate the virus it is still capable of infecting a susceptible host. Thus the proposed virulence factor in the nsP1/nsP2 cleavage site may be one of several mechanisms that work in concert to overcome the mammalian host innate immunity.

5.10 Possible rationale for A533V-induced phenotype

Given that a major role of nsP1 is in effecting 5' capping of RNA transcripts, it is possible that the engineered amino acid substitution at the P3 position may adversely affect this process, thereby exposing an increased volume of un-capped RNA to host cell pattern recognition receptors. This would result in the induction of increased levels of IFN through the pathways triggered by RIG-1 or PKR. Alternatively the failure of efficient cleavage at the nsP1/nsP2 junction may inhibit the translocation of nsP2 to the host cell nucleus, a process believed to be instrumental in inhibiting the induction of IFNs through shut-off of host protein synthesis (Montgomery and Johnson 2007).

5.11 Future work

The infectious clone developed in this study has been shown to be a useful tool to investigate the infectious cycle and pathogenesis of CHIKV. The principles used in its construction might also be adapted for the development of similar constructs based on other alphaviruses. In recent years the re-emergence of several of other Old World alphaviruses including ONNV and MAYV (Lanciotti *et al* 1998, Gomes *et al* 2012), with close evolutionary relationships to CHIKV, have been documented. In view of the impact on vector specificity and pathogenic consequences, attributed to the acquisition of the E2 A226V mutation in CHIKV, the potential for other species to emerge in a similar way may be significant.

Several questions arising from the findings in this study in the context of a powerful research tool, will form the basis of interesting future work. The SL-R233 isolate on which the clones in this work were based was shown to consist of a heterogeneous population with respect to the presence of the alternative codons CGA or TGA (arginine or the opal termination codon) near to the 3' end of nsP3. The arginine-containing version was incorporated into the clones pCHIK-SL(wt) and pCHIK-SL(A533V) as this appeared to be the dominant species present. However the construction of a w/t clone containing the alternative loci would be of use in investigating whether either version is more pathogenic in the mouse model, also to monitor the acquisition of mutations when both are passaged in insect and mammalian cells.

Although evidence of arthritic disease was observed in the mouse model selected for the study the outcomes differed in some respects from those reported by Gardner *et al* (2010). In addition to the timing of the leg swelling previously mentioned, in the original study more extensive histopathologic changes were observed in the synovium and subcutaneous regions, which were largely absent in the present study. It is possible that adaption of the SL-R233-based virus by conducting serial passages in C57BL/6 mice would have resulted in symptoms that more closely mirror those seen in human patients. Were this process to be conducted, it would be possible to monitor changes in the genomic sequence and determine loci that were important for adaption to the mammalian host.

In summary this thesis describes the successful development of a reverse genetics system for the study of CHIKV and demonstates the utility of this tool by investigating the hypothesis that a virulence determinant is present within the nsP1/nsP2 cleavage domain. Finally evidence is presented of its role in the suppression of the type 1 IFN response in the mammalian host.

BIBLIOGRAPHY

Abramides, GC. Roiz, D. Guitart, R. Quintana, S. Guerrero, I. and Giménez, N. (2011) Effectiveness of a multiple intervention strategy for the control of the tiger mosquito (Aedes albopictus)in Spain. *Trans. R. Soc. Trop. Med. Hyg.* **105:** 281-288.

Aggarwal, M. Tapas, S. Preeti1, Siwach, A. Kumar, P.Richard J. Kuhn, RJ. and Tomar, S. (2012) Crystal structure of Aura virus capsid protease and its complex with dioxane: new insights into capsid-glycoprotein molecular contacts. *PLOS One* **7(12):** e51288

Aguilar, PV. Weaver, SC. and Basler, CF. (2007) Capsid Protein of Eastern Equine Encephalitis Virus Inhibits Host Cell Gene Expression. *J. Virol.* **81(8)**: 3866-3876

Ahola, T. and Kääriäinen, L. (1995) Reaction in alphavirus mRNA capping: formation of a covalent complex of nonstructural protein nsPl with 7-methyl-GMP. *Proc. Natl. Acad. Sci.* **92:** 507-511

Akahata, W. Yang, Z-Y. Andersen, H. Sun, S. Holdaway, HA. Kong, W-P. Lewis, MG. Higgs, S. Rossmann, MG. Rao, S. Nabel, GJ. (2010) A virus-like particle vaccine for Chikungunya virus protects non-human primates against infection. *Nature Medicine* **16(3):** 334-338

Akhrymuk, I. Kulemzin, S. Frolova, E. (2012) Evasion of the innate immune response: the Old World Alphavirus nsP2 protein induces rapid degradation of Rpb1, a catalytic subunit of RNA polymerase II. *J. Virol.* **86(13):** 7180-7191

Ansumana, R. Jacobsen, KH. Leski, TA. Covington, AL. Bangura, U. Hodges, MH. Lin, B. Bockarie, AS. Lamin, JM. Bockarie, MJ. and Stenger, DA. (2013) Reemergence of chikungunya virus in Bo, Sierra Leone. *Emerging Infect.Dis.*. **19(7):** 1108-1110

Apandi, Y. Nazni, WA. Noor Alzeen, ZA. Vythilingam, I. Noorazian, MY. Azahari, AH. Zainah, S. and Lee, HL. (2009) The first isolation of chikungunya virus from non-human primates in Malaysia. *J. Gen. Mol. Virol.* **1(3):** 25-39

Arankalle, VA. Shrivastava, S. Cherian, S. Gunjikar, RS. Walimbe, AM. Jadhav, SM. Sudeep, AB. and Mishra, AC. (2007) Genetic divergence of Chikungunya viruses in India (1963-2006) with special reference to the 2005-2006 explosive epidemic. *J. Gen. Virol.* **88:** 1967-1976

Attoui, H. Sailleau, C. Jaafar, FM. Belhouchet, M. Biagini, P. Cantaloube, JF. De Micco, P. Mertens, P. Zientara, S. (2007) Complete nucleotide sequence of Middelburg virus, isolated from the spleen of a horse with severe clinical disease in Zimbabwe. *J. Gen. Virol.* **88:** 3078-3088

Baltimore, D. (1971) Expression of animal virus genomes. *Bacteriol. Rev.* **35(3):** 235-242

Barth, BU. Wahlberg, JM. Garoff, H. (1995) The oligomerization reaction of the Semliki Forest virus membrane protein sub-units. *J. Cell Biol.* **128:** 283-291

Benedict, MQ. Levine, RS. Hawley, WA. and Lounibos, LP. (2007) Spread of the tiger: global risk of invasion by the mosquito Aedes albopictus. *Vect. Borne Zoonotic. Dis.* **7(1):** 76-85

Bernard, E. Solignat, M. Gay, B. Chazal, N. Higgs, S. Devaux, C. and Briant, L. (2010) Endocytosis of Chikungunya virus into mammalian cells: Role of clathrin and early endosomal compartments. *PLoS One* **5(7):** e11479

Bernard, K. Klimstra, WB. and Johnston, RE. (2000) Mutations in the E2 glycoprotein of Venezuelan equine encephalitis virus confer heparin sulphate interaction, low morbidity and rapid clearance from the blood of mice. *Virology* **276(1):** 93-103

Binder, GK. and Griffin, DE. (2001) Interferon-gamma-mediated site-specific clearance of alphavirus from CNS neurons. *Science* **293(5528):** 303-306

Blasius, AL. and Beutler, B. (2010) Intracellular toll-like receptors. *Immunity* **32:** 305-315

Borgherini, G. Poubeau, P. Jossaume, A. Gouix, A. Cotte, L. Michault, Arvin-Berod, C. Paganin, F. (2008) Persistent Arthralgia Associated with Chikungunya Virus: A Study of 88 Adult Patients on Reunion Island *Clin Infect Dis.***47(4):** 469-475

Breakwell, L. Dosenovic,P. Karlsson, Hedestam, GB. D'Amato, M. Liljeström, P. Fazakerley, J. and McInerney, GM. (2007) Semliki Forest virus nonstructural protein 2 is involved in suppression of the type I interferon response. *J. Virol.* **81(16):** 8677-8684

Briolant, S. D. Garin, D. Scaramozzino, N. Jouan, A. Crance, JM. (2004) In vitro inhibition of Chikungunya and Semliki Forest viruses replication by antiviral compounds: synergistic effect of interferon and ribavirin combination. *Antiviral Res.* **61:** 111-117

Burt, F. Rolph, MS. Rulli, NE. Mahalingam, S. Heise, MT. (2012) Chikungunya: a re-emerging virus. *Lancet* **379:** 662-671

Calisher, CH. Shope, RE. Brandt, WE. Casals, J. Karabatsos, N. Murphy, FA. Tesh, RB. and Wiebe, ME. (1980) Proposed antigenic classification of registered arboviruses I. Togaviridae, Alphavirus *Intervirology* **14:** 229-232:

Calisher, CH. el-Kafrawi**,** AO. Al-Deen Mahmud, MI. Travassos da Rosa, AP. Bartz, CR. Brummer-Korvenkontio, M. Haksohusodo, S. and Suharyono, W. (1986) Complex-specific immunoglobulin M antibody patterns in humans infected with alphaviruses. *J. Clin. Microbiol.* **23:** 155-159

Calisher, CH. Karabatsos, N. Dalrymple, JM. Shope, RE. Porterfield, JS. Westway, EG. and Brandt, WE. (1989) Antigenic relationships between flaviviruses as determined by cross-neutralization tests with polyclonal antisera. *J. Gen. Virol.* **70:** 37-43

Carey, DE. (1971) Chikungunya and dengue: a case of mistaken identity? *J. Hist. Med. Allied Sci.* **26:** 243-262

Cassadou, S. Boucau, S. Petit-Sinturel, M. Huc, P.I Leparc-Goffart, PI. and Ledrans, M. (2014) Emergence of chikungunya fever on the French side of St Martin Island, October to December 2013. *Eurosurveillance* **19(13):** Article 2

Cavrini, F. Gaibani, P. Pierro, AM. Rossini, G. Landini, MP. Sambrini, V. (2009) Chikungunya: an emerging and spreading arthropod-borne viral disease. *J. Infect. Dev. Ctries.* **3(10):** 744-752

Cheng, RH. Kuhn, RJ. Olson, NH. Rossmann, MG. Choi, HK. Smith, TJ. and Baker, TS. (1995) Nucleocapsid and glycoprotein organization in an enveloped virus. *Cell* **80:** 621-630

Choi, HK. Tong, L. Minor, W. Dumas, P. Boege, U. Rossman, MG. and Wengler, G. (1999) Sructure of Sindbis viruscore protein reveals a chymotrypsin-like serine proteinase and the oganisation of the virion. *Nature* **354:** 37-43

Chopra, A. Anuradha, V. Lagoo-Joshi, V. Kunjir, V. Salvi, S. and Saluja, M. (2008) Chikungunya virus aches and pains: an emerging challenge. *Arthritis Rheum*.**58:** 2921-2922

Chung, BY-W. Firth, AE. Atkins, JF. (2010) Frameshifting in alphaviruses: a diversity of 3' stimulatory structures. *J. Mol. Biol.* **397 :** 448-456

Couderc, T. Chrétien, F. Schilte, C. Disson O. Brigitte, M. Guivel-Benhassine, F. Touret, Y. Barau, G. Cayet, N.Schuffenecker, I. Despre`, P. Arenzana-Seisdedos, F. Michault, A. Matthew L. Albert, M. Lecuit, M.(2008) A Mouse Model for Chikungunya: Young Age and Inefficient Type-I Interferon Signaling Are Risk Factors for Severe Disease *PloS Pathogens* **4(2):** e29

Clarke DH. and Casals J. (1958) Techniques for hemagglutination and hemagglutination-inhibition with arthropod-borne viruses. *Am J Trop Med Hyg* **7:** 561–573.

Couderc, T. Khandoudi, N. Grandadam, M. Visse, C. Gangneux, N. Bagot, S. Prost, J. Lecuit, M. (2009) Prophylaxis and therapy for chikungunya virus infection. *J. Infect.Dis.* **200:** 516-523

Cross (1983) Identification of a unique guanine-7-methyltransferase in Semliki Forest Virus (SFV) infected cell extracts. *Virology* **130:** 452-463

Cruz, CC. Suthar, MS. Montgomery, SA. Shabman, R. Simmonds, J. Johnston, RE. Morrison, TE. and Heise, MT. (2010) Modulation of type I IFN induction by a virulence determinant within the alphavirus nsP1. *Virology* **399(1):** 1-10

Davis, NL. Willis, LV. Smith, JF. and Johnston, RE. In vitro synthesis of infection Venezuelan equine encephalitis virus RNA from a cDNA clone: analysis of a viable mutant. (1989) *Virology* **171:** 189-204

De Groot, RJ. Hardy, WR. Shirako, Y. Strauss, JH. (1990) Cleavage site preferences of Sindbis virus polyprotein containing the non-structural proteinase. Evidence for temporal regulation of polyprotein processing *in vivo*. *EMBO J.* **9(8):** 2631-2638

De Lamballerie, X. Leroy, E. Charrel, RN. Ttsetsarkin, K. Higgs, S and Gould, EA. (2008) Chikungunya virus adapts to tiger mosquito via evolutionary convergence: a sign of things to come? *Virol. J.* **5: 33**

Delatte, H. Dehecq, JS. Thira, J. Domerg, C. Paupy, C. and Fontenille, D. (2008) Geographic distribution and development sites of *Aedes albopictus* (Diptera: Culicidae) during a chikungunya epidemic event. *Vect. Borne Zoonotic Dis.* **8(1):** 25-34

Desmyter, J. Melnick, J. and Rawls, WE. (1968) Defectiveness of interferon production and of rubella virus interference in a line of African green monkey kidney cells (Vero). J. Virol. 2(10): 955-961

DeTulleo, L. and Kirchhausen, T. (1998) The clathrin endocytic pathway in viral infection. *EMBO J.* 17**(16):** 4585-4593

Deuber, SA. and Pavlovic, J (2007) Virulence of a mouse-adapted Semliki Forest virus strain is associated with reduced susceptibility to interferon. *J. Gen Virol.* **88:** 1952-1959

Dhanwani, R. Khan, M. Bhaskar, ASB, Singh, R. Patro, IK. Rao, PVL. Parida, MM. (2012) Characterization of chikungunya virus infection in human neuroblastoma SH-SY5Y cells: Role of apoptosis in neuronal cell death. *Virus Res.* **163(2):** 563-572

Dhanwani, R. Khan, M, Venkata, Rao, PVL. Ly, H. Parida, M. (2014) Characterization of chikungunya virus induced host response in a mouse model of myositis. *PLOS One* **9(3):** e92813

Diallo, M. Thonnon, J. Traore-Lamizana, M. and Fontenille, D. (1999) Vectors of Chikungunya virus in Senegal : current data and transmission cycles. *Am. J. Trop. Med. Hyg.* **60 (2):** 281-286

Dieffenbach, CW. Lowe, TM and Dveksler, GS. (1993) General concepts for PCR primer design *Genome Res.* **3:** S30-S37

Dobryszycka, W. (1997) Biological Functions of Haptoglobin - New Pieces to an Old Puzzle. *Eur. J. Clin. Chem. Clin. Biochem.* **35(9):** 647-654

Doxsey, S. Brodsky, FM. Blank, G.and Helenius, A. (1987) Inhibition of endocytosis by anti-clathrin antibodies. *Cell* **50(3):** 453–463.

Dupont-Rouzeyrol, M. Caro, V. Guillaumot, L. Vazeille, M. D'Ortenzio, E. Thiberge, JM. Baroux, N. Gourinat, AC. Grandadam and M. Falloux, AB. (2012) Chikungunya

virus and the mosquito vector *Aedes aegyptii* in New Caledonia (South Pacific Region). *Vector Borne Zoonotic Dis.* **12(12):** 1036-41

Dutta, P Khan, SA. Khan, AM. Borah, J. Chowdhury, P. and Mahanta, J.(2011) First evidence of chikungunya infection in Assam, Northeast India. *Trans. R. Soc. Trop. Med Hyg*. **105:** 355–357

Eckels, KH. Harrison, VR. and Hetrick, FM. (1970) Chikungunya virus vaccine prepared by Tween-ether extraction. *Appl. Microbiol.* **19(2):** 321-325

Edleman, R. Tacket, CO. Wasserman, SS. Bodison, SA. Perry, JG. and Manggiafico, JA. (2000) Phase II Safety and Immunogenicity of Live Chikungunya Virus Vaccine TSI-GSD-218. *Am. J. Med. Hyg.* **62(6):** 681-685

Edwards, CJ. Welch, SR. Chamberlain, J. Hewson, R. Tolley, H. Cane, PA. and Lloyd, G.(2007) Molecular diagnosis and analysis of Chikungunya virus. *J. Clin. Virol.* **39:** 271-275

Eleazer and Hill (1994) Highlands J virus-associated mortality in chukar partridges. *J. Vet. Invest.* **6:** 98-99

Emeny and JE. Morgan, MJ. (1978) Regulation of the interferon system: evidence that vero cells have a genetic defect in interferon production *J. Gen. Virol.* **43:** 247-252

Fata, C. Sawicki, S. and Sawicki, D. (2002) Alphavirus minus-strand RNA synthesis: Identification of a role for Arg183 of the nsP4 polymerase. *J. Virol.* **76(17):** 8632-8640

Fayzulin, R.and Frolov, I. (2004) Changes of the secondary structure of the 5’ end of the Sindbis virus genome inhibit virus growth in mosquito cells and lead to accumulation of adaptive mutations. *J. Virol.* **78(10):** 4953-4964

Firth, AE. Chung, BYW., Fleeton, MN. and Atkins, JF. (2008) Discovery of frameshifting in Alphavirus 6K resolves a 20-year enigma. *Virol. J.* **5:** 108

Forrester, NL. Palacios, G. Tesh, RB. Savji, N. H. Guzman, H. M. Sherman, M. Weaver, SC. and Lipkinb, WI. (2012) Genome-scale phylogeny of the Alphavirus genus suggests a marine origin. *J. Virol.* **86(5):** 2729-2738

Fric, J. Bertin-Maghit, S. Wang, CI.Nardin, A. and Warter, L. (2013) Use of human monoclonal antibodies to treat chikungunya virus infection. *J. Infect. Dis.* **207:** 319-322

Fritel, X. Rollot, O. Gérardin, P. Gaüzère, B-A. Bideault, J. Lagarde, L. Dhuime, B. Orvain, E. Cuillier, F. Ramful, D. Sampériz, S. Jaffar-Bandjee, M-C. Michault, A. Cotte, L. Kaminski, M. Fourmaintraux, A. and the Chikungunya-Mère-Enfant Team (2010) Chikungunya Virus Infection during Pregnancy, Réunion, France, 2006. *Emerging Infect. Dis.* **16(3):** 418-425

Frolov, I. Hardy, R. Rice, CM.Cis-acting RNA elements at the 5' end of Sindbis virus genome RNA regulate minus – and plus strand RNA synthesis. (2001) *RNA* **7(11):** 1638-1651

Frovlova, E. Frovlov, I. Schlesinger, S. (1997) Packaging signals in Alphaviruses. *J. Virol.* **71(1):** 248-258

Frolova, EI. Fayzulin, RZ. Cook, SH. Griffin, DE. Rice, CM. and Frolov, I. (2002) Roles of nonstructural protein nsP2 and alpha/beta interferons in determining the outcome of Sindbis virus infection. *J. Virol.* **76(22):** 11254-11264

Fros, JJ. Lui, WJ. Prow, NA. Geertsema, C. Ligtenberg, M. Vanlandingham, DL. Schnettler, E. Vlak, JM. Suhrbier, A. Khromykh, AA.and Pijlman, GP. (2010) Chikungunya virus non-structural protein 2 inhibits type I/II interferon-stimulated JAK-STAT signalling. *J. Virol.* **84(20):** 10877-10887

Gaedigk-Nitschko, K. Ding, MX. Levy, MA. Schlesinger, MJ. (1990) Site-directed mutagenesis in the Sindbis virus 6Kprotein reveal sites for fatty acylation and the underacylated protein affects virus release and virus structure. *Virology* **175(1):** 282-291

Gardner, CL. Yin, J. Burke, CW. Klimstra, WB.Ryman, KD. (2009) Type I interferon induction is correlated with attenuation of a South American eastern equine encephalitis virus strain in mice. *Virology* **390:**338-347

Gardner, CL. Burke, CL. Higgs, ST. Klimstra, WB. and Ryman, KD. (2012) Interferon-alpha/beta deficiency greatly exacerbates arthritogenic disease in mice infected with wild-type chikungunya virus but not with the cell culture-adapted live attenuated 181/25 vaccine candidate. *Virology* **425(2):** 103-112

Gardner, J. Anraku, I. Le, TT. Larcher, T. Major, L. Roques, P. Schroder, WA. Higgs, S. Suhrbier, A. (2010) Chikungunya virus arthritis in adult wild-type mice. *J. Virol.* **84(16):** 8021-8032

Garmashova, NR. Gorchakov, E. Frolova E. and I. Frolov, I. (2006) Sindbis virus nonstructural protein nsP2 is cytotoxic and inhibits cellular transcription. *J. Virol.* **80:** 5686–5696.

Garmashova, N.Gorchakov, R. Volkova, E. Paessler, S. Frolova, E. and Frolov I. (2007a) The Old World and New World alphaviruses use different virus-specificproteins for induction of transcriptional shutoff. *J. Virol.* **81(5):** 2472-2484

Garmashova, N. Atasheva, S. Kang, W. Weaver, SC. Frovlova, E.and Frovlov, I. (2007b) Analysis of Venezuelan Equine Encephalitis virus capsid protein function in the inhibition of cellular transcription. *J. Virol.* **81(24):** 13552-13565

Garoff, H. and Simons, K. (1974) Isolation and characterization of the membrane proteins of Semliki Forest virus. *Virology* **61:** 493-504

Garoff, H. Wilschut, J. Liijestrom, P. Wahlberg, JM. Bron, R. Soumalainen, M. Smyth, J. Barth, BU. Zhao, H. Forsell, K. Ekström, M. (1994) Assembly and entry mechanisms of Semliki Forest virus. *Arch.Virol. Suppl.* **9:** 329-338

Gauri, LA. Ranwa, BL. Nagar, K. Vyas, A. and Fatima, Q. (2012) Post chikungunya brain stem encephalitis. *J. Assoc. Physicians India* **60:** 68-69

Gentilomi, GA. Cricca1, M. Giovanna De Luca, G. Rossella Sacchetti, and R. Zanetti, F. (2008) Rapid and sensitive detection of MS2 coliphages in wastewater samples by quantitative reverse transcriptase PCR. *New Microbiol.* **31:** 273-280

Gérardin, P. Barau, G. Michault, A. Blintner, M. Randrianaivo, H. Choker, G. Lenglet, Y. Touret,Y. Bouveret, A. Grivard, P. Le Roux, K. and Blanc, S. (2008) Multidisciplinary Prospective Study of Mother-to-Child Chikungunya Virus Infections on the Island of La Réunion. *PLos Med* **5(3):** e60. doi:10.1371

Glasgow, GM. McGee, MM. Sheahan, BJ. and Atkins, GJ. (1997) Death mechanisms in cultured cells infected by Semliki Forest virus. *J. Gen. Virol.* **78(7):** 1559-1563

Gomes, MMP. de Souza Bastos, M. Pinto de Figueiredo, R. Lima Gimaque, JB. dos Santos Galusso, E. Kramer, VM. Costa de Oliveira, CM. Gomes Naveca, F. and Moraes Figueiredo, LT. (2012) Mayaro Fever in the City of Manaus, Brazil, 2007–2008 *Vector Borne Zoonotic Dis.* **12(1):** 42–46

Gomez de Cedron, M. Ehsani, N. Mikkola, ML. Garcia, JA. and Kääriäinen, L. (1999) RNA helicase activity of Semliki Forest virus replicase protein NSP2. *FEBS Letters* **448(1):** 19-22

Gould, EA. and Higgs, S. (2009) Impact of climate change and other factors on emerging arbovirus diseases. *Trans. R. Soc Trop. Med. Hyg.* **103:**109-121

Grandadam, M. Caro, V. Plumet, S. Thiberge, J-M. Souarès, Y. Failloux, A-B. Tolou, HJ. Budelot, M. Cosserat, D. Leparc-Goffart, I. and Desprès, P. (2011) Chikungunya virus in southeastern France. *Emerg. Infect. Dis.* **17(5):** 910-913

Gratz, NG. (2004) Critical review of the vector status of *Aedes albopictus*. *Med. Vet. Entomol.* **18:** 215-227

Griffin, DE (2013) Alphaviruses. In: *Fields Virology* 6th Edition. Knipe DM. and Howley PM. (eds) 651-686. Lippincott, Williams and Wilkins, Philadelphia

Hahon N. and Zimmerman WD. (1970) Chikungunya virus infection of cell monolayers by cell-to-cell and extracellular transmission. *Appl. Microbiol.* **19:** 389-391

Hahn, CS. Lustig, S. Strauss, EG. and Strauss, JH. (1988) Western equine encephalitis virus is a recombinant virus. *Proc. Natl. Acad. Sci.* **85:** 6997-6001

Haller, O. Weber, F. Kochs, G. (2005 Intracellular antiviral defence mechanisms: the power of interferon-regulated restriction factors. In: *Molecular pathogenesis of virus infections.* Digard, P. Nash, AA. and Randall, RA. (eds) 253-268 Cambridge University Press, New York.

Hapuarachchi, HC.Bandara, KBA. Sumanadasa, SDM. Hapugoda, MD. Lai, Y. Lee, KS. Tan, LK. Lin, RTP. Ng, LFP. Bucht, G. Abeyewickreme, W. Ng, LC. (2010) Re-emergence of Chikungunya virus in South-east Asia : virological evidence from Sri Lanka and Singapore. *J. Gen. Virol.* **91:**1067-1076

Hardy, RW. and Rice, CM. (2005) Requirements at the 3' end of the *Sindbis virus* genome for efficient synthesis of minus-strand RNA. *J. Virol.* **79(8):** 4630-4639

Hardy, WR. Straus, JH. (1989) Processing the non-structural proteins of Sindbis virus: non-structural proteinase. J. Virol. 63: 4653-4664

Hardy, WR. (2006) The role of the 3' terminus of the Sindbis virus genome in the minus strand initiation site selection. *Virology* **354(2):** 520-531

Harrison, VR. Binn, LN. and Randall, R. (1967) Comparative Immunogenicities of Chikungunya Vaccines Prepared in Avian and Mammalian Tissues. *Am. J. Trop. Med. Hyg. 16(6):* 786-791

Hasebe, F. Parquet, MC. Pandey, BD. Mathenge, EGM. Morita, K. Balasubramaniam, V. Saat, Z. Yusop, A. Sinniah, M. Natkunam, S. and Igarashi, A. (2002) Combined detection and genotyping of chikungunya virus by specific reverse transcription-polymerase chain reaction. *J. Med. Virol.* **67(3):** 370-374

Hawman, DW. Stoermer, KA. Montgomery, SA. Pal, P. Oko, L. Diamond, MS. and Morrison, TE. (2013) Chronic joint disease caused by chronic chikungunya virus infection is controlled by the adaptive immune response. *J. Virol.* **87(24):** 13878-13888

Heil, ML. Albee, A. Strauss, JH. and JM. Kuhn, RJ. (2001) An amino acid substitution in the coding region of the E2 glycoprotein adapts Ross River virus To utilize heparan sulfate as an attachment moiety. *J. Virol.* **75(14):** 6303-6309

Heise, MT. Simpson, DA. and Johnson, RE. (2000)A single amino acid change in nsP1 attenuates neurovirulence of the Sindbis-group alphavirus SA AR86. *J. Virol.* **74(9):** 4207-4213

Heise, MT. White, LJ. Simpson, DA. Leonard, C. Bernard, KA. Meeker, RB. and Johnson, RE. (2003) An attenuating mutation in nsP1 of the Sindbis-group virus SAAR86 accelerates non-structural protein processing and up-regulates viral 26S RNA synthesis. *J. Virol.* **77(2):** 1149-1156

Helenius, A. Morein, B. Fries, E. Simons, K. Robinson, P. Schirrmachert, V. Terhorst, C. and Strominger, JL. (1978) Human (HLA-A and HLA-B) and murine (H-2K and H-2D) histocompatibility antigens are cell surface receptors for Semliki Forest virus. *Proc. Nati. Acad. Sci.* **75(8):** 3846-3850

Helenius, A. Kartenbeck, J. Simons, and K. Fries, E. (1980) On the entry of Semliki Forest virus into BHK-21 cells. *J. Cell Biol.* **84:** 404-420

Hernandez, R. Luo, and T. Brown, DT. (2001) Exposure to low pH is not required for penetration of mosquito cells by Sindbis virus. *J. Virol.* **75(4):** 2010-2013

Hill, KR. Hajou, M. Hu, JY. Raju, R. (1997) RNA-RNA recombination in Sindbis virus: roles of the 3' conserved motif, poly-A tail and non-viral sequences of template RNAs in polymerase recognition and template switching. *J. Virol.* **71(4):** 2693-2704

Hoarau, JJ. Jaffar Bandjee, M.C. Krejbich Trotot,P. Das,T. Li-Pat-Yuen,G. Dassa, B. Denizot, M. Guichard, E. Anne Ribera, A.Tawfiq Henni,T. Frank Tallet, F.Marie Pierre Moiton, M. Gauzère, BA. Sandrine Bruniquet, S. Jaffar Bandjee, Z. Morbidelli, Martigny, G. Jolivet ,M Gay,F. Marc Grandadam, M. Tolou, H. Vieillard,V. Debrè, P. Autran,B. and Philippe Gasque, P. (2010) Persistent chronic inflammation and infection by chikungunya arthritogenic alphavirus in spite of a robust host immune response . *J. Immunol.* **184:** 5914-5927

Hornung, V. Ellegast, J. Kim, S. Brzózka, K. Jung, A. Kato, H. Poeck, H. Akira, S. Conzelmann, K-K. Schlee, M. Endres, S. and Hartmann G. (2006) 5'Triphosphate RNA Is the Ligand for RIG-I. *Science* **314:** 994-997

Horwood, PF. Reimer,LJ. Dagina, R. Susapu, M. Bande, G. Katusele, M. Koimbu, G. Jimmy, S. Ropa, B. Siba, PM. and Pavlin, BI. (2013) Outbreak of Chikungunya Virus Infection, Vanimo, Papua New Guinea. *Emerging Infect. Dis.* **19(9):** 1535-1538

Huang, X. Li, and Y.Zheng, C. (2009) A novel single-cell quantitative real-time RT-PCR method for quantifying foot-and-mouth disease viral RNA. *J. Virol. Methods* **155:** 150-156

HSE http://www.hse.gov.uk

Jan, JT. and Griffin, DE. (1999) Induction of apoptosis by sindbis virus occurs at cell entry and does not require virus replication. *J. Virol.* **73(12):** 10296-10302

Janeway, CA. Travers, P. Walport, M. Shlomchik, MJ. (2006) In: *Immunobiology*, 6th edition New York: Garland Science Publishing

Jansen, MD. Gjerset, B. Modahl, I. Bohlin, J. (2010) Molecular epidemiology of salmonid alphavirus subtype 3 in Norway. *Virol. J.* **7:** 188

Jordan, GW. (1973) Interferon Sensitivity of Venezuelan Equine Encephalomyelitis Virus. *Infect. Immun.* **7(6):** 911-917

Jose, J. Snyder, JE. and Kuhn, RJ. (2009) A structural and functional perspective of alphavirus replication and assembly. *Future Microbiol.* **4:** 837-856

Jose, J. Przybyla, L. Edwards, TJ. Perera, R. Burgner, JW. Kuhn, RJ. (2012) Interactions of the cytoplasmic domain of Sindbis virus E2 with nucleocapsid cores promote alphavirus budding. *J. Virol.* **86(5):** 2585-2599

Judith, D. Mostowy, S. Bourai, M. Gangneux, N. Lelek, M.Lucas-Hourani, M. Cayet, N. Yves Jacob, Y. Prévost, M-C. Pierre1, P. Tangy, F. Zimmer, C. Pierre-Olivier Vidalain, P-O. Couderc, T. and Lecuit, M. (2013) Species-specific impact of the autophagy machinery on Chikungunya virus infection. *EMBO reports* **14(6):** 534-544

Kääriäinen, L. and Ahola, T. (2002) Functions of alphavirus non-structural proteins in RNA replication. Progress in Nucleic acid Research **71:**187-222

Kariuki Njenga, M. Nderitu, L. Ledermann, JP. Ndirangu, A. Logue, CH. Kelly, CHL. Sang, R. Sergon, K. Breiman, R. and Powers, AM. (2008) Tracking epidemic Chikungunya virus into the Indian Ocean from East Africa. *J. Gen. Virol.* **89:** 2754-2760

Karp, YA. Aher, PP. Lole, KS. (2011) NTPase and 5′-RNA Triphosphatase Activities of Chikungunya Virus nsP2 Protein. *PLoS ONE* **6(7):** e22336

Karras, GI. Kustatscher, G. Buhecha, HR. Allen, MD. Pugieux, C. Sait, F. Bycroft, M. and Ladurner, AG. (2005) The macro domain is an ADP-ribose binding module. EMBO J. **24(11):** 1911-1920

Kaur, P. and Jang Hann Chu, J. (2013) Chikungunya virus: an update on antiviral development and challenges. *Drug Discovery Today* **18(19/20):** 969-983

Kaur, P. Thiruchelvan, M. Ching Hua Lee, R. Chen, H. Caiyun Chen, K. Lee Ng, M. Jang Hann Chu, J. (2013) Inhibition of Chikungunya virus replication by harringtonine, a novel antiviral that suppresses viral protein expression. *Antimicrob. Agents Chemother.* **57(1):** 157-167

Khan, AH. Morita, K. Parquet, MC. Hasebe, F. Mathenge, EGM and Igarashi, A. (2002) Complete nucleotide sequence of chikungunya virus and evidence for an internal polyadenylation site. *J. Gen. Virol.* **83:** 3075-3084

Kiellan, M. Chanel-Vos, C. and Liao, M. (2010) Alphavirus entry and membrane fusion. *Viruses* **2:** 796-825 doi:10.3390

Kim, HK. Rümenapf, T. Strauss, EG. and Strauss, JH. (2004) Regulation of Semliki Forest virus RNA replication: a model for the control of alphavirus pathogenesis in invertebrate hosts. Virology **323:** 153-163

Kim, TK and Eberwine, JH. (2010) Mammalian cell transfection: the present and the future. *Anal. Bioanal.Chem.* **397:** 3173-3178

King, AMQ. Adams, MJ. Carstens, EB. and Lefkowitz, E. J. (Edits) (2011) Virus Taxonomy: Ninth Report of the International Committee on Taxonomy of Viruses (ICTV).

Klimstra, WB. Ryman, KD. Johnston, RE. (1998) Adaption of Sindbis virus to BHK cells selects for use of Heparan sulphate as an attachment receptor. *J. Virol.* **72(9):** 7357-7366

Krejbich-Torot, P. Denizot, M. Hoarau, JJ. Jaffar-Bandjee, MC. Das, T. and Gasque, P. (2011) Chikungunya virus mobilizes the apoptotic machinery to invade host cell defences. *FASEB J.* **25:** 314-325

Kuhn, RJ. Hong, Z.and Strauss,JH. (1990) Mutagenesis of the 3' nontranslated region of Sindbis virus RNA. *J. Virol.* **64(4):** 1465-1476

Kuhn, RJ. Griffin, DE. Zhang, H. Niesters, HGM. Strauss, and JH. (1992) Attenuation of Sindbis virus neurovirulence by using defined mutations in nontranslated regions of the genome RNA. *J. Virol.* **66(12):** 7121-7127

Kuhn, RJ. (2013) Togaviridae: The viruses and their replication. In*: Fields Virology* 6th Edition. Knipe DM. and Howley PM. (eds) 1002-1022. Lippincott, Williams and Wilkins Philadelphia

Kumar, NP. Joseph, R, Kamara, T and Jambulingam, P. (2008) A226V mutation in virus during the 2007 chikungunya outbreak in Kerala, India. *J. Gen. Virol*. **89:** 1945-1948

Labadie, K. Larcher, T. Joubert, C. Mannioui, A.Delache, B. Brochard, P. Guigand, L. Dubreil, L. Lebon, P. Verrier, B. deLamballerie, X. Suhrbier, A. Cherel, Y. Le Grand, R. and Roques, P. (2010) Chikungunya disease in non-human primates involves long-term viral persistence in macrophages. *J. Clin Invest.* **120(3):** 894- 906

Lahariya, C. and Pradhan, SK.(2006) Emergence of chikungunya virus in Indian sub-continent after 32 years: a review. *J. Infect. Borne Dis*. **43:** 151-160

Laakkonen, P. Hyvönen, M. Peränen, J. and Kääriäinen, L. (1994) Expression of Semliki Forest virus nsP1-specific methyl transferase in insect cells and in *E.coli*. *J. Virol.* **68(11):** 7418- 7425

Lakshmi, V. Neeraja, M Subbalaxmi, MVS. Parida, MM. Dash, PK. Santhosh, and SR Rao, PVL (2008). Clinical features and molecular diagnosis of chikungunya fever in South India. *Clin. Infect. Dis.* **46:** 1436-1442

La Linn, M. Gardner, J. Warrilow, D. Darnell, GA. McMahon, CR. Field, I. Hyatt, AD. Slade, RW. and Suhrbier, A.(2001) Arbovirus of marine mammals: a new alphavirus isolated from the elephant seal louse, *Lepidophthirus macrorhini*. *J. Virol.* **75(9):** 4103-9

La Linn, M. Eble, JA. Lübken, C. Slade, RW. Heino, J. Davies, J. Suhrbier, A. (2005) An arthritogenic alphavirus uses the α1β1 integrin collagen receptor. *Virology* **366(2):** 229-239

Lanciotti, RS. Ludwig, ML. Rwaguma, EB. Lutwama, JJ. Kram, TM. Karabatsos, N. C. Cropp, BC. and Barry R. Miller, BR. (1998) Emergence of Epidemic O'nyong-nyong Fever in Uganda after a 35-Year Absence: Genetic Characterization of the Virus *Virology* **252:** 258–268

Laras, K. Sucri, NC. Larasati, RP. Bangs, MJ. Kosim, R. Djauzi, Wandra, T. Master, J. Kosasih, H. Hartati, S. Becket, C. Sedyaningsih, ER. Beecham III, HJ. and Corwin, AL.(2005) Tracking the re-emergence of epidemic chikungunya virus in Indonesia. *Trans. R. Soc. Trop. Med. Hyg.* **99:** 128-141

Lavergne, A. De Thoisy, B. Lacoste, V. Pascalis, H. Pouliquen, J-F. Mercier, V. Tolou, H. Dussart, P. Morvan, J. Talarmin, A. and Kazanji, M. (2006) Mayaro virus: Complete nucleotide sequence and phylogenetic relationships with other alphaviruses. *Virus Res.* **117:** 283-290

Lescar, J. Roussel, A. Wien, MW. Navaza, J. Fuller, SD. Wengler, G. Wengler, G. and Rey, FA. (2001) The fusion glycoprotein shell of Semliki Forest virus: an icosahedral assembly primed for fusogenic activation at endosomal pH. *Cell* **105(1):** 137-148

Levitt, NH. Ramsburg, HH. Hasty, SE. Repik, PM. Cole, FE. and Lupton, HW. (1986) Development of an attenuated strain of chikungunya virus for use in vaccine production. *Vaccine* **4:** 157-162

Lewthwaite, P. Begum, A. Veerahsankar, M. Ravikumar, R. Desai, A. Osborne, J. Plank, J. Hewson, R. Ravi, V. Beeching, N. and Solomon, T. (2009) Chikungunya virus and central nervous system infections in children, India. *Emerg. Infect. Dis.* **15(2):** 329-331

Li, G. and Rice, CM. (1989) Mutagenesis of the in-frame opal termination codon preceeding nsP4 of Sindbis virus: studies of translational readthrough and its effect on virus replication. *J. Virol.* **63(3):** 1326-1336

Liijeström, P. and Garoff, H. (1991) Internally located cleavable signal sequences direct the formation of Semliki Forest virus membrane proteins from a polyprotein precursor. *J. Virol.* **65(1):** 147-154

Liijeström, P. Lusa, S. Huylebroeck, D. and Garoff, H. (1991) In vitro mutagenesis of a full-length cDNA clone of Semliki Forest virus: the small 6,000-molecular-weight membrane protein modulates virus release. *J. Virol.* **65(8):** 4107-4113

Litzba, N. Shufffenecker, I. Zeller, H. Drosten, C. Emmerich, P. Charrel, R. Kreher, P. and Niedrig, M. (2008) Evaluation of the first commercial chikungunya virus indirect immunofluorescence test. *J. Virol. Meth.* **149:** 175-179

Lloyd, G. Alphaviruses. in: Principles and Practice of Clinical Virology. (5^{th} edition) Zuckerman, AJ. Banatvala, JE. Pattison, JR. Griffiths, PD. Schoub, BD. (eds) 509-529 John Wiley & Sons, Ltd.

Lobigs, M. and Garoff, H. (1990) Fusion function of the Semliki Forest virus spike is activated by proteolytic cleavage of the envelope glycoprotein precursor p62. J. Virol. 64(3): 1233-1240

Loewy, A. Smyth, J. Von Bonsdorff, CH. Liijestrom, P. and Schlesinger, MJ. (1995) The 6-kilodalton membrane protein of Semliki Forest virus is involved in the budding process. *J. Virol.* **69(1):**469-475.

Ludwig, GV., Kondig, JP. and Smith, JF. (1996) A putative receptor for Venezuelan Equine Encephalitis virus from mosquito cells. *J. Virol.* **70(8):** 5592-5599

Luers, AJ. Adams, SD. Smalley, and Campanella, J. (2005) A phylogenomic study of the genus Alphavirus employing whole genome comparison. *Comp. Func. Genom.* **6:** 217-227

Lulla, A. Lulla, and V. Merits, A. (2012) Macromolecular assembly-driven processing of the 2/3 cleavage site in the alphavirus replicase polyprotein. *J. Virol.* **86(1):** 553-65

Lum, F-M. Teo, T-H. Lee, WWL. Kam, Y-W. Rénia, L. and Ng, LFP. (2011) An Essential Role of Antibodies in the Control of Chikungunya Virus Infection. *J. Immunol.* **190(12):** 6295-6302

Lusa, S. Garoff, H. and Liljeström, P. (1991) Fate of the 6K membrane protein of Semliki Forest virus during virus assembly. *Virology* **185(2):** 843-6

Malet, H. Gould, EA. Jamal, S. Dutartre, H. Papageorgiou, N. Neuvonen, M. Ahola, T. Forrester, N. Gould, EA. Lafitte, D. Ferron, F. Lescar, J. Gorbalenya, AE. De Lamballerie, X. and Canard, B. (2009) The crystal structures of Chikungunya and Venezuelan equine encephalitis virus nsP3 macro domains define a conserved adenosine binding pocket. *J. Virol.* **83(13):** 6534-6545

Mareike Kümmerer, B. Klaus Grywna, K. Gläsker, S. Wieseler, J. and Christian Drosten C. (2012) Construction of an infectious Chikungunya virus cDNA clone and stable insertion of mCherry reporter genes at two different sites. *J. Gen. Virol.* **93:** 1991–1995

Mai, J. Sawicki, S. and Sawicki, D. (2009) Fate of minus-strand templates and replication complexes produced by a P23-cleavage defective mutant of Sindbis virus. *J. Virol.* **83(17):** 8553-8564

Mallilankaraman, K. Shedlock, DJ. Huihui Bao, H. Omkar U. Kawalekar, OU. Fagone, P. Ramanathan, AA. Ferraro, B. Stabenow, J. Vijayachari, P. Sundaram, SG. Muruganandam, N. Sarangan, G. Srikanth, P. Khan, AS. Lewis, MG. Kim, JJ.

Sardesai, NY. Muthumani, K. and Weiner, DB. (2011) A DNA Vaccine against Chikungunya Virus Is Protective in Mice and Induces Neutralizing Antibodies in Mice and Nonhuman Primates. *PLOS Negl. Trop. Dis.* **5(1)**: e928

Marsh, M. and HeleniusA. (1980) Adsorptive endocytosis of Semliki Forest virus. *J. Mol. Biol.* **142:** 439-454

Mayuri, Geders, TW. Smith, JL. Kuhn, RJ. (2008) Role for conserved residues of Sindbis virus nonstructural protein 2 methyltransferase-like domain in regulation of minus-strand synthesis and development of cytopathic infection. *J. Virol.* **82(15):** 7284-7297

McInerny, GM. Smit, JM. Liijestrom, P. and Wilsschut, J. (2004) Semliki Forest virus produced in the absence of the 6K protein has an alterd spike structure as revealed by decreased membrane fusion capacity. *Virology* **325(2):** 200-206

Merits, A., Vasiljeva, L., Ahola, T., Kääriäinen, L., and Auvinen, P. (2001) Proteolytic processing of Semliki Forest virus-specific non-structural polyprotein by nsP2 protease. *J. Gen. Virol.* **82:** 765–773.

Messaoudi, I. Vomaske, J. Totonchy, T. Kreklywich, TC. Haberthur, K. Laura Springgay, L. Brien, JD. Diamond, MS. DeFilippis and VR. Streblow, DN. (2013) Chikungunya virus infection results in higher and persistent viral replication in aged Rhesus macaques due to defects in anti-viral immunity. *PLoS Negl. Trop. Dis.* **7(7):**1-13

Metsikkö, K and Garoff, H. (1990) Oligomers of the cytoplasmic domain of the p62/E2 membrane protein of Semliki Forest virus bind to the nucleocapsid *in vitro*. *J. Virol.* ***64*(10):** 4678-4683

Metz, SW. Gardner, Geertsema, C. Le, TT. Goh, L. Vlak, JM. Suhrbier, A. and Pijlman, GP. (2013) Effective Chikungunya Virus-like Particle Vaccine Produced in Insect Cells. *PLOS Negl. Trop. Dis.* **7(3)**: e2124

Meylan E, Curran J, Hofmann K, Moradpour D, Binder M, Bartenschlager R, and Tschopp J. (2005) Cardif is an adaptor protein in the RIG-I antiviral pathway and is targeted by hepatitis C virus. *Nature* **437:**1167–1172.

Mi, S. and Stollar, V. (1991) Expression of sindbis virus nsP1 and methyltransferase activity inEscherichia coli. *Virology* **184:** 423-427.

Montgomery, SA. and Johnston, RE. (2007) Nuclear import and export of Venezuelan Equine Encephalitis Virus Nonstructural Protein 2. *J. Virol.* **81(19):** 10268- 10279

Moriette, C. LeBerre, M. Lamoureux, A. Lai, T-L. and Brémont, M. (2006) Recovery of recombinant salmonid alphavirus fully attenuated and protective for rainbow trout. *J. Virol.* **80(8):** 4088-4098

Morrison, TE. Oko, L. Montgomery, SA. Whitmore, AC. Lotstein AR. Gunn, BM. Elmore, SA. Heise, MT. (2011) A mouse model of Chikungunya virus-induced musculoskeletal inflammatory disease. *Am. J. Path.* **78(1):** 32-40

Myles, KM. Kelly, CLH. Ledermann, JP. and Powers, AM. (2006) Effects of an opal termination codon preceding the nsP4 gene sequence in the O'nyong nyong virus genome on *Anopheles gambiae* infectivity. *J. Virol.* **80(10):** 4229-4997

Nakaya, HI. Gardner, J. Poo, Y-S. Major,L. Pulendran, B. and Suhrbier A. (2012) Gene profiling of chikungunya virus arthritis in a mouse model reveals significant overlap with rheumatoid arthritis. *Arthritis Rheum.* **64(11):** 3553-3563

Nasar , F. Palacios, G. Gorchakov, RV. Guzman, H. Travassos Da Rosa, AP. Savji, N. Popov, VL. Sherman, MB. Lipkin, WI. Tesh, RB. and Weaver, SC. (2012) Eilat virus, a unique alphavirus with host range restricted to insects by RNA replication. *PNAS* **109(36):** 14622–14627

Nicola, AV. Chen, W. and Helenius, A. (1999) Co-translational folding of an alphavirus capsid protein in the cytosol of living cells. *Nature Cell Biol.* **1:**341-345

Niesters, HGM.and Strauss, JH. (1990) Defined mutations in the 5' nontranslated sequence of Sindbis virus RNA. *J. Virol.* **64(9):** 4162-4168

Njenga, MK. Nderitu, L. Ledermann, JP. Ndirangu, A. Logue, CH. Kelly, CHL. Sang, R. Sergon, K. Breiman, R. and Powers, AM. (2008) Tracking epidemic Chikungunya virus into the Indian Ocean from East Africa. *J. Gen. Virol.* 89: 2754-2760

Ou, J-H. Strauss, EG. Strauss, JH (1983)The 5'-terminal sequences of the genomic RNAs of several alphaviruses. *J. Mol. Biol.* 168: 1-15

Ozden, S. Huerre, M. Riviere, J-P. Coffey, LL. Afonso, PV. Mouly, V. de Monredon, J. Roger, JC. El Amrani, M. Yvin, JL. Jaffar, MC. Frenkiel, MP. Sourisseau, M. Schwartz, O. Butler-Browne, G. Desprès, P. Gessain, A. Ceccald, PE. (2007) Human muscle satellite cells as targets of chikungunya virus infection. *PLoS ONE* **2(6):** e527. doi:10.1371

Panning, M. Grywna, K. van Esbroeck, M. Emmerich, P.and Drosten, C. (2008) Chikungunya fever in travelers returning to Europe from the Indian Ocean region, 2006. *Emerging Infect. Dis.* **14(3):** 416-422

Paredes, AM. Heidner, H. Thuman-Commike, P. Venkataram Prasad, BV. Johnson, RE. Chui, W. (1998) Structural localization of the E3 glycoprotein in attenuated Sindbis virus mutants *J. Virol.* **72(2):** 1534-1541

Parrott, MM. Sitarski, SA. Arnold, RJ. Picton, LK. Hill, RB. and Mukhopadhyay, S. (2009) Role of conserved cysteines in alphavirus E3 protein. *J. Virol.* **83(6):** 2584-2591

Pastorino, B. Muyembe-Tafum, JJ. Bessaud, M. Tock, F. Tolou, H. Durand, JP. And Peyrefitte, CN. (2004) Epidemic resurgence of Chikungunya virus in democratic Republic of the Congo: Identification of a new central African strain. *J. Med. Virol.* **74:** 277-282

Paupy, C. Kassa, FK. Caron, M. Nkoghé, D. and Leroy, EM. (2012) A chikungunya outbreak associated with the vector Aedes albopictus in remote villages of Gabon. *Vector-Borne Zoonotic Dis.* **2(2):** 167-169

Pedicone, LD. Brass, CA. Albrecht, JK. *et al.* (2009) Peginterferon alfa-2b or alfa-2a with ribavirin for treatment of hepatitis C infection, *N. Engl. J. Med.* **361(6):** 580–593,

Pehrson, and R. Fuji, RN. (1998) Evolutionary conservation of histone macro H2A subtypes and domains. Nucleic Acids Res. **26:** 2837-2842

Pepys, MB. Baltz, M. Gomer, K. Davies, AJS. and Doenhoff, M.(1979) Serum amyloid P-component is an acute phase reactant in the mouse. *Nature* **278:** 259-261

Pfeffer, M. Kinney, RM. Kaaden and O-R. (1998) The Alphavirus 3′-nontranslated region: size heterogeneity and arrangement of repeated sequence elements. *Virology* **240(1):** 100-108

Pialoux, G. Gauzere, BA. Jaureguiberry, S. and Strobel, M. (2007) Chikungunya, an epidemic arbovirus. *Lancet Infect. Dis.* **7:** 319-327

Plante, K. Wang, E. Partidos, CD. Weger, J. Gorchakov, R. Tsetsarkin, K. Borland, EM. Powers, AM. Seymour, R. Stinchcomb, DT. Osorio, JE. Frolov, I. Weaver, SC. (2011) Novel Chikungunya Vaccine Candidate with an IRES-Based Attenuation and Host Range Alteration Mechanism. *PLoS* **7(7):** e1002142

Powers, AM. Brault, AC. Tesh, RB. and Weaver, SC. (2000) Re-emergence of chikungunya and o'nyong-nyong viruses: evidence for distinct geographical lineages and distant evolutionary relationships. *J. Gen. Virol.* **81:** 471-479

Powers, AM. Brault, AC. Shirako, Y. Straus, EG. Kang, W. Straus, JH. and Weaver, SC. (2001) Evolutionary relationships and systematics of the alphaviruses. *J. Virol* **75(21):** 1011-31

Powers, AM. Aguilar, PV. Chandler, LJ. Brault, AC. Meakins, TA. Watts, D. Russell, KL. Olson, J. Vasconcelos, PFC. Da Rossa, AT. Weaver, SC. and Tesh, RB. (2006)Genetic relationships among Mayaro and Una viruses suggest distinct patterns of transmission. *Am. J. Trop. Med. Hyg.* **75(3):** 461-469

Powers, AM. and Logue, CH. (2007) Changing patterns of Chikungunya virus: re-emergence of a zoonotic arbovirus. *J. Gen. Virol.* **88:** 2363-2377

Powers, AM. (2008) Epidemic Emergence of Chikungunya Virus: Options for Control of an Enzootic Virus. In: *Emerging Infections 8* Scheld, WM. Hammer, SM. and Hughes, SM. (eds) 125-136 ASM Press, Washington, DC.

Precious, SW. Webb, HE. and Bowen, ETW. (1974) Isolation and persistence of chikungunya virus in cultures of mouse brain cells. *J. Gen. Virol.* **23:** 271-279

Puiprom, O. Morales Vargas, RE. Potiwat, R. Chaichana, P. Ikuta, K. Pongrama Ramasoota, P. and Okabayashi, T. (2013) Characterization of chikungunya virus infection of a human keratinocyte cell line: Role of mosquito salivary gland protein in suppressing the host immune response. *Infect. Genet. Evol.***17:** 210-215

Quetglas, JI. Ruiz-Guillen, M. Alejandro, A. Casales, E. Bezunartea, J. and Smerdou, C. (2010) Alphavirus vectors for cancer therapy. *V. Res.***153:** 179-196

Queyriaux, B, Simon F, Grandadam M, Michel R, Tolou H and Boutin JP. (2008) Clinical burden of chikungunya virus infection. *Lancet Infect Dis.* **8(1):** 2–3

Randall, RE. and Goodbourn, S. (2008) Interferons and viruses: an interplay between induction, signalling, antiviral responses and virus countermeasures. *J. Gen. Virol.* **89:** 1-47

Ravichandran, R. Manian, M. (2008) Ribavirin therapy for Chikungunya arthritis. *J. Infect. Developing Countries* **2(2):** 140-142

Rayner, JO. Dryga, SA. and Kamrud, KL. (2002) Alphavirus vectors and vaccination. *Rev. Med. Virol.* **12;** 279-296

Renault, P. Solet, J-L. Sissoko, D. Balleydier, E. Larrieu, S. Filleul, L.Lassalle, C. Thiria, J. Rachou, E. de Valk, H. Ilef, D. Ledrans, M. Quatresous, I. Quenel, P. and Pierre, V. (2008) A Major Epidemic of Chikungunya Virus Infection on Réunion Island, A Major Epidemic of Chikungunya Virus Infection on Réunion Island, France, 2005–2006. *Am. J. Trop. Med. Hyg.* **77(4):** 727-731

Rezza, G., Nicholetti, L. Angelini, R. Romi, R. Finarelli, AC. Panning, M. Cordioli, P. Fortuna, C. Boros, S. Magurano, F. Silvi, G. Angelini, P. Dottori, M. Ciufolini, MG. Majori, GC. and Cassone, A. (2007) Infection with Chikungunya virus in Italy: an outbreak in a temperate region. *Lancet* **370**: 1840-1846

Rhim, J. S., Schell, K., Creasy, B. and Case, W. (1969) Biological characteristics and viral susceptibility of an African green monkey kidney cell line (Vero). *Proc. Soc. Exp. Biol. Med.* **132:** 670–678.

Rikkonen, M. Peränen, J. Kääriäinen, L. (1992) Nuclear targeting signals of Semliki Forest Virus non-structural protein nsP2. *Virology* **189:** 462-473

Rikkonen, M. Peränen, J. Kääriäinen, L. (1994) Nuclear targeting of Semliki Forest Virus nsP2. *Arch Virol. Suppl.* **9:** 369-377

Robinson, MC. (1955) An epidemic of virus disease in Southern Province, Tanganyika Territory, in 1952-53. I. Clinical features. *Trans. R. Soc. Trop. Med. Hyg.* **49:** 28-32

Rosanov, MN. Koonin, EV. And Gorbalenya, AE. (1992) Conservation of the putative methyltransferase domain: a hallmark of the "Sindbis-like" supergroup of positive-strand RNA viruses. *J. Gen. Virol.* **73:** 2129-2134

Ross, RW. (1956) The Newala epidemic. III. The virus: isolation, pathogenic properties and relationship to the epidemic. *J. Hyg. (Lond)* **54(2):** 177-91

Rubak, JK. Wasik, BR. Rupp, JC. Kuhn, RJ. Hardy, RW. Smith, JL. (2009) Characterization of purified Sindbis virus nsP4 DNA-dependent RNA polymerase activity in vitro. *Virology* **384:** 201-208

Rümenapf, T. Strauss, EG. And Strauss, JH. (1994) Sub-genomic mRNA of Aura alphavirus is packaged into virions. *J. Virol.* **69(1):** 56-62

Salonen, A. Vasiljeva, L. Merits, A. Magden, J. Jokitalo, E, and Kääriäinen, L. (2003) Properly folded non-structural polyprotein directs the Semliki Forest virus replication complex to the endosomal compartment. *J. Virol.* **81(2):** 872-883

Salonen, A. Ahola, T. and Kääräinen, L. (2004)Viral RNA replication in association with cellular membranes. *Curr. Top. Microbiol. Immunol.* **285:** 139-173

Sambrook, J. Fritsch, EF. Maniatis, T. (1989) *Molecular Cloning, A Laboratory Manual* (2nd ed.) Appendix E5. Cold Spring Harbor Laboratory Press New York.

Sam, I-C. Loong, S-K. Michael, JC. Chua, C-L. Sulaiman, WYW. Vythilingam, I. Chan, S-Y. Chiam, C-W. Yeong, Y-S. AbuBakar, S. and Chan, YF (2012) Genotypic and Phenotypic Characterization of Chikungunya Virus of Different Genotypes from Malaysia. *PLoS One* **7(11):** e50476

Santosh, SR. Dash, PK. Parida, MM. Khan, M. Tiwari, M. and Lakshmana Rao, PV. (2008) Comparative full genome analysis revealed E1: A226V Indian Chikungunya virus isolates. *Virus Res.* **135:**36-41

Sarkar, JK. Chatterjee, SN. Chakravarti and SK. Mitra, AC. (1965) Chikungunya virus infection with haemorrhagic manifestations. *Ind J. Med. Res.* **53:** 921-923

Saxton-Shaw, KD. Ledermann, JP. Borland, EM. Stovall JL, Mossel, EC. Singh, AJ. Wilusz, J. and Powers, AM. (2013) O'nyong nyong Virus Molecular Determinants of Unique Vector Specificity Reside in Non-Structural Protein 3. *PLOS. Negl. Trop. Dis.* **7(1):** 1-9

Schilte, C. Couderc, T. Chretien, F. Sourisseau, M.Gangneux, N Guivel-Benhassine, F. Kraxner, A. Tschopp, J. Higgs, S. Michault, A. Arenzana-Seisdedos, F. Colonna, M. Peduto,L. Schwartz, O. Lecuit, M and Albert, ML. (2010) Type I IFN controls chikungunya virus via its action on nonhematopoietic cells *J. Exp. Med.* **207:** 429-442

Schmid, S. Fuchs, R. Kielian, M. Helenius, A. Mellman, I. (1989) Acidification of sub-populations in wild-type chinese hamster ovary cells and temperature sensitive acidification-defective mutants. *J. Cell Biol.* **108:** 1291-1300

Schuffenecker, I. Iteman, I. Michault, A. Frangeul, L. Vaney, MC. Lavenir, R. Pardigon, N. Reynes, JM. Pettinelli, F. Biscornet, L. Diancourt, L. Michel, S. Duquerroy, S. Guigon, G. Frenkeil, MP. Bréhin, AC. Cubito, N. Desprès, P. Kunst, F. Rey, FA. Zeller, H. and Brisse, S. (2006) Genome Microevolution of Chikungunya Viruses Causing the Indian ocean Outbreak. *PLoS* Medicine **3 (7):** 1058-1070

Schultz-Cherry, S. Dybing, JK. Davis, NL.Williamson, C. Suarez, DL. Johnston, R. and Perdue, ML. (2000) Influenza virus (A/HK/156/97) hemagglutinin expressed by an alphavirus replicon system protects chickens against lethal infection with Hong Kong-origin H5N1 Viruses *Virology* **278**: 55-59

Schwartz, O. and Albert, ML. (2010) Biology and pathogenesis of chikungunya virus. *Nature Rev.* **8:** 491-500

Sergon, K. Njuguna, C. Kalani, R. Ofula, V. Onyango, C. Konongoi, LS. Bedno, S. Burke, H. DumillaAM. Konde, J. Njenga, MK. Sang, R. and Breiman, RF. (2008) Seroprevalence of Chikungunya Virus (CHIKV) Infection on Lamu Island, Kenya, October 2004. *Am. J. Trop. Med. Hyg.* **78 (2):** 333-337

Shin, G. Yost, SA. Miller, MT. Elrod, EJ. Grakoui, A. Marcotrigliano, J. (2012) Structural and functional insights into alphavirus polyprotein processing and pathogenesis. *PNAS.* 109(41): 16534-16539

Shirako, Y. and Strauss, JH. (1994) Regulation of Sindbis virus RNA replication: uncleaved P123 and nsP4 function in minus-strand RNA synthesis, whereas cleaved products from P123 are required for efficient plus-strand RNA synthesis. *J. Virol.* **68(3):** 1874-1885

Shirako, Y. Strauss, EG. Strauss, JH. (2000) Suppressor mutations that allow Sindbis virus RNA polymerase to function with nonaromatic amino acids at the N-terminus: Evidence for interaction between nsP1 and nsP4 in minus-strand RNA synthesis. *Virology* **276(1):** 148-160

Simmons, JD. Wollish, AC. and Heise, MT. (2010) A determinant of Sindbis virus neurovirulence enables efficient disruption of Jak/STAT signalling. *J. Virol.* **84(21):** 11429-11439

Simzu, B. Yamamoto, K. Hashimoto, K. and Ogata, T. (1984) Structural proteins of chikungunya virus. *J. Virol.* **51(1):** 254-258

Singh, L. and Helenius, A. (1992) Role of ribosomes in Semliki Forest nucleocapsid uncoating. J. Virol. **66:** 7049-7058

Singh, SS. Manimunda, SP. Sugunan, AP. Sahina, Vijayachari, P (2008) Four cases of acute flaccid paralysis associated with chikungunya virus infection. *Epidemiol. Infect.* **136(9):** 1277-80

Sjöberg, M. Lindqvist, B. and Garoff, H. (2011) Activation of the alphavirus spike protein is suppressed by bound E3. *J. Virol.* **85(11):** 5644-5650

Smee, DF. Alaghamandan, HA. Kini, GD. and Robins, RK. (1988) Antiviral action and mode of action of ribavirin 5'sulfamate against Semliki Forest virus. *Antiviral Res.* **10 :** 253-262

Snyder, JE. Kulcsar, KA. Schultz, KLW. Riley, CP. Neary, JT. Marr, S. Jose, J. Griffin, DE. and Kuhn, RJ. (2013) Functional Characterization of the Alphavirus TF Protein. *J. Virol.* **87(15):** 8511-8523

Sourisseau, M. Schilte, C. Casartelli, N. Trouillet, C. Guivel-Benhassine, F. Rudnicka, D.Sol-Foulon, N. Le Roux, K. Prevost, MC. Fsihi, H. Frenkiel, MP. Blanchet, F. Afonso, PV. Ceccaldi, PE. Ozden, S. Gessain, A. Schuffenecker, I. Verhasselt, B. Zamborlini, A. Saïb, A. Rey, FA. Arenzana-Seisdedos, F. Desprès, P. Michault, A. Albert, ML. and Schwartz, O. (2007) Characterization of re-emerging chikungunya virus. *PLoS Pathog.* **3(6):** e8917604450

Spuul, P. Salonen, A Merits, A. Jokitalo, E. Kääriäinen, L. and Ahola, T. (2007)Role of amphipathic peptide of Semliki Forest virus replicase protein nsP1 in membrane association and virus replication. *J. Virol.* **81(2):** 872-883

Staples, JE. Breiman, RF. and Powers, AM. (2009) Chikungunya fever: an epidemiological review. *Clin. Infect. Dis.* **49:** 942-948

Stout, JT. and Caskey, CT. (1985) HPRT: gene structure, expression and mutation. *Ann. Rev. Genet.* **19:** 127-48

Strauss, EG. Rice, CM. and Strauss, JH. (1983) Sequence coding for the alphavirus nonstructural proteins is interrupted by an opal termination codon. *Proc. Natl. Acad. Sci.* **80:** 5271-5275

Strauss, JH. and Strauss, EG. (1994) The Alphaviruses: Gene Expression, Replication and Evolution. *Microbiol. Rev.* **58 (3):** 491-562

Strauss, JH. Wang, K-S. Schmaljohn, AL. Kuhn, RJ. and Strauss, EG. (1994) Host cell receptors for Sindbis virus. *Arch. Virol. (Suppl)* **9:** 473-484

Strauss, JH. and Strauss, EG. (2002) in: *Viruses and Human Disease* Academic Press

Sun, B. skaeveland, I. Svingerud, T. Zou, J. Jorgensen, J. and Robertsen, B. (2011) Antiviral activity of salmonid gamma interferon against infectious pancreatic necrosis

virus and salmonid alphavirus and its dependency on type 1 interferon. J. Virol. 85(17): 9188-9198

Sun, Q. Sun, L. Lui, H-H. Chen, X. Seth, RB. Forman, J. Chen, ZJ. (2006) The specific and essential role of MAVS an antiviral innate immune response. *Immunity* **24:** 633-642

Suthar, MS. Shabman, R. Madric, K Lambeth, C. and Heise, MT. (2005) Identification of Adult Mouse Neurovirulence Determinants of the Sindbis Virus Strain AR86. *J. Virol.* **79(7):** 4219-4228

Teo, T-H. Lum, F-M. Claser, C. Lulla, V. Lulla, A. Merits, A. Rénia, L. and Ng, LFP. (2013) A pathogenic role for CD4+ T cells during chikungunya virus infection in mice. *J. Immunol.* **190:** 259-269

Tesh, RB. (1982)Arthritides caused by mosquito-borne viruses. *Ann. Rev. Med.* **33:** 31-40

Thangamani, S. Higgs, S. Ziegler, S. Vanlandingham, D. Tesh and R. Wikel, S. (2010) Host immune response to mosquito-transmitted chikungunya virus differs from that elicited by needle inoculated virus. *PLoS ONE* 5(8): e12137

Thein, S. La Linn, Aaskov, J. Aung, MM. Zaw, A. and Myint, A (1992) Development of a simple indirect enzyme-linked immunosorbent assay for the detection of immunoglobulin M antibody in serum from patients following an outbreak of chikungunya virus infection in Yangon, Myanmar. *Trans. R. Soc. Trop. Med. Hyg*. **86:** 438-442

Thomas, S. Rai, J. John, L. Günther, S. Drosden, C. Pützer and Schaefer, S. 2010) Functional dissection of the alphavirus capsid protease: sequence requirements for activity. *Virol. J.*7:327 doi:10:1186

Thon-Hon, VG. Denizot, M. Li-Pat-Yuen, Giry, GC. Marie-Christine Jaffar-Bandjee, M-C. and Gasque, P. (2012) Deciphering the differential response of two human fibroblast cell lines following Chikungunya virus infection. *Virol. J.* **9**:213

Tomar, S. Hardy, RW. Smith, JL. Kuhn, RJ. (2006) Catalytic core of alphavirus non-structural protein nsP4 possesses terminal adenyltransferase activity. *J. Virol.* **80(20):** 9962-9969

Travassos Da Rosa, AP.et al (2001) Trocara virus: a newly recognised Alphavirus (Togavirus) isolated from mosquitoes in the Amazon Basin. *Am. J. Trop. Med. Hyg.* **64:** 93-97

Tsetsarkin, K. Higgs, S. McGee, CE. De Lamballerie, X. Charrel, RN, Vanlandingham, DL. (2006) Infectious clones of chikungunya virus (La Réunion isolate) for vector competence studies. *Vector-Borne Zoonotic Dis.* **6(4):** 325-336

Tsetsarkin, KA. Vanlandingham, DL. McGee, CE. and Higgs, S. (2007) A single mutation in Chikungunya Virus affects vector specificity and epidemiological potential. *PLoS Pathol*. **3 (12):** 1895-1905

Tsetsarkin, KA. McGee, CE. Volk, SM. Vanlandingham, Weaver, SC. and Higgs, S. (2009) Epistatic roles of E2 glycoprotein mutations in adaption of chikungunya virus to Aedes Albopictus and Ae.aegypti mosquitoes. *PLoS ONE* **4(8):** e6835. doi:10.1371/journal.pone.0006835

Tsetsarkin, KA. Vanlandingham, DL. McGee, CE. and Higgs, S. (2007) A single mutation in Chikungunya Virus affects vector specificity and epidemiological potential. *PLoS Pathol*. **3 (12):** 1895-1905

Tsetsarkin, KA. Chen, R. Leal, G. Forrester, N. Higgs, S. Huang, J. Weaver, SC. (2011) Chikungunya virus emergence is constrained in Asia by lineage-specific adaptive landscapes. *PNAS.* **108(19):** 7872-7877

Tuittilla, M. and Hinkkanen, AE. (2003) Amino acid mutations in the replicase protein nsP3 of Semliki Forest virus cumulatively effect neurovirulence. *J. Gen. Virol.* **84:** 1525-1533

Ubol and Griffin (1991) Identification of a putative alphavirus receptor on mouse neural cells. *J. Virol.* **65(12):** 6913-6921

Uhlar, CM. and Whitehead, AS. (1999) Serum amyloid A, the major vertebrate acute-phase reactant. *Eur. J. Biochem.* **265(2):** 501-523

Urbinelli, S. Bellini, B. Carrieri, M. Sallicandro, P. and Celli, G. (2000) population structure of Aedes albopictus (Skuse) : the mosquito which is colonising Mediterranean countries. *Heredity* **84:** 331-337

Van Bortel, W. Dorleans, F. Rosine, J. Blateau, A. Rousset, D. Matheus, S. Leparc-Goffart, I. Flusin, O. Prat, CM. Césaire, R. Najioullah, F. Ardillon, V. Balleydier, E. Carvalho, L. Lemaître, A. Noël, H. Servas, V. Six, C. Zurbaran, M. Léon, L. Guinard, A. van den Kerkhof, J. Henry, M. Fanoy, E. Braks, M. Reimerink, J. Swaan, C. Georges, R. Brooks, L. Freedman, J. Sudre, B. and Zeller H. (2014) Chikungunya outbreak in the Caribbean region, December 2013 to March 2014, and the significance for Europe. *Eurosurveillance* **19(13):** Article 5

Vasiljeva, L. Merits, A. Auvinen, P. Kääriäinen, L. (2000) Identification of a novel function of the alphavirus capping apparatus: RNA5'triphosphatase activity of nsP2. *J. Biol. Chem.* **275:** 172881-17287

Vazeille, M. Sara Moutailler, S.Daniel Coudrier, D. Rousseaux, C. Khun, H. Huerre, M. Thiria, J. Dehecq, J-S. Fontenille, D. Schuffenecker, I. Despres, P and Failloux, A-B. (2007) Two Chikungunya isolates from the outbreak of La Reunion (Indian Ocean) exhibit different patterns of infection in the mosquito, Aedes albopictus. *PLoS ONE* **2(11):** e1168. doi:10.1371

Vihinen, H. Ahola, T. Tuitila, M. Merits, A.and Kääriäinen, L. (2001) Elimination of phosphorylation sites of Semliki Forest virus replicase protein nsP3. J. *Biol. Chem.* **276(8):** 5745-5752

Villoing, S. Bearzotti, M Chilmonczyk, S. Castric, J. and Bremont M. (2000) Rainbow trout sleeping sickness disease virus is an atypical alphavirus. *J. Virol*. **74:** 173-183

Wang, D. Suhrbier, A. Penn-Nicholson, A. Woraratanadharm, J. Gardner, J. Luo, M. Le, TT. Anraku, I. Sakalian, M. Einfeld, D. and Y. Dong, JY. (2011) A complex adenovirus vaccine against chikungunya virus provides complete protection against viraemia and arthritis. *Vaccine* **29:** 2803-2809

Wang, E, Volkova, E. Paige Adams, A. Forrester, N. Xiao, S-Y. Frolov, I. and Weaver, SC. (2008) Chimeric alphavirus vaccine candidates for chikungunya. *Vaccine* **26:** 5030-5039

Wang, K-S. Schmaljohn, AL. Kuhn, RJ. and Strauss, JH. (1991) Antiidiotypic Antibodies as Probes for the Sindbis Virus Receptor. *Virology* **181:** 694-702

Wang, K-S. Kuhn, Strauss, RJ. Ou, S. and Strauss, JH. (1992) High-Affinity Laminin Receptor Is a Receptor for Sindbis Virus in Mammalian Cells. *J. Virol.* **66(8):** 4992-5001

Wang, Y. Sawicki, S. Sawicki, D. (1991) Sindbis virus nsP1 functions in negative-strand RNA synthesis. *J. Virol.* **65(2):** 985-988

Waquier, N. Becquart, P. Nkoghe, D. Padilla, C. Ndjoyi-Mbiguino, A. and Leroy, EM. (2011) The acute phase of chikungunya infection in humans is associated with strong innate immunity and T CD8 cell activation. *J. Infect. Dis.* **204:** 115-124

Weaver SC, Rico-Hesse R, Scott TW (1992). "Genetic diversity and slow rates of evolution in New World alphaviruses". *Curr. Top. Microbiol. Immunol.* **176**: 99–117.

Weaver SC, Hagenbaugh A, Bellew LA, Netesov SV, Volchkov VE, Chang GJ, Clarke DK, Gousset L, Scott TW, Trent DW (November 1993). "A comparison of the nucleotide sequences of eastern and western equine encephalomyelitis viruses with those of other alphaviruses and related RNA viruses". *Virology* **197 (1):** 375–90

Weaver, S. C., W. Kang, Y. Shirako, T. Rumenapf, E. G. Strauss, and J. H.Strauss. 1997. Recombinational history and molecular evolution of western equine encephalomyelitis complex alphaviruses. *J. Virol.* **71:** 613–623.

Weaver, SC. Frey, TK. Huang, HV. Kinney, RM. Rice, CM. Roehrig, JT. Shope, RE. and Strauss, EG. (2005) in: *Togaviridae, Virus Taxonomy: Eighth Report of the International Committee on Taxonomy of Viruses.* (Fauquet, CM. Mayo, MA. Maniloff, J. Desselberger, U. and Ball, LA., eds) 999-1008.

Weiss, B. Geigenmüller-Gnirke, U. and Schlesinger, S. (1994) Interactions between Sindbis virus RNAs and a 68 amino acid derivative of the nucleocapsid protein further defines the capsid binding site. *Nucleic Acids Res.* **22(5):** 780- 786

Wengler, G. Würkner, D. and Wengler, G. (1992) Identification of a sequence element in the alphavirus core protein which mediates interaction of cores with ribosomes and the disassembly of cores. *Virology* **191(2):** 880-888

Wengler, G. Koschinski, A. Wengler, G. and Dreyer, F. (2003) Entry of alphaviruses at the plasma membrane converts the viral surface proteins into an ion permeable pore that can be detected by electrophysiological analyses of whole-cell membrane currents. *J. Gen. Virol.* **84(1):** 173-181

Weston, JH. Welsh, MD. McLoughlin, MF. and Todd, D. (1999) Salmon pancreas disease virus, an alpha virus infecting farmed Atlantic salmon, Salmo salar. *Virology* **256:** 188-195

White, LJ. Wang, J-G. Davis, NL. Johnson, RE. (2001) Role of alpha-beta interferon in Venezuelan equine encephalitis virus pathogenesis: effect of an attenuating mutation in the 5' untranslated region. *J. Virol.* **75(8):** 3706-3718

Wilkinson (2005) The discovery of ubiquitin-dependent proteolysis. *PNAS* **102(43):** 15280-15282

Wintachai, P. Wikan N. Kuadkitkan, A. Jaimipuk, T. Ubol, S. Pulmanausahakul, R. Auewarakul, P. Kasinrerk, W. Weng, W-Y. Mingkwan Panyasrivanit, M. Atchara Paemanee, A. Kittisenachai, S. Roytrakul, S. and Smith, DR. (2012) Identification of prohibitin as a Chikungunya virus receptor protein. *J. Med. Virol.* **84:** 1757-1770

Xu, C. Guo, TC. Mutoloki, S. Haugland, Ø. Marjara, IS. and Evensen, Ø. (2010) Alpha interferon and not gamma interferon inhibits salmonid alphavirus subtype 3 replication *in vitro.* *J. Virol.* **84(17):** 8903-8912

Yap, G. Pok, KY. Lai, YL. Hapuarachchi, HC. Chow, A. Leo, YS. Tan, LC. and Ng, LK. (2010) Evaluation of Chikungunya diagnostic assays: differences in sensitivity of serology assays in two independent outbreaks. *PLoS* **4(7):** e753 1-9

Ziegler, SA. Lu, L. Travassos da Rossa, APA. Xiao and S. Tesh, RB. (2008) An animal model for studying the pathogenesis of Chikungunya virus infection. *Am. J. Trop. Med. Hyg.* **79(1):** 133-139

APPENDICES

Appendix A: Proprietary Protocols

A1 Qiagen®QIAquick® PCR purification kit

QIAquick PCR Purification Kit Protocol using a microcentrifuge

This protocol is designed to purify single- or double-stranded DNA fragments from PCR and other enzymatic reactions. For cleanup of other enzymatic reactions, follow the protocol as described for PCR samples or use the new MinElute Reaction Cleanup Kit. Fragments ranging from 100 bp to 10 kb are purified from primers, nucleotides, polymerases, and salts using QIAquick spin columns in a microcentrifuge.

Notes: • Add ethanol (96–100%) to Buffer PE before use (see bottle label for volume).
• All centrifuge steps are at ε10,000 x *g* (~13,000 rpm) in a conventional tabletop microcentrifuge.

1. Add 5 volumes of Buffer PB to 1 volume of the PCR sample and mix. It is not necessary to remove mineral oil or kerosene.
For example, add 500 µl of Buffer PB to 100 µl PCR sample (not including oil).
2. Place a QIAquick spin column in a provided 2 ml collection tube.
3. To bind DNA, apply the sample to the QIAquick column and centrifuge for 30–60 s.
4. Discard flow-through. Place the QIAquick column back into the same tube.
Collection tubes are re-used to reduce plastic waste.
5. To wash, add 0.75 ml Buffer PE to the QIAquick column and centrifuge for 30–60 s.
6. Discard flow-through and place the QIAquick column back in the same tube.
Centrifuge the column for an additional 1 min at maximum speed.
IMPORTANT: Residual ethanol from Buffer PE will not be completely removed unless the flow-through is discarded before this additional centrifugation.
7. Place QIAquick column in a clean 1.5 ml microcentrifuge tube.
8. To elute DNA, add 50 µl Buffer EB (10 mM Tris·Cl, pH 8.5) or H2O to the center of the QIAquick membrane and centrifuge the column for 1 min. Alternatively, for increased DNA concentration, add 30 µl elution buffer to the center of the QIAquick membrane, let the column stand for 1 min, and then centrifuge.

IMPORTANT: Ensure that the elution buffer is dispensed directly onto the QIAquick membrane for complete elution of bound DNA. The average eluate volume is 48 µl from 50 µl elution buffer volume, and 28 µl from 30 µl elution buffer. Elution efficiency is dependent on pH. The maximum elution efficiency is achieved between pH 7.0 and 8.5. When using water, make sure that the pH value is within this range, and store DNA at –20°C as DNA may degrade in the absence of a buffering agent. The purified DNA can also be eluted in TE (10 mM Tris·Cl, 1 mM EDTA, pH 8.0), but the EDTA may inhibit subsequent enzymatic reactions.

A2 Gel extraction - Qiagen®QIAquick® Gel Extraction kit

QIAquick Gel Extraction Kit Protocol using a microcentrifuge
This protocol is designed to extract and purify DNA of 70 bp to 10 kb from standard or low-melt agarose gels in TAE or TBE buffer. Up to 400 mg agarose can be processed per spin column. This kit can also be used for DNA cleanup from enzymatic reactions
For DNA cleanup from enzymatic reactions using this protocol, add 3 volumes of Buffer QG and 1 volume of isopropanol to the reaction, mix, and proceed with step 6 of the protocol. Alternatively, use the new MinElute Reaction Cleanup Kit.
Notes: • The yellow color of Buffer QG indicates a pH δ7.5.
• Add ethanol (96–100%) to Buffer PE before use (see bottle label for volume).
• Isopropanol (100%) and a heating block or water bath at 50°C are required.
• All centrifugation steps are carried out at ε10,000 x *g* (~13,000 rpm) in a conventional table-top microcentrifuge.
• 3 M sodium acetate, pH 5.0, may be necessary.
1. Excise the DNA fragment from the agarose gel with a clean, sharp scalpel.
Minimize the size of the gel slice by removing extra agarose.
2. Weigh the gel slice in a colorless tube. Add 3 volumes of Buffer QG to 1 volume of gel (100 mg ~ 100 µl).
For example, add 300 µl of Buffer QG to each 100 mg of gel. For >2% agarose gels, add 6 volumes of Buffer QG. The maximum amount of gel slice per QIAquick column is 400 mg; for gel slices >400 mg use more than one QIAquick column.
3. Incubate at 50°C for 10 min (or until the gel slice has completely dissolved). To help dissolve gel, mix by vortexing the tube every 2–3 min during the incubation.
IMPORTANT: Solubilize agarose completely. For >2% gels, increase incubation time.
4. After the gel slice has dissolved completely, check that the color of the mixture is yellow (similar to Buffer QG without dissolved agarose).
If the color of the mixture is orange or violet, add 10 µl of 3 M sodium acetate, pH 5.0, and mix. The color of the mixture will turn to yellow. The adsorption of DNA to the QIAquick membrane is efficient only at pH δ7.5. Buffer QG contains a pH indicator which is yellow at pH δ7.5 and orange or violet at higher pH, allowing easy determination of the optimal pH for DNA binding.
5. Add 1 gel volume of isopropanol to the sample and mix.
For example, if the agarose gel slice is 100 mg, add 100 µl isopropanol. This step increases the yield of DNA fragments <500 bp and >4 kb. For DNA fragments between 500 bp and 4 kb, addition of isopropanol has no effect on yield.
6. Place a QIAquick spin column in a provided 2 ml collection tube.
7. To bind DNA, apply the sample to the QIAquick column, and centrifuge for 1 min.

The maximum volume of the column reservoir is 800 µl. For sample volumes of more than 800 µl, simply load and spin again.

8. Discard flow-through and place QIAquick column back in the same collection tube.

Collection tubes are re-used to reduce plastic waste.

9. (Optional): Add 0.5 ml of Buffer QG to QIAquick column and centrifuge for 1 min.

This step will remove all traces of agarose. It is only required when the DNA will subsequently be used for direct sequencing, in vitro transcription or microinjection.

10. To wash, add 0.75 ml of Buffer PE to QIAquick column and centrifuge for 1 min.

Note: If the DNA will be used for salt sensitive applications, such as blunt-end ligation and direct sequencing, let the column stand 2–5 min after addition of Buffer PE, before centrifuging.

11. Discard the flow-through and centrifuge the QIAquick column for an additional 1 min at ε10,000 x *g* (~13,000 rpm).

IMPORTANT: Residual ethanol from Buffer PE will not be completely removed unless the flow-through is discarded before this additional centrifugation.

12. Place QIAquick column into a clean 1.5 ml microcentrifuge tube.

13. To elute DNA, add 50 µl of Buffer EB (10 mM Tris·Cl, pH 8.5) or H2O to the center of the QIAquick membrane and centrifuge the column for 1 min at maximum speed. Alternatively, for increased DNA concentration, add 30 µl elution buffer to the center of the QIAquick membrane, let the column stand for 1 min, and then centrifuge for 1 min.

A3 GeneElute™ Plasmid miniprep kit

Preparation Instructions

1. Thoroughly mix reagents Examine reagents for precipitation. If any reagent forms a precipitate, warm at 55–65 °C until the precipitate dissolves and allow to cool to room temperature before use.
2. Resuspension Solution Spin the tube of the RNase A Solution (Catalog No. R6148) briefly to collect the solution in the bottom of the tube. Add 13 µl (for 10 prep package), 78 µl (for 70 prep package) or 500 µl (for 350 prep package) of the RNase A Solution to the Resuspension Solution prior to initial use. Store at 4 °C.
3. Wash Solution Dilute the Wash Solution Concentrate with 10 ml (10 prep package), 100 ml (70 prep package), or 300 ml (350 prep package) of 95–100% ethanol prior to initial use. After each use, tightly cap the diluted wash solution to prevent the evaporation of ethanol.

Procedure

Note: All centrifugation speeds are given in units of *g*. Please refer to Table 1 for information on converting *g*-force to rpm. If centrifuges/rotors for the required *g*-forces are not available, use the maximum *g*-force possible and increase the spin time proportionally. Spin until all liquid passes through the column.

All steps are carried out at room temperature. Harvest cells Pellet 1–5 ml of an overnight recombinant *E. coli* culture by centrifugation. The optimal volume of culture to use depends upon the plasmid and culture density. For best yields, follow the instructions in the note below. Transfer the appropriate volume of the recombinant *E. coli* culture to a microcentrifuge tube and pellet cells at ;12,000 3 *g* for 1 minute. Discard the supernatant.

Note: For best results with recombinant *E. coli* grown in LB (Luria Broth), use 1–3 ml of culture for high copy plasmids or 1–5 ml of culture for low copy plasmids. With recombinant *E. coli* grown in rich media such as TB (Terrific Broth) or 2X YT, use only 1 ml of culture. Higher volumes can cause a reduction in yield.

1. Resuspend cells Important Reminder: *Verify that appropriate volume RNase A Solution was added to the Resuspension Solution.*

Completely resuspend the bacterial pellet with 200 µl of the Resuspension Solution. Vortex or pipette up and down to thoroughly resuspend the cells until homogeneous. Incomplete resuspension will result in poor recovery. Another rapid way to resuspend the cell pellets is to scrape the bottoms of the microcentrifuge tubes back and forth 5 times across the surface of a polypropylene microcentrifuge tube storage rack.

2. Lyse cells Lyse the resuspended cells by adding 200 µl of the Lysis Solution. Immediately mix the contents by gentle inversion (6–8 times) until the mixture becomes clear and viscous. Do not vortex. Harsh mixing will shear genomic DNA, resulting in chromosomal DNA contamination in the final recovered plasmid DNA. Do not allow the lysis reaction to exceed 5 minutes. Prolonged alkaline lysis may permanently denature supercoiled plasmid DNA that may render it unsuitable for most downstream applications.

3. Neutralize Precipitate the cell debris by adding 350 µl of the Neutralization/Binding Solution. Gently invert the tube 4–6 times. Pellet the cell debris by centrifuging at ;12,000 3 *g* or maximum speed for 10 minutes. Cell debris, proteins, lipids, SDS, and chromosomal DNA should fall out of solution as a cloudy, viscous precipitate. If the supernatant contains a large amount of floating particulates after centrifugation, recentrifuge the supernatant before proceeding to step 6.

4. Prepare Column Insert a GenElute Miniprep Binding Column into a provided microcentrifuge tube, if not already assembled.

Add 500 µl of the Column Preparation Solution to each miniprep column and centrifuge at 12,000 3 *g* for 30 seconds to 1 minute. Discard the flow-through liquid. Note: The Column Preparation Solution maximizes binding of DNA to the membrane resulting in more consistent yields.

5. Load cleared lysate Transfer the cleared lysate from step 3 to the column prepared in step 4 and centrifuge at ;12,000 3 *g* for 30 seconds to 1 minute. Discard the flow-through liquid.

6. Optional wash (use only with EndA+ strains) Add 500 µl of the Optional Wash Solution to the column. Centrifuge at ;12,000 3 *g* for 30 seconds to 1 minute. Discard the flow-through liquid. Note: When working with bacterial strains containing the wild-type EndA+ gene, such as HB101, JM101, and the NM and PR series, the Optional Wash step is necessary to avoid nuclease contamination of the final plasmid DNA product.

7. Wash column Important Reminder: *Verify that ethanol has been added to the bottle of Wash Solution 2.* Add 750 µl of the diluted Wash Solution to the column. Centrifuge at ;12,000 3 *g* for 30 seconds to 1 minute. The column wash step removes residual salt and other contaminants introduced during the column load. Discard the flow-through liquid and centrifuge again at maximum speed for 1 to 2 minutes without any additional Wash Solution to remove excess ethanol.

8. Elute DNA Transfer the column to a fresh collection tube. Add 100 µl of Elution Solution or molecular biology reagent water to the column. For DNA sequencing and other enzymatic applications, use water or 5 mM Tris-HCl, pH 8.0, as an eluant. Centrifuge at ;12,000 3 *g* for 1 minute. The DNA is now present in the eluate and is ready for immediate use or storage at –20 °C. Note: If a more concentrated plasmid DNA preparation is required, the elution volume may be reduced to a minimum of 50 µl. However, this may result in a reduction in the total plasmid DNA yield.

A4 Qiagen® QIAfilter Plasmid Midi kit

Procedure

1. Pick a single colony from a freshly streaked selective plate and inoculate a starter culture of 2–5 ml LB medium containing the appropriate selective antibiotic. Incubate for approx. 8 h at 37°C with vigorous shaking (approx. 300 rpm).

Use a tube or flask with a volume of at least 4 times the volume of the culture.

2. Dilute the starter culture 1/500 to 1/1000 into selective LB medium. For high-copy plasmids, inoculate ▲25 ml or ● 100 ml medium with ▲25–50 µl or ● 100–200 µl of starter culture. For low-copy plasmids, inoculate ▲ 50–100 ml or ● 250 ml medium with ▲ 100–200 µl or ● 250–500 µl of starter culture. Grow at 37°C for 12–16 h with vigorous shaking (approx. 300 rpm).

Use a flask or vessel with a volume of at least 4 times the volume of the culture. The culture should reach a cell density of approximately 3–4 x 109 cells per milliliter, which typically corresponds to a pellet wet weight of approximately 3 g/liter medium.

3. Harvest the bacterial cells by centrifugation at 6000 x *g* for 15 min at 4°C.

ƒ If you wish to stop the protocol and continue later, freeze the cell pellets at –20°C.

4. Resuspend the bacterial pellet in ▲ 4 ml or ● 10 ml Buffer P1.

For efficient lysis it is important to use a vessel that is large enough to allow complete mixing of the lysis buffers. Ensure that RNase A has been added to Buffer P1.

If LyseBlue reagent has been added to Buffer P1, vigorously shake the buffer bottle before use to ensure LyseBlue particles are completely resuspended. The bacteria should be resuspended completely by vortexing or pipetting up and down until no cell clumps remain.

5. Add ▲4 ml or ● 10 ml Buffer P2, mix thoroughly by vigorously inverting the sealed tube 4–6 times, and incubate at room temperature (15–25°C) for 5 min.

Do not vortex, as this will result in shearing of genomic DNA. The lysate should appear viscous. Do not allow the lysis reaction to proceed for more than 5 min. After use, the bottle containing Buffer P2 should be closed immediately to avoid acidification from CO2 in the air. If LyseBlue has been added to Buffer P1 the cell suspension will turn blue after addition of Buffer P2. Mixing should result in a homogeneously colored suspension. If the suspension contains localized colorless regions or if brownish cell clumps are still visible, continue mixing the solution until a homogeneously colored suspension is achieved.

During the incubation prepare the QIAfilter Cartridge:

Screw the cap onto the outlet nozzle of the QIAfilter Midi or QIAfilter Maxi Cartridge. Place the QIAfilter Cartridge in a convenient tube.

6. Add ▲ 4 ml or ● 10 ml chilled Buffer P3 to the lysate, and mix immediately and thoroughly by vigorously inverting 4–6 times. Proceed directly to step 7. Do not incubate the lysate on ice.

Precipitation is enhanced by using chilled Buffer P3. After addition of Buffer P3, a fluffy white material forms and the lysate becomes less viscous. The precipitated material contains genomic DNA, proteins, cell debris, and KDS. The lysate should be mixed thoroughly to ensure even potassium dodecyl sulfate precipitation. If the mixture still appears viscous, more mixing is required to completely neutralize the solution. It is important to transfer the lysate into the QIAfilter Cartridge immediately in order to prevent later disruption of the precipitate layer. If LyseBlue reagent has been used, the suspension should be mixed until all trace of blue has gone and the suspension is colorless. A homogeneous colorless suspension indicates that the SDS has been effectively precipitated.

7. Pour the lysate into the barrel of the QIAfilter Cartridge. Incubate at room temperature (15–25°C) for 10 min. Do not insert the plunger!

Important: This 10 min incubation at room temperature is essential for optimal performance of the QIAfilter Midi or QIAfilter Maxi Cartridge. Do not agitate the QIAfilter Cartridge during this time. A precipitate containing proteins, genomic DNA, and detergent will float and form a layer on top of the solution. This ensures convenient filtration without clogging. If, after the 10 min incubation, the precipitate has not floated to the top of the solution, carefully run a sterile pipet tip around the walls of the cartridge to dislodge it.

8. Equilibrate a QIAGEN-tip 100 or QIAGEN-tip 500 by applying 4ml or 10 ml Buffer QBT, and allow the column to empty by gravity flow.

Flow of buffer will begin automatically by reduction in surface tension due to the presence of detergent in the equilibration buffer. Allow the QIAGEN-tip to drain completely. QIAGEN-tips can be left unattended, since the flow of buffer will stop when the meniscus reaches the upper frit in the column.

9. Remove the cap from the QIAfilter Cartridge outlet nozzle. Gently insert the plunger into the QIAfilter Midi or QIAfilter Maxi Cartridge and filter the cell lysate into the previously equilibrated QIAGEN-tip.

Filter until all of the lysate has passed through the QIAfilter Cartridge, but do not apply extreme force. Approximately **10 ml** and **25 ml** of the lysate are generally recovered after filtration.

☞ Remove a 40 µl or 120 µl sample of the filtered lysate and save for an analytical gel (sample 1) in order to determine whether growth and lysis conditions were optimal.

10. Allow the cleared lysate to enter the resin by gravity flow.

☞ Remove a ▲ 240 µl or ● 120 µl sample from the flow-through and save for an analytical gel (sample 2) in order to determine the efficiency of DNA binding to the QIAGEN Resin.

11. Wash the QIAGEN-tip with ▲ 2 x 10 ml or ● 2 x 30 ml Buffer QC.

Allow Buffer QC to move through the QIAGEN-tip by gravity flow. The first wash is sufficient to remove all contaminants in the majority of plasmid DNA preparations. The second wash is especially necessary when large culture volumes or bacterial strains producing large amounts of carbohydrates are used.

☞ Remove a ▲ 400 µl or ● 240 µl sample from the combined wash fractions and save for an analytical gel (sample 3).

12. Elute DNA with ▲ 5 ml or ● 15 ml Buffer QF.

Collect the eluate in a 15 ml or 50 ml tube (not supplied). Use of polycarbonate centrifuge tubes is not recommended as polycarbonate is not resistant to the alcohol used in subsequent steps.

A5 QIAamp® Viral RNA Mini Kit

QIAamp Viral RNA Mini Spin Protocol

• Equilibrate samples to room temperature (15–25°C).
• Equilibrate Buffer AVE to room temperature for elution in step 10.
• Check that Buffer AW1, Buffer AW2, and Carrier RNA have been prepared
• Redissolve precipitate in Buffer AVL/Carrier RNA by heating, if necessary, and cool to room temperature before use.
• All centrifugation steps are carried out at room temperature.

1. Pipet 560 µl of prepared Buffer AVL containing Carrier RNA into a 1.5-ml microcentrifuge tube.

If the sample volume is larger than 140 µl, increase the amount of Buffer AVL/Carrier RNA proportionally (e.g., a 280-µl sample will require 1120 µl Buffer AVL/Carrier RNA).

2. Add 140 µl plasma, serum, urine, cell-culture supernatant, or cell-free body fluid to the Buffer AVL/Carrier RNA in the microcentrifuge tube. Mix by pulse-vortexing for
15 sec.

To ensure efficient lysis, it is essential that the sample is mixed thoroughly with Buffer AVL to yield a homogeneous solution. Frozen samples that have only been thawed once can also be used.

3. Incubate at room temperature (15–25°C) for 10 min.

Viral particle lysis is complete after lysis for 10 min at room temperature. Longer incubation times have no effect on the yield or quality of the purified RNA. Potentially infectious agents and RNases are inactivated in Buffer AVL.

4. Briefly centrifuge the 1.5-ml microcentrifuge tube to remove drops from the inside of the lid.

5. Add 560 µl of ethanol (96–100%) to the sample, and mix by pulse-vortexing for 15 sec.
After mixing, briefly centrifuge the 1.5-ml microcentrifuge tube to remove drops from inside the lid.

Only ethanol should be used since other alcohols may result in reduced RNA yield and purity. If the sample volume is greater than 140 µl, increase the amount of ethanol proportionally (e.g., a 280-µl sample will require 1120 µl of ethanol). In order to ensure efficient binding, it is essential that the sample is mixed thoroughly with the ethanol to yield a homogeneous solution.

6. Carefully apply 630 µl of the solution from step 5 to the QIAamp spin column (in a 2-ml collection tube) without wetting the rim. Close the cap, and centrifuge at 6000 x g
(8000 rpm) for 1 min. Place the QIAamp spin column into a clean 2-ml collection tube, and discard the tube containing the filtrate.

Close each spin column in order to avoid cross-contamination during centrifugation. Centrifugation is performed at 6000 x g (8000 rpm) in order to limit microcentrifuge noise. Centrifugation at full speed will not affect the yield or purity of the viral RNA. If the solution has not completely passed through the membrane, centrifuge again at a higher speed until all of the solution has passed through.

7. Carefully open the QIAamp spin column, and repeat step 6.

If the sample volume was greater than 140 µl, repeat this step until all of the lysate has been loaded onto the spin column.

8. Carefully open the QIAamp spin column, and add 500 µl of Buffer AW1. Close the cap, and centrifuge at 6000 x g (8000 rpm) for 1 min. Place the QIAamp spin column in a clean 2-ml collection tube (provided), and discard the tube containing the filtrate.

It is not necessary to increase the volume of Buffer AW1 even if the original sample

volume was larger than 140 µl.

9. Carefully open the QIAamp spin column, and add 500 µl of Buffer AW2. Close the cap and centrifuge at full speed (20,000 x g; 14,000 rpm) for 3 min. Continue directly with step 10, or to eliminate any chance of possible Buffer AW2 carryover, perform step 9a, and then continue with step 10.

Note: Residual Buffer AW2 in the eluate may cause problems in downstream applications. Some centrifuge rotors may vibrate upon deceleration, resulting in flow-through, containing Buffer AW2, contacting the QIAamp spin column. Removing the QIAamp spin column and collection tube from the rotor may also cause flowthrough to come into contact with the QIAamp spin column. In these cases, the optional step 9a should be peformed.

9a. (Optional): Place the QIAamp spin column in a new 2-ml collection tube (not provided), and discard the old collection tube with the filtrate. Centrifuge at full speed for 1 min.

10. Place the QIAamp spin column in a clean 1.5-ml microcentrifuge tube (not provided).

Discard the old collection tube containing the filtrate. Carefully open the QIAamp spin column and add 60 µl of Buffer AVE equilibrated to room temperature. Close the cap, and incubate at room temperature for 1 min. Centrifuge at 6000 x g (8000 rpm) for 1 min.

A single elution with 60 µl of Buffer AVE is sufficient to elute at least 90% of the viral RNA from the QIAamp spin column. Performing a double elution using 2 x 40 µl of Buffer AVE will increase yield by up to 10%. Elution with volumes of less than 30 µl will lead to reduced yields and will not increase the final concentration of RNA in the eluate.

Viral RNA is stable for up to one year when stored at –20°C or –70°C.

A6 Qiagen® Minielute gel extraction kit

MinElute Gel Extraction Kit Protocol
using a microcentrifuge

This protocol is designed to extract and purify DNA of 70 bp to 4 kb from standard or low-melt agarose gels in TAE or TBE buffer resulting in high end-concentrations of DNA.
Up to 400 mg agarose can be processed per MinElute column.

Important points before starting

- The yellow color of Buffer QG indicates a pH δ7.5.
- Add ethanol (96–100%) to Buffer PE before use (see bottle label for volume).
- All centrifugation steps are carried out at ε10,000 x g in a conventional table-top microcentrifuge at room temperature.

Procedure

1. Excise the DNA fragment from the agarose gel with a clean, sharp scalpel.
Minimize the size of the gel slice by removing extra agarose.

2. Weigh the gel slice in a colorless tube. Add 3 volumes of Buffer QG to 1 volume of gel (100 mg or approximately 100 µl).
For example, add 300 µl of Buffer QG to each 100 mg of gel. For >2% agarose gels, add 6 volumes of Buffer QG. The maximum amount of gel slice per spin column is 400 mg; for gel slices >400 mg use more than one MinElute column.

3. Incubate at 50°C for 10 min (or until the gel slice has completely dissolved). To help
dissolve gel, mix by vortexing the tube every 2–3 min during the incubation.
IMPORTANT: Solubilize agarose completely. For >2% gels, increase incubation time.

4. After the gel slice has dissolved completely, check that the color of the mixture is yellow (similar to Buffer QG without dissolved agarose).
Note: If the color of the mixture is orange or violet, add 10 µl of 3 M sodium acetate, pH 5.0, and mix. The color of the mixture will turn to yellow.
The adsorption of DNA to the membrane is efficient only at pH δ7.5. Buffer QG contains a pH indicator which is yellow at pH δ7.5 and orange or violet at higher pH, allowing easy determination of the optimal pH for DNA binding.

5. Add 1 gel volume of isopropanol to the sample and mix by inverting the tube several times.
For example, if the agarose gel slice is 100 mg, add 100 µl isopropanol. Do not centrifuge the sample at this stage.

6. Place a MinElute column in a provided 2 ml collection tube in a suitable rack.

7. To bind DNA, apply the sample to the MinElute column, and centrifuge for 1 min.
For maximum recovery, transfer all traces of sample to the column. The maximum volume of the column reservoir is 800 µl. For sample volumes of more than 800 µl, simply load and spin again.

8. Discard the flow-through and place the MinElute column back in the same collection tube.
9. Add 500 µl of Buffer QG to the spin column and centrifuge for 1 min.
10. Discard the flow-through and place the MinElute column back in the same collection tube.
11. To wash, add 750 µl of Buffer PE to the MinElute column and centrifuge for 1 min.
Note: If the DNA will be used for salt-sensitive applications, such as blunt-end ligation and direct sequencing, let the column stand 2–5 min after addition of Buffer PE, before centrifuging.
12. Discard the flow-through and centrifuge the MinElute column for an additional
1 min at ε10,000 x g.
IMPORTANT: Residual ethanol from Buffer PE will not be completely removed unless the flow-through is discarded before this additional centrifugation.
13. Place the MinElute column into a clean 1.5 ml microcentrifuge tube.
14. To elute DNA, add 10 µl of Buffer EB (10 mM Tris·Cl, pH 8.5) or water to the center
of the membrane, let the column stand for 1 min, and then centrifuge for 1 min.
IMPORTANT: Ensure that the elution buffer is dispensed directly onto the center of the membrane for complete elution of bound DNA. The average eluate volume is 9 µl from 10 µl elution buffer volume.

A7 Qiagen® RNeasy Mini Kit

Procedure

1. Harvest cells according to step 1a or 1b.

1a. Cells grown in suspension (do not use more than 1 x 107 cells):

Determine the number of cells. Pellet the appropriate number of cells by centrifuging for 5 min at 300 x *g* in a centrifuge tube (not supplied).

Carefully remove all supernatant by aspiration, and proceed to step 2.

Note: Incomplete removal of cell-culture medium will inhibit lysis and dilute the lysate, affecting the conditions for binding of RNA to the RNeasy membrane. Both effects may reduce RNA yield.

1b. Cells grown in a monolayer (do not use more than 1 x 107 cells):

Cells can be either lysed directly in the cell-culture vessel (up to 10 cm diameter) or trypsinized and collected as a cell pellet prior to lysis. Cells grown in cell-culture flasks should always be trypsinized.

To lyse cells directly:

Determine the number of cells. Completely aspirate the cell-culture medium, and proceed immediately to step 2.

Note: Incomplete removal of cell-culture medium will inhibit lysis and dilute the lysate, affecting the conditions for binding of RNA to the RNeasy membrane. Both effects may reduce RNA yield.

To trypsinize and collect cells:

Determine the number of cells. Aspirate the medium, and wash the cells with PBS.

Aspirate the PBS, and add 0.1–0.25% trypsin in PBS. After the cells detach from the dish or flask, add medium (containing serum to inactivate the trypsin), transfer the cells to an RNase-free glass or polypropylene centrifuge tube (not supplied) and centrifuge at 300 x *g* for 5 min. Completely aspirate the supernatant, and proceed to step 2.

Note: Incomplete removal of cell-culture medium will inhibit lysis and dilute the lysate, affecting the conditions for binding of RNA to the RNeasy membrane. Both effects may reduce RNA yield.

2. Disrupt the cells by adding Buffer RLT.

For pelleted cells, loosen the cell pellet thoroughly by flicking the tube. Add the appropriate volume of Buffer RLT. Vortex or pipet to mix, and proceed to step 3.

Note: Incomplete loosening of the cell pellet may lead to inefficient lysis and reduced RNA yields.

For direct lysis of cells grown in a monolayer, add the appropriate volume of Buffer RLT (see Table 6) to the cell-culture dish. Collect the lysate with a rubber policeman.

Pipet the lysate into a microcentrifuge tube (not supplied). Vortex or pipet to mix, and ensure that no cell clumps are visible before

* Regardless of the cell number, use the buffer volumes indicated to completely cover the surface of the dish.

3. Homogenize the lysate according to step 3a, 3b, or 3c.

If processing δ1 x 105 cells, homogenize by vortexing for 1 min. After homogenization, proceed to step 4.

Note: Incomplete homogenization leads to significantly reduced RNA yields and can cause clogging of the RNeasy spin column. Homogenization with a

rotor–stator or QIAshredder homogenizer generally results in higher RNA yields than with a syringe and needle.

3a. Pipet the lysate directly into a QIAshredder spin column placed in a 2 ml collection tube, and centrifuge for 2 min at full speed. Proceed to step 4.

3b. Homogenize the lysate for 30 s using a rotor–stator homogenizer. Proceed to step 4.

3c. Pass the lysate at least 5 times through a blunt 20-gauge needle (0.9 mm diameter) fitted to an RNase-free syringe. Proceed to step 4.

4. Add 1 volume of 70% ethanol to the homogenized lysate, and mix well by pipetting. Do not centrifuge.

Note: The volume of lysate may be less than 350 µl or 600 µl due to loss during homogenization.

Note: When purifying RNA from certain cell lines, precipitates may be visible after addition of ethanol. This does not affect the procedure.

5. Transfer up to 700 µl of the sample, including any precipitate that may have formed, to an RNeasy spin column placed in a 2 ml collection tube (supplied). Close the lid gently, and centrifuge for 15 s at ε8000 x *g* (ε10,000 rpm). Discard the flow-through.*

Reuse the collection tube in step 6.

If the sample volume exceeds 700 µl, centrifuge successive aliquots in the same RNeasy spin column. Discard the flow-through after each centrifugation.*

Optional: If performing optional on-column DNase digestion

, follow steps D1–D4 after performing this step.

* Flow-through contains Buffer RLT or Buffer RW1 and is therefore not compatible with bleach.

for safety information.

Add 700 µl Buffer RW1 to the RNeasy spin column. Close the lid gently, and centrifuge for 15 s at ε8000 x *g* (ε10,000 rpm) to wash the spin column membrane. Discard the flow-through.*

Reuse the collection tube in step 7.

Note: After centrifugation, carefully remove the RNeasy spin column from the collection tube so that the column does not contact the flow-through. Be sure to empty the collection tube completely.

Skip this step if performing optional on-column DNase digestion.

7. Add 500 µl Buffer RPE to the RNeasy spin column. Close the lid gently, and centrifuge for 15 s at ε8000 x *g* (ε10,000 rpm) towash the spin columnmembrane. Discard the flow-through.

Reuse the collection tube in step 8.

Note: Buffer RPE is supplied as a concentrate. Ensure that ethanol is added to

Buffer RPE before use (see “Things to do before starting”).

8. Add 500 µl Buffer RPE to the RNeasy spin column. Close the lid gently, and centrifuge for 2min at ε8000 x *g* (ε10,000 rpm) to wash the spin columnmembrane.

The long centrifugation dries the spin column membrane, ensuring that no ethanol is carried over during RNA elution. Residual ethanol may interfere with downstream reactions.

9. Optional: Place the RNeasy spin column in a new 2 ml collection tube (supplied), and discard the old collection tube with the flow-through. Close the lid gently, and centrifuge at full speed for 1 min.
Perform this step to eliminate any possible carryover of Buffer RPE, or if residual flow-through remains on the outside of the RNeasy spin column after step 8.
10. Place the RNeasy spin column in a new 1.5 ml collection tube (supplied). Add 30–50 µl RNase-free water directly to the spin column membrane. Close the lid gently, and centrifuge for 1 min at ε8000 x *g* (ε10,000 rpm) to elute the RNA.
11. If the expected RNA yield is >30 µg, repeat step 10 using another 30–50 µl RNasefree water, or using the eluate from step 10 (if high RNA concentration is required). Reuse the collection tube from step 10.
If using the eluate from step 10, the RNA yield will be 15–30% less than that obtained using a second volume of RNase-free water, but the final RNA concentration will be higher.

A8 Megaclear™ kit - Ambion

E. MEGAclear™ Kit Procedure

CAUTION

Filter Cartridges should not be subjected to RCFs over 16,000 x g because it could cause mechanical damage and/or may deposit glass filter fiber in the final sample.

1. Bring the RNA sample to 100 µL with Elution Solution. Mix gently but thoroughly.

2. Add 350 µL of Binding Solution Concentrate to the sample. Mix gently by pipetting.

3. Add 250 µL of 100% ethanol to the sample. Mix gently by pipetting.

4. Apply the sample to the filter.

Centrifuge users:

a. Insert a Filter Cartridge into 1 of the Collection and Elution Tubes supplied.

b. Pipet the RNA mixture onto the Filter Cartridge.

c. Centrifuge for ~15 sec to 1 min, or until the mixture has passed through the filter. Centrifuge at RCF 10,000–15,000 x g (typically 10,000–14,000 rpm). Spinning harder than this may damage the filters.

d. Discard the flow-through and reuse the Collection and Elution Tube for the washing steps.

Vacuum manifold users:

a. Put 5 mL syringe barrels on the vacuum manifold, load them with Filter Cartridges, and apply the vacuum.

b. Pipet the RNA mixture onto the Filter Cartridge. The vacuum will draw it through the filter. Do not be concerned if the RNA mixture is pulled through very quickly, the RNA will bind instantly.

E. MEGAclear™ Kit Procedure

5. Wash with 2 x 500 µL Wash Solution

Make sure that the ethanol has been added to the Wash Solution Concentrate before using it.

a. Apply 500 µL Wash Solution. Draw the Wash Solution through the filter as in the previous step.

b. Repeat with a second 500 µL aliquot of Wash Solution.

c. After discarding the Wash Solution, continue centrifugation or leave the Filter Cartridge on the vacuum manifold for 10–30 sec to remove the last traces of Wash Solution.

6. Elute RNA with 50 µL Elution Solution

Elute the RNA from the filter using either one of the methods described below; they are equivalent in terms of RNA recovery.

RNA elution option 1

a. Place the Filter Cartridge into a new Collection/Elution Tube.

b. Apply 50 µL of Elution Solution to the center of the Filter Cartridge. Close the cap of the tube and incubate in a heat block set to 65–70°C for 5–10 min.

c. Recover eluted RNA by centrifuging for 1 min at RT (RCF

10,000–15,000 x g).
d. To maximize RNA recovery, repeat this elution procedure with a second 50 µL aliquot of Elution Solution. Collect the eluate into the same tube.

RNA elution option 2

a. Pre-heat 110 µL of Elution Solution per sample to 95°C.
b. Apply 50 µL of the pre-heated Elution Solution to the center of the Filter Cartridge, close the cap of the tube and centrifuge for 1 min at room temperature (RCF 10,000–15,000 x g) to elute the RNA.
c. To maximize RNA recovery, repeat this elution procedure with a second pre-heated 50 µL aliquot of Elution Solution. Collect the eluate into the same Collection/Elution Tube

A9 Stratagene QuikChange® II Site-Directed Mutagenesis Kit

PROTOCOL

Mutant Strand Synthesis Reaction (Thermal Cycling)

.

1. Synthesize two complimentary oligonucleotides containing the desired mutation, flanked by unmodified nucleotide sequence. Purify these oligonucleotide primers prior to use in the following steps (see *Mutagenic Primer Design*).
2. Prepare the control reaction as indicated below:

5 μl of 10× reaction buffer

2 μl (10 ng) of pWhitescript 4.5-kb control plasmid (5 ng/μl)

1.25 μl (125 ng) of oligonucleotide control primer #1 [34-mer (100 ng/μl)]

1.25 μl (125 ng) of oligonucleotide control primer #2 [34-mer (100 ng/μl)]

1 μl of dNTP mix

38.5 μl ddH2O (to bring the final reaction volume to 50 μl)

Then add

1 μl of *PfuUltra* HF DNA polymerase (2.5 U/μl)

3. Prepare the sample reaction(s) as indicated below:

Note *Stratagene recommends setting up a series of sample reactions using various amounts of dsDNA template ranging from 5 to 50 ng (e.g., 5, 10, 20, and 50 ng of dsDNA template) while keeping the primer concentration constant.*

5 μl of 10× reaction buffer

X μl (5–50 ng) of dsDNA template

X μl (125 ng) of oligonucleotide primer #1

X μl (125 ng) of oligonucleotide primer #2

1 μl of dNTP mix

ddH2O to a final volume of 50 μl

Then add

1 μl of *PfuUltra* HF DNA polymerase (2.5 U/μl)

4. If the thermal cycler to be used does not have a hot-top assembly, overlay each reaction with ~30 μl of mineral oil.

TABLE I

Cycling Parameters for the QuikChange II Site-Directed Mutagenesis Method

Segment	Cycles	Temperature	Time
1	1x	95°C	30 seconds
		95°C	30 seconds
		55°C	1 minute
2	12–18x	68°C	1 minute/kb of plasmid length*

* For example, a 5-kb plasmid requires 5 minutes at 68°C per cycle.

5. Cycle each reaction using the cycling parameters outlined in Table I. (For the control reaction, use a 5-minute extension time and run the reaction for 12 cycles.)

6. Adjust segment 2 of the cycling parameters according to the type of mutation desired (see the following table):

Type of mutation desired	Number of cycles
Point mutations	12
Single amino acid changes	16
Multiple amino acid deletions or insertions	18

7. Following temperature cycling, place the reaction on ice for 2 minutes to cool the reaction to ≤37°C.

Note If desired, amplification may be checked by electrophoresis of 10 µl of the product on a 1% agarose gel. A band may or may not be visualized at this stage. In either case proceed with Dpn *I digestion and transformation.*

QuikChange® II Site-Directed Mutagenesis Kit 9

Dpn I Digestion of the Amplification Products

Note It is important to insert the pipet tip below the mineral oil overlay when adding the Dpn *I restriction enzyme to the reaction tubes during the digestion step or when transferring the 1 µl of* Dpn *Itreated DNA to the transformation reaction. Stratagene suggests using specialized aerosol-resistant pipet tips, which are small and pointed, to facilitate this process.*

1. Add 1 µl of the *Dpn* I restriction enzyme (10 U/µl) directly to each amplification reaction below the mineral oil overlay using a small, pointed pipet tip.
2. Gently and thoroughly mix each reaction mixture by pipetting the solution up and down several times. Spin down the reaction mixtures in a microcentrifuge for 1 minute and immediately incubate each reaction at 37°C for 1 hour to digest the parental (i.e., the nonmutated) supercoiled dsDNA.

Transformation of XL1-Blue Supercompetent Cells

Notes Please read the Transformation Guidelines *before proceeding with the transformation protocol.*

XL1-Blue cells are resistant to tetracycline. If the mutagenized plasmid contains only the tetR resistance marker, an alternative tetracycline-sensitive strain of competent cells must be used.

1. Gently thaw the XL1-Blue supercompetent cells on ice. For each control and sample reaction to be transformed, aliquot 50 µl of the supercompetent cells to a *prechilled* Falcon® 2059 polypropylene tube.
2. Transfer 1 µl of the *Dpn* I-treated DNA from each control and sample reaction to separate aliquots of the supercompetent cells.

Note Carefully remove any residual mineral oil from the pipet tip before transferring the Dpn *I-treated DNA to the transformation reaction.*

As an optional control, verify the transformation efficiency of the XL1-Blue supercompetent cells by adding 1 µl of the pUC18 control plasmid (0.1 ng/µl) to a 50-µl aliquot of the supercompetent cells. Swirl the transformation reactions gently to mix and incubate the reactions on ice for 30 minutes.

3. Heat pulse the transformation reactions for 45 seconds at 42°C and then place the reactions on ice for 2 minutes.

4. Add 0.5 ml of NZY+ broth preheated to 42°C and incubate the transformation reactions at 37°C for 1 hour with shaking at 225–250 rpm.
5. Plate the appropriate volume of each transformation reaction, as indicated in the table below, on agar plates containing the appropriate antibiotic for the plasmid vector.
For the mutagenesis and transformation controls, spread cells on LB–ampicillin agar plates containing 80 μg/ml X-gal and 20 mM IPTG (see *Preparing the Agar Plates for Color Screening*).

Transformation reaction plating volumes

Reaction Type	Volume to Plate
pWhitescript mutagenesis control	250 μl
pUC18 transformation control	5 μl (in 200 μl of NZY+ broth)*
Sample mutagenesis (entire transformation reaction)	250 μl on each of two plates

* Place a 200-μl pool of NZY+ broth on the agar plate, pipet the 5 μl of the transformation reaction into the pool, then spread the mixture.

6. Incubate the transformation plates at 37°C for >16 hours.

A10 mMESSAGE mMACHINE® Kit *mMESSAGE mMACHINE® Kit Procedure*

Capped transcription reaction assembly

1. Thaw the frozen reagents

Place the RNA Polymerase Enzyme Mix on ice, it is stored in glycerol and will not be frozen at –20°C.

Vortex the 10X Reaction Buffer and the 2X NTP/CAP until they are completely in solution. Once thawed, store the ribonucleotides (2X NTP/CAP) on ice, but ***keep the 10X Reaction Buffer at room temperature while assembling the reaction***.

All reagents should be microfuged briefly before opening to prevent loss and/or contamination of material that may be present around the rim of the tube.

2. Assemble transcription reaction at room temperature.

The spermidine in the 10X Reaction Buffer can coprecipitate the template DNA if the reaction is assembled on ice.

Add the 10X Reaction Buffer after the water and the ribonucleotides are already in the tube.

The following amounts are for a single 20 µL reaction. Reactions may be scaled up or down if desired.

Amount	Component
to 20 µL	Nuclease-free Water
10 µL	2X NTP/CAP
2 µL	10X Reaction Buffer
(1 µL) (optional)	[‹-32P]UTP as a tracer
0.1–1 µg	linear template DNA†
2 µ	Enzyme Mix

† Use 0.1–0.2 µg PCR-product template or ~1 µg linearized plasmid template.

IMPORTANT! The following reaction setup is recommended when the RNA produced will be 300 bases to 5 kb in length. For transcripts longer or shorter than this,

3. Mix thoroughly

Gently flick the tube or pipette the mixture up and down gently, and then microfuge tube briefly to collect the reaction mixture at the bottom of the tube.

4. Incubate at 37°C, 1 hr

Typically, 80% yield is achieved after a 1 hr incubation. For maximum yield, we recommend a 2 hr incubation. Since SP6 reactions are somewhat slower than T3 and T7 reactions, they especially may benefit from the second hour of incubation.

A second hour of incubation is recommended for synthesis of <300 base transcripts and for inefficiently transcribed templates.

If the reaction is trace-labeled:

After the incubation (before or after TURBO DNase treatment), remove an aliquot of trace-radiolabeled reactions to assess yield by TCA precipitation

5. (optional) Add 1 µL TURBO DNase, mix well and incubate 15 min at 37°C

This DNase treatment removes the template DNA. For many applications it may not be necessary because the template DNA will be present at a very low concentration relative to the RNA.

a. Add 1 µL TURBO DNase, and mix well.

b. Incubate at 37°C for 15 min.

A11 USB® Poly(A) Tail-LengthAssay Kit

Protocol

Step 1: G/I tailing

Use the following protocol to add poly(G/I) tails to a total RNA sample. For the positive control, substitute the provided HeLa total RNA for an experimental sample.

This standard protocol applies to a single 20 μl G/I tailing reaction.

1. Thaw frozen reagents on ice and mix thoroughly by vortexing enzyme mixes should be gently flicked to mix. Centrifuge briefly.
2. Add the following reagents in Table 1 to a nuclease-free tube. Mix gently by pipetting up and down and then centrifuge the tube briefly to collect the contents. Keep samples on ice.

G/I tailing mix

Reagent Per reaction

Total RNA sample, 1 μg (0.1 - 2 μg) up to 14 μl
5X Tail Buffer Mix 4 μl
10X Tail Enzyme Mix 2 μl
Water, Nuclease-Free to 20 μl

3. Incubate at 37°C for 60 minutes
4. Add 2 μl 10X Tail Stop Solution and mix well.
5. Proceed to Step 2: Reverse transcription. *Alternatively, tailed RNA samples can be stored at -20°C until ready to proceed to Step 2.*

Step 2: Reverse transcription

Use the following protocol to reverse transcribe the poly(G/I) tailed RNA. This standard protocol applies to a single 20 μl reverse transcription reaction. Master mixes for multiple reactions can be made by increasing the volumes of reaction components proportionally.

1. Thaw frozen reagents on ice and mix thoroughly by vortexing. Enzyme mixes should be gently flicked to mix. Centrifuge briefly.
2. Add the following reagents in Table 2 to a nuclease-free tube. Mix gently and briefly spin down the tube contents. Keep on ice.

RT mix:

Reagent	RT +	RT - (control)
G/I Tailed RNA Sample	5 μl	5 μl
5X RT Buffer Mix	4 μl	4 μl
10X RT Enzyme Mix	2 μl	-
Water, Nuclease-Free	9 μl	11 μl

Note: Each kit supports 20 x 20 μl reactions.

3. Incubate at 44°C for 60 minutes; 92°C for 10 minutes; and at 4°C hold.
4. Proceed to Step 3: PCR amplification. *Alternatively, cDNA samples can be stored at -20°C until ready to proceed to Step 3.*

Step 3: PCR amplification

Use the following protocol to PCR amplify the poly(G/I) tailed cDNA. This standard protocol applies to a single 25 μl PCR reaction. Master mixes for multiple reactions
can be made by increasing the volumes of reaction components proportionally.

1. Dilute each RT sample by adding 20 μl Nuclease-Free Water (40 μl final volume).
2. Thaw frozen reagents on ice and mix thoroughly by vortexing. Mix HotStart-ITR Taq DNA Polymerase by gently flicking. Centrifuge briefly.

3. Add the following reagents in Table 3 to a nuclease-free tube. Mix gently and briefly spin down the tube contents. Keep on ice.

Step 4: Detection

The size of PCR products can be assessed by running an aliquot of the reaction on an agarose or polyacrylamide gel. To start, we recommend loading one half of each PCR reaction (12.5 μl) per lane on a 2.5% agarose TAE gel. For increased resolution,
load one half of each PCR reaction (12.5 μl) per lane on a 5% non-denaturing polyacrylamide
TBE gel. Stain gels with ethidium bromide or SYBRR Gold and visualize
with a standard ultraviolet transilluminator or fluorescence image scanner.
See the Supplementary information section for guidelines on gel electrophoresis and data analysis.

A12 QuantiFast® Probe RT-PCR Plus Kit

1. Thaw 2x QuantiFast Mix 1, 2x QuantiFast Mix 2 (Probe), template RNA, primer and probe solutions, RNase-free water, and High-ROX Dye Solution or ROX Dye Solution. Mix the individual solutions. QuantiFast RT Mix should be taken from –20°C immediately before use, and returned to storage at –20°C immediately after use.

2. Prepare a reaction mix for removal of genomic DNA according to Table 1.

3. Mix the reaction mix thoroughly, and dispense appropriate volumes into PCR tubes, PCR capillaries, or the wells of a PCR plate.
Note: Do not keep the PCR vessels or plates on ice.
4. Add template RNA (≤100 ng) to the individual PCR tubes, PCR capillaries, or wells and incubate for 5 min at room temperature (15–25°C).

Note: The incubation step can be prolonged up to 15 min.
5. Prepare a QuantiFast Reaction mix.

6. Mix the QuantiFast reaction mix thoroughly and dispense appropriate volumes into PCR vessels or plates containing the genomic DNA removal reaction.

7. Program the real-time cycler according to Table 3.
Note: Check the real-time cycler's user manual for correct instrument setup for multiplex analysis. Be sure to activate the detector for each reporter dye used. Depending on your instrument, it may be also necessary to perform a calibration procedure for each of the reporter dyes before they are used for the first time.

8. Perform data analysis. Before performing data analysis, select the analysis settings for each probe (i.e., baseline settings and threshold values). Optimal analysis settings are a prerequisite for accurate quantification data.

A13 MEGAshortscript™ Kit

III.B. Transcription Reaction Assembly and Incubation

NOTE

B. Transcription Reaction Assembly and Incubation

Thaw the T7 10X Reaction Buffer, four ribonucleotide solutions, and Water at room temperature. Briefly vortex the T7 10X Reaction Buffer and ribonucleotide solutions. Microfuge all reagents briefly before opening to prevent loss and/or contamination of material that may be present around the rim of the tube. Keep the T7 Enzyme Mix on ice during assembly of the reaction.

1. Assemble the reaction mix

Assemble the reaction in an RNase-free microfuge tube at ***room temperature*** in the order shown. For convenience, all four nucleotides can be premixed; add 8 µL of the mixture to a standard 20 µL reaction instead of adding the ribonucleotides separately. The following amounts are for a single 20 µL reaction. Reactions may be scaled as needed.

2 µL T7 10X Reaction Buffer
2 µL T7 ATP Solution (75 mM)
2 µL T7 CTP Solution (75 mM)
2 µL T7 GTP Solution (75 mM)
2 µL T7 UTP Solution (75 mM)
~1 µL (optional) Labeled ribonucleotide
<8 µL Template DNA
2 µL T7 Enzyme Mix
Water (Nuclease-free) to 20 µL final volume.

Components in the transcription buffer can lead to precipitation of the template DNA if the reaction is assembled on ice.

2. Mix the reaction gently Mix contents thoroughly by gently flicking the tube, then microfuge the tube briefly to collect the reaction mixture at the bottom of the tube.

3. Incubate the reaction at 37°C for ε2 hr

Incubate the reaction at 37°C for at least 2 hr. For most applications 2–4 hr incubation is sufficient; however, the optimal incubation time will be template-dependent. To determine the optimum incubation time for maximum yield with a given template, a time-course experiment should be done.

4. (optional) Add 1 µL of TURBO DNase and incubate at 37°C for 15 min

To remove the DNA template, add 1 µL of TURBO DNase to the reaction, mix well, and continue the incubation at 37°C for 15 min. If very large mass amounts of DNA template were used, more TURBO DNase may be required.

A14 Invitrogen Mouse Interferon-Gamma (Ms IFN-γ) ELISA (product KMC4022)

Assay Procedure

Allow all reagents to reach room temperature before use. Gently mix all liquid reagents prior to use.

Note: A standard curve must be run with each assay.

1. Determine the number of 8-well strips needed for the assay. Insert these in the frame(s) for current use. (Re-bag extra strips and frame. Store these in the refrigerator for future use.)
2. Dilute serum, plasma and tissue culture samples 1:4 with *Standard Diluent Buffer* (See **Preparation of Reagents**). Alternatively, samples may be diluted directly in the microtiter well by adding 75 µL of the *Standard Diluent Buffer* to each well, followed by 25 µL of serum, plasma or tissue culture sample.
3. Add 100 µL of the *Standard Diluent Buffer* to the zero standard wells. Well(s) reserved for chromogen blank should be left empty.
4. Add 100 µL of standards, controls or samples (serum, plasma and TCS prediluted) to the appropriate microtiter wells.
5. Cover plate with *plate cover* and incubate for **2 hour at room temperature**.
6. Thoroughly aspirate or decant solution from wells and discard the liquid. Wash wells 4 times. See **Directions for Washing**.
7. Add 100 µL of biotinylated anti-Ms IFN-γ solution into each well except the chromogen blank(s).
8. Cover plate with the *plate cover* and incubate for **1 hour at room temperature**.
9. Thoroughly aspirate or decant solution from wells and discard the liquid. Wash wells 4 times. See **Directions for Washing**.
10. Add 100 µL Streptavidin-HRP Working Solution to each well except the chromogen blank(s). See **Preparation of Reagents**.
11. Cover plate with the *plate cover* and incubate for **30 minutes at room temperature.**
12. Thoroughly aspirate or decant solution from wells and discard the liquid. Wash wells 4 times. See **Directions for Washing**.
13. Add 100 µL of *Stabilized Chromogen* to each well. The liquid in the wells will begin to turn blue.
14. Incubate for **30 minutes at room temperature and in the dark**. ***Note*: Do not cover the plate with aluminum foil or metalized mylar**. The incubation time for chromogen substrate is often determined by the microtiter plate reader used. Many plate readers have the capacity to record a maximum optical density (O.D.) of 2.0. The O.D. values should be monitored and the substrate reaction stopped before the O.D. of the positive wells exceed the limits of the instrument. The O.D. values at 450 nm can only be read after the *Stop Solution* has been added to each well. If using a reader that records only to 2.0 O.D., stopping the assay after 20 to 25 minutes is suggested.
15. Add 100 µL of *Stop Solution* to each well. Tap side of plate gently to mix. The solution in the wells should change from blue to yellow.
16. Read the absorbance of each well at 450 nm having blanked the plate reader against a chromogen blank composed of 100 µL each of *Stabilized Chromogen* and *Stop Solution*. Read the plate within 2 hours after adding the

Stop Solution.
17. Use a curve-fitting software to generate the standard curve. A four parameter algorithm provides the best standard curve fit.
18. Read the Ms IFN-γ concentrations for unknown samples and controls from the standard curve. Multiply value(s) obtained for sample(s) by 4 to correct for the 1:4 dilution in Step 2. (Samples producing signals greater than that of the highest standard (300 pg/mL) should be diluted in *Standard Diluent Buffer* and reanalyzed, multiplying the concentration found by the appropriate dilution factor).

A 15 VeriKine-HS™ Mouse IFN Beta Serum ELISA Kit

Catalog No. 42410 Assay Range: 0.94 – 60 pg/ml Store **all** components at 2 - 8°C

PREPARATION OF REAGENTS

Before starting the assay, the plate(s), Wash Solution
Concentrate, Serum Buffer, TMB Substrate and Stop Solution should be equilibrated to room temperature (RT), 22-25ºC. Supplied Mouse IFN-β Standard, Antibody Concentrate, HRP Conjugate Concentrate, Sample Diluent, Antibody Diluent and HRP Diluent should be kept on ice (4ºC) throughout the assay.

Wash Solution: The Wash Solution Concentrate may contain crystals. Place the bottle in a warm water bath and gently mix until completely dissolved. Prepare a 1:10 working wash solution (e.g. Add 50 ml of Wash Solution Concentrate to 450 ml of distilled or deionized water and mix thoroughly). Diluted Wash Solution can be stored at RT (22-25ºC) when not in use.

Mouse Interferon Beta Solution: Using the Mouse IFN-β Standard, construct a standard curve (0.94-60 pg/ml), as shown in figure 1, in Sample Diluent.

Standard Curve Preparation:

a) Prepare a 1:16.7 *working stock* of mouse IFN-β Standard by pipetting 60 µl of IFN Standard into 940 µl of Sample Diluent. Mix thoroughly by gently pipetting up and down 10 times.
b) Label seven polypropylene tubes (S1-S7).
c) Fill tubes with Sample Diluent as indicated in Figure 1.
d) Add 100 µl of the working stock of Mouse IFN-β Standard to S7 and mix thoroughly to recover all material adhered to the inside of the pipette tip.
e) Using a pipette set at 500 µl, mix S7 thoroughly by pipetting up and down. Transfer 500 µl of S7 to S6 and mix thoroughly by pipetting up and down. Repeat to complete series to S1.
f) **Set aside on ice (4ºC)** until use in step 1 of the Assay Procedure.

ASSAY PROCEDURE

All incubations should be performed at room temperature (RT), 22-25°C, keeping the plate away from drafts and other temperature fluctuations. Use plate sealers to cover the plates as directed. During all wash steps, remove contents of plate by inverting and shaking over a sink and blotting the plate on lint-free absorbent paper; tap the plate. Wash each well with a minimum of 250 µl of diluted Wash Solution at each wash step. Refer to Preparation of Reagents for dilution of concentrated solutions.

1a. **For testing serum or plasma samples:**
- Add 50 µl of Serum Buffer to each well
- Overlay 50 µl of diluted Standard, Test Sample or Blank

1b. **For testing tissue culture samples:**
- Add 50 µl of Sample Diluent to each well
- Overlay 50 µl of diluted Standard, Test Sample or Blank

Cover with plate sealer and shake plate at 650 rpm at RT (22-25°C) for 1 hour.
After 1 hour, empty the contents of the plate and wash the wells four times with at least 250 µl of working Wash Solution (refer to Preparation of Reagents).
2. **Antibody Solution:** Add 50 µl of diluted Antibody Solution (refer to Preparation of Reagents) to each well. Cover with plate sealer and shake plate at 650 rpm at RT (22-25°C) for 30 minutes.
After 30 minutes, empty the contents of the plate and wash the wells four times with at least 250 µl of working Wash Solution.
3. **HRP:** Add 50 µl of diluted HRP Solution (refer to Preparation of Reagents) to each well. Cover with plate sealer and shake plate at 650 rpm at RT (22-25°C) for 10 minutes.
After 10 minutes, empty the contents of the plate and wash the wells four times with at least 250 µl of working Wash Solution.
4. **TMB Substrate:** Add 100 µl of the TMB Substrate Solution to each well. Incubate, in the dark, at RT (22-25°C), for 10 minutes. Do not use a plate sealer and do not shake during the incubation.

5. **Stop Solution:** After the 10 minute incubation of TMB, DO NOT EMPTY THE WELLS AND DO NOT WASH. Add 100 µl of Stop Solution to each well.
6. **Read:** Using a microplate reader, determine the absorbance at 450 nm within 5 minutes after the addition of the Stop Solution.

A16 VeriKine™ Mouse Interferon Alpha ELISA kit PBL-42120

ASSAY PROCEDURE—DAY 1

All incubations should be performed in a closed chamber at RT (22-25ºC) keeping the plate away from drafts and other temperature fluctuations. Set plate shaker speed to 450 rpm where indicated. Use plate sealers to cover the plates as directed. During all wash steps, remove contents of plate by inverting and shaking over a sink and blotting the plate on lint-free absorbent paper; tap the plate. Wash each well with a minimum of 300 µl of diluted Wash Solution for each wash step. See Preparation of Reagents for details on dilution of concentrated solutions.

1. **Standards, Test Samples and Diluted Antibody Solution**: Determine the number of microplate strips required to test the desired number of samples plus the appropriate number of wells needed to run blanks and standards. We recommend running both the IFN-α standard, blanks and samples in duplicate. Remove extra microtiter strips from the frame, seal in the foil bag provided and store at 2-8ºC. Unused strips can be used in later assays

Step A: Adding Standards, Test Samples and Blanks Add 100 µl of Standard (refer to Preparation of Reagents), Test Samples or Blanks per well.

Step B: Adding diluted Antibody Solution Add 50 µl of diluted Antibody Solution (refer to Preparation of Reagents) to each well (Total volume = 150 µl/well). Change pipette tips between each addition.

. Cover with a Plate Sealer and incubate for 1 hour at RT (22-25°C) with shaking at 450 rpm.

After 1 hour, transfer the plate to 4°C and incubate 20-24 hours without shaking.

ASSAY PROCEDURE—DAY 2

After 20-24 hours, empty the contents of the plate and wash the wells four times with diluted Wash Solution (refer to Preparation of Reagents).

2. **HRP:** Add 100 µl of diluted HRP Solution (refer to Preparation of Reagents) to each well. Cover with Plate Sealer and incubate for 2 hours at RT (22-25°C) with shaking at 450 rpm.

After 2 hours, empty the contents of the plate and wash the wells four times with diluted Wash Solution.

3. **TMB Substrate:** Add 100 µl of the TMB Substrate Solution to each well. Incubate, in the dark, at RT (22-25ºC), for 15minutes. Do not use a plate sealer during the incubation. DO NOT SHAKE.

4. Stop Solution: After the 15 minute incubation of TMB, DO NOT EMPTY THE WELLS AND DO NOT WASH. Add 100 µl of Stop Solution to each well.

5. Read: Using a microplate reader, determine the absorbance at 450 nm within 5 minutes after the addition of the Stop Solution.

CALCULATION OF RESULTS

By plotting the optical densities (OD) using a 4-parameter fit for the standard curve, the interferon titer in the samples can be determined. Blank ODs should be subtracted from the standards and sample ODs to eliminate background. A typical standard curve for this assay is shown in the enclosed pages. This example is for the purpose of illustration only, and should not be used to calculate unknowns.

A shift in optical densities is typical between users and kit lots. The back fit concentration extrapolated from the standard curve is a more accurate determination of the sample titer and performance of the kit. Variations from the typical curve provided can be a result of operator technique, altered incubation time, fluctuations in temperature and kit age.

Because the interferon samples are titrated against the international standard, the values from the curves can be determined in units/ml as well as pg/ml. The conversion factor of about 10-20 pg/unit is applicable for mouse interferon alpha.3 Nevertheless, this conversion factor is only a

A17 MOUSE HAPTOGLOBIN ELISA Life Diagnostics, Inc., Catalog Number: 2410-1

INTRODUCTION

Haptoglobin is an acute phase protein that is elevated in mouse serum as a result of injury, infection or disease. Studies at Life Diagnostics, Inc. and by others[1-3] indicate that haptoglobin levels may increase 10-fold or more. Haptoglobin therefore provides a useful acute phase biomarker in mice.

PRINCIPLE OF THE ASSAY

The mouse haptoglobin test kit is based on a solid phase enzymelinked immunosorbent assay (ELISA). The assay uses affinity-purified anti-mouse haptoglobin antibodies for solid phase (microtiter wells) immobilization and horseradish peroxidase (HRP) conjugated anti-mouse haptoglobin antibodies for detection. The test sample is diluted and incubated in the microtiter wells for 45 minutes. The microtiter wells are subsequently washed and HRP conjugate is added and incubated for 30 minutes. This results in haptoglobin molecules being sandwiched between the immobilization and detection antibodies. The wells are then washed to remove unbound HRP-labeled antibodies and TMB Reagent is added and incubated for 20 minutes at room temperature. This results in the development of a blue color. Color development is stopped by the addition of Stop Solution, changing the color to yellow, and optical density is measured spectrophotometrically at 450 nm. The concentration of haptoglobin is proportional to the optical density of the test sample.

MATERIALS AND COMPONENTS

Materials provided with the kit:

- Anti-mouse haptoglobin antibody coated microtiter plate with 96 wells (provided as 12 detachable strips of 8)
- Enzyme Conjugate Reagent, 11 ml
- Reference standard (lyophilized), containing 2 mg/ml mouse haptoglobin
- 10x Wash Buffer, 60 ml
- 10x Diluent, 25 ml
- TMB Reagent (One-Step), 11 ml
- Stop Solution (1N HCl), 11 ml

Materials required but not provided:

- Precision pipettes and tips
- Distilled or deionized water
- Polypropylene or glass tubes
- Vortex mixer
- Absorbent paper or paper towels
- Micro-Plate incubator/shaker with an approximate mixing speed of 150 rpm
- A microtiter plate reader at 450 nm wavelength, with a bandwidth of 10 nm or less and an optical density range of 0-4
- Graph paper (PC graphing software is optional).

STORAGE

The unopened kit should be stored at 2-8 °C and the microtiter plate should be kept in a sealed bag with desiccant to minimize exposure to damp air. Test kits will remain stable for six months from the date of purchase provided that the components are stored as described above.

GENERAL INSTRUCTIONS

1. All reagents should be allowed to reach room temperature (18-25°C) before use.
2. Serum or plasma samples should be diluted ~25,000 fold with 1x diluent in order to obtain values within the standard range.

DILUENT PREPARATION

The diluent is provided as a 10x stock. Prior to use estimate the final volume of diluent required for your assay and dilute one (1) volume of the 10x stock with nine (9) volumes of distilled or deionized water.

WASH SOLUTION PREPARATION

The wash solution is provided as a 10x stock. Prior to use dilute the contents of the bottle (60 ml) with 540 ml of distilled or deionized water.

STANDARD PREPARATION

1. The standard is provided as a lyophilized stock. Add the

volume of distilled or deionized water indicated on the vial
label and mix gently until dissolved to obtain a 2 ㎎/ml rat
CRP stock ***(the reconstituted standard should be aliquoted***
and frozen at -20ºC after reconstitution if future use is
intended).
2. Label 8 polypropylene microcentrifuge tubes as 125, 62.5,
31.3, 15.6, 7.8, 3.9, 1.95, and 0 ng/ml.
3. Dispense 468.8 ㎖ of diluent into the tube labeled 125 ng/ml
and 250 ㎖ of diluent into the remaining tubes.
4. Pipette 31.25 ㎖ of the 2 ㎎/ml haptoglobin standard into the
tube labeled 125 ng/ml and mix. This provides the working
125 ng/ml haptoglobin standard.
5. Prepare a 62.5 ng/ml standard by diluting and mixing 250 ㎖ of
the 125 ng/ml standard with 250 ㎖ of diluent in the tube
labeled 62.5 ng/ml. Similarly prepare the 31.2, 15.6, 7.8, 3.9,
and 1.95 ng/ml standards by serial dilution.

SAMPLE PREPARATION

General Note: Haptoglobin is generally present in mouse serum at
concentrations ranging from 0.1 – 2 mg/ml. In order to obtain
values within the range of the standard curve we suggest that
samples be diluted 25,000 fold. The following procedure may be
used for each sample to be tested:
1. Dispense 497.5 ㎖ and 248 ㎖ of 1x diluent into separate
polypropylene tubes.
2. Pipette and mix 2.5 ㎖ of the serum/plasma sample into the
tube containing 497.5 ㎖ of diluent. This provides a 200 fold
diluted sample.
3. Mix 2.0 ㎖ of the 200 fold diluted sample with the 248 ㎖ of
diluent in the second tube. This provides a 25,000 fold dilution
of the sample.
4. Repeat this procedure for each sample to be tested.

ASSAY PROCEDURE

1. Secure the desired number of coated wells in the holder.
2. Dispense 100 ㎖ of standards and samples into the wells (we
recommend that samples be tested in duplicate).
3. Incubate on an orbital micro-plate shaker at 100-150 rpm at
room temperature (18-25° C) for 45 minutes.
4. Remove the incubation mixture by flicking plate contents into
an appropriate Bio-waste container or using a plate washer.
5. Wash and empty the microtiter wells 4-5 times with 1x wash
solution. This may be performed using either a plate washer
(350 ㎖/well) or a squirt bottle. The entire wash procedure
should be performed as quickly as possible.
6. Strike the wells sharply onto absorbent paper or paper towels
to remove all residual water droplets.
7. Add 100 ㎖ of enzyme conjugate reagent into each well.
8. Incubate on an orbital micro-plate shaker at 100-150 rpm at
room temperature (18-25° C) for 30 minutes.
9. Wash as detailed in 4 to 5 above.
10. Strike the wells sharply onto absorbent paper or paper towels
to remove residual water droplets.
11. Dispense 100 ㎖ of TMB Reagent into each well.
12. Gently mix on an orbital micro-plate shaker at 100-150 rpm at
room temperature (18-25° C) for 20 minutes.
13. Stop the reaction by adding 100 ㎖ of Stop Solution to each
well.
14. Gently mix. *It is important to make sure that all the blue color*
changes to yellow.
15. Read the optical density at 450 nm with a microtiter plate
reader *within 15 minutes*.

CALCULATION OF RESULTS

1. Calculate the average absorbance values (A_{450}) for each set of
reference standards and samples.
2. Construct a standard curve by plotting the mean absorbance
obtained from each reference standard against its
concentration in ng/ml on linear graph paper, with absorbance

values on the vertical or Y-axis and concentrations on the horizontal or X-axis.
3. Using the mean absorbance value for each sample, determine the corresponding concentration of haptoglobin in ng/ml from the standard curve.
4. Multiply the derived concentration by the dilution factor to determine the actual concentration of haptoglobin in the serum/plasma sample.
5. PC graphing software may be used for the above steps.
6. If the OD_{450} values of samples fall outside the standard curve when tested at a 25,000 fold dilution, samples should be diluted appropriately and re-tested.

REPRESENTATIVE STANDARD CURVE

A typical standard curve with optical density readings at 450nm on the Y-axis against haptoglobin concentrations on the X-axis is shown below. This curve is for the purpose of illustration only, and should not be used to calculate unknowns. Each user should obtain his or her data and standard curve in each experiment.

LIMITATIONS OF THE PROCEDURE

1. Reliable and reproducible results will be obtained when the assay procedure is carried out with a complete understanding of and in accordance with the instructions detailed above.
2. The wash procedure is critical. Insufficient washing will result in poor precision and falsely elevated absorbance readings.

A 18 MOUSE SERUM AMYLOID A (SAA) ELISA TEST KIT Life Diagnostics, Inc., Catalog Number: 3400-1 Mouse SAA ELISA

INTRODUCTION

SAA is an acute phase serum protein that is elevated in mice approximately 50-fold following lipopolysaccharide injection.[1] In mice, two major forms of SAA are induced during the acute phase response, SAA1 and SAA2. Studies have shown that the two forms are similarly increased in response to different inflammatory stimuli.[2] This ELISA kit uses antibodies that preferentially detect SAA2.[A] Measurement of SAA provides a useful biomarker of inflammation and disease.

PRINCIPLE OF THE TEST

The mouse SAA test kit is based on a solid phase enzymelinked immunosorbent assay (ELISA). The assay uses affinity purified peptide-specific polyclonal anti-mouse SAA2 antibodies for solid phase (microtiter wells) immobilization and horseradish peroxidase (HRP) conjugated polyclonal peptide-specific anti-mouse SAA1/2 antibodies for detection.

The test sample is diluted and incubated in the microtiter wells together with the HRP conjugate for one hour. This results in SAA2 molecules being sandwiched between the immobilization and detection antibodies. The wells are then washed to remove unbound HRP-labeled antibodies, and TMB Reagent is added and incubated for 20 minutes at room temperature. This results in the development of a blue color.

Color development is stopped by the addition of Stop Solution, changing the color to yellow, and optical density is measured spectrophotometrically at 450 nm. The concentration of SAA2 is proportional to the optical density of the test sample.

MATERIALS AND COMPONENTS

Materials provided with the kit:

· Anti-mouse SAA2 antibody coated microtiter plate with 96 wells (provided as 12 detachable strips of 8)
· HRP Conjugate Reagent, 11 ml
· Reference standard (0.20 ml, lyophilized), containing mouse SAA (concentration and dilution instructions are detailed on the vial label)
· 20x Wash Buffer, 50 ml
· Diluent, 30 ml
· TMB Reagent (One-Step), 11 ml
· Stop Solution (1N HCl), 11 ml

Materials required but not provided:

· Precision pipettes and tips
· Distilled or deionized water
· Polypropylene tubes
· Vortex mixer
· Absorbent paper or paper towels
· Micro-Plate incubator/shaker with an approximate mixing speed of 150 rpm
· Plate reader capable of measuring OD at 450 nm
· Graph paper (PC graphing software is optional)

[A] Studies at Life Diagnostics, Inc. indicate that this kit has less than 5% cross reactivity with mouse SAA1 polypeptide compared to mouse SAA2 polypeptide.

STORAGE OF TEST KIT

The lyophilized reference standard should be stored at or below -20°C for optimum stability (it can be safely shipped at 2-8°C). The remainder of the kit should be stored at 2-8°C and the microtiter plate should be kept in a sealed bag with desiccant to minimize exposure to damp air. Test kits will remain stable for six months from the date of purchase provided that the components are stored as described above.

GENERAL INSTRUCTIONS

1. All reagents should be allowed to reach room temperature (18- 25°C) before use.
2. Serum or plasma samples should generally be diluted ~100 fold or more with diluent in order to obtain values within the standard range.

WASH SOLUTION PREPARATION

The wash solution is provided as a 20x stock. Prior to use, dilute the contents of the bottle (50 ml) with 950 ml of distilled or deionized water.

STANDARD PREPARATION

The mouse SAA standard is comprised of lyophilized mouse serum of known SAA concentration. The SAA content was determined by reference to a synthetic mouse SAA2 polypeptide.

1. Reconstitute the lyophilized mouse SAA reference standard by addition of 200 ml of deionized or distilled
water. Mix gently several times over a period of 5-10 minutes. The concentration of SAA in the reconstituted stock is indicated on the vial label.
2. Label 7 polypropylene tubes as 500, 250, 125, 62.5,
31.25, 15.6, and 7.8 ng/ml.
3. Into the tube labeled 500 ng/ml, pipette the volume of
diluent detailed on the SAA reference standard vial label.
Then add the indicated volume of reference SAA
standard and mix gently. This provides the working 500
ng/ml standard.
4. Dispense 250 ml of diluent into the tubes labeled 250,
125, 62.5, 31.25, 15.6, and 7.8 ng/ml.
5. Pipette 250 ml of the 500 ng/ml SAA standard into the
tube labeled 250 ng/ml and mix. This provides the
working 250 ng/ml SAA standard.
6. Prepare a 125 ng/ml standard by diluting and mixing
250 ml of the 250 ng/ml standard with 250 ml of diluent in
the tube labeled 125 ng/ml. Similarly prepare the 125,
62.5, 31.25, 15.6 and 7.8 ng/ml standards by serial
dilution.

Please Note: The reconstituted reference standard
should be aliquoted and stored frozen at or below -20oC
(within 1 hour of reconstitution) if future use is intended.

SAMPLE PREPARATION

General Note: Because SAA levels can increase as
much as 50 fold or more during inflammation, optimal
dilutions should be determined empirically. However, as
a good starting point, samples may be tested at a 100
fold dilution using the following procedure for each
sample to be tested:

1. Dispense 297 ml of diluent into a polypropylene tube.
1. Secure the desired number of coated wells in the holder.
2. Dispense 100 ml of standards and diluted samples into
the wells (we recommend that standards and samples
be tested in duplicate).
3. Add 100 ml of HRP conjugate reagent into each well.
4. Incubate on an orbital micro-plate shaker at 150 rpm at room temperature (18-25° C) for one hour.
5. Wash and empty the microtiter wells 6 times with 1x wash solution. This may be performed using either a
plate washer (400 ml/well) or a squirt bottle. The entire
wash procedure should be performed as quickly as
possible.
6. Strike the wells sharply onto absorbent paper or paper
towels to remove all residual wash solution.
7. Dispense 100 ml of TMB Reagent into each well.
8. Gently mix on an orbital micro-plate shaker at 150 rpm
at room temperature (18-25° C) for 20 minutes.
9. Stop the reaction by adding 100 ml of Stop Solution to
each well.
10. Gently mix. It is important to make sure that all the blue
color changes to yellow.
11. Read the optical density at 450 nm with a microtiter
plate reader within 5 minutes.

CALCULATION OF RESULTS

1. Calculate the average absorbance values (A_{450}) for each
set of reference standards and samples.
2. Construct a standard curve by plotting the mean
absorbance obtained from each reference standard
against its concentration in ng/ml on linear graph paper,
with absorbance values on the vertical or Y-axis and
concentrations on the horizontal or X-axis.
3. Using the mean absorbance value for each sample,
determine the corresponding concentration of SAA in
ng/ml from the standard curve.
4. Multiply the derived concentration by the dilution factor
to determine the actual concentration of SAA in the
serum sample.
5. If available, PC graphing software should be used for the
above steps. We find that good a good fit of the data is
obtained to a two site binding equation.
6. If the OD_{450} values of samples fall outside the standard
curve when tested at a dilution of 100, samples should
be diluted appropriately and re-tested.

A 19 MOUSE SERUM AMYLOID P (SAP) ELISA TEST KIT
Life Diagnostics, Inc., Catalog Number: 3410-1
Mouse SAP ELISA

INTRODUCTION

SAP is a member of the pentraxin family of acute phase proteins that includes C-reactive protein. It circulates in blood as a decamer of a single polypeptide chain of mwt 25 kDa. It is a positive acute phase protein in all strains of mice. Levels may increase 50-100 fold during the acute phase response but basal levels vary with strain (refs. 1-3). SAP is an excellent acute phase biomarker in mice.

PRINCIPLE OF THE TEST

The mouse SAP ELISA uses two peptide-specific antibodies developed at Life Diagnostics, Inc. that recognize different epitopes on mouse SAP. One is used for solid phase immobilization and the other, conjugated to horseradish peroxidase (HRP), is used for detection. Diluted serum samples (100 ㎖) are incubated in the antibody-coated microtiter wells together with HRP conjugate (100 ㎖) for one hour. As a result, SAP molecules are sandwiched between the immobilization and detection antibodies. The wells are then washed to remove unbound HRP-conjugate and TMB Reagent is added and incubated for 20 minutes. This results in the development of a blue color. Color development is stopped by the addition of Stop Solution, changing the color to yellow, and optical density is measured at 450 nm. The concentration of SAP is proportional to the optical density of the test sample and is derived from a standard curve.

MATERIALS AND COMPONENTS

Materials provided with the kit:

· Anti-mouse SAP coated 96-well microtiter (12x8 wells)
· HRP Conjugate, 11 ml
· SAP stock, 1 vial (lyophilized)[1]
· 20x Wash Buffer, 50 ml
· Diluent, 50 ml
· TMB Reagent (One-Step), 11 ml
· Stop Solution (1N HCl), 11 ml

Materials required but not provided:

· Precision pipettes and tips
· Distilled or deionized water
· Polypropylene tubes
· Vortex mixer
· Absorbent paper or paper towels
· Plate incubator/shaker with an approximate mixing speed of 150 rpm
· 96-well plate reader capable of measuring absorbance at 450 nm
· PC graphing software or graph paper

STORAGE

Upon receiving the kit, please store the SAP standard in a freezer at or below -20^{o}C. The remaining components of the kit should be stored in a refrigerator at 2-8° C. It is important that the microtiter plate be kept in a sealed bag with desiccant to minimize exposure to damp air. Test kits will remain stable for six months from the date of purchase, provided that the components are stored as described above.

[1] The SAP standard was calibrated using recombinant mouse SAP from an independent laboratory.

GENERAL INSTRUCTIONS

1. All reagents should be allowed to reach room temperature (25^{o}C) before use.
2. Please take the time to completely read and understand this kit insert before starting your assay. Don't hesitate to contact Life Diagnostics by telephone or email should you require technical assistance or clarification.

WASH SOLUTION PREPARATION

The wash solution is provided as a 20x stock. Prior to use, dilute the contents of the bottle (50 ml) with 950 ml of distilled or deionized water.

SAMPLE PREPARATION

Samples should be diluted at least 40-fold in diluent. Optimum dilutions should be determined empirically.

STANDARD PREPARATION

1. Reconstitute the SAP stock as described on the vial label. Mix gently several times before use.
2. Label 8 polypropylene tubes as 500, 250, 125, 62.5, 31.25, 15.63, 7.81 and 0 ng/ml.
3. Into the tube labeled 500 ng/ml, pipette the volume of

diluent detailed on the SAP stock vial label. Then add
the indicated volume of SAP stock (also shown on the
vial label) and mix gently. This provides the working 500
ng/ml standard.
4. Dispense 250 µl of diluent into the tubes labeled 250,
125, 62.5, 31.25, 15.63, 7.81 and 0 ng/ml.
5. Pipette 250 µl of the 500 ng/ml SAP standard into the
tube labeled 250 ng/ml and mix. This provides the
working 250 ng/ml SAP standard.
6. Similarly prepare the 125, 62.5, 31.25, 15.63, and 7.81
ng/ml standards by serial dilution.
Please Note: Unused reconstituted reference standard
stock should be stored frozen at or below -20°C if future
use is intended. Sufficient standard stock is provided for
two standard curves to be run in duplicate or 4 standard
curves run as singlets.

ASSAY PROCEDURE

1. Secure the desired number of coated wells in the holder.
2. Dispense 100 µl of standards and diluted samples into
the wells (we recommend that standards and samples
be tested in duplicate).
3. Add 100 µl of HRP conjugate reagent into each well.
4. Incubate on an orbital micro-plate shaker at 150 rpm at
room temperature (25° C)[2] for one hour.
5. Wash and empty the microtiter wells 6 times with 1x
wash solution using a plate washer (400 µl/well). The
entire wash procedure should be performed as quickly
as possible.
6. Strike the wells sharply onto absorbent paper or paper
towels to remove all residual wash solution.
[2] The ELISA was validated using a shaking incubator at 25°C and 150
rpm. Lower temperatures and/or mixing speeds will give lower
absorbance values.
7. Dispense 100 µl of TMB Reagent into each well.
8. Gently mix on an orbital micro-plate shaker at 150 rpm
at room temperature (25° C) for 20 minutes.
9. Stop the reaction by adding 100 µl of Stop Solution to
each well.
10. Gently mix. It is important to make sure that all the blue
color changes to yellow.
11. Read the optical density at 450 nm with a microtiter
plate reader within 5 minutes.

CALCULATION OF RESULTS

1. Calculate the average absorbance values (A_{450}) for each
set of reference standards and samples.
2. Construct a standard curve by plotting the mean
absorbance obtained from each reference standard
against its concentration in ng/ml on linear graph paper,
with absorbance values on the vertical or Y-axis and
concentrations on the horizontal or X-axis.
3. Using the mean absorbance value for each sample,
determine the corresponding concentration of SAP in
ng/ml from the standard curve.
4. Multiply the derived concentration by the dilution factor
to determine the actual concentration of SAP in the
serum sample.
5. If available, PC graphing software should be used for the
above steps. We find that good a good fit of the data is
obtained to either a two site binding equation or a
second order polynomial equation.
6. If the A_{450} values of samples fall outside the standard
curve samples should be diluted appropriately and retested.

TYPICAL STANDARD CURVE

A representative standard curve with optical density readings
at 450 nm on the Y-axis against SAP concentrations on the
X-axis is shown below. This curve is for the purpose of
illustration only and should not be used to calculate
unknowns. Each user should obtain his or her data and
standard curve in each experiment.

Appendix B: Plasmid Maps

B1 TOPO 2.1, DNA pCR®

Map of pCR™2.1-TOPO®

pCR™2.1-TOPO® map

The following map shows the features of the pCR™2.1-TOPO® vector and the sequence surrounding the TOPO® Cloning site. Restriction sites are labeled to indicate the actual cleavage site. The arrow indicates the start of transcription for T7 polymerase. The sequence of the pCR™2.1-TOPO® vector is available from www.lifetechnologies.com/support or by contacting Technical Support (page 32).

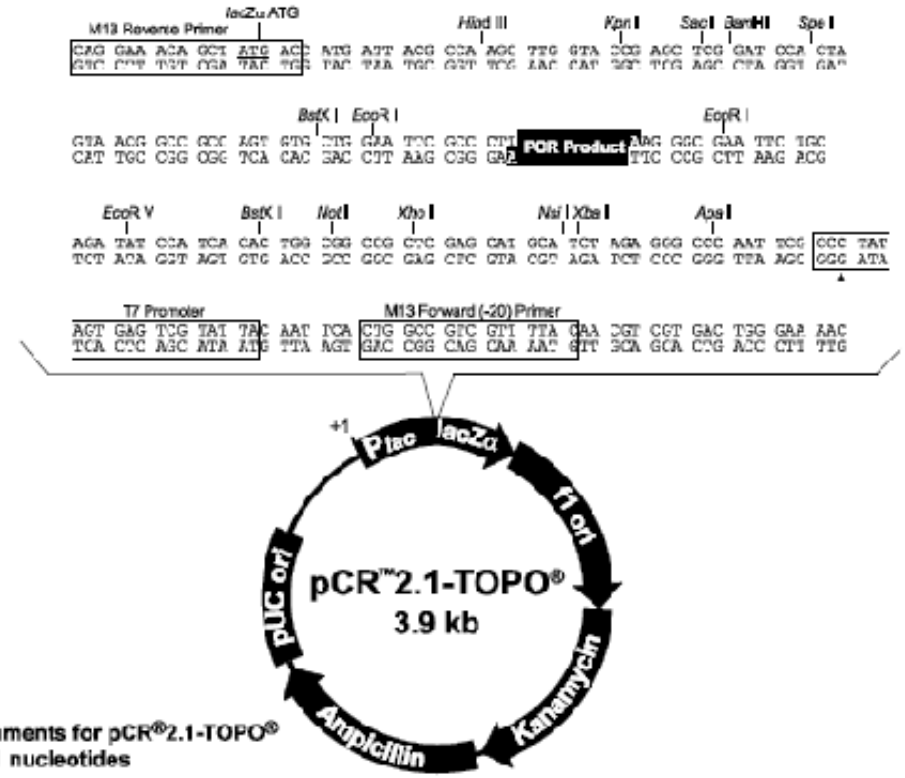

Comments for pCR®2.1-TOPO®
3931 nucleotides

LacZα fragment: bases 1-547
M13 reverse priming site: bases 205-221
Multiple cloning site: bases 234-357
T7 promoter/priming site: bases 364-383
M13 Forward (-20) priming site: bases 391-406
f1 origin: bases 548-985
Kanamycin resistance ORF: bases 1319-2113
Ampicillin resistance ORF: bases 2131-2991
pUC origin: bases 3136-3809

B2 pCR™ -Blunt II-TOPO®

Map of pCR™-Blunt II-TOPO®

pCR™-Blunt II-TOPO® map

The following map shows the features of pCR™-Blunt II-TOPO® and the sequence surrounding the TOPO® Cloning site. Restriction sites are labeled to indicate the actual cleavage site. The arrows indicate the start of transcription for the T7 and SP6 polymerases. **The sequence of the vector** is available from www.lifetechnologies.com/support or by contacting Technical Support (page 29).

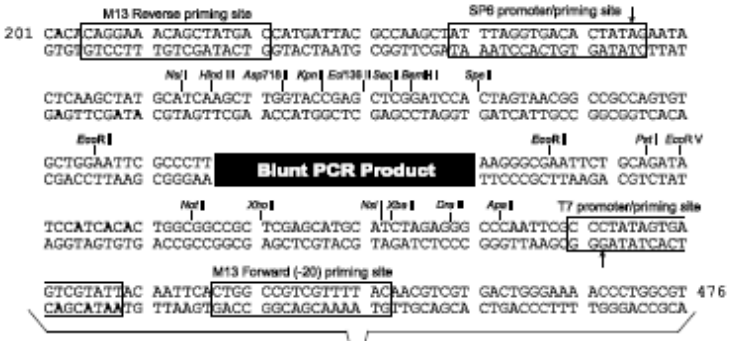

Comments for pCR™-Blunt II-TOPO®
3519 nucleotides

lac promoter/operator region: bases 95-216
M13 Reverse priming site: bases 205-221
LacZ-alpha ORF: bases 217-576
SP6 promoter priming site: bases 239-256
Multiple Cloning Site: bases 269-399
TOPO®-Cloning site: bases 336-337
T7 promoter priming site: bases 406-425
M13 (-20) Forward priming site: bases 433-448
Fusion joint: bases 577-585
ccdB lethal gene ORF: bases 586-888
kan gene: bases 1099-2031
kan promoter: bases 1099-1236
Kanamycin resistance gene ORF: bases 1237-2031
Zeocin resistance ORF: bases 2238-2612
pUC origin: bases 2724-3397

B3 Promega pGEM7Zf(+)

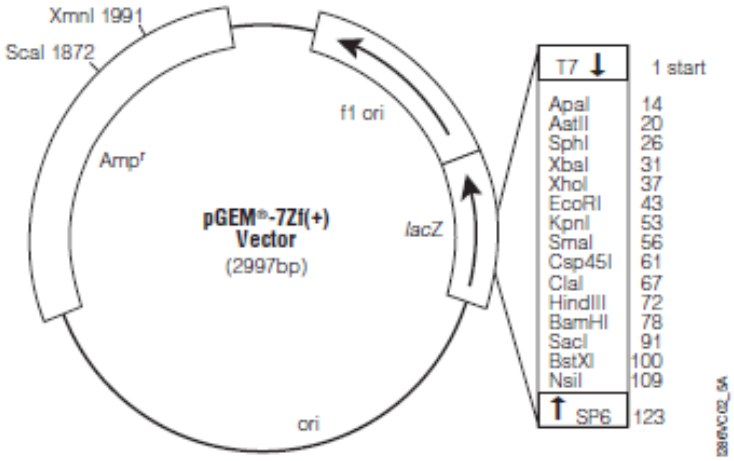

Figure 2. pGEM®-7Zf(+) Vector circle map and sequence reference points. The pGEM®-7Zf(+) and pGEM®-7Zf(–) Vectors are identical except for the orientation of the f1 origin. Use the T7 Promoter Primer or pUC/M13 Forward Primer to sequence ssDNA produced by the pGEM®-7Zf(+) Vector.

pGEM®-7Zf(+) Vector sequence reference points:

T7 RNA polymerase transcription initiation site	1
SP6 RNA polymerase transcription initiation site	123
T7 RNA polymerase promoter (–17 to +3)	2981–3
SP6 RNA polymerase promoter (–17 to +3)	121–140
multiple cloning region	10–110
binding site of pUC/M13 Reverse Sequencing Primer	158–174
*lac*Z start codon	162
lac operon sequences	2818–2978; 148–377
lac operator	182–198
β-lactamase (Amp^r) coding region	1319–2179
phage f1 region	2362–2817
binding site of pUC/M13 Forward Sequencing Primer	2938–2954

B4 Promega pGEM5Zf(+)

Promega

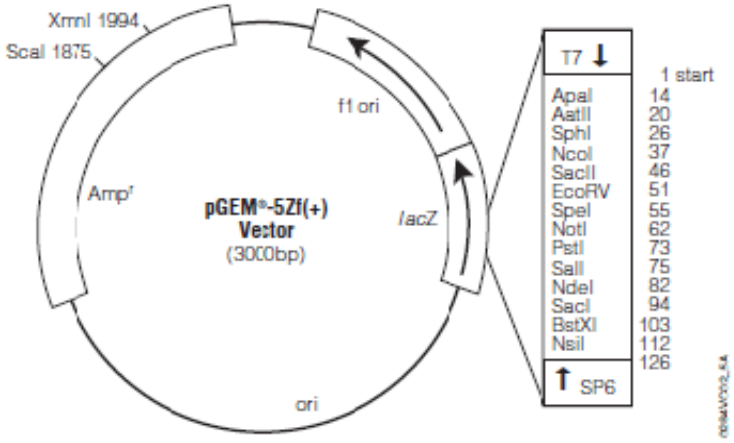

Figure 2. pGEM®-5Zf(+) Vector map.

The pGEM®-5Zf(+) and pGEM®-5Zf(-) Vectors are identical except for the orientation of the f1 origin.

pGEM®-5Zf(+) Vector sequence reference points:

T7 RNA Polymerase transcription initiation site	1
Multiple cloning region	10–113
SP6 RNA Polymerase promoter (–17 to +3)	124–143
SP6 RNA Polymerase transcription initiation site	126
Binding site of pUC/M13 Reverse Sequencing Primer	161–177
lacZ start codon	165
lac operon sequences	151–380; 2821–2981
lac operator	185–201
β-lactamase coding region	1322–2182
phage f1 region	2365–2820
binding site of pUC/M13 Forward Sequencing Primer	2941–2957
T7 RNA Polymerase promoter (–17 to +3)	2984–3

B5 pMK-T –based CHIKV qRT-PCR amplicon clone

life technologies™

Quality Assurance Documentation: 12ABYWDP

Ref. No.: 1314264

Designation:	E.coli K12 (dam+ dcm+ tonA rec-)
Gene name:	**CHIKV_qPCR_amplicon**
Gene size:	139 bp
Vector backbone:	pMK-T
Cloning sites:	SfiI / SfiI
Quantity:	~5 µg Plasmid DNA
Note:	Please dissolve lyophilized DNA in 50 µl distilled water or 10 mM Tris-HCl (pH 8.0). We recommend sequence verification after each transformation step.

Plasmid Map:

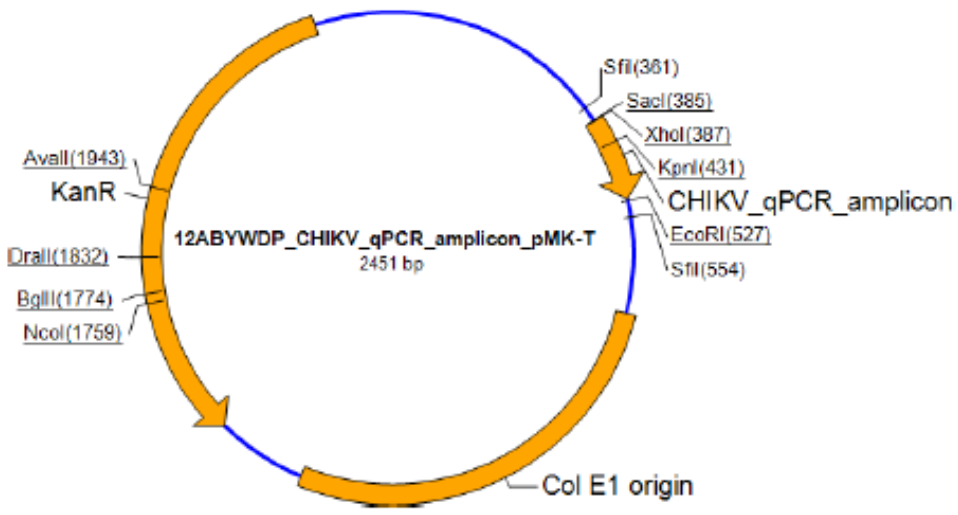

B6 CHIKV cDNA clone pCHIK-SL(wt)

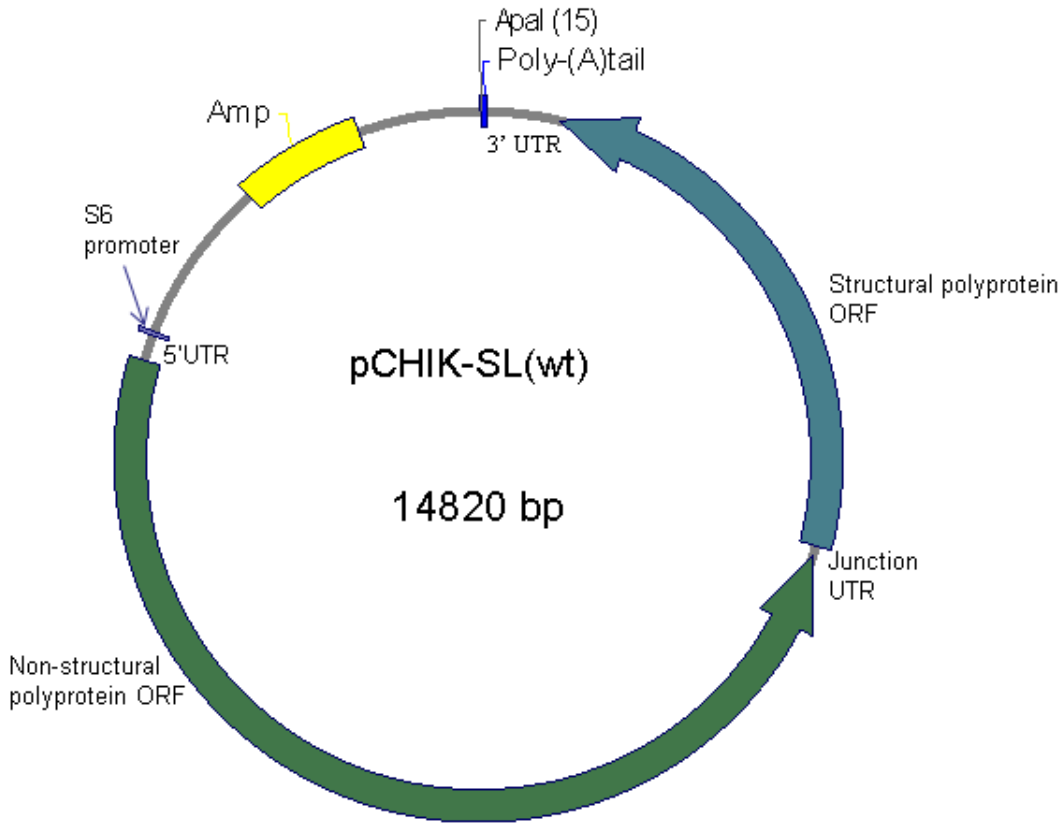

Appendix C: Supplementary data

C1: The cDNA sequence of CHIKV SL-R233 (excluding the poly-A tail).

Italics are used to indicate untranslated regions, open reading frames are shown in bold lettering and stop codons are underlined.

```
   1 atggctgcgt gagacacacg tagcctacca gtttcttact gctctactct
  51 gcaaagcaag agattaataa cccatcatgg atcctgtgta cgtggacata
 101 gacgctgaca gcgccttttt gaaggccctg caacgtgcgt accccatgtt
 151 tgaggtggaa ccaaggcagg tcacaccgaa tgaccatgct aatgctagag
 201 cgttctcgca tctagctata aaactaatag agcaggaaat tgaccccgac
 251 tcaaccatcc tggatatcgg cagtgcgcca gcaaggagga tgatgtcgga
 301 caggaagtac cactgcgtct gcccgatgcg cagtgcggaa gatcccgaga
 351 gactcgctaa ttatgcgaga aagctagcat ctgccgcagg aaaagtcctg
 401 gacagaaaca tctctggaaa gatcggggac ttacaagcag taatggccgt
 451 gccagacaag gagacgccaa cattctgctt acacacagac gtctcatgta
 501 gacagagagc agacgtcgct atataccaag acgtctatgc tgtacacgca
 551 cccacgtcgc tataccacca ggcgattaaa ggggtccaag tggcgtactg
 601 ggttgggttc gacacaaccc cgttcatgta caatgccatg gcgggtgcct
 651 acccctcata ctcgacaaac tgggcagatg agcaggtact gaaggctaag
 701 aacataggat tatgttcaac agacctgacg gaaggtagac gaggcaagtt
 751 gtctattatg agagggaaaa agctaaaacc gtgcgaccgt gtgctgttct
 801 cagtagggtc aacgctctac ccggaaagcc gcaagctact taagagctgg
 851 cacctgccat cggtgttcca tttaaagggc aaactcagct tcacatgccg
 901 ctgtgataca gtggtttcgt gtgagggcta cgtcgttaag agaataacga
 951 tgagcccagg cctttatgga aaaaccacag ggtatgcggt aacccaccac
1001 gcagacggat tcctgatgtg caagactacc gacacggttg acggcgaaag
1051 agtgtcattc tcggtgtgca catacgtgcc ggcgaccatt tgtgatcaaa
1101 tgaccggcat ccttgctaca gaagtcacgc cggaggatgc acagaagctg
1151 ttggtggggc tgaaccagag aatagtggtt aacggcagaa cgcaacggaa
1201 tatgaacacc atgaaaaatt atctgcttcc cgtggtcgcc caagccttca
1251 gtaagtgggc aaaggagtgc cggaaagaca tggaagatga aaaactcctg
1301 ggggtcagag aaagaacact gacctgctgc tgtctatggg cattcaagaa
1351 gcagaaaaca cacacggtct acaagaggcc ggatacccag tcaattcaga
1401 aggttcaggc cgagtttgac agctttgtgg taccgagtct gtggtcgtcc
1451 gggttgtcaa tccctttgag gactagaatc aaatggttgt taagcaaggt
1501 gccaaaaacc gacctgatcc catacagcgg agacgcccga gaagcccggg
1551 acgcagaaaa agaagcagag gaagaacgag aagcagaact gactcgcgaa
1601 gccctaccac ctctacaggc agcacaggaa gatgttcagg tcgaaatcga
1651 cgtggaacag cttgaggaca gagcgggcgc aggaataata gagactccga
1701 gaggagctat caaagttact gcccaaccaa cagaccacgt cgtgggagag
1751 tacctggtac tctccccgca gaccgtacta cgtagccaga agctcagtct
1801 gattcacgct ttggcggagc aagtgaagac gtgcacgcac aacggacgag
1851 cagggaggta tgcggtcgaa gcgtacgacg gccgagtcct agtgccctca
1901 ggctatgcaa tctcgcctga agacttccag agtctaagcg aaagcgcaac
1951 gatggtgtat aacgaaagag agttcgtaaa cagaaagcta caccatattg
2001 cgatgcacgg accagccctg aacaccgacg aagagtcgta tgagctggtg
2051 agggcagaga ggacagaaca cgagtacgtc tacgacgtgg atcagagaag
2101 atgctgtaag aaggaagaag ccgcaggact ggtactggtg ggcgacttga
2151 ctaatccgcc ctaccacgaa ttcgcatatg aagggctaaa aatccgccct
2201 gcctgcccat acaaaattgc agtcatagga gtcttcggag taccgggatc
2251 tggcaagtca gctattatca agaacctagt taccaggcag gacctggtga
2301 ctagcggaaa gaaagaaaac tgccaagaaa tcaccaccga cgtgatgaga
2351 cagagaggtc tagagatatc tgcacgtacg gttgactcgc tgctcttgaa
2401 tggatgcaac agaccagtcg acgtgttgta cgtagacgag gcgtttgcgt
2451 gccactctgg aacgctactt gctttgatcg ccttggtgag accaaggcag
2501 aaagttgtac tttgtggtga cccgaagcag tgcggcttct tcaatatgat
2551 gcagatgaaa gtcaactata atcacaacat ctgcacccaa gtgtaccaca
```

2601 **aaagtatctc caggcggtgc acactgcctg tgaccgccat tgtgtcatcg**
2651 **ttgcattacg aaggcaaaat gcgcactacg aatgagtaca acaagccgat**
2701 **tgtagtggac actacaggct caacaaaacc tgaccctgga gacctcgtgt**
2751 **taacgtgctt cagagggtgg gttaaacaac tgcaaattga ctatcgtgga**
2801 **tacgaggtca tgacagcagc cgcatcccaa gggttaacca gaaaaggagt**
2851 **ttacgcagtt agacaaaaag ttaatgaaaa cccgctctat gcatcaacgt**
2901 **cagagcacgt caacgtactc ctaacgcgta cggaaggtaa actggtatgg**
2951 **aagacacttt ccggcgaccc gtggataaag acgctgcaga acccaccgaa**
3001 **aggaaacttc aaagcaacta ttaaggagtg ggaggtggag catgcatcaa**
3051 **taatggcggg catctgcagt caccaaatga ccgtcgatac attccaaaat**
3101 **aaagccaacg tttgttgggc taagagcttg gtccctatcc tcgaaacagc**
3151 **ggggataaaa ctaaatgata ggcagtggtc tcagataatt caagccttca**
3201 **aagaagacaa agcatactca cctgaagtag ccctgaatga aatatgtacg**
3251 **cgcatgtatg gggtggatct agacagcggg ctattttcta aaccgttggt**
3301 **gtctgtgtat tacgcggata accactggga taataggcct ggagggaaaa**
3351 **tgttcggatt taaccccgag gcagcatcca ttctagaaag aaagtaccca**
3401 **ttcacaaaag ggaagtggaa catcaacaag cagatctgcg tgactaccag**
3451 **gaggatagaa gactttaacc ctaccaccaa catcataccg gccaacagga**
3501 **gactaccaca ctcattagtg gccgaacacc gcccagtaaa aggggaaaga**
3551 **atggaatggc tggttaacaa gataaacggc caccacgtgc tcctggtcag**
3601 **tggctataac cttgcactgc ctactaagag agtcacttgg gtagcgccgt**
3651 **taggtgtccg cggagcggac tacacataca acctagagtt gggtctgcca**
3701 **gcaacgcttg gtaggtatga ccttgtggtc ataaacatcc acacaccttt**
3751 **tcgcatacac cattaccaac agtgcgtcga ccacgcaatg aaactgcaaa**
3801 **tgctcggggg tgactcattg agactgctca aaccgggcgg ctctctattg**
3851 **atcagagcat atggttacgc agatagaacc agtgaacgag tcatctgcgt**
3901 **attgggacgc aagtttagat cgtctagagc gttgaaacca ccatgtgtca**
3951 **ccagcaacac tgagatgttt ttcctattca gcaactttga caatggcaga**
4001 **aggaatttca caactcatgt catgaacaat caactgaatg cagccttcgt**
4051 **aggacaggtc acccgagcag gatgtgcacc gtcgtaccgg gtaaaacgca**
4101 **tggacatcgc gaagaacgat gaagagtgcg tagtcaacgc cgctaaccct**
4151 **cgcgggttac cgggtgacgg tgtttgcaag gcagtataca aaaaatggcc**
4201 **ggagtccttt aagaacagtg caacaccagt gggaaccgca aaaacagtta**
4251 **tgtgcggtac gtatccagta atccacgctg ttggaccaaa cttctctaat**
4301 **tattcggagt ctgaagggga ccgggaattg gcagctgcct atcgagaagt**
4351 **cgcaaaggaa gtaactaggc tgggagtaaa tagtgtagct atacctctcc**
4401 **tctccacagg tgtatactca ggagggaaag acaggctgac ccagtcactg**
4451 **aaccacctct ttacagccat ggactcgacg gatgcagacg tggtcatcta**
4501 **ctgccgcgac aaagaatggg agaagaaaat atctgaggcc atacagatgc**
4551 **ggacccaagt agagctgctg gatgagcaca tctccataga ctgcgatatt**
4601 **gttcgcgtgc accctgacag cagcttggca ggcagaaaag gatacagcac**
4651 **cacggaaggc gcactgtact catatctaga agggacccgt tttcatcaga**
4701 **cggctgtgga tatggcggag atacatacta tgtggccaaa gcaaacagag**
4751 **gccaatgagc aagtctgcct atatgccctg ggggaaagta ttgaatcgat**
4801 **caggcagaaa tgcccggtgg atgatgcaga cgcatcatct ccccccaaaa**
4851 **ctgtcccgtg cctttgccgt tacgctatga ctccagaacg cgtcacccgg**
4901 **cttcgcatga accacgtcac aagcataatt gtgtgttctt cgtttccact**
4951 **cccaaagtac aaaatagaag gagtgcaaaa agtcaaatgc tctaaggtaa**
5001 **tgctatttga ccacaacgtg ccatcgcgcg taagtccaag ggaatataga**
5051 **tcttcccagg agtctgcaca ggaggcgagt acaatcacgt cactgacgca**
5101 **tagtcaattc gacctaagcg ttgatggcga gatactgccc gtcccgtcag**
5151 **acctggatgc tgacgcccca gccctagaac cagcactaga cgacggggcg**
5201 **acacacacgc tgccatccac aaccggaaac cttgcggccg tgtctgactg**
5251 **ggtaataagc accgtacctg tcgcgccgcc cagaagaagg cgagggagaa**
5301 **acctgactgt gacatgtgac gagagagaag ggaatataac acccatggct**
5351 **agcgtccgat tctttagggc agagctgtgt ccggtcgtac aagaaacagc**
5401 **ggagacgcgt gacacagcaa tgtctcttca ggcaccaccg agtaccgcca**
5451 **cggaaccgaa tcatccgccg atctccttcg gagcatcaag cgagacgttc**
5501 **cccattacat ttggggactt caacgaagga gaaatcgaaa gcttgtcttc**
5551 **tgagctacta actttcggag acttcttacc aggagaagtg gatgacttga**
5601 **cagacagcga ctggtccacg tgctcagaca cggacgacga gttacgacta**

5651 **gacagggcag gtgggtatat attctcgtcg gacaccggtc caggtcattt**
5701 **acaacagaag tcagtacgcc agtcagtgct gccggtgaac accctggagg**
5751 **aagtccacga ggagaagtgt tacccaccta agctggatga agcaaaggag**
5801 **caactattac ttaagaaact ccaggagagt gcatccatgg ccaacagaag**
5851 **caggtatcag tcgcgcaaag tagaaaacat gaaagcagca atcatccaga**
5901 **gactaaagag aggctgtaga ctatacttaa tgtcagagac cccaaaagtc**
5951 **cctacttacc ggactacata tccggcgcct gtgtactcgc ctccgatcaa**
6001 **cgttcgattg tccaatcccg agtccgcagt ggcagcatgc aatgagttct**
6051 **tagctagaaa ctatccaact gtctcatcat accaaattac cgacgagtat**
6101 **gatgcatatc tagacatggt ggacgggtcg gagagttgcc tggaccgagc**
6151 **gacattcaat ccgtcaaaac tcaggagcta cccgaaacag cacgcttacc**
6201 **acacgccctc catcagaagc gctgtaccgt ccccattcca gaacacacta**
6251 **cagaatgtac tggcagcagc cacgaaaaga aactgcaacg tcacacagat**
6301 **gagggaatta cccactttgg actcagcagt attcaacgtg gagtgtttca**
6351 **aaaaattcgc atgcaaccaa gaatactggg aagaatttgc tgccagccct**
6401 **attaggataa caactgagaa tttagcaacc tatgttacta aactaaaagg**
6451 **gccaaaagca gcagcgctat tcgcaaaaac ccataatcta ctgccactac**
6501 **aggaagtacc aatggatagg ttcacagtag atatgaaaag ggacgtgaag**
6551 **gtgactcctg gtacaaagca tacagaggaa agacctaagg tgcaggttat**
6601 **acaggcggct gaacccttgg cgacagcata cctatgtggg attcacagag**
6651 **agctggttag gaggctgaac gccgtcctcc tacccaatgt acatacacta**
6701 **tttgacatgt ctgccgagga tttcgatgcc atcatagccg cacactttaa**
6751 **gccaggagac actgttttgg aaacggacat agcctccttt gataagagcc**
6801 **aagatgattc acttgcgctt actgctttga tgctgttaga ggatttaggg**
6851 **gtggatcact ccctgctgga cttgatagag gctgctttcg gagagatttc**
6901 **cagctgtcac ctaccgacag gtacgcgctt caagttcggc gccatgatga**
6951 **aatcaggtat gttcctaact ctgttcgtca acacattgtt aaacatcacc**
7001 **atcgccagcc gagtgctgga agatcgtctg acaaaatccg cgtgcgcggc**
7051 **cttcatcggc gacgacaaca taatacatgg agtcgtctcc gatgaattga**
7101 **tggcagccag atgtgccact tggatgaaca tggaagtgaa gatcatagat**
7151 **gcagttgtat ccttgaaagc cccttacttt tgtggagggt ttatactgca**
7201 **cgatactgtg acaggaacag cttgcagagt ggcagacccg ctaaaaaggc**
7251 **tttttaaact gggcaaaccg ctagcggcag gtgacgaaca agatgaagat**
7301 **agaagacgag cgctggctga cgaagtgatc agatggcaac gaacagggct**
7351 **aattgatgag ctggagaaag cggtatactc taggtacgaa gtgcagggta**
7401 **tatcagttgt ggtaatgtcc atggccacct ttgcaagctc cagatccaat**
7451 **ttcgagaagc tcagaggacc cgtcataact ttgtacggcg gtcctaaa**ta
7501 *ggtacgcact acagctacct attttgcaga agccgacagc aagtatctaa*
7551 *acactaatca gctaca***atgg agttcatccc aacccaaact ttttacaata**
7601 **ggaggtacca gcctcgaccc tggactccgc gctctactat ccaaatcatc**
7651 **aggcccagac cgcgccctca gaggcaagct gggcaacttg cccagctgat**
7701 **ctcagcagtt aataaactga caatgcgcgc ggtaccccaa cagaagccac**
7751 **gcaggaatcg gaagaataag aagcaaaagc aaaaacaaca ggcgccacaa**
7801 **aacaacacaa atcaaaagaa gcagccacct aaaaagaaac cggctcaaaa**
7851 **gaaaaagaag ccgggccgca gagagaggat gtgcatgaaa atcgaaaatg**
7901 **attgtatttt cgaagtcaag cacgaaggta aggtaacagg ttacgcgtgc**
7951 **ctggtggggg acaaagtaat gaaaccagca cacgtaaagg ggaccatcga**
8001 **taacgcggac ctggccaaac tggcctttaa gcggtcatct aagtatgacc**
8051 **ttgaatgcgc gcagataccc gtgcacatga agtccgacgc ttcgaagttc**
8101 **acccatgaga aaccggaggg gtactacaac tggcaccacg gagcagtaca**
8151 **gtactcagga ggccggttca ccatccctac aggtgctggc aaaccagggg**
8201 **acagcggcag accgatcttc gacaacaagg gacgcgtggt ggccatagtc**
8251 **ttaggaggag ctaatgaagg agcccgtaca gccctctcgg tggtgacctg**
8301 **gaataaagac attgtcacta aaatcacccc cgaggggccc gaagagtgga**
8351 **gtcttgccat cccagttatg tgcctgttgg caaacaccac gttcccctgc**
8401 **tcccagcccc cttgcacgcc ctgctgctac gaaaaggaac cggaggaaac**
8451 **cctacgcatg cttgaggaca acgtcatgag acctgggtac tatcagctgc**
8501 **tacaagcatc cttaacatgt tctccccacc gccagcgacg cagcaccaag**
8551 **gacaacttca atgtctataa agccacaaga ccatacttag ctcactgtcc**
8601 **cgactgtgga gaagggcact cgtgccatag tcccgtagca ctagaacgca**
8651 **tcagaaatga agcgacagac gggacgctga aaatccaggt ctccttgcaa**

8701 **atcggaataa agacggatga cagccacgat tggaccaagc tgcgttatat**
8751 **ggacaaccac atgccagcag acgcagagag ggcggggcta tttgtaagaa**
8801 **catcagcacc gtgtacgatt actggaacaa tgggacactt catcctggcc**
8851 **cgatgtccaa aaggggaaac tctgacggtg ggattcactg acagtaggaa**
8901 **gattagtcat tcatgtacgc acccatttca ccacgaccct cctgtgatag**
8951 **gtcgggaaaa attccattcc cgaccgcagc acggtaaaga gctaccttgc**
9001 **agcacgtacg tgcagagcac cgccgcaact accgaggaga tagaggtaca**
9051 **catgccccca gacacccctg atcgcacatt aatgtcacaa cagtccggca**
9101 **acgtaaagat cacagtcaat ggccagacgg tgcggtacaa gtgtaattgc**
9151 **ggtggctcaa atgaaggatt aacaactaca gacaaagtga ttaataactg**
9201 **caaggttgat caatgtcatg ccgcggtcac caatcacaaa aagtggcagt**
9251 **ataactcccc tctggtcccg cgtaatgctg aacttgggga ccgaaaagga**
9301 **aaaattcaca tcccgtttcc gctggcaaat gtaacatgca gggtgcctaa**
9351 **agcaaggaac cccaccgtga cgtacgggaa aaaccaagtc atcatgctac**
9401 **tgtatcctga ccacccaaca ctcctgtcct accggaatat gggagaagaa**
9451 **ccaaactatc aagaagagtg ggtgatgcat aagaaggaag tcgtgctaac**
9501 **cgtgccgact gaagggctcg aggtcacgtg gggcaacaac gagccgtata**
9551 **agtattggcc gcagttatct acaaacggta cagcccatgg ccacccgcat**
9601 **gagataattc tgtattatta tgagctgtac cctactatga ctgtagtagt**
9651 **tgtgtcagtg gccacgttca tactcctgtc gatggtgggt atggcagcgg**
9701 **ggatgtgcat gtgtgcacga cgcagatgca tcacaccgta tgaactgaca**
9751 **ccaggagcta ccgtcccttt cctgcttagc ctaatatgct gcatcagaac**
9801 **agctaaagcg gccacatacc aagaggctgc gatatacctg tggaacgagc**
9851 **agcaaccttt gttttggcta caagccctta ttccgctggc agccctgatt**
9901 **gttctatgca actgtctgag actcttacca tgctgctgta aaacgttggc**
9951 **ttttttagcc gtaatgagcg tcggtgccca cactgtgagc gcgtacgaac**
10001 **acgtaacagt gatcccgaac acggtgggag taccgtataa gactctagtc**
10051 **aatagacctg gctacagccc catggtattg gagatggaac tactgtcagt**
10101 **cactttggag ccaacactat cgcttgatta catcacgtgc gagtacaaaa**
10151 **ccgtcatccc gtctccgtac gtgaagtgct gcggtacagc agagtgcaag**
10201 **gacaaaaacc tacctgacta cagctgtaag gtcttcaccg gcgtctaccc**
10251 **atttatgtgg ggcggcgcct actgcttctg cgacgctgaa aacacgcagt**
10301 **tgagcgaagc acatgtggag aagtccgaat catgcaaaac agaatttgca**
10351 **tcagcataca gggctcatac cgcatctgca tcagctaagc tccgcgtcct**
10401 **ttaccaagga aataacatca ctgtaactgc ctatgcaaac ggcgaccatg**
10451 **ccgtcacagt taaggacgcc aaattcattg tggggccaat gtcttcagcc**
10501 **tggacacctt tcgacaacaa aattgtggtg tacaaaggtg acgtctataa**
10551 **catggactac ccgccctttg gcgcaggaag accaggacaa tttggcgata**
10601 **tccaaagtcg cacacctgag agtaaagacg tctatgctaa tacacaactg**
10651 **gtactgcaga gaccggctgc gggtacggta cacgtgccat actctcaggc**
10701 **accatctggc tttaagtatt ggctaaaaga acgcggggcg tcactgcagc**
10751 **acacagcacc atttggctgc caaatagcaa caaacccggt aagagcggtg**
10801 **aactgcgccg tagggaacat gcccatctcc atcgacatac cggaagcggc**
10851 **cttcactagg gtcgtcgacg cgccctcttt aacggacatg tcgtgcgagg**
10901 **taccagcctg cacccattcc tcagactttg ggggcgtcgc cattattaaa**
10951 **tatgcagcca gcaagaaagg caagtgtgcg gtgcattcga tgactaacgc**
11001 **cgtcactatt cgggaagctg agatagaagt tgaagggaat tctcagctgc**
11051 **aaatctcttt ctcgacggcc ttagccagcg ccgaattccg cgtacaagtc**
11101 **tgttctacac aagtacactg tgcagctgag tgccaccccc cgaaggacca**
11151 **catagtcaac tacccggcgt cacataccac cctcggggtc caggacatct**
11201 **ccgctacggc gatgtcatgg gtgcagaaga tcacgggagg tgtgggactg**
11251 **gttgttgctg ttgccgcact gattctaatc gtggtgctat gcgtgtcgtt**
11301 **cagcaggcac taacttgaca at**taa*gtatg aaggtatatg tgtcccctaa*
11351 *gagacacact gtacatagca aataatctat agatcaaagg gctacgcaac*
11401 *ccctgaatag taacaaaata caaaatcact aaaaattata aaaacagaaa*
11451 *aatacataaa taggtatacg tgtcccctaa gagacacatt gtatgtaggt*
11501 *gataagtata gatcaaaggg ccgaataacc cctgaatagt aacaaaatat*
11551 *gaaaatcaat aaaaatcata aaatagaaaa accataaaca gaagtagttt*
11601 *aaagggctat aaaacccctg aatagtaaca aaacataaag ttaataaaaa*
11651 *tcaaatgaat accataattg gcaaacggaa gagatgtagg tacttaagct*
11701 *tcctaaaagc agccgaactc actttgagaa gtaggcatag cataccgaac*

11751 *tcttccacga ttctccgaac ccacagggac gtaggagatg ttattttgtt*
11801 *tttaatattt c*

C2 Virus titres obtained by conducting plaque assays in triplicate using Vero cells in 6 well (35mm) assay dishes for (a) w/t and (b) A533V mutant viruses.

(a)

Time (hr)	w/t 1 pfu/ml	w/t 2 pfu/ml	w/t 3 pfu/ml	wt Ave pfu/ml
1	6.50E+04	5.46E+04	3.50E+04	5.15E+04
2	5.20E+04	4.00E+04	4.80E+04	4.67E+04
4	6.30E+04	4.26E+04	4.40E+04	4.99E+04
7	1.28E+06	4.20E+06	4.09E+06	3.19E+06
9	1.83E+07	1.81E+07	1.37E+07	1.67E+07
20	2.89E+08	5.60E+08	4.53E+08	4.34E+08
24	4.60E+07	2.49E+08	2.00E+08	1.65E+08
48	3.30E+07	9.81E+07	1.62E+08	9.77E+07

(b)

Time(hr)	mut vero 1	mut vero 2	mut vero 3	Ave pfu/ml
1	1.40E+04	1.20E+04	1.40E+04	1.33E+04
2	1.40E+04	1.20E+04	1.60E+04	1.40E+04
4	2.20E+04	3.10E+04	2.90E+04	2.73E+04
7	7.60E+05	1.04E+06	1.02E+06	9.40E+05
9	3.60E+06	4.00E+06	2.00E+06	3.20E+06
20	1.09E+08	1.83E+08	1.29E+08	1.40E+08
24	2.06E+08	1.92E+08	2.60E+08	2.19E+08
48	8.71E+07	9.23E+07	1.01E+08	9.35E+07

C3 Virus titres obtained by conducting plaque assays in triplicate using L929 cells in 6 well (35mm) assay dishes for (a) w/t and (b) A533V mutant viruses.

(a)

Time (hr	w/t 1 pfu/ml	pfu/ml	pfu/ml	wt Ave pfu/ml
1	1.28E+04	1.20E+04	1.06E+04	1.18E+04
3	7.20E+03	8.20E+03	6.40E+03	7.27E+03
6	5.00E+03	6.80E+03	7.50E+03	6.43E+03
8	4.20E+04	4.40E+04	5.50E+04	4.70E+04
20	9.80E+04	1.30E+05	1.14E+05	1.14E+05
26	5.47E+05	4.93E+05	5.60E+05	5.33E+05
50	3.87E+05	4.27E+05	4.26E+05	4.13E+05

(b)

Time	mut 1	mut 2	mut 3	Ave pfu/ml
1	4.20E+03	5.20E+03	4.80E+03	4.73E+03
3	8.00E+03	1.10E+04	7.20E+03	8.73E+03
6	1.28E+04	9.80E+03	1.20E+04	1.15E+04
8	1.00E+05	1.00E+05	1.08E+05	1.03E+05
20	3.60E+05	3.64E+05	3.30E+05	3.51E+05
26	7.00E+04	1.10E+05	1.08E+05	9.60E+04
	3.40E+04	2.80E+04	3.60E+04	3.27E+04